CLOSED-LOOP INTERFACES FOR NEUROELECTRONIC DEVICES AND ASSISTIVE ROBOTS

EDITED BY: Loredana Zollo, Max Ortiz-Catalan, Nicolas Garcia-Aracil, Christian Antfolk and Elsa Andrea Kirchner

PUBLISHED IN: Frontiers in Neuroscience

frontiers Research Topics

frontiers

ISSN 1664-8714
ISBN 978-2-88976-027-5
DOI 10.3389/978-2-88976-027-5

About Frontiers

Frontiers is more than just an open-access publisher of scholarly articles: it is a pioneering approach to the world of academia, radically improving the way scholarly research is managed. The grand vision of Frontiers is a world where all people have an equal opportunity to seek, share and generate knowledge. Frontiers provides immediate and permanent online open access to all its publications, but this alone is not enough to realize our grand goals.

Frontiers Journal Series

The Frontiers Journal Series is a multi-tier and interdisciplinary set of open-access, online journals, promising a paradigm shift from the current review, selection and dissemination processes in academic publishing. All Frontiers journals are driven by researchers for researchers; therefore, they constitute a service to the scholarly community. At the same time, the Frontiers Journal Series operates on a revolutionary invention, the tiered publishing system, initially addressing specific communities of scholars, and gradually climbing up to broader public understanding, thus serving the interests of the lay society, too.

Dedication to Quality

Each Frontiers article is a landmark of the highest quality, thanks to genuinely collaborative interactions between authors and review editors, who include some of the world's best academicians. Research must be certified by peers before entering a stream of knowledge that may eventually reach the public - and shape society; therefore, Frontiers only applies the most rigorous and unbiased reviews.
Frontiers revolutionizes research publishing by freely delivering the most outstanding research, evaluated with no bias from both the academic and social point of view. By applying the most advanced information technologies, Frontiers is catapulting scholarly publishing into a new generation.

What are Frontiers Research Topics?

Frontiers Research Topics are very popular trademarks of the Frontiers Journals Series: they are collections of at least ten articles, all centered on a particular subject. With their unique mix of varied contributions from Original Research to Review Articles, Frontiers Research Topics unify the most influential researchers, the latest key findings and historical advances in a hot research area! Find out more on how to host your own Frontiers Research Topic or contribute to one as an author by contacting the Frontiers Editorial Office: frontiersin.org/about/contact

CLOSED-LOOP INTERFACES FOR NEUROELECTRONIC DEVICES AND ASSISTIVE ROBOTS

Topic Editors:
Loredana Zollo, Campus Bio-Medico University, Italy
Max Ortiz-Catalan, Chalmers University of Technology, Sweden
Nicolas Garcia-Aracil, Miguel Hernández University of Elche, Spain
Christian Antfolk, Lund University, Sweden
Elsa Andrea Kirchner, Robotik-Innovationszentrum, Deutsches Forschungszentrum für Künstliche Intelligenz (DFKI), Germany

Citation: Zollo, L., Ortiz-Catalan, M., Garcia-Aracil, N., Antfolk, C., Kirchner, A. E., eds. (2022). Closed-loop Interfaces for Neuroelectronic Devices and Assistive Robots. Lausanne: Frontiers Media SA. doi: 10.3389/978-2-88976-027-5

Table of Contents

frontiers in Neuroscience

ORIGINAL RESEARCH
published: 19 February 2020
doi: 10.3389/fnins.2020.00120

Long-Term Home-Use of Sensory-Motor-Integrated Bidirectional Bionic Prosthetic Arms Promotes Functional, Perceptual, and Cognitive Changes

*Jonathon S. Schofield[1], Courtney E. Shell[2,3], Dylan T. Beckler[2], Zachary C. Thumser[2,4] and Paul D. Marasco[2,3]**

[1] Department of Mechanical and Aerospace Engineering, University of California, Davis, Davis, CA, United States,
[2] Department of Biomedical Engineering, Lerner Research Institute-Cleveland Clinic, Cleveland, OH, United States,
[3] Advanced Platform Technology Center, Louis Stokes Cleveland VA Medical Center, Cleveland, OH, United States,
[4] Research Service, Louis Stokes Cleveland VA Medical Center, Cleveland, OH, United States

OPEN ACCESS

Edited by:
Max Ortiz-Catalan, Chalmers University of Technology, Sweden

Reviewed by:
Strahinja Dosen, University Medical Center Göttingen, Germany
Sliman J. Bensmaia, University of Chicago, United States

***Correspondence:**
Paul D. Marasco
marascp2@ccf.org

Specialty section:
This article was submitted to Neural Technology, a section of the journal Frontiers in Neuroscience

Received: *10 September 2019*
Accepted: *30 January 2020*
Published: *19 February 2020*

Citation:
Schofield JS, Shell CE, Beckler DT, Thumser ZC and Marasco PD (2020) Long-Term Home-Use of Sensory-Motor-Integrated Bidirectional Bionic Prosthetic Arms Promotes Functional, Perceptual, and Cognitive Changes. Front. Neurosci. 14:120. doi: 10.3389/fnins.2020.00120

Cutaneous sensation is vital to controlling our hands and upper limbs. It helps close the motor control loop by informing adjustments of grasping forces during object manipulations and provides much of the information the brain requires to perceive our limbs as a part of our bodies. This sensory information is absent to upper-limb prosthesis users. Although robotic prostheses are becoming increasingly sophisticated, the absence of feedback imposes a reliance on open-loop control and limits the functional potential as an integrated part of the body. Experimental systems to restore physiologically relevant sensory information to prosthesis users are beginning to emerge. However, the impact of their long-term use on functional abilities, body image, and neural adaptation processes remains unclear. Understanding these effects is essential to transition sensate prostheses from sophisticated assistive tools to integrated replacement limbs. We recruited three participants with high-level upper-limb amputation who previously received targeted reinnervation surgery. Each participant was fit with a neural-machine-interface prosthesis that allowed participants to operate their device by thinking about moving their missing limb. Additionally, we fit a sensory feedback system that allowed participants to experience touch to the prosthesis as touch on their missing limb. All three participants performed a long-term take-home trial. Two participants used their neural-machine-interface systems with touch feedback and one control participant used his prescribed, insensate prosthesis. A series of functional outcome metrics and psychophysical evaluations were performed using sensate neural-machine-interface prostheses before and after the take-home period to capture changes in functional abilities, limb embodiment, and neural adaptation. Our results demonstrated that the relationship between users and sensate neural-machine-interface prostheses is dynamic and changes with long-term use. The presence of touch sensation had a near-immediate impact on how the users operated their prostheses. In the multiple independent measures of users' functional abilities employed, we observed

a spectrum of performance changes following long-term use. Furthermore, after the take-home period, participants more appropriately integrated their prostheses into their body images and psychophysical tests provided strong evidence that neural and cortical adaptation occurred.

Keywords: perceptual engineering, sensory restoration, take-home trial, human-machine interface, prosthesis

INTRODUCTION

The human hand is extremely versatile, capable of performing tasks with remarkable variations in the required dexterity, power, and precision of grasps. These range from tasks as delicate as microsurgeries to those as demanding as rock climbing. Cutaneous sensation is vital to controlling our hands and upper limbs. In nearly every activity performed with our hands, cutaneous sensation shapes how we achieve that task. Specifically, it closes the motor control loop by informing the real-time adjustments of grasping forces and responses to perturbations during object manipulations (Johansson, 1996). Cutaneous sensation also plays a critical role beyond limb control by providing much of the necessary information the brain requires to perceive our limbs as a part of our bodies (embodiment) (Botvinick and Cohen, 1998), which helps us distinguish ourselves as separate from the world around us.

Prosthesis solutions have become increasingly sophisticated and advanced robotic limbs are beginning to rival healthy limbs in dexterity (Belter et al., 2013). Unfortunately, the increased sophistication of these devices reveals that the lack of natural sensory feedback and reliance on open-loop control limits the functional potential of these devices. Humans naturally seek to close the loop through sensory information. This can be seen clearly in prosthesis users who typically adopt indirect feedback strategies in an effort to compensate for the lack of sensation. This involves continual visual attention paid to prostheses and monitoring of other indirect cues such as the sound of the motors, vibrations, and changes in pressure or leverage between the prosthetic socket and the residual limb (Gonzalez et al., 2012; Schofield et al., 2014). This substituted sensory information is cognitively demanding to interpret and can leave users feeling overwhelmed and frustrated (Gonzalez et al., 2012). Addressing the challenges associated with the absence of sensation is a highly active field of study, and attempts to provide prosthesis users with sensory feedback have been reported as early as the 1950s (Siehlow, 1951). More recently, the use of mechanotactile and vibrotactile feedback has been used to provide sensations of proportional tactile force (Marasco et al., 2011; Antfolk et al., 2013; Rombokas et al., 2013; Cipriani et al., 2014; Hebert et al., 2014; De Nunzio et al., 2017), and movement sensation (Sharma et al., 2014; Witteveen et al., 2014; Hasson and Manczurowsky, 2015; Marasco et al., 2018) in both amputee and able-bodied populations. These methods have proven effective in patient performance of tasks such as precise force generation (De Nunzio et al., 2017), force discrimination (Hebert et al., 2014), stiffness discrimination (Hebert et al., 2014; Witteveen et al., 2014), stimuli localization (Antfolk et al., 2013), and multi-site sensory discrimination (Antfolk et al., 2013). Other approaches are also being pursued, including electrical stimulation of peripheral nerves (e.g., Christie et al., 2017), electrocutaneous stimulation (e.g., Paredes et al., 2015), and direct cortical stimulation of the primary somatosensory cortex (e.g., Tabot et al., 2013; Hiremath et al., 2017).

When a limb is lost, there is a disruption of one's body image (Rybarczyk and Behel, 2008), which is likely potentiated by the absence of sensory feedback (Marasco et al., 2011). The perception that our limbs belong to our bodies is largely a product of visual and tactile information; when touch to a body part is seen and felt appropriately, our brains assume ownership over that body part (Botvinick and Cohen, 1998). Therefore, the absence of sensation in upper-limb prostheses significantly impedes these devices from being perceived as integrated parts of the body. When taken together, operating an insensate prosthesis leaves the user to pilot a numb, cognitively demanding, and disconnected tool rather than an integrated replacement limb. Although no commercially available prostheses actively provide physiologically relevant sensory feedback, efforts to achieve intuitive touch feedback, among other sensory modalities, are on the experimental horizon.

The implications of sensory loss extend far beyond the direct impediments to prosthesis use and the disruptions to body image. Amputation damages all the nerves that once connected to the limb, which promotes structural and functional reorganization of sensory-motor pathways (Cohen et al., 1991; Flor et al., 1995; Makin et al., 2013). Regular prosthesis use appears to have an important influence on how the brain adapts to limb loss. There is evidence to suggest that the regularity and the extent to which one uses a conventional mechatronic (myoelectric) prosthesis correlates with reduction in this cortical reorganization (Lotze et al., 1999) and may even influence the network of brain areas from which body schema and representation are processed (Boccia et al., 2019).

Although conventional insensate prosthesis use may have a long-term influence on cortical adaptation, it is important to make the distinction that these devices still do not leverage the same residual neural pathways that the intact limb once did. Communicating with the user and brain via these same mechanisms is perhaps the most direct way to truly replace a limb. Taking advantage of existing circuitry that the body and user are pre-wired to accept can enable intuitive control, physiologically relevant feedback, and rapid incorporation as part of the body. In recent years, there has been an emergence of surgical interventions that interface and communicate with the residual neural anatomy of a limb post-amputation. For example, targeted motor reinnervation and targeted sensory reinnervation [TMR and TSR, respectively (Kuiken et al., 2004; Hebert et al., 2014)] are surgical techniques that create motor

and sensory neural-machine-interfaces (NMIs) for intuitive closed-loop control of mechatronic prostheses. These procedures surgically redirect motor and sensory nerves, which once served the patient's amputated hand, to proximal muscle and cutaneous sites in the residual limb (Kuiken et al., 2004; Hebert et al., 2014). When a patient attempts to move their missing limb, the reinnervated muscle sites will contract. This muscle activity can be measured and used to control mechatronic prosthesis movements (Kuiken et al., 2004). Furthermore, cutaneous stimulation of the reinnervated skin sites is experienced as occurring on the missing limb (Kuiken et al., 2007a). Patients can experience sensations of touch, force, vibration, temperature, and pain in the missing limb with near-normal detection thresholds (Kuiken et al., 2007a). By instrumenting a prosthetic limb to detect touch and force, and mapping these signals to touch feedback devices located on a patient's reinnervated skin sites, participants can experience touch and grasp forces of a prosthesis as though it is their missing limb (Hebert et al., 2014).

With a newly restored sense of touch, TSR participants have demonstrated improvements in functional tasks requiring the ability to detect prosthetic digit touch and discriminate forces (Hebert et al., 2014). Furthermore, psychophysical and metabolic evidence suggests that TSR participants using a touch feedback interface receive the appropriate sensory information to begin re-embodying artificial limbs (Marasco et al., 2011). Imaging data suggest that reinnervated participants attempting to activate a prosthetic hand produce similar activation in the primary motor cortex as healthy controls, which was not the case with a non-reinnervated participant group (Serino et al., 2017). Similarly, touch on the reinnervated skin activated the primary sensory cortex in patterns similar to those of a healthy control group, although activation strength was reduced (Serino et al., 2017). Taken together, it is evident that TMR-TSR participants operating an NMI mechatronic prosthesis are equipped with all the necessary pieces to operate and feel an artificial limb as though it were an integrated part of the body. However, NMI prostheses are still machines that must communicate with the user. Although the neural mechanisms of this communication are native to the user, the relationship is likely dynamic over time as the user learns to optimally interact with their device, and the brain adapts to the newly restored sensory-motor channels. Performing long-term take-home trials with sensate NMI prostheses can help us understand how users learn, embody, and adapt to these systems. This is an important next step to unlocking artificial limbs that are truly reintegrated and functional beyond the laboratory.

We recruited TMR-TSR participants to perform long-term take-home trials of touch-integrated NMI robotic prostheses. Participants completed assessments before and after the take-home period that captured changes in functional ability, prosthesis embodiment, as well as cognitive changes. We hypothesized that following the take-home period, we would see indications of limb reintegration in the form of improved functional outcomes, increased scores on prosthesis embodiment surveys, and changes in psychophysical-cognitive tests.

MATERIALS AND METHODS

Take-Home Study Structure

Prior to the take-home period, we benchmarked the performance of each participant on a series of experiments with their NMI prosthesis, with various touch conditions, described in a later subsection. Participants repeated these experiments after the take-home period. The experiments completed were touch mapping of reinnervated skin (Kuiken et al., 2007a), a temporal order judgment task [TOJ; (Marasco et al., 2011)], a block-foraging stiffness discrimination task (Beckler et al., 2019), a psychophysical Fitts' law grasp force task (Thumser et al., 2018), the Box and Block task (Mathiowetz et al., 1985), and the Clothespin Relocation task (Miller et al., 2008). These experiments are briefly described below and additional procedural details are available in the references cited above. After baseline performance was assessed in their initial visit, participants completed a minimum 9-month take-home period. SD and TH completed this take-home period with their sensate NMI prostheses while CTRL completed this period with his normal (insensate) TMR-controlled NMI myoelectric prosthesis. During this take-home period, all participants logged their prosthesis use and completed a diary describing activities performed with their prostheses.

Participants and Technical Setup

This study was carried out under a protocol approved by the Institutional Review Boards of the Cleveland Clinic and Department of the Navy Human Research Protection Program. Participants gave written informed consent prior to study procedures. All participants had previously undergone both TMR and TSR surgeries following amputation and trained to use a myoelectric prosthesis system with their reinnervated muscles. All participants perceived touch on the reinnervated skin of their residual limbs (touch sites) as touch on their missing hand. We created a closed-loop NMI prosthesis for each participant. A certified prosthetist fitted a new myoelectric prosthesis system, using components comparable to their familiar, prescribed system. We added touch feedback by placing robotic, four-bar haptic pushing devices (touch tactors) on the reinnervated skin at their touch sites (HDT Global, Fredericksburg, VA, United States) (Kim et al., 2010). Photographs of one participant's prosthesis are shown in **Figure 1**. Tactor activation was mapped to matching sensorized locations on the prosthetic hand, thereby translating touch on the prosthesis to touch on the missing hand at the corresponding location. Details of each participant's NMI prosthesis are described below.

To detect touch on the prosthesis, we retrofitted the first, second, and third digits of a SensorHand Speed (Ottobock, Duderstadt, Germany) with strain gauges, and the palm and fourth and fifth digits of a System Inner hand shell (Ottobock, Duderstadt, Germany) with force-sensitive resistors. Sensors were paired with tactors so that when touch was detected by one of the six sensors in the prosthetic hand, a tactor pushed on the site where participants perceived touch on their missing hand corresponding to the activated sensor.

The sensors and tactors were configured to simultaneously apply two different touch feedback modes – proportional touch and tap detection. The proportional touch mode mapped the amount of force generated on the sensorized prosthetic hand to force applied by the tactors. The tap detection mode relayed the sensation of object contact or tapping to the missing hand by causing the tactors to quickly and forcefully extend based on the speed and amplitude of the force applied to the sensorized prosthesis, and then rapidly retract. Together, the proportional mode continuously dictated the end position of the tactor, while contact events and other transient forces applied an additional, brief extension of the tactors, which then rapidly returned to the proportional mode command. To tune touch feedback forces, participants watched an investigator touch their prosthetic hand as well as touched it with their intact hand; tactor force gains (mapping forces on the prosthesis to touch force feedback) were adjusted until the participants reported satisfaction with the subjective experience and were able to uniquely identify touch on each digit. Both the proportional and tap modes could be tuned independently, and while this may be a slight departure from the way an intact individual experiences touch and force sensation, it allowed participants to be sensitive to light touches which, in a pure proportional mode, might fail to make tactor-skin contact. In practice a combination of both was preferred for most digits by the participants.

The completed NMI prostheses were self-contained and required no extra work from the participants to don/doff and maintain beyond the requirements of a standard myoelectric prosthesis. The touch feedback system drew power from the same battery used to power the myoelectric prosthesis, so the participants only had to charge the standard battery for a Boston Digital Arm Systems Elbow (LTI/Liberating Technologies, Inc., Holliston, MA, United States) to ensure power for the entire system. Furthermore, the touch feedback system was fully integrated, with no external components. The sensors were integrated into the terminal device and the cosmesis, with no visible or protruding pieces. The touch tactors were integrated into the socket and shrouded to protect them from damage and streamline appearance. This integration also meant that the feedback system was placed using the repeatability of socket donning. To use the touch-enabled NMI, participants simply donned their prosthesis as normal; no additional technical knowledge or training was necessary.

Participant With a Shoulder Disarticulation, TMR, and TSR

The first participant, SD, had previously received targeted motor and sensory reinnervations and regularly used a left shoulder disarticulation, socket-fit myoelectric prosthesis system with proportional EMG control (Kuiken et al., 2007a,b; Marasco et al., 2011). For the take-home period and experimental testing, SD used a myoelectric prosthesis system comparable to her familiar, prescribed system. The prosthesis used a custom (Advanced Arm Dynamics, Redondo Beach, CA, United States) silicone-lined, electrode-embedded socket with chest plate, harness, and dropped shoulder, a Boston Digital Arm Systems Elbow, a SensorHand Speed set to speed 0, System Inner hand shell, and proportional EMG control. This system afforded her three active simultaneous degrees-of-freedom – elbow flexion/extension, wrist pronation/supination, and hand open/close – as well as three passive degrees-of-freedom – shoulder flexion/extension, shoulder abduction/adduction, and humeral rotation. We located six touch sites, one each on all five digits and her palm, where touch on the reinnervated skin of the residual limb site caused sensation of touch on her missing hand. All of the touch sites were located on the skin over her pectoral muscle, so we mounted six four-bar, linear-actuating tactors to the prosthesis chest plate, positioned over her touch sites. Thus, pressure on the prosthetic hand caused SD to perceive congruent touch sensation on her missing hand. This system provided distinct touch sensation in physiologically correct locations for her five digits and palm.

Participant With a Transhumeral Amputation, TMR, and TSR

The second participant, TH, had previously received targeted motor and sensory reinnervations, and regularly used a left transhumeral myoelectric prosthesis system with a socket liner, controlled by pattern recognition (Dumanian et al., 2009; Marasco et al., 2011, 2018). For this study, TH used a comparable prosthesis system, consisting of a custom-made thermoplastic socket and harness, electrode-embedded liner (The Ohio Willow Wood Company, Mt. Sterling, OH, United States), Boston Digital Arm Systems Elbow, SensorHand Speed set to speed 0, System Inner hand shell, and pattern recognition control (CoAPT, Chicago, IL, United States). This system afforded her three active degrees-of-freedom – elbow flexion/extension, wrist pronation/supination, and hand open/close – as well as passive humeral rotation. Tactors extended through holes drilled in the socket and pushed on TH's touch sites through thinned areas of the liner. This system provided distinct touch sensation in physiologically correct locations for her five digits and palm.

Control Participant With a Transhumeral Amputation, TMR, and TSR

The third participant, CTRL, had previously received targeted motor and sensory reinnervations, and regularly used a left suction-socket, myoelectric prosthesis system with proportional EMG control (Hebert et al., 2014; Marasco et al., 2018). For testing, CTRL used a comparable prosthesis system, consisting of a custom-made, electrode-embedded thermoplastic socket and harness, Boston Digital Arm Systems Elbow, SensorHand Speed set to speed 0, System Inner hand shell, and proportional EMG control. This system afforded him two active simultaneous degrees-of-freedom – elbow flexion/extension and hand open/close – as well as passive humeral rotation and wrist pronation/supination. CTRL had two touch sites, one where touch on the residual limb site caused sensations of touch on his thumb and index finger, and the other sensation of touch primarily on his index finger (and faint middle finger). Therefore, two sensors and two tactors were configured, the first sensitive to touch on the prosthetic thumb and the second to the index finger. Prior to testing, CTRL reported distinct touch sensation in physiologically correct locations for both tactors. CTRL elected to have his tactors configured to operate only on proportional mode

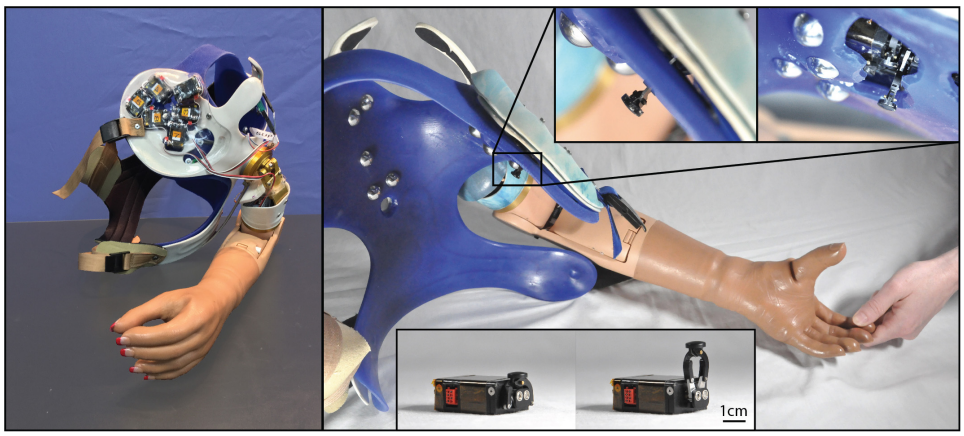

FIGURE 1 | Photographs of the closed-loop NMI prosthesis system created for and used by the participant with a shoulder disarticulation (SD). Touch tactors placed in the chest plate are shown in the left panel, while dome electrodes and bump switches used for control are shown in the right main panel. Touch tactors extended when sensors embedded in the prosthetic hand detected touch. Close-up views of the touch tactors extended are shown in the top inset, and an unmounted tactor in the rest and extended position is shown in the bottom inset.

as this was subjectively more appropriate to him. Although CTRL was fitted with a sensate prosthesis for experiments in the lab, he did not take this touch-enabled prosthetic limb home during the take-home period. He instead used his own non-touch, TMR-controlled myoelectric arm as his home-use limb.

Touch Conditions

During the experiments described below, participants completed tasks with the touch tactors configured in four different ways (touch conditions). In the *touch-off* condition, the tactors were powered off, and no touch feedback was provided. In the *touch-on* condition, participants received spatially and temporally congruent touch feedback. In the *lagged* condition, the tactors provided feedback after a 1000-ms delay, i.e., spatially congruent but temporally incongruent. In the *scrambled* condition, the sensor-tactor mapping was pseudo-randomized such that activating a sensor caused a mismatched tactor to actuate, so touch feedback was spatially incongruent but temporally congruent with touches on the prosthetic hand. Touch conditions were completed in blocks. Note that during CTRL's visits the lagged and scrambled conditions were omitted from relevant tests when needed to accommodate time constraints related to the participant's work schedule and international travel.

Experiments

Touch Mapping

Experimental procedure

To determine where to place touch tactors, we queried participants about the locations at which they experienced touch on their missing hand when we stimulated reinnervated skin. We also repeated this process after the take-home period to assess any changes in touch sensation locations. For all participants, we prepared for touch mapping by identifying reproducible sites on their reinnervated skin to be tested for touch sensation. We used skin-based landmarks, such as scars or freckles, and where possible, we used a thermoplastic reference socket with a 1 × 1 cm grid of holes drilled through it. We passed a felt marker through the holes to consistently draw the 1 × 1 cm alphanumeric grid. This ensured that we could interrogate the same locations before and after the take-home period. We applied pressure to each point in a randomized order with a cotton swab, which was attached to a 300 g Von Frey monofilament to ensure equal pressure was applied to each point of the grid. Participants were given schematic diagrams of hands that they drew on to indicate where they felt touch sensation on their missing hand [percept drawings (Kuiken et al., 2007a)]. It should be noted that following TMR-TSR procedures, touch on reinnervated skin is felt only in the missing hand (Kuiken et al., 2007a; Hebert et al., 2014). If participants felt touch on only their native skin (i.e., upper arm or chest), they were instructed to inform the investigator but not to draw anything as this indicated that the location touched was not reinnervated. This procedure was performed twice for each participant: once before and then again following the take-home period. Also note that CTRL's initial touch map was created with the cotton swab placed on a 300 g Von Frey monofilament. However, instead of using a reference grid, the point placement was guided by the points shown in Hebert et al. (2016) (a study in which he was previously involved). There were fewer points represented in Hebert et al. (2016) because that earlier study used a thresholding approach to define touch areas. In CTRL's final touch map session this change in point referencing methodology was corrected and the mapping procedure was conducted in alignment with the mapping procedure for all participants as described above.

Data analysis

We digitally transcribed each participant's percept drawings and layered all points onto two representative schematics (touch maps) for each participant, one per visit. Transparencies of individual percept drawings were normalized across participants and visits such that equal shades of color indicated that an equal

proportion of tested points caused sensation in that region. For each participant's touch mapping session, we first looked for a change in proportion of touch map locations, for which the participant reported sensation, using a standard *z*-test. Then, we divided their hand drawings coarsely into twelve regions (five individual digits, plus the remainder of the hand/palm, for both ventral and dorsal surfaces) and compared shifts in the proportion of sensation reported in each of the different locations for each participant, comparing their initial to final visit. This analysis of proportions was designed to ensure validity by allowing for differences in the amount/exact location of tested points in the initial and final maps.

We also wanted to isolate the areas of reinnervated skin that were targeted by the touch tactors to understand how perceptions of touch at these areas might change when stimulated long-term. This analysis was performed *post hoc* using experimental photographs to identify where each touch tactor was located relative to the alphanumeric points used in the touch mapping experiments. Since the exact points at which tactors contacted the skin may have varied slightly day-to-day due to normal differences in donning, we also included the percept drawings from tested points adjacent to the tactor locations when compiling touch maps for these areas (with shading normalized as described above).

Temporal Order Judgment Task

Experimental setup

This task assessed relative weighting of sensory processing between the intact and amputated sides by asking the participants to judge which of two nearly simultaneous events, one on each side, occurred first. Participants were seated at a table across from an investigator, with a partition placed in between them. While their view of each other was occluded, a small window in the partition allowed the participant and investigator to interact. Participants placed their prosthetic hand within reach of the investigator through the window and could view their prosthesis as it was touched by the investigator. Each participant had a commercially available vibratory unit (C2 tactor, Engineering Acoustics Inc., Casselberry, FL, United States) taped to their skin near the distal end of their residual limb, and another vibratory unit in a mirrored position on their intact limb. For each participant, we placed two foot pedals under the table, near their feet. During the experiment, participants wore disposable earplugs and noise-canceling headphones that played gray noise.

Experimental procedure

Participants were instructed to watch their prosthetic hand at all times during the experiment, unless it was covered, in which case they watched a small marker placed on the partition just above the prosthetic hand. Each experimental trial started and ended with a 1-min rest period where the prosthetic hand was covered with a white sheet. After the initial rest period, the white sheet was removed, and the seated investigator repeatedly touched the prosthesis in different randomized locations in an experimental protocol similar to Marasco et al. (2011). After 5 min of stimulation, the vibratory units placed on the left and right sides activated asynchronously, with the delay between activation of the unit on one side and activation of the unit of the other side varying (10, 20, 30, 60, 90, or 120 ms), while hand stimulation continued. Half of the time vibration occurred on the left side first, and the other half of the time right-side vibration was first. Participants were instructed to decide (two-alternative forced choice) which unit vibrated first, and to press the foot pedal on the side that vibrated first. Foot pedal presses were recorded. Time interval and left-first/right-first order was pseudo-randomized in sets of 12 presentations, with each combination of time interval and left-first/right-first occurring once per set. One experimental trial contained seven sets, for a total of 84 presentations. Blocks of testing consisted of five trials: the four touch conditions (touch-off, touch-on, lagged, and scrambled) and a fixation trial (where the prosthetic hand remained covered and the investigator did not interact with the prosthetic hand). Within each experimental block, the order of conditions was randomized. Participants completed three blocks of testing.

After each TOJ trial was completed (each touch condition), participants were given a nine-statement, seven-point Likert scale survey to measure the degree to which they embodied the prosthetic hand (Marasco et al., 2011). Participants were asked to indicate their level of agreement with each statement, from *strongly disagree* to *strongly agree*. Of the nine statements, three were related to embodiment, and the remaining six were used to control for suggestibility and task compliance.

Note that SD participated in two initial visits (before the take-home period). The temporal order judgment data were collected on the first visit, while the remaining data were collected in the second visit upon receiving a satisfactorily fitting prosthesis that she could wear over the time course of the take-home period.

Data analysis

For each participant, we calculated a *point of subjective simultaneity* (PSS) (Keetels and Vroomen, 2012). We first calculated the proportion of left-first/right-first responses for each time interval presented (12 in total, described above). A sigmoid was then fit across these 12 proportions. The time interval for which left-first and right-first responses were modeled as being equal was taken as the PSS.

Embodiment was calculated by averaging questionnaire statements following each TOJ trial. The three statements of embodiment were averaged and the six control statements were averaged for each participant according to each touch condition (touch-off, touch-on, lagged, scrambled, and fixation). Participants were considered to have embodied the prosthesis for a particular touch condition if their average response was greater than or equal to one (Kalckert and Ehrsson, 2012).

Block-Foraging Stiffness Discrimination Task

Experimental setup

The block-foraging stiffness discrimination task is a scientifically validated sensory-motor function test that was specifically designed to be sensitive to touch feedback. This is achieved through quantifying performance during selection of rubber blocks with a target stiffness from a pool of target and distractor blocks (Beckler et al., 2019). This task provides separable assessment of motor and sensory performance as well as insight into strategy. Following the procedure described by

Beckler et al. (2019), we placed rubber blocks (25.4 mm cubes) of varying stiffness in the testing area (approximately 500 mm long and 400 mm wide, with 3 mm walls to contain the blocks) on a table in front of the participants. There were 60 blocks total, 20 "hard blocks" of 80A durometer, 20 "medium blocks" of 60A durometer, and 20 "soft blocks" of 40A durometer. One reference block of each hardness was labeled and placed outside the box, within participants' reach. To reduce auditory cues, participants wore disposable earplugs and noise-canceling headphones playing gray noise. Participants wore frosted lenses that mitigated discrimination by visual cues, but still allowed them to visually locate the blocks. Two video recorders were used to film the experiment from different angles.

Experimental procedure

Participants were informed that the testing area contained soft, medium, and hard blocks, and that they would be searching for either soft or hard blocks. We instructed the participants which hardness to search for by tapping the corresponding reference block. Participants tapped the target reference block to indicate they were starting the trial. They then searched for and removed five blocks, one at a time, from the testing area that they thought were the target hardness. We recorded the number of blocks the participants squeezed, the number of correct blocks the participants selected, and trial duration. Participants also performed baseline trials where they were instructed to select five blocks of any hardness and move them outside the testing area. Soft, hard, and baseline trial order was randomized and completed in blocks of about 20% of the entire task. Blocks of testing alternated between touch-off and touch-on conditions. For each touch condition, participants selected 100 rubber blocks total.

Data analysis

We divided the trial durations into three different sub-sections: *search time*, the time it took a participant to find the block they ultimately selected; *involvement time*, the time a participant spent discriminating block stiffness and transporting the block they ultimately selected; and *handling time*, the time a participant spent transporting a block during the baseline trials (where no discrimination was made). We also calculated *recognition time*, the time a participant spent making their discrimination decision when selecting a block, as the difference between *involvement time* and *handling time*. Time values were derived through frame-by-frame analysis of video footage captured at 30 frames per second.

We calculated each participant's *accuracy* by dividing the number of correct blocks that were selected by the total number of blocks selected. We used their accuracy, the total number of blocks they encountered, and the known proportions of blocks to calculate a *false positive rate* (the probability a participant incorrectly selected a non-target block when they encountered one) and a *false negative rate* (the probability a participant incorrectly rejected a target block when they encountered one) for each participant.

Efficiency, calculated by dividing accuracy by the average time it took to select a block, provided an overall performance measure. *Discrimination efficiency*, calculated by dividing accuracy by average recognition time, provided a discrimination performance measure.

To determine if changes across touch condition and visit were statistically significant, z-tests of proportion were used for accuracy, Wilcoxon rank-sum tests were used for search times, and t-tests were used for recognition and handling times. A significance level of 0.05 was used for all tests.

Psychophysical Fitts' Law Grasp Force Task

Experimental setup

The psychophysical Fitts' law grasp force task is a scientifically validated sensory-motor function test developed to quantify the user's ability to quickly and accurately produce a desired grasping force (Downey et al., 2018; Thumser et al., 2018). This speaks to participants' abilities to incorporate sensory feedback into their control scheme. Each participant sat at a table in front of a television screen with their prosthetic hand in reach of a grip force manipulandum. A partition was used to block the participant's view of the manipulandum. A keyboard was placed within reach of the participant's healthy hand. Participants were instructed to rest their open prosthetic hand around the manipulandum, but not to touch it between trials. An investigator monitored the prosthetic hand to ensure task compliance.

Experimental procedure

Before the experiment began, we asked each participant to squeeze the manipulandum with the full force of their prosthesis to record the maximum grip force, analogous to their maximum voluntary contraction. Their maximum force was measured three times, and the average was considered their maximum prosthesis grip force.

During the task, participants watched the television screen and were shown an image of a familiar, everyday item (e.g., apple, wine glass, milk carton, or eggshell). When they were ready to start the trial, they pressed the keyboard spacebar, which initiated a red-yellow-green "traffic light" countdown. When the green light lit, an audible tone played, and the participant squeezed the manipulandum with the force needed to pick up the displayed object without dropping or damaging it. We instructed the participants to grasp the manipulandum as quickly and accurately as possible. When the participant achieved their desired grip force, they pressed the spacebar again to end the trial. We recorded the maximum force generated by the participant, and the time elapsed from force onset until the maximum force was reached. Participants were shown eight unique items, and the order of items was randomized. With items that had multiple grasping possibilities, such as the wine glass, we asked participants to choose one single way that they imagined they would grasp that object and consistently use that imagined grasp every time they saw the object. The task was completed in blocks of 32 trials, and blocks alternated between touch-off and touch-on conditions. Participants were shown each unique item a total of 20 times per condition, for a total of 160 trials per touch condition.

During TH's initial visit we noticed that she prioritized speed over precision, hindering the ability to identify her maximum

grasp force precision. To capture this for future participants and sessions, we added a "precision" version of the task, in which the instructions were identical, except participants were shown the same object (milk carton) every trial, and they were told to be as accurate as possible, but that speed was not important. The precision block was 20 trials long per touch condition.

Data analysis

Consistent with Thumser et al. (2018), we calculated three outcome measures from the grasp force task: *objects successfully handled*, *peak precision,* and *speed*. Adopting their definitions for this test, an object was considered *successfully handled* if it was statistically different from the participant's maximum prosthesis force. Successful handling purposefully does not include information about object-damage threshold or force required to lift an object; rather, it focuses the metric on a participant's ability to repeatably achieve their intention, without grading them on their knowledge of object durability or weight. Each object's target difficulty was determined from the ratio of average force amplitude to force variability. *Peak precision* was the maximum difficulty of successful objects [calculated as maximum effective index of difficulty (IDe) in units of bits]. Each participant's "*speed*" was determined as the average ratio of target difficulty to average trial duration for all successful objects (calculated as *throughput* in units of bits per second). Throughput describes the tradeoff between speed and precision, where a higher value indicates that the user does not slow down much as task difficulty increases, and low values indicate that difficult tasks result in a dramatic reduction in speed. This is in notable contrast to the participant being fast or slow in absolute terms, which is not described by this metric.

For all participants except TH in her initial visit, the peak precision measured during the "precision" version of the task replaces the peak precision if it is higher than what was produced during the primary task.

Box and Block and Clothespin Relocation Tasks

Experimental setup

Standard tasks to characterize manual dexterity were performed to assess motor control. Both of these tasks involve manipulating and relocating small objects under time constraints and are used in clinical practice but were developed prior to the clinical availability of sensory feedback in prostheses. For the Box and Block task, a standard two-compartment Box and Block box (Mathiowetz et al., 1985) with center partition was placed on a table in front of the participant. One side of the box was filled with 25.4 mm wooden cubes and placed on the same side as the participant's prosthesis. For the Clothespin Relocation task, we placed a standard Clothespin Relocation setup (Miller et al., 2008) on a table in front of the participant. The setup included a horizontal bar, with three clothespins positioned equidistantly, and a vertical bar. For both tests, we quantified eye gaze patterns as a proxy for the visual attention required to complete each task. The participant wore an eye-tracking headset (ETL500, ISCAN, Woburn, MA, United States) that automatically tracked gaze in space as well as detected and tracked the participant's hand relative to their gaze vector by color-based object detection of a brightly colored glove worn on the prosthetic hand during the task. In half of the trials we also employed a visual distractor. A laptop placed just beyond the box or clothespin setup played a distractor video, which showed three blocks that were randomly moved on and off screen and periodically prompted the participant to report how many blocks were shown on screen.

Experimental procedure

For the Box and Block task, participants started with their prosthetic hand on the table and were given a "3, 2, 1" countdown to begin the trial, then had 60 s to move as many blocks as they could from the filled compartment, over the center partition, to the other compartment. Participants were instructed to move only one block at a time; if multiple blocks were moved, only one was counted. At the end of the 60-s period, the number of blocks correctly transferred was recorded. For the Clothespin Relocation task, participants were instructed to move each clothespin from the horizontal bar to the vertical bar, one at a time without dropping them. After the three clothespins were successfully transferred, they were reset equally spaced on the vertical bar, and participants transferred them back down to the horizontal bar. If a clothespin was dropped, the trial was reset to the last completed transfer. Successfully transferring the clothespins to and from the vertical bar concluded a single trial. Both the time taken to move the clothespins up and down were recorded. For both tasks, each block of testing contained four trials of different touch conditions: touch-off, touch-on, lagged, and scrambled. Each trial was completed twice, first with and then without the visual distractor. Participants completed three blocks, and within each block the touch condition order was randomized. Participants also completed three trials using their intact limb to assess their able-bodied level of performance in those tasks.

Data analysis

Box and Block scores for each touch condition were calculated as the average number of blocks successfully transferred in 60 s across the three trials. Clothespin Relocation scores for each touch condition were calculated as the average time needed to successfully transfer three clothespins to the vertical bar and back to the horizontal bar, across the three trials. Failed trials (i.e., when a clothespin was dropped) were not included in the time calculation, although the number of failed trials per condition was recorded.

To quantify visual attention paid to each participant's hand, we calculated the root-mean-squared (RMS) gaze deviation, which is the angular difference between their gaze vector and the center of their hand, less the average radius of the detected hand area (to a minimum difference of zero). Thus, a higher RMS gaze deviation, in degrees, represents more time spent looking farther away from their hand, and a lower RMS gaze deviation represents more time looking at or near their hand.

RESULTS

Take-Home Period

SD had her touch-enabled arm for 2 years and we received activity diaries for 25 weeks. During the 2-month period immediately before her final visit, she wore the arm for an average of

4.9 ± 3.7 h per week. TH also had her touch-enabled arm for 2 years and we received activity diaries for 17 weeks. She wore her arm an average of 5.6 ± 1.1 h per week in the 2-month period prior to her final visit. CTRL wore his regularly prescribed (insensate), TMR-controlled NMI myoelectric arm during his workday until the battery drained, typically 9–10 h. Over the course of one and a half years, he provided activity diaries for 40 weeks. During this time, for 22 weeks in which he wore his myoelectric arm and reported wear time, he wore it an average of 5 ± 2 days per week.

Both of the participants who used the take-home system were unilateral amputees and felt that they could perform their jobs and day-to-day activities without their prostheses, conventional or sensate. TH reported needing her prosthesis for various tasks around her house (e.g., laundry, cutting vegetables, opening items) but that it was hard to wear for long periods of time due to eventual discomfort and the weight of the device. SD reported that she did not feel that she needed her prosthesis for many tasks, other than some use in preparing meals and eating. Both SD and TH avoided wearing their prosthetic arm system if there was a possibility that it might get wet (e.g., rain, going to the beach, participating in aquatic activities), and both lived in areas and had hobbies where this occurred frequently. In contrast, CTRL has a physically demanding job that requires carrying multiple, large, and/or bulky items. As a result, he wore his arm for long periods of time throughout his workday unless in wet, muddy, or extremely cold conditions.

Touch Mapping

Both SD and TH reported a significantly greater proportion of touch-sensitive locations on areas tested on their reinnervated skin in their visit after the take-home period compared to their initial visit, while CTRL did not (SD: 91.7 vs. 79.2%, $p = 0.034$; TH: 79.8 vs. 59.1%, $p < 0.0001$; CTRL: 93.9 vs. 90.0%, $p = 0.66$; z-test). The increase in SD's reported sensations comes primarily from her ventral thumb and palm; TH's increase is concentrated in the ventral ring finger, index finger, and palm, and on the dorsal index and middle fingers (**Figures 2**–**5**). There was a high degree of spatial congruency between the instrumented regions on the prosthetic hand and the corresponding percepts on the missing hand (**Figure 2B**). From the initial to final visit: TH demonstrated an increase in the amount of missing hand represented at tactor-stimulated areas; SD demonstrated an increase in how much of the palm and index finger was felt, a focusing of the area represented on the thumb, and a decrease in the area reported for the ventral hand; CTRL demonstrated relatively minimal changes (**Figure 2B**). **Figures 3**–**6** highlight the individual points tested on each participant's reinnervated skin and the reported sensations projected to the missing hand, with tactor placements and control electrodes overlaid. Together these results suggest that with regular stimulation of the reinnervated skin, the representation of each participant's missing hand expanded and strengthened over time.

PSS

During the initial visit, all participants demonstrated asymmetries in the point of subjective simultaneity (PSS) across all touch conditions (**Figure 7**, average PSS across all conditions SD: 92 ms, TH: 20 ms, CTRL: 59 ms), suggesting that participants' brains weighted sensory information from the amputated side asymmetrically from the intact side. In the final visit SD demonstrated symmetry in PSS scores (average PSS across all conditions 1 ms). TH also demonstrated reduced PSS bias (average PSS across all conditions 12 ms). The remaining 12 ms difference was entirely due to the lagged and scrambled conditions (32 and 29 ms, respectively), whereas the other three conditions had an average PSS of 0 ms. CTRL again demonstrated asymmetric PSS during the final visit (average PSS across all conditions was 58 ms). The decreased PSS asymmetry for SD and TH, but not CTRL, suggest that extended exposure to touch feedback led to more comparable processing of sensory information from the two sides.

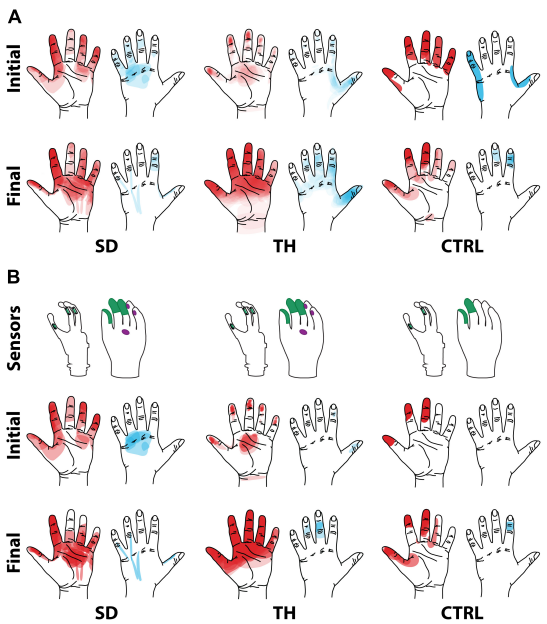

FIGURE 2 | Regions of the hand where the participant with a shoulder disarticulation (SD), the participant with a transhumeral amputation (TH), and the control participant (CTRL) felt sensation when their reinnervated skin was touched in the initial visit and final visit are shown. Red shading indicates where sensation was felt on the ventral side of their hand, and blue shading indicates where sensation was felt on the dorsal side of their hand. The intensity of the shaded areas indicates the proportion of probed locations on the reinnervated skin for which sensation was perceived at that location on the missing hand. **(A)** Shows sensations reported from all points tested on each individual participant's reinnervated skin. **(B)** Shows the reported sensations arising from the reinnervated skin near/surrounding the tactor locations. The areas of each participant's prosthetic hand that were instrumented are shown in the top row. The locations of the strain gauges in the digits of the SensorHand Speed are shown in green on the schematic of the prosthetic hand. The regions where the sensors responded are shown on the cosmesis in green for the strain gauges and purple for the force sensitive resistors.

Embodiment Questionnaires

During the initial visit, SD's and TH's survey responses indicated that they embodied their prostheses in the touch-on condition.

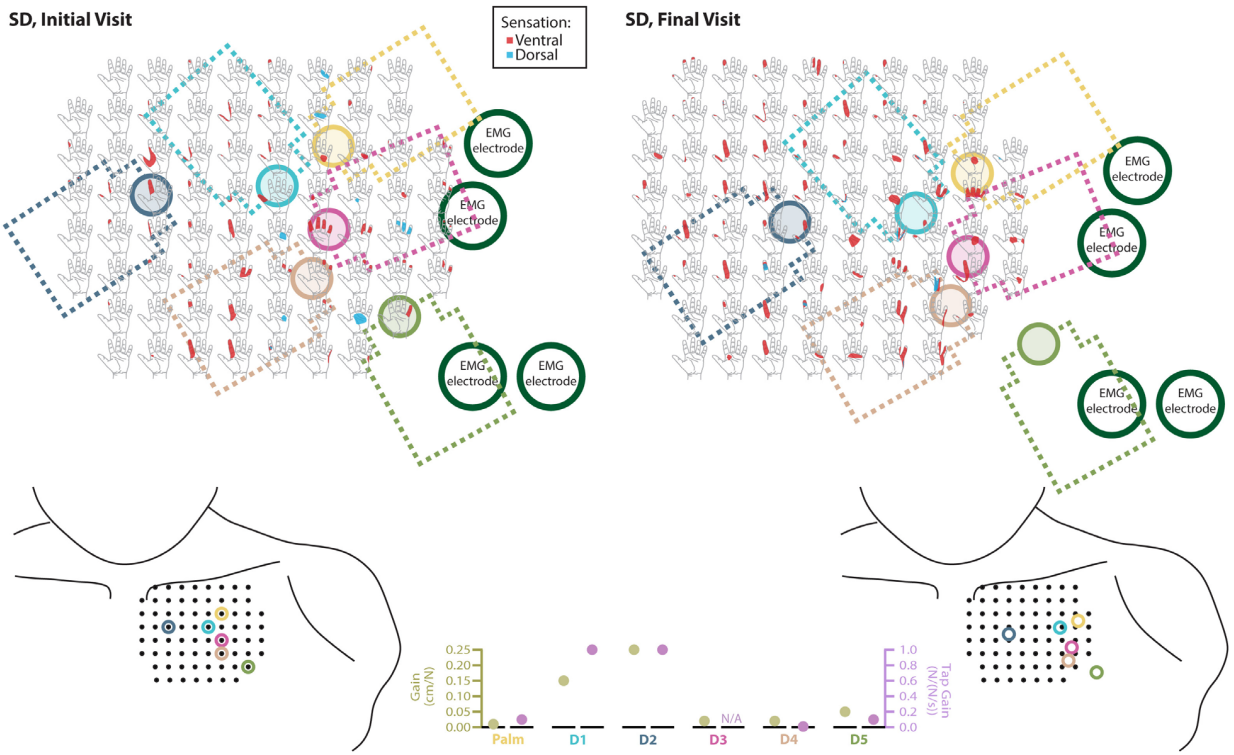

FIGURE 3 | Responses to touch mapping for the participant with a shoulder disarticulation (SD). The initial visit is shown on the left while the final visit is shown on the right. Sensations that were reported as projected to the ventral or dorsal side of the missing hand are shown in red and blue, respectively. The locations of the tactor heads that pushed on SD's skin are depicted as shaded circles and the tactor motor bodies are outlined with dotted lines; these correspond to sensors located on the prosthesis palm (yellow), thumb (D1, light blue) index finger (D2, medium blue), middle finger (D3, magenta), ring finger (D4, tan), and little finger (D5, light green). Locations of EMG electrodes near the reinnervated skin are portrayed as dark green circles. The line drawings below the maps for each visit depict the locations of the points mapped and the tactor heads (colored circles) on SD's upper chest. The proportional (gold markers) and tap (mauve markers) gains for each of the six tactors are shown in the panel in the bottom center.

They also both embodied their prostheses in the lagged condition (**Figure 8**). In the scrambled condition, SD embodied her prosthesis while TH approached embodiment. During the final visit, SD and TH both indicated embodiment for the touch-on condition but no longer embodied the lagged and scrambled touch conditions. CTRL did not indicate embodiment for any condition during the initial or final visit. All participants responded below the cutoff for agreement to the control questions, indicating that their embodiment scores were not due to participant suggestibility (**Supplementary Figure 1**).

Block-Foraging Stiffness Discrimination Task

Both during the initial and final visits, all participants demonstrated an increase in discrimination ability when given touch (**Figure 9**). SD demonstrated an improvement in accuracy that was statistically significant during the initial and final visits ($p < 0.00001$ and $p = 0.00022$, respectively). During TH's initial visit, providing touch sensation allowed her to achieve an accuracy score that was statistically different from chance, whereas without touch sensation she was unable to discriminate the blocks. This effect was not observed in the final visit. When using touch, SD and TH demonstrated decreases in false positive errors with increases in false negative errors, indicating that participants were more selective.

Both SD and TH showed significant changes in the time spent searching for blocks when touch was turned on ($p < 0.00001$), both during the initial and final visits (**Figure 9**). CTRL did not demonstrate any significant changes in search time behavior during either visit. During the initial visit, SD and TH showed significantly increased recognition time when touch was turned on ($p < 0.00001$). This may indicate that the participants slowed down to engage with the sensory feedback to help inform decisions. This effect was not present in CTRL. During the final visit, however, TH and CTRL showed significantly increased recognition time when touch was turned on ($p < 0.00001$ and $p = 0.00035$, respectively), whereas SD did not. During both initial and final visits, TH had recognition times that were not significantly different from zero when touch was turned off ($p = 0.75$ and $p = 0.89$, respectively), indicating that without touch feedback discrimination decisions were not attempted. No participant demonstrated any significant changes to handling time during either visit when touch was turned on. However, comparing initial visit to final, TH and CTRL demonstrated significantly faster handling times ($p < 0.00007$), whereas SD had

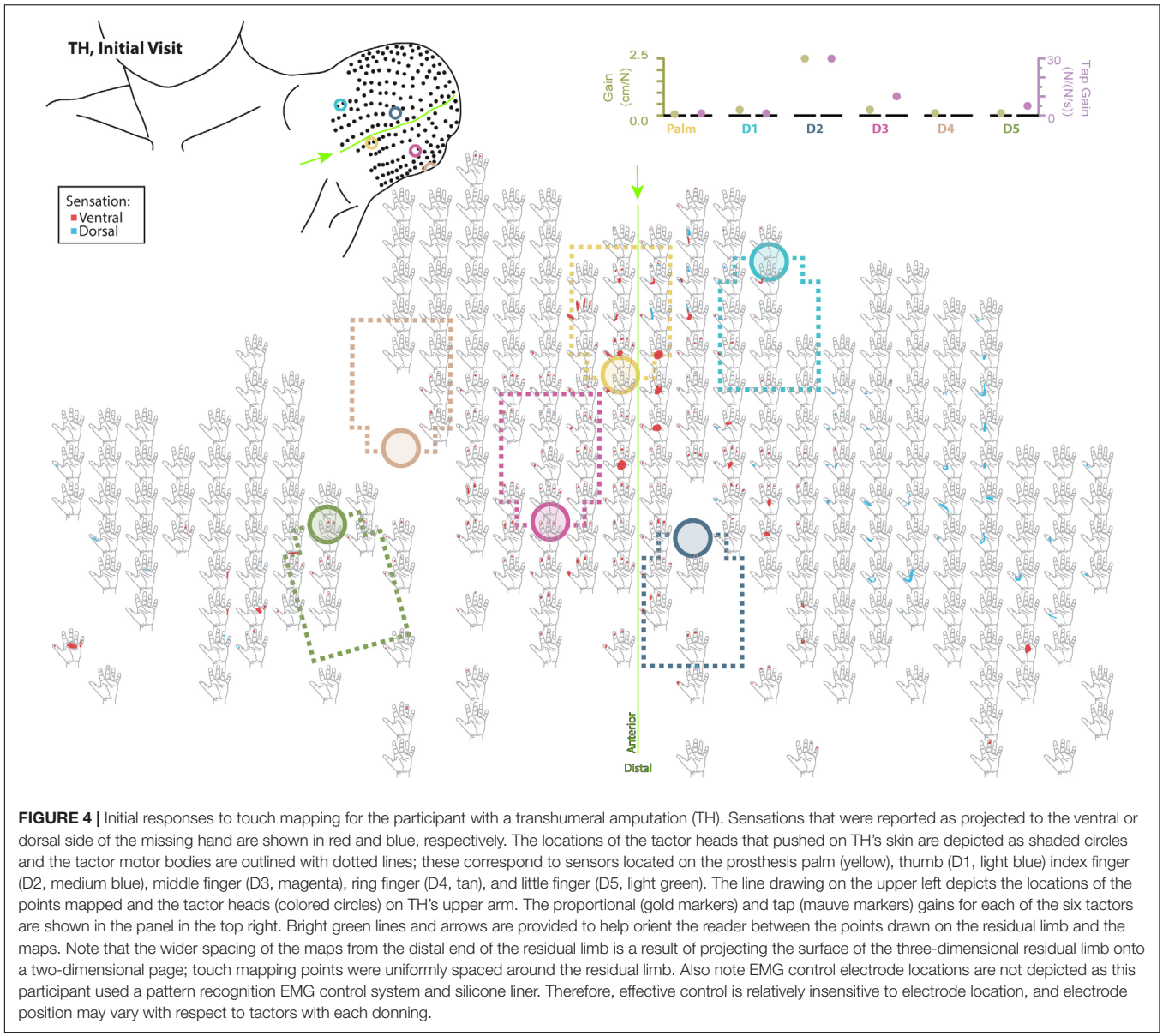

FIGURE 4 | Initial responses to touch mapping for the participant with a transhumeral amputation (TH). Sensations that were reported as projected to the ventral or dorsal side of the missing hand are shown in red and blue, respectively. The locations of the tactor heads that pushed on TH's skin are depicted as shaded circles and the tactor motor bodies are outlined with dotted lines; these correspond to sensors located on the prosthesis palm (yellow), thumb (D1, light blue) index finger (D2, medium blue), middle finger (D3, magenta), ring finger (D4, tan), and little finger (D5, light green). The line drawing on the upper left depicts the locations of the points mapped and the tactor heads (colored circles) on TH's upper arm. The proportional (gold markers) and tap (mauve markers) gains for each of the six tactors are shown in the panel in the top right. Bright green lines and arrows are provided to help orient the reader between the points drawn on the residual limb and the maps. Note that the wider spacing of the maps from the distal end of the residual limb is a result of projecting the surface of the three-dimensional residual limb onto a two-dimensional page; touch mapping points were uniformly spaced around the residual limb. Also note EMG control electrode locations are not depicted as this participant used a pattern recognition EMG control system and silicone liner. Therefore, effective control is relatively insensitive to electrode location, and electrode position may vary with respect to tactors with each donning.

significantly slower handling times ($p < 0.00001$). Efficiency and discrimination efficiency consistent with Beckler et al. (2019) are presented in **Supplementary Figure 2**.

Psychophysical Fitts' Law Grasp Force Task

For the initial visit, both SD and TH demonstrated tradeoffs in performance when given touch; SD achieved greater precision at the cost of speed, and TH showed increased speed and objects successfully handled at the cost of some precision (**Figure 10**). However, both participants successfully handled more objects with touch feedback. CTRL made an objective improvement when given touch, successfully handling objects with greater precision and faster speed. During the final visit, the benefits of touch were more pronounced, as both SD and CTRL improved in each of the three outcome measures. Additionally, providing touch allowed both participants to achieve a peak precision outside of the area in which, statistically, there was not reliable grasp production (i.e., force greater than zero). TH could only complete the task with touch during her final visit (zero successful objects without touch), thus touch provided a clear improvement. In all cases, providing touch improved at least two of the three outcome measures.

Box and Block Task

Participant Box and Block scores were insensitive to the touch conditions presented (**Figure 11**, top two rows). Additionally, the presence of the visual distractor had little effect on Box and Block scores (**Figure 11**). Gaze deviation away from the prosthetic hand generally increased when the visual distractor was present (**Figure 11**, bottom row); touch conditions had a

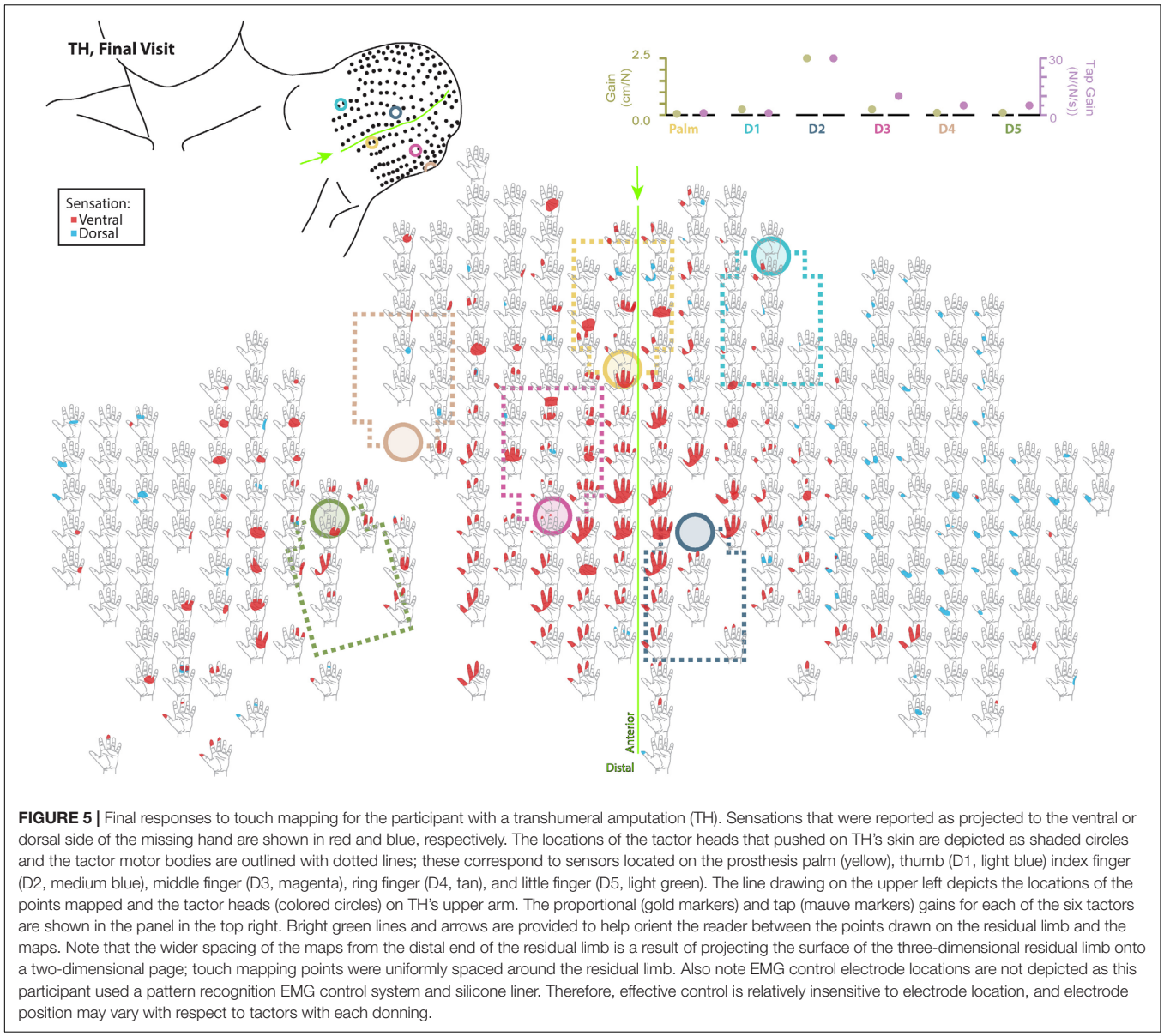

FIGURE 5 | Final responses to touch mapping for the participant with a transhumeral amputation (TH). Sensations that were reported as projected to the ventral or dorsal side of the missing hand are shown in red and blue, respectively. The locations of the tactor heads that pushed on TH's skin are depicted as shaded circles and the tactor motor bodies are outlined with dotted lines; these correspond to sensors located on the prosthesis palm (yellow), thumb (D1, light blue) index finger (D2, medium blue), middle finger (D3, magenta), ring finger (D4, tan), and little finger (D5, light green). The line drawing on the upper left depicts the locations of the points mapped and the tactor heads (colored circles) on TH's upper arm. The proportional (gold markers) and tap (mauve markers) gains for each of the six tactors are shown in the panel in the top right. Bright green lines and arrows are provided to help orient the reader between the points drawn on the residual limb and the maps. Note that the wider spacing of the maps from the distal end of the residual limb is a result of projecting the surface of the three-dimensional residual limb onto a two-dimensional page; touch mapping points were uniformly spaced around the residual limb. Also note EMG control electrode locations are not depicted as this participant used a pattern recognition EMG control system and silicone liner. Therefore, effective control is relatively insensitive to electrode location, and electrode position may vary with respect to tactors with each donning.

comparatively smaller effect on gaze deviation away from the prosthetic hand (**Figure 11**, bottom two rows). The most notable trend was that during the final visit, SD, and TH both looked at the prosthetic hand more during the touch-off condition (decreased gaze deviation), and were able to look away from the prosthetic hand more (increased gaze deviation) during the touch-on condition. Although gaze deviation was generally highest during the touch-on condition, gaze deviation tended to be greater when touch feedback was on, lagged, or scrambled than that in the touch-off condition.

Clothespin Relocation Task

Performance in the Clothespin Relocation task was also mostly insensitive to the touch condition. SD demonstrated slower task completion times for the scrambled touch condition, especially during the final visit, whereas task completion times for the other touch conditions were relatively consistent during both visits (**Figure 12**, top two rows). During the initial visit, TH demonstrated the fastest task completion times in the touch-on condition. This effect was not present in the final visit. Rather, completion times were consistent except for the scrambled condition, when participants showed faster completion times. The addition of a visual distractor did not cause systematic changes in completion time across touch conditions (**Figure 12**). There were no systematic trends in eye gaze deviation relative to touch condition (**Figure 12**, bottom two rows); furthermore, the addition of a visual distractor had little effect on eye gaze deviation (**Figure 12**, bottom two rows). Clothespin drops (**Supplementary Figure 3**) were relatively low across all participants, visits, and touch conditions, with one or zero drops during the majority of test conditions. No systematic trends between initial and final visits were identified.

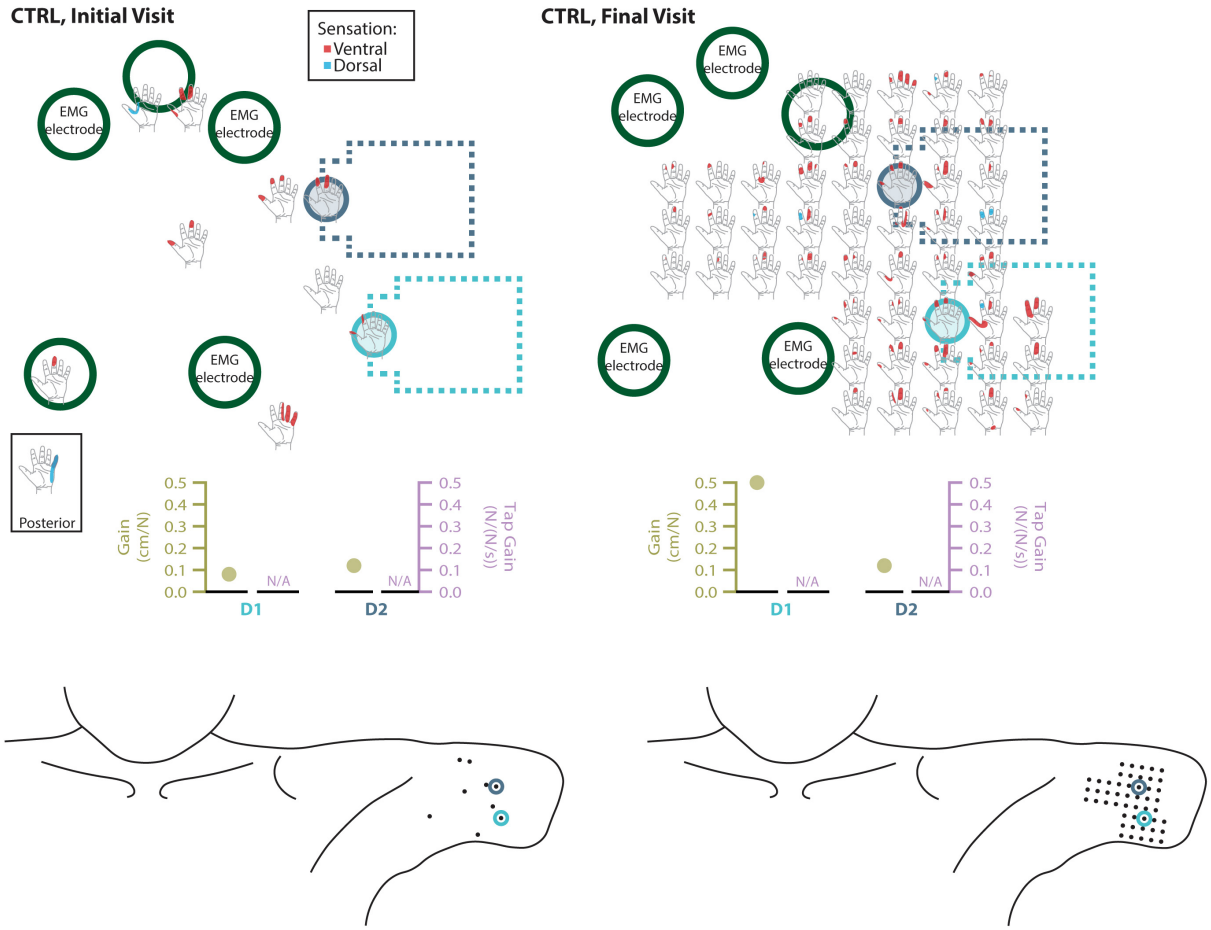

FIGURE 6 | Responses to touch mapping for the control participant (CTRL). The initial visit is shown on the left while the final visit is shown on the right. Sensations that were reported as projected to the ventral or dorsal side of the missing hand are shown in red and blue, respectively. The locations of the tactor heads that pushed on CTRL's skin are depicted as shaded circles and the tactor motor bodies are outlined with dotted lines; these correspond to sensors located on the prosthesis thumb (D1, light blue) and index finger (D2, medium blue). Locations of EMG electrodes near the reinnervated skin are portrayed as dark green circles. The line drawings below the maps for each visit depict the locations of the points mapped and the tactor heads (colored circles) on CTRL's upper arm. The proportional (gold markers) and tap (mauve markers) gains for each of the two tactors are shown below the maps. Note that one point was probed on the posterior side of the residual limb; the map showing the response for that point is shown in the box labeled 'Posterior.' Also note, while the number of tested points varied between initial and final mapping sessions, the points tested in the final mapping session were an expanded data set. This expansion captured the sensations reported over the same area of reinnervated skin but with greater resolution. Subsequent analyses based on data from these points (**Figure 2**) were designed to mathematically accommodate this methodological difference. All points tested are shown, regardless of whether or not the participant reported feeling sensation projected to their missing hand when touched at that location.

DISCUSSION

This work demonstrates that the relationship between users and sensate NMI prostheses is dynamic and changes over time with long-term use. Taken together, these results suggest that although the restoration of touch sensation can provide a near-immediate impact on operation of a prosthesis, long-term use may lead to further functional improvements, more appropriate integration of artificial limbs as a part of the body, and adaptation of higher-level neural-cortical systems.

Neural Adaptation

The touch mapping experiments support that neural and cortical adaptation processes occurred with the long-term use of NMI prostheses that provided physiologically relevant touch feedback. It appears that continual exposure to, and use of, this restored sense of touch allowed the sensory architecture of the missing hand to conform to this new sensory information. Following the take-home period, CTRL, an NMI-prosthesis user who did not take home a touch-integrated device, demonstrated no significant changes in the proportion of skin producing missing hand percepts. In contrast, we found that the proportion of reinnervated skin producing sensations projected to the missing hand increased significantly for both SD and TH. The areas of the missing hand whose proportional representation most increased were often the same areas targeted by the touch tactors (ventral side of the five digits and distal palm). Not only did the proportion increase, but participants also reported feeling

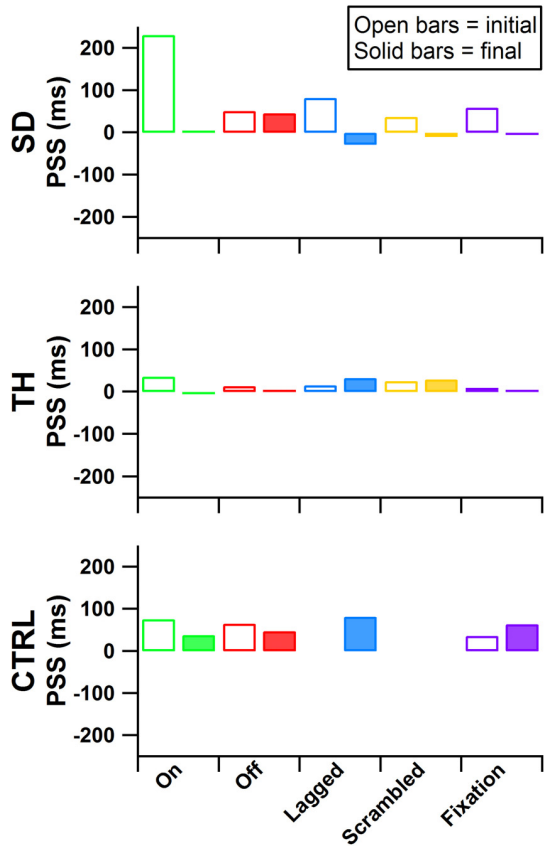

FIGURE 7 | Point of subjective simultaneity (PSS) is presented for the participant with a shoulder disarticulation (SD, top row), the participant with a transhumeral amputation (TH, center row), and the control participant (CTRL, bottom row) for their visits before (open bars) and after (filled bars) the take-home period. From left to right, participants' results from the touch-on (green), touch-off (red), lagged (blue), scrambled (yellow), and fixation (purple) conditions are shown. Values further from zero indicate greater asymmetry in the PSS between the intact and amputated sides.

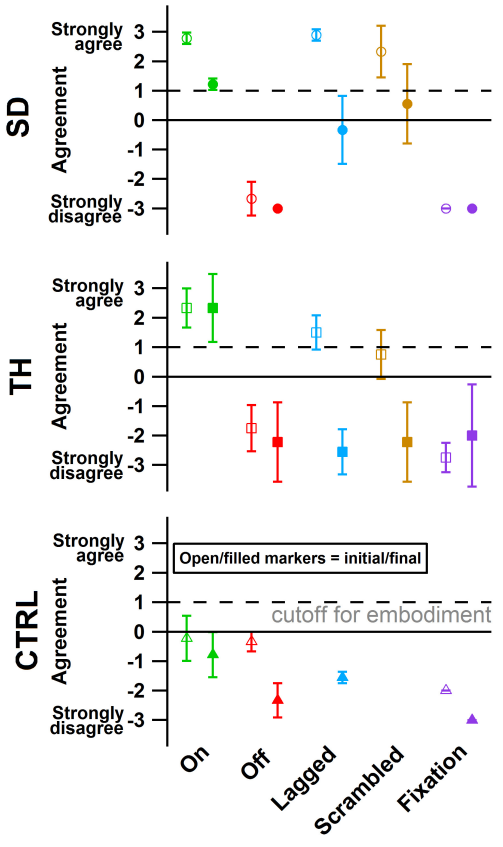

FIGURE 8 | The degree of agreement with questionnaire statements is shown for the participant with a shoulder disarticulation (SD, top row, circles), the participant with a transhumeral amputation (TH, center row, squares), and the control participant (CTRL, bottom row, triangles) in their visit before (open markers) and after (filled markers) the take-home period. Responses to control questions are provided in **Supplementary Figure 1**. All participants responded below the cutoff for agreement to the control questions. Markers are colored according to touch feedback condition: touch-on (green), touch-off (red), lagged (blue), scrambled (yellow), and fixation (purple). Participants were considered to have embodied their prosthesis if their agreement with embodiment questions was greater than or equal to one (Kalckert and Ehrsson, 2012), indicated by the dashed line.

larger areas within these missing hand regions. These areas were also spatially congruent with the instrumentation installed on their prostheses. Inconsistent or minimal increases were observed in the missing hand areas that were not directly targeted by participants' touch feedback systems. Across our participants, little to no growth was observed in the proximal palms (near the wrist) and minimal increases in proportion of projected sensation were observed in the dorsal side of the hands.

The implementation of sensory feedback within the constraints of a prosthetic fitting is complex. There are a number of functional constraints that must be considered. Foremost is the limited surface area available for both touch feedback tactors and EMG-control electrode placement. Here, a balance must be struck between the available touch percepts on the skin and the available motor control points in the reinnervated muscle. SD is an excellent example of this. We focused primarily on the touch feedback system targeting the most functionally relevant digits for the use of a three-jaw-chuck myoelectric terminal device (thumb and index finger). Multiple strong thumb and index finger touch percepts were available for SD, so we identified locations where reported sensation was most congruent to sensor locations on the prosthesis. We also set the pressure and tap settings (gains) for those two tactors to follow what the participant suggested 'felt most correct' (**Figure 3**). The remaining tactors were placed in areas that most closely approximated the palm and middle, ring, and little fingers. These positions were under more constraints with respect to placement on the remaining socket and skin areas. At these locations, the pressure and tap gains were set to provide reliable touch sensation to minimize the possibility of interference with the EMG control, either by electrical crosstalk or by displacing the skin that was in contact with the control electrodes.

We found changes in SD's final percept map that appeared to reflect both physical aspects of the prosthesis and the spatial accommodations made for the sensory feedback and control

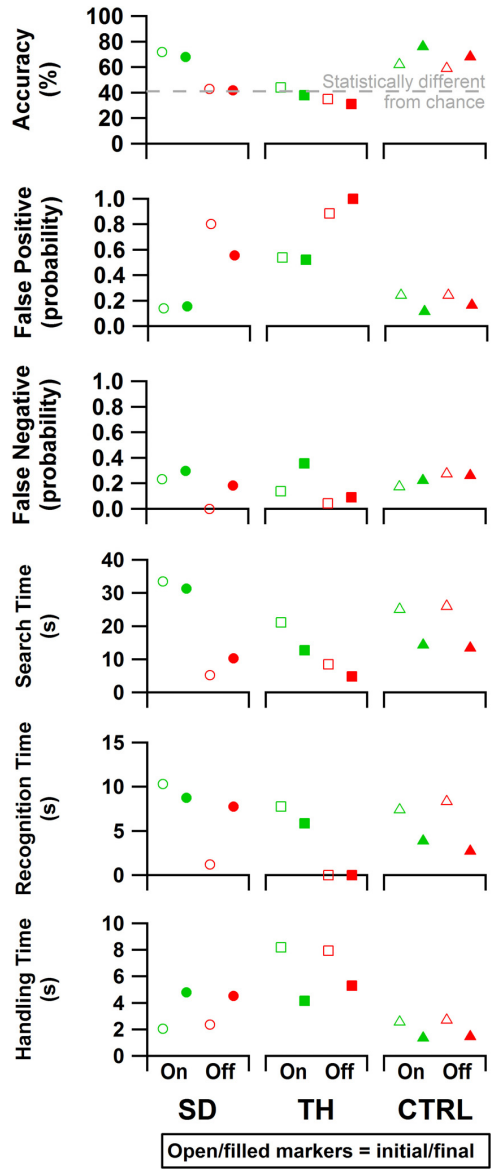

FIGURE 9 | From top to bottom: accuracy, false positive rate, false negative rate, search time, recognition time, and handling time data are presented. Results are shown for the participant with a shoulder disarticulation (SD, left column, circles), the participant with a transhumeral amputation (TH, center column, squares), and the control participant (CTRL, right column, triangles) in their visit before (open markers) and after (filled markers) the take-home period. Data are presented for the touch-on (green) and touch-off (red) conditions. The gray dashed line in the accuracy plot indicates the smallest statistically detectable change (41%) from chance accuracy (33%).

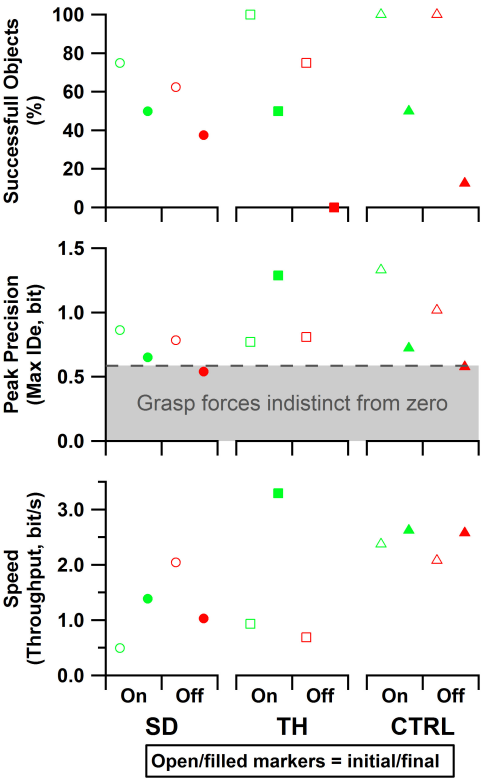

FIGURE 10 | Results are shown for the participant with a shoulder disarticulation (SD, left column, circles), the participant with a transhumeral amputation (TH, center column, squares), and the control participant (CTRL, right column, triangles) in their visit before (open markers) and after (filled markers) the take-home period. Data presented are from the touch-on (green) and touch-off (red) conditions. The dashed line and shading indicate the area in which, statistically, there was not reliable grasp production (i.e., force greater than zero). Note that since TH's initial visit did not include precision trials, the peak precision values for the initial visit may be slightly underestimated. Also note that since TH did not successfully handle any objects without touch feedback in the final visit, peak precision and throughput are undefined for that case.

systems. For example, we found that the thumb and index finger appeared to blend together. This may be an effect of the coupling between the main digits on three-jaw-chuck myoelectric hands, where digits 1–3 (thumb, index finger, and middle finger) always operate together. Moreover, the proportional and tap gains were higher, which made the thumb and index finger more sensitive. In the final hand map, we saw a focus on the thumb and index finger without the addition of the coupled middle finger. Similarly, the ring and little fingers also appeared to blend together in the final percept map. Both of these digits are passive in the myoelectric hand and are physically coupled together by an internal wire frame. In contrast, the separate palm tactor appeared to remain largely focused toward palm percepts. More broadly, we found an expansion of the thumb/index-finger and ring/little finger percepts across the final touch map. The thumb and index finger demonstrated the most expansion across the mapping space. Similarly, the ring-/little-finger representations also expanded; however, this effect was less pronounced than the thumb/index-finger changes. There is a possibility that the expansion was related to the roughly 1.5 cm lateral shifting of the tactor heads (**Figure 3**). This shifting was related to body shape changes experienced by SD over the duration of the take-home period. Although socket fit was impacted, the thumb- and index-finger-focused expansion also extended medially on the final

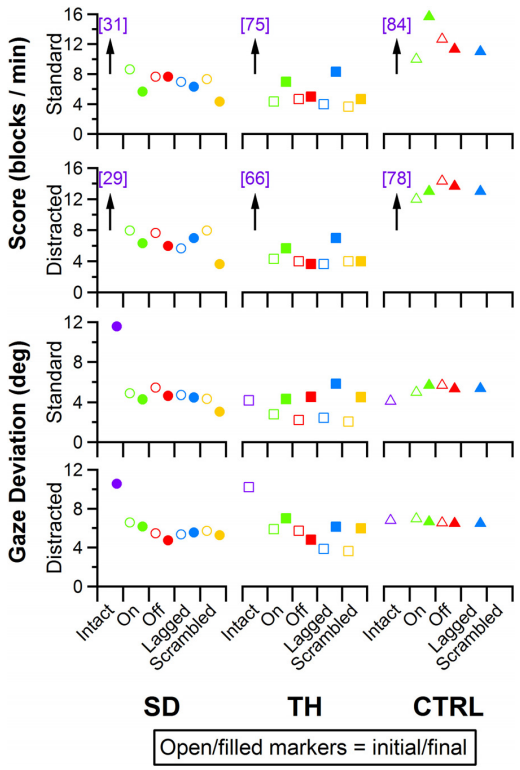

FIGURE 11 | Score and gaze deviation during the Box and Block task are presented in the top two and bottom two rows, respectively. In both pairs, the top row shows the results during the standard task while the bottom row shows the results during the trials when a visual distractor was present. Results are shown for the participant with a shoulder disarticulation (SD, left column, circles), the participant with a transhumeral amputation (TH, center column, squares), and the control participant (CTRL, right column, triangles) in their visit before (open markers) and after (filled markers) the take-home period. Participants' performance with their intact side are presented on the left (purple), followed by performance with the amputated side during the (from left to right) touch-on (green), touch-off (red), lagged (blue), and scrambled (yellow) conditions. Able-bodied scores that are outside of the *y*-axis range are shown in brackets.

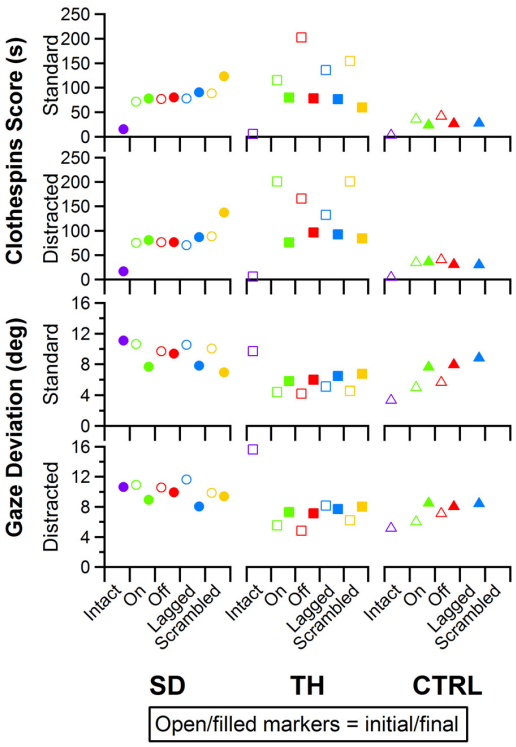

FIGURE 12 | Score and gaze deviation during the Clothespin Relocation task are presented in the top two and bottom two rows, respectively. In both pairs, the top row shows the results during the standard task while the bottom row shows the results during the trials when a visual distractor was present. Results are shown for the participant with a shoulder disarticulation (SD, left column, circles), the participant with a transhumeral amputation (TH, center column, squares), and the control participant (CTRL, right column, triangles) in their visit before (open markers) and after (filled markers) the take-home period. Participants' performance with their intact side are presented on the left (purple), followed by performance with the amputated side during the (from left to right) touch-on (green), touch-off (red), lagged (blue), and scrambled (yellow) conditions.

touch map and the relatively small position shift did not impact EMG function.

Although the changes in TH's final percept map were different than SD's, they appear to be driven by the sensory-motor constraints and accommodations unique to her prosthesis fitting. Unlike SD, whose socket rested against her chest and allowed tactors to press directly on the chest skin (see: **Figures 1**, **3**), TH used a silicone liner between the residual limb and the hard plastic socket where the tactors were mounted. In this setup the tactors could not touch the skin directly. They instead pressed into the reinnervated skin through the liner, which had thinned-out sections to improve sensation while maintaining traction and socket suspension on the residual limb. Furthermore, TH used a pattern recognition system for controlling her prosthesis, which is not sensitive to electrode positioning. In TH we saw a widespread increase in the strength of the touch percepts projected to the missing hand. We also saw an expansion of the percept areas that correspond to the digit and palm placement of the tactors. However, instead of focusing the percepts in the final touch map, we saw a fusing of multiple digits, similar to SD. Although this may have involved the coupling of the three-jaw-chuck myoelectric fingers, it is possible that other factors related to the prosthetic fitting also influenced the perceptual changes. Since TH's tactors had to press through a liner to reach the reinnervated skin, the tactor influence may not have been as locally focused as it was for SD. Instead, each time the tactor pushed in on a specific spot, the surrounding reinnervated skin may have experienced indirect stimulation. This may have activated other local touch percepts simultaneously. Also, from a practical perspective, since TH wore a socket liner, there may have been minor changes in position each time it was donned. Changes in position due to donning compounded with activation of adjacent percepts due to pushing through the liner likely account for the "smearing" of tactor-elicited sensations in TH's final touch map.

Although we cannot rule out that changes to the sensory reinnervation of the skin itself may have occurred due to repeated stimulation over the course of the take-home period, our data suggest that brain processing may be impacted by the long-term restoration of physiologically relevant touch. Psychophysical temporal order judgment tasks can be used to study the interplay between different senses, such as vision, hearing, and touch (Keetels and Vroomen, 2012). PSS is a time-based evaluation of perceptual shifts, derived from responses in a temporal order judgment task, that implicitly measures weighting given by the brain to different sensory information channels (Moseley et al., 2008). PSS occurs when two streams of sensory information are perceived as occurring at the same time. Therefore, when two sensory channels receive equal weighting they will yield a PSS of 0, while a larger magnitude correlates to greater differences in weightings (Vroomen et al., 2004). Similar to Marasco et al. (2011), we applied PSS measures to investigate the equivalency of sensory processing from the amputated side relative to the intact side, and how the brain may adapt its weightings with long-term restored touch sensation. We used an experimental paradigm that applied equivalent vibratory stimuli to non-reinnervated skin at mirrored positions on each participant's limbs to probe central tactile processing mechanisms. Before the take-home period, when two equivalent vibratory stimuli were provided at the exact same time, we found that all the participants were more likely to identify stimuli on the amputated side as occurring first. This suggests the brain weighted the sensory information from the amputated side asymmetrically from the intact side (regardless of the feedback condition: touch-off, touch-on, lagged, scrambled, or fixation). In contrast, following the take-home period, SD and TH demonstrated more symmetric PSS results regardless of feedback conditions. Before and after the take-home period CTRL remained largely unchanged. These findings support the idea that the brain changed its processing of sensory information and became more comparable to that of the intact side. Of particular relevance, in the touch-off and fixation conditions, the peripheral sensory receptors associated with the missing hand were not receiving any touch feedback stimulation; yet, PSS measures were more symmetric. The persistence of increased symmetry without touch feedback supports the idea that these changes were occurring above the peripheral neural level. Additionally, since results remained relatively consistent across feedback conditions within a test session, this symmetry may be a longer-term result of the brain adapting to the returned touch sensation of the amputated side rather than an immediate system response.

The sense of limb ownership arises from the integration of visual and tactile information; that is, when a stimulus is seen and felt appropriately (temporally and spatially congruent), the brain assumes ownership over that part of the body (Botvinick and Cohen, 1998). In the initial embodiment experiments, SD and TH demonstrated a tendency to embody their prostheses under conditions where touch was either temporally (lagged) or spatially (scrambled) mismatched in addition to the normal temporally and spatially appropriate (touch-on) condition (**Figure 8**). After the take-home period, this tendency was abolished – SD and TH only showed embodiment during the touch-on condition, where all multisensory temporal and spatial inputs were appropriately aligned. The initial tendency of the participants to take ownership of the prosthesis in conditions with mismatched touch indicates abnormal brain processing that is overly permissive when establishing body ownership. This permissiveness in ownership can also be seen in individuals who inappropriately experience the pain of others as their own, or experience touch when they see others being touched (Aimola Davies and White, 2013; Botan et al., 2018). This condition arises when the brain incorrectly assumes ownership of external features due to simple correlations of multisensory information, despite the temporal and/or spatial relationships between sensory channels being inappropriate. Similar to these populations, SD and TH also integrated inappropriate yet correlated information to establish embodiment during their initial visits. In the lagged condition, participants received touch input from the tactors 1000 ms after seeing the actual touch by the investigator on the prosthesis. Although the timing between what was seen and what was felt was shifted, the two sensory events were still correlated. Similarly, in the scrambled condition, the touch tactors were connected to mismatched sites on the reinnervated skin (e.g., when the investigator touched the thumb of the prosthesis, the participant felt touch on a different digit). Although touch on the prosthesis was spatially mismatched with touch felt on the missing hand, the timing was correlated. The prolonged return of sensation matched to relevant prosthesis activity during the take-home period appears to have provided the contextual cues necessary for restoring these individuals to a more normal mode of multisensory processing (Heed and Azañón, 2014). Interestingly, previous work with one of the participants shows that their prosthetic limb was not embodied when there was a complete lack of temporal correlation between touch and vision when touches experienced by the participant through the touch tactor system were randomly associated with observed touches to the prosthetic hand (Marasco et al., 2011). Furthermore there appears to be a limit to the cortical-representational distance that can lead to permissiveness in body attribution. In the earlier study discussed above, there was a similar temporal correlation between mismatched spatial locations, yet the participant did not embody the prosthesis when touch seen on the prosthesis forearm was felt on the missing hand (Marasco et al., 2011), which was representationally located much farther away than the mismatched locations in the study reported here. In the present study, during the initial visits, the incorrectly correlated input from different digits in the scrambled condition promoted overly permissive embodiment. Long-term use of a touch-integrated prosthesis likely helped build a stronger perceptual representation of the fingers, which contributed to a less permissive yet more normal mode of limb ownership.

Participants performed this study using a single-degree-of-freedom prosthetic hand that provided a three-jaw-chuck grasp configuration. However, there are numerous dexterous prostheses available that can perform multiple hand grasping configurations. With these devices, not all digits are involved in each possible grasp configuration and each configuration is visually distinguishable from the next. Therefore, in more dexterous systems, the impact of spatial congruency in what

is seen and felt is likely to be even more important than with a single-degree-of-freedom hand. As prostheses become increasingly sophisticated, the quality and congruency of sensory feedback will progressively become more important to integrating these systems as a true limb replacement.

Functional Changes

Our block-foraging and psychophysical grasp tasks are standardized, scientifically validated tests that, when applied to upper-limb prosthesis use, can parse out the contributions of control and sensory feedback in relation to successful task completion (Thumser et al., 2018; Beckler et al., 2019). We found that across all three participants, there appeared to be an immediate improvement in functional performance when touch was turned on. Interestingly, SD's and TH's functional performance following the take-home period remained near the initial levels and did not improve substantially over that.

Our block-foraging task examines sensory discrimination and evaluates how sensation influences discrimination strategies and decision-making. Across all participants both before and after the take-home period, when provided with touch feedback, trials took longer. This test isolates cutaneous force as the primary sensory channel informing participant decision-making. When no touch feedback is present, prosthesis control is open-loop and participants have no sensory information outside of vision on which to base decisions. However, when touch is turned on, participants slow down as they engage with the sensory information to make more careful, informed decisions when searching for blocks of a target stiffness. The addition of this sensory channel improved the accuracy of selecting a correct target block; however, the likelihood of interrogating a correct block but not selecting it also increased (false negative rates). With touch feedback, participants were willing to interrogate more blocks and improve accuracy at the cost of speed. Handling time is a measure of one's ability to pilot the prosthesis, and it generally did not change in relation to touch feedback. This suggests that the changes in search time were primarily due to interaction with sensory feedback. Following the take-home period, the initial improvements in accuracy with touch feedback remained. These results provide evidence that the cutaneous force information provided through the NMI is readily used by the brain with little learning required.

Our psychophysical grasp task is designed to evaluate how quickly and precisely individuals can reach their intended grasping force. Similar to results found with our block-foraging task, turning on the touch feedback system resulted in immediate changes in task performance across all three participants. Touch enabled all participants to more reliably achieve intermediate grasp forces. However, in their initial visits, both SD and TH had to make compromises, either improving grasp force precision at the cost of speed (SD) or improving speed at the cost of precision (TH), whereas CTRL improved both speed and precision. In contrast, following the take-home period, both SD and TH were able to use the sensation of touch to improve both speed and precision. Similar to conclusions drawn from the block-foraging task results, it appears that initially the sensory information provided through the NMI was readily interpreted by the brain, and the use of the touch system during the take-home period provided the brain with additional context for the sensory information. This appears to have helped the users integrate their restored sense of touch into their prosthesis control strategies. For example, TH was unable to complete the psychophysical grasp task without touch in her final visit, indicating that touch feedback had become an essential part of her control strategy and without it, achieving intermediate grasping forces was extremely difficult. These results suggest that long-term use of NMI touch feedback can promote more effective closed-loop control that enables users to more quickly and precisely achieve intended grasping forces.

We observed significant changes in function, as well as cognition and perception, in response to touch sensation across multiple measures; however, these changes were not represented in the Box and Block or Clothespin Relocation tasks. We attempted to capture changes caused by touch feedback by adding eye gaze tracking and trials with a distractor video to the Box and Block and Clothespin Relocation tasks. Our intent was to use the eye gaze data as a proxy to capture visual attention during the task. We found that for the Box and Block task the participants demonstrated slightly more gaze deviation in the touch-on condition. However, this result did not translate to the Clothespin Relocation task. Relocating a clothespin requires a higher amount of visual attention to pinch, rotate, transfer, and release an object in a precise location. Here, there is little opportunity for gaze deviation from the hand, which is reflected in the results. Eye tracking data may provide complementary information to quantify the attention and visual demand when operating a sensate prosthesis; however, tasks must be carefully designed to permit looking away from the prosthesis and/or require decisions based on sensory feedback to reflect the true impact of this sensation.

Integrating a prosthesis as a functional body part is a complex challenge. Although sensation fundamentally underpins body perception and limb function, its contributions are difficult to quantify as its influence is multifaceted and dependent on many factors (Markovic et al., 2018). For example, we found minimal performance difference with and without touch sensation in the standard clinical measures of Box and Block and Clothespin Relocation tasks. We argue that these tasks did not sufficiently challenge users to engage with touch sensation to shape task behaviors. Rather, visual cues and motor control drove task performance. The block-foraging and psychophysical grasp tasks were specifically designed to require that participants engage with touch feedback (Thumser et al., 2018; Beckler et al., 2019). In these tasks, participants displayed a near-immediate improvement in performance when touch sensation was provided; however, no additional improvements were seen after the take-home period. This lack of additional long-term improvement may be attributed to the touch feedback system utilizing the residual neural anatomy associated with the now-missing hand. Following amputation, the brain retains a representation of the missing hand and is likely able to readily use sensations generated through this residual architecture with minimal learning. This is because the restored touch information is felt as an equivalent touch in the missing hand. In the same

way that we would anticipate minimal performance changes if a healthy, intact hand were tested before and after a 2-year span, our participant cohort performed similarly on functional tasks over a comparable time span. It was only through the employed cognitive and perceptual measures that the long-term effects of restored touch became evident. Here, we employed multiple measures to better understand the relationship between the newly restored sense of touch and higher-level sensory processing. Across multiple independent measures, we found evidence to suggest neural-cognitive adaptation processes occur with the long-term use of NMI prostheses. Therefore, we argue that evaluation of sensate prostheses must extend beyond functional tasks and performance measures to further capture the integration of the system as a part of the body. Quantifying this process is complex and requires multiple independent measures to capture changes in functional abilities, the user's explicit perceptions that the device is a body part, and the implicit processes in which sensory-motor mechanisms adapt and are learned.

CONCLUSION

Restoring touch sensation through NMI prostheses brings us one step closer to true limb replacement. However, achieving this goal will require a paradigm shift in the way we study and evaluate advanced robotic limbs. Rather than viewing prostheses as tools used to improve function, we must begin evaluating these devices as integrated body parts. Future investigations following the development and growth of this dynamic relationship over the long term are important next steps in this exciting process of unlocking the next generation of integrated artificial limbs.

DATA AVAILABILITY STATEMENT

The data sets generated for this study are available upon reasonable request to the corresponding author.

ETHICS STATEMENT

The studies involving human participants were reviewed and approved by the Cleveland Clinic Institutional Review Board and the Department of the Navy Human Research Protection Program. The patients/participants provided their written informed consent to participate in this study. Written informed consent was obtained from the individual(s) for the publication of any potentially identifiable images or data included in this article.

AUTHOR CONTRIBUTIONS

All authors contributed to the manuscript preparation. PM, ZT, and DB contributed to the experimental design and development, and fabrication of the experimental prostheses. ZT, DB, CS, and JS performed the experimental data collection and data analysis. PM and CS coordinated with participants. PM was the principal investigator, provided scientific direction, and performed overall project coordination. ZT, CS, and DB performed technical support for participants during the take-home period.

FUNDING

This project was developed with funding through Defense Advanced Research Projects Agency (DARPA) contract numbers #61732-LS-DRP: P-1108-114403/DARPA-BAA-11-08 Reliable Peripheral Interfaces (RPI) under the auspices of Dr. Jack Judy and N66001-15-C-4015 under the auspices of Drs. Doug Weber and Al Emondi. JS received support through the Canadian Institutes of Health Research Fellowship Program.

SUPPLEMENTARY MATERIAL

The Supplementary Material for this article can be found online at: https://www.frontiersin.org/articles/10.3389/fnins.2020.00120/full#supplementary-material

REFERENCES

Aimola Davies, A. M., and White, R. C. (2013). A sensational illusion: vision-touch synaesthesia and the rubber hand paradigm. *Cortex* 49, 806–818. doi: 10.1016/j.cortex.2012.01.007

Antfolk, C., D'Alonzo, M., Controzzi, M., Lundborg, G., Rosen, B., Sebelius, F., et al. (2013). Artificial redirection of sensation from prosthetic fingers to the phantom hand map on transradial amputees: vibrotactile versus mechanotactile sensory feedback. *IEEE Trans. Neural Syst. Rehabil. Eng.* 21, 112–120. doi: 10.1109/TNSRE.2012.2217989

Beckler, D. T., Thumser, Z. C., Schofield, J. S., and Marasco, P. D. (2019). Using sensory discrimination in a foraging-style task to evaluate human upper-limb sensorimotor performance. *Sci. Rep.* 9, :5806. doi: 10.1038/s41598-019-42086-0

Belter, J. T., Segil, J. L., Dollar, A. M., and Weir, R. F. (2013). Mechanical design and performance specifications of anthropomorphic prosthetic hands: a review. *J. Rehabil. Res. Dev.* 50, 599–618. doi: 10.1682/JRRD.2011.10.0188

Boccia, M., Di Vita, A., Palermo, L., Nemmi, F., Traballesi, M., Brunelli, S., et al. (2019). Neural modifications in lower limb amputation: an fMRI study on action and non-action oriented body representations. *Brain Imaging Behav.* 1–10. doi: 10.1007/s11682-019-00142-3 [Epub ahead of print].

Botan, V., Fan, S., Critchley, H., and Ward, J. (2018). Atypical susceptibility to the rubber hand illusion linked to sensory-localised vicarious pain perception. *Conscious. Cogn.* 60, 62–71. doi: 10.1016/j.concog.2018.02.010

Botvinick, M., and Cohen, J. (1998). Rubber hands "feel" touch that eyes see. *Nature* 391, :756. doi: 10.1038/35784

Christie, B. P., Freeberg, M., Memberg, W. D., Pinault, G. J. C., Hoyen, H. A., Tyler, D. J., et al. (2017). Long-term stability of stimulating spiral nerve cuff electrodes on human peripheral nerves. *J. Neuroeng. Rehabil.* 14, 1–13. doi: 10.1186/s12984-017-0285-3

Cipriani, C., Segil, J. L., Clemente, F., Richard, R. F., and Edin, B. (2014). Humans can integrate feedback of discrete events in their sensorimotor control of a robotic hand. *Exp. Brain Res.* 232, 3421–3429. doi: 10.1007/s00221-014-4024-8

Cohen, L. G., Bandinelli, S., Findley, T. W., and Hallett, M. (1991). Motor reorganization after upper limb amputation in man: a study with focal magnetic stimulation. *Brain* 114, 615–627. doi: 10.1093/brain/114.1.615

De Nunzio, A. M., Dosen, S., Lemling, S., Markovic, M., Schweisfurth, M. A., Ge, N., et al. (2017). Tactile feedback is an effective instrument for the training of

grasping with a prosthesis at low- and medium-force levels. *Exp. Brain Res.* 235, 2547–2559. doi: 10.1007/s00221-017-4991-7

Downey, J. E., Weiss, J. M., Flesher, S. N., Thumser, Z. C., Marasco, P. D., Boninger, M. L., et al. (2018). Implicit grasp force representation in human motor cortical recordings. *Front. Neurosci.* 12:801. doi: 10.3389/fnins.2018.00801

Dumanian, G. A., Ko, J. H., O'Shaughnessy, K. D., Kim, P. S., Wilson, C. J., and Kuiken, T. A. (2009). Targeted reinnervation for transhumeral amputees: current surgical technique and update on results. *Plast. Reconstr. Surg.* 124, 863–869. doi: 10.1097/PRS.0b013e3181b038c9

Flor, H., Elbert, T., Knecht, S., Wienbruch, C., Pantev, C., Birbaumer, N., et al. (1995). Phantom-limb pain as a perceptual correlate of cortical reorganization following arm amputation. *Nature* 375, 482–484. doi: 10.1038/375482a0

Gonzalez, J., Soma, H., Sekine, M., and Yu, W. (2012). Psycho-physiological assessment of a prosthetic hand sensory feedback system based on an auditory display: a preliminary study. *J. Neuroeng. Rehabil.* 9, :33. doi: 10.1186/1743-0003-9-33

Hasson, C. J., and Manczurowsky, J. (2015). Effects of kinematic vibrotactile feedback on learning to control a virtual prosthetic arm. *J. Neuroeng. Rehabil.* 12, :31. doi: 10.1186/s12984-015-0025-5

Hebert, J. S., Chan, K. M., and Dawson, M. R. (2016). Cutaneous sensory outcomes from three transhumeral targeted reinnervation cases. *Prosthet. Orthot. Int.* 40, 303–310. doi: 10.1177/0309364616633919

Hebert, J. S., Olson, J. L., Morhart, M. J., Dawson, M. R., Marasco, P. D., Kuiken, T. A., et al. (2014). Novel targeted sensory reinnervation technique to restore functional hand sensation after transhumeral amputation. *IEEE Trans. Neural Syst. Rehabil. Eng.* 22, 765–773. doi: 10.1109/TNSRE.2013.2294907

Heed, T., and Azañón, E. (2014). Using time to investigate space: a review of tactile temporal order judgments as a window onto spatial processing in touch. *Front. Psychol.* 5:76. doi: 10.3389/fpsyg.2014.00076

Hiremath, S. V., Tyler-Kabara, E. C., Wheeler, J. J., Moran, D. W., Gaunt, R. A., Collinger, J. L., et al. (2017). Human perception of electrical stimulation on the surface of somatosensory cortex. *PLoS One* 12:e0176020. doi: 10.1371/journal.pone.0176020

Johansson, R. S. (1996). "Sensory and memory information in the control of dexterous manipulation," in *Neural Bases of Motor Behaviour*, eds F. Lacquaniti, and P. Viviani (Dordrecht: Springer), 205–260. doi: 10.1007/978-94-017-2403-6_10

Kalckert, A., and Ehrsson, H. H. (2012). Moving a rubber hand that feels like your own: a dissociation of ownership and agency. *Front. Hum. Neurosci.* 6:40. doi: 10.3389/fnhum.2012.00040

Keetels, M., and Vroomen, J. (2012). "Perception of synchrony between the senses," in *The Neural Bases of Multisensory Processes*, eds M. M. Murray, and M. T. Wallace (Boca Raton, FL: CRC Press).

Kim, K., Colgate, J. E., Santos-Munne, J. J., Makhlin, A., and Peshkin, M. A. (2010). On the design of miniature haptic devices for upper extremity prosthetics. *IEEE ASME Trans. Mechatron.* 15, 27–39. doi: 10.1109/TMECH.2009.2013944

Kuiken, T. A., Dumanian, G. A., Lipschutz, R. D., Miller, L. A., and Stubblefield, K. A. (2004). The use of targeted muscle reinnervation for improved myoelectric prosthesis control in a bilateral shoulder disarticulation amputee. *Prosthet. Orthot. Int.* 28, 245–253. doi: 10.3109/03093640409167756

Kuiken, T. A., Marasco, P. D., Lock, B. A., Harden, R. N., and Dewald, J. P. A. (2007a). Redirection of cutaneous sensation from the hand to the chest skin of human amputees with targeted reinnervation. *Proc. Natl. Acad. Sci. U. S. A.* 104, 20061–20066. doi: 10.1073/pnas.0706525104

Kuiken, T. A., Miller, L. A., Lipschutz, R. D., Stubblefield, K., Marasco, P. D., Zhou, P., et al. (2007b). Targeted reinnervation for enhanced prosthetic arm function in a woman with a proximal amputation: a case study. *Lancet* 369, 371–380. doi: 10.1016/S0140-6736(07)60193-7

Lotze, M., Grodd, W., Birbaumer, N., Erb, M., Huse, E., and Flor, H. (1999). Does use of a myoelectric prosthesis prevent cortical reorganization and phantom limb pain? *Nat. Neurosci.* 2, 501–502. doi: 10.1038/9145

Makin, T. R., Scholz, J., Filippini, N., Henderson Slater, D., Tracey, I., and Johansen-Berg, H. (2013). Phantom pain is associated with preserved structure and function in the former hand area. *Nat. Commun.* 4, 1570–1578. doi: 10.1038/ncomms2571

Marasco, P. D., Hebert, J. S., Sensinger, J. W., Shell, C. E., Schofield, J. S., Thumser, Z. C., et al. (2018). Illusory movement perception improves motor control for prosthetic hands. *Sci. Transl. Med.* 10, :eaao6990. doi: 10.1126/scitranslmed.aao6990

Marasco, P. D., Kim, K., Colgate, J. E., Peshkin, M. A., and Kuiken, T. A. (2011). Robotic touch shifts perception of embodiment to a prosthesis in targeted reinnervation amputees. *Brain* 134, 747–758. doi: 10.1093/brain/awq361

Markovic, M., Schweisfurth, M. A., Engels, L. F., Bentz, T., Wüstefeld, D., Farina, D., et al. (2018). The clinical relevance of advanced artificial feedback in the control of a multi-functional myoelectric prosthesis. *J. Neuroeng. Rehabil.* 15, :28. doi: 10.1186/s12984-018-0371-1

Mathiowetz, V., Volland, G., Kashman, N., and Weber, K. (1985). Adult norms for the box and block test of manual dexterity. *Am. J. Occup. Ther.* 39, 386–391. doi: 10.5014/ajot.39.6.386

Miller, L. A., Lipschutz, R. D., Stubblefield, K. A., Lock, B. A., Huang, H., Williams, T. W., et al. (2008). Control of a six degree of freedom prosthetic arm after targeted muscle reinnervation surgery. *Arch. Phys. Med. Rehabil.* 89, 2057–2065. doi: 10.1016/j.apmr.2008.05.016

Moseley, G. L., Olthof, N., Venema, A., Don, S., Wijers, M., Gallace, A., et al. (2008). Psychologically induced cooling of a specific body part caused by the illusory ownership of an artificial counterpart. *Proc. Natl. Acad. Sci. U.S.A.* 105, 13169–13173. doi: 10.1073/pnas.0803768105

Paredes, L. P., Dosen, S., Rattay, F., Graimann, B., and Farina, D. (2015). The impact of the stimulation frequency on closed-loop control with electrotactile feedback. *J. Neuroeng. Rehabil.* 12, :35. doi: 10.1186/s12984-015-0022-8

Rombokas, E., Stepp, C. E., Chang, C., Malhotra, M., and Matsuoka, Y. (2013). Vibrotactile sensory substitution for electromyographic control of object manipulation. *IEEE Trans. Biomed. Eng.* 60, 2226–2232. doi: 10.1109/TBME.2013.2252174

Rybarczyk, B., and Behel, J. (2008). "Limb loss and body image," in *Psychoprosthetics*, eds P. Gallagher, D. Desmond, and M. MacLachlan (London: Springer), 23–31. doi: 10.1007/978-1-84628-980-4_3

Schofield, J. S., Evans, K. R., Carey, J. P., and Hebert, J. S. (2014). Applications of sensory feedback in motorized upper extremity prosthesis: a review. *Expert Rev. Med. Devices* 11, 499–511. doi: 10.1586/17434440.2014.929496

Serino, A., Akselrod, M., Salomon, R., Martuzzi, R., Blefari, M. L., Canzoneri, E., et al. (2017). Upper limb cortical maps in amputees with targeted muscle and sensory reinnervation. *Brain* 140, 2993–3011. doi: 10.1093/brain/awx242

Sharma, A., Torres-Moreno, R., Zabjek, K., and Andrysek, J. (2014). Toward an artificial sensory feedback system for prosthetic mobility rehabilitation: examination of sensorimotor responses. *J. Rehabil. Res. Dev.* 51, 907–918. doi: 10.1682/JRRD.2013.07.0164

Siehlow, K. (1951). The Vadux arm, a phantom-controlled electric prosthesis. *Zentralbl. Chir.* 76, 1128–1135.

Tabot, G. A., Dammann, J. F., Berg, J. A., Tenore, F. V., Boback, J. L., Vogelstein, R. J., et al. (2013). Restoring the sense of touch with a prosthetic hand through a brain interface. *Proc. Natl. Acad. Sci. U.S.A.* 110, 18279–18284. doi: 10.1073/pnas.1221113110

Thumser, Z. C., Slifkin, A. B., Beckler, D. T., and Marasco, P. D. (2018). Fitts' law in the control of isometric grip force with naturalistic targets. *Front. Psychol.* 9:560. doi: 10.3389/fpsyg.2018.00560

Vroomen, J., Keetels, M., De Gelder, B., and Bertelson, P. (2004). Recalibration of temporal order perception by exposure to audio-visual asynchrony. *Cogn. Brain Res.* 22, 32–35. doi: 10.1016/j.cogbrainres.2004.07.003

Witteveen, H. J. B., Luft, F., Rietman, J. S., and Veltink, P. H. (2014). Stiffness feedback for myoelectric forearm prostheses using vibrotactile stimulation. *IEEE Trans. Neural Syst. Rehabil. Eng.* 22, 53–61. doi: 10.1109/TNSRE.2013.2267394

Conflict of Interest: The authors declare that the research was conducted in the absence of any commercial or financial relationships that could be construed as a potential conflict of interest.

frontiers in Neuroscience

TECHNOLOGY AND CODE
published: 19 February 2020
doi: 10.3389/fnins.2020.00117

Wireless Electrical Stimulators and Sensors Network for Closed Loop Control in Rehabilitation

David Andreu[1], Benoît Sijobert[1], Mickael Toussaint[1,2], Charles Fattal[3], Christine Azevedo-Coste[1] and David Guiraud[1]**

[1] CAMIN, INRIA, University of Montpellier, CNRS, Montpellier, France, [2] Vivaltis, Montpellier, France, [3] CRF La Châtaigneraie, Menucourt, France

This paper presents a wireless distributed Functional Electrical Stimulation (FES) architecture. It is based on a set of, potentially heterogeneous, distributed stimulation and measurement units managed by a wearable controller. Through a proof-of-concept application, the characterization of the wireless network performances was assessed to check the adequacy of this solution with open-loop and closed-loop control requirements. We show the guaranteed time performances over the network through the control of quadriceps and hamstrings stimulation parameters based on the monitoring of the knee joint angle. Our solution intends to be a tool for researchers and therapists to develop closed-loop control algorithms and strategies for rehabilitation, allowing the design of wearable systems for a daily use context.

Keywords: functional electrical stimulation, neuroprosthesis, sensory-motor deficiencies, motor rehabilitation, wireless FES architecture

OPEN ACCESS

Edited by:
Max Ortiz-Catalan, Chalmers University of Technology, Sweden

Reviewed by:
Kevin Lloyd Kilgore, MetroHealth, United States
Jit Muthuswamy, Arizona State University, United States

****Correspondence:***
Christine Azevedo-Coste
Christine.Azevedo@inria.fr
David Guiraud
David.Guiraud@inria.fr

Specialty section:
This article was submitted to Neural Technology, a section of the journal Frontiers in Neuroscience

Received: *09 September 2019*
Accepted: *29 January 2020*
Published: *19 February 2020*

Citation:
Andreu D, Sijobert B, Toussaint M, Fattal C, Azevedo-Coste C and Guiraud D (2020) Wireless Electrical Stimulators and Sensors Network for Closed Loop Control in Rehabilitation. Front. Neurosci. 14:117. doi: 10.3389/fnins.2020.00117

1. INTRODUCTION

Electrical Stimulation (ES) induces Action Potentials (AP) by depolarizing the membrane of the targeted cells in particular axons or muscle fibers at the motor point. Since the 1950's, ES has been successfully used in a growing set of applications linked to motor and sensory impairments. Attempts to use ES have been made in movement rehabilitation, such as drop foot syndrome correction for post-stroke hemiplegic patients (Liberson et al., 1961) and more complex movements or functions for patients with a spinal cord injury (Kralj and Bajd, 1989; Davis et al., 1997; Kobetic et al., 1997, 1999; Rijkhoff, 2004; Guiraud et al., 2006a,b). In Smith et al. (1998), the functional results are substantial including, for instance, recovery of the grasp function for quadriplegic patients, who might then be able to grab and hold objects, eat, and even, in the best cases, write with a pen. Although not optimal, Functional ES (FES) systems remain the only way to date to restore paralyzed muscle's contraction so they are valuable tools for acute clinical rehabilitation. Besides, recently, researches for movement restoration through muscle's activation of the lower limb in particular, regained interest through new surgical approaches and stimulation targets (Possover et al., 2010; Harkema et al., 2011; Angeli et al., 2018; Wagner et al., 2018). In these papers, the authors described the abilities of the spinal cord to generate useful muscle activation that may provide standing and even walking patterns. However, as commonly stated in literature, available stimulators, both implanted and external, remain too limited to explore widely all the possibilities that these techniques could provide. Among these limitations, functional movements controlled in a closed loop way are still unused, except in focused research protocols, although it is known that the human nervous system is controlling movement through complex multilevel closed loops. Indeed,

an efficient functional movement would need for closed loop control (balance control, fatigue compensation) or optimized synthesized patterns (sit to stand movement, grasping). It means that several stimulation points and sensors have to be placed on the body. It leads to complex donning and doffing in particular due to classical wired links. Thus, wireless systems appear to be a neat solution, *a fortiori* wearable to meet the need for mobility, however it leads to issues when safety and guaranteed performances to achieve closed loop control are mandatory.

The first network based FES system available was the BION (Loeb et al., 2001). The implantable, thus invasive, technology faced the difficulty to power the system through external inductive antennas over wide areas of the body, even with its rechargeable version. Moreover, closed loop control, as far as we know, was never used on such network finally dedicated to acute rehabilitation. Some external FES stimulators already use wireless technology, mainly to allow portability (Broderick et al., 2008; Chae et al., 2008), i.e., stimulators that can be worn by the patient without being physically connected to a computer. Some of these stimulators are standalone units, meaning that one of the available programs can directly be selected or parameterized on the stimulator itself. Some examples of existing products are the Compex Wireless from Compex, the NESS L300 from Bioness (Hausdorff and Ring, 2008; Dunning et al., 2009; Laufer et al., 2009), the WalkAid from Innovative Neurotronics (Weber et al., 2005). These systems are designed to carry out a unique thus specific FES-application. Even if these stimulators can be used in different FES therapies, it is still impossible to use the technology for multi-site FES applications despite their 4-channel outputs for some. Indeed, to treat different functional deficiencies eventually simultaneously, it is necessary to coordinate stimulation and acquisition on distributed sites on the human body. To achieve this task, it is necessary to connect and coordinate stimulators via the network, and today, very few external wireless FES stimulators attempt to do so: Jovicic et al. propose a prototype but discusses mainly the problem of transmission and relay between units and a host computer (Jovicic et al., 2012). An efficient routing protocol has been proposed to face frame losses (due to signals' attenuation) when communicating with the mandatory remote computer since the system is not fully wearable, and thus not adapted to daily life context.

To guarantee safety and performances through wireless link, the key issue is the Medium Access Control (MAC) protocol. Prototypes of networked implantable neuroprothesis for which we already designed stimulation units (Andreu et al., 2009), present another application with close MAC protocol design but not used on a wireless medium. The purpose of the paper is to detail the adequacy of our open, potentially heterogeneous, wireless architecture—hardware, software, and protocol—with closed loop control requirements over a distributed FES system.

The paper is organized as follows: the distributed architecture is described, then wireless network properties are related to the closed loop control requirements, quantitative results show the real performances of the system followed by a relevant illustrative clinical application.

2. MATERIALS AND METHODS

2.1. Distributed FES Architecture

The underlying principle of distributed architectures is to decentralize parts of the processing on a set of physical distributed units (DU). Activities of these entities are coordinated at higher levels of the architecture to provide complex functionalities. According to this principle, we designed an external wireless FES architecture based on:

- Distributed Stimulation Units (DSU): a DSU executes locally the stimulation profile and thus generates the stimulus.
- Distributed Measurement Units (DMU): currently, DMU can acquire EMG or physical data such as angles (goniometers), 3D accelerations, or inertial sensors. Thus, a DMU locally performs the acquisition of the signals and processes data, such as digital filtering, envelope computation, or threshold detection.
- Control Unit (CU): the controller is in charge of coordinating activities of DSUs and DMUs to offer high level functionalities according to the running FES application. CU configures, coordinates and schedules all DUs. CU remotely modulates relevant parameters of DSUs and collects processed data from DMUs for closed loop control purposes. Finally, CU supervises and controls the network Quality of Service (QoS).

  CU can be used in a standalone mode—within a "homogeneous" architecture implying only the CU and a set of DSUs and DMUs—or as a gateway between this networked FES system and a wearable controller (or a computer) that then ensures the closed loop control and the connections (wired or wireless ones) with other types of sensors, leading to a "heterogeneous" architecture involving multiple networks (e.g., sensor networks). This allows interfacing with any kind of sensors while keeping the most critical part, i.e., the DSU, unchanged. The 2 types of architectures are illustrated through the paper.

2.2. Wireless Communication Link

Communication is a critical issue as it directly has an impact on the performances, the reliability and the safety of the system. Indeed, compared to wired or centralized systems, a wireless system over has to face: (i) avoidance of collision, (ii) optimization of bandwidth occupation, (iii) determinism, (iv) bounded time latencies for robust control, (v) safety against frame losses.

Wifi technology (802.11) cannot be used since the CSMA/CA method does not offer a deterministic MAC, and its PCF (Point Coordination Function) mode is not efficient, even not always implemented. Bluetooth solution (IEEE 802.15.1) has an important drawback considering the need for network synchronization delays in scatter-nets of multiple piconets (small networks up to 8 slaves). ZigBee technology (IEEE 802.15.4) provides deterministic medium access through guaranteed time slots within the contention free period on beacon-enabled network. It is moreover efficient in its use of power and able to support a network with thousands of devices thanks to a cluster tree or mesh network's topology. However, it is more adequate for communication between devices and services dedicated to remote monitoring than for real-time FES closed-loop control.

Indeed, Zigbee is used for applications where the latency of transmission is not critical (transmit GTS and/or receive GTS nodes' request and coordinator GTSs management impacts efficiency, and the routing layer as well). Its software architecture, protocol stack and services, remains complex. However, it relies on a low-power digital radio based on the IEEE 802.15.4 standard which is efficient in terms of receiver sensitivity, link quality indication, transmit power adjustment. We thus use only the physical layer of this technology.

We developed a communication solution based on a 3-layer protocol stack (reduced OSI model): physical, MAC and application layers. The physical layer (2.4 GHz RF link, IEEE 802.15.4) has a bit-rate of 250 Kbs^{-1}. The less occupied channel is detected to limit interference and then enhance the QoS of the wireless link; reception and emission power are measured and adapted to optimize power consumption and link reliability. Besides, this physical layer can be changed if needed, according to new communication standard, enhanced technology or local country rules *a fortiori* in medical-context applications (Baker and Hoglund, 2008; Panescu, 2008). The application layer supports configuration, programming and remote operating of the DUs and allows for a very flexible evolution toward new type of DU without changing physical and MAC layers.

The main issue remains the MAC aspects. Due to limitations of existing solutions, an original MAC protocol was designed in order to minimize the risk of collisions between frames and to optimize medium sharing, both for efficiency and reactivity purposes. We designed the Sliding Time Interval Medium Access Protocol (STIMAP). It ensures that only one DU communicates over the network at a given time while optimizing the bandwidth use through a smart adjustment of time slots duration (Godary et al., 2007; Godary-Dejean and Andreu, 2013). STIMAP is based on the Master/Slaves model—the CU being the master and other DUs being slaves—and dynamic TDMA (Time Division Multiple Access, see **Appendix**). STIMAP offers unicast, multicast, and broadcast addressing. Multicast addressing allows grouping of DUs. A DU can be member of up to 8 groups. Address space allows for defining 64 groups and 64 DUs over one network; this being, the maximum number of units that can be involved in this wireless architecture depends both on the time constraints of the application and on the number of sensors (since it is the exchange of sensor data that consumes the most bandwidth). The main properties of this original MAC protocol are:

- Multicast provides: (i) simultaneous addressing of several DUs with a unique frame minimizing medium occupancy (ii) network level synchronization (beacons like) (Godary-Dejean and Andreu, 2013).
- Adjustable and optimized time-slot allocation ensures a better trade-off between reactivity / answer to a request from a DU, and time slot occupancy through dynamic unused time-slot recovery.

2.3. Hardware and Software Architectures of Units

A CE-marked external FES system based on our distributed wireless architecture was developed in collaboration with Vivaltis Company (Montpellier, France). The CU board can be connected to a wearable controller or a computer via an USB link, allowing the practitioner to configure and program the complete system through application specific GUIs. The CU, worn by the patient, ensures all communications with DUs and provides for the scheduling of DU activities including closed-loop control in standalone mode (i.e., homogeneous architecture). DU relies on a 2-board based architecture: a generic board embedding the communication protocol stack and a specific board composed of digital and analog electronics adapted to stimulation or acquisition (**Figure 1**, left). Unit's volume and weight are respectively $80*55*30$ mm^3 and 98 g.

2.3.1. Distributed Stimulation Unit

The stimulation unit is a regulated-current 2-channel stimulator, able to sequentially deliver a stimulus on each channel. The features are: maximal current 100 mA, 0.1 mA step on a maximum load of 1 $k\Omega$, stimulation frequency 1 Hz to 1 kHz, pulse-width 50 μs min., 1 μs step, and electrical polarity can be configured. All parameters are dynamically and remotely adjustable (**Figure 2**).

2.3.2. Distributed Measurement Unit

Specific boards can be developed to interface with various types of sensors such as accelerometers or Inertial Motion Units (IMU). The 2-channel EMG unit (Vivaltis, France) can alternately sample two input signals. The features are: a bandwidth from 10 Hz to 1 kHz, sampling frequency of 2.5 kHz per channel, 3 programmable input ranges (80, 200, and 400 μV), and a digital resolution of 12 bits. The DMU can numerically rectify and filter EMG with a programmable cut-off frequency to get the envelope thus limiting the necessary bandwidth on the medium by using under-sampling. A second DMU was designed with a 2D goniometer (Biometrics). This DMU samples both angles at 25 Hz with a 12-bit resolution.

2.3.3. Hardware and Software Implementations

For DSU and DMU, the software architecture is based on the same set of tasks deployed on two microprocessors (**Figure 3**), for the generic (ARM7 of Freescale MC1322X, with the RTOS CMX-RTX) and specific boards (Renesas R8C27).

The CU is based on a microprocessor board (ARM7 of Freescale MC1322X), (**Figure 1**). Its software application is multitask (**Figure 3**), running on a real-time operating system (RTOS CMX-RTX).

2.3.4. Safety Issues

There are 2 levels of safety; the first one concerns stimulation generation. On the stimulation board, a 10-bit ADC measures the effective output current on a serial shunt resistor (2 Ω). Open-circuit or saturated output can be detected (due for instance to high impedance of the electrode). This current is checked on the DSU and limited by software depending on the application. It ensures that the DSU cannot deliver more current than it is supposed to. It is all the more important on wireless systems, that transmission failures may occur more easily than on wired systems.

The second level of safety deals with the wireless link issue. Since the DU is an autonomous unit being remotely controlled,

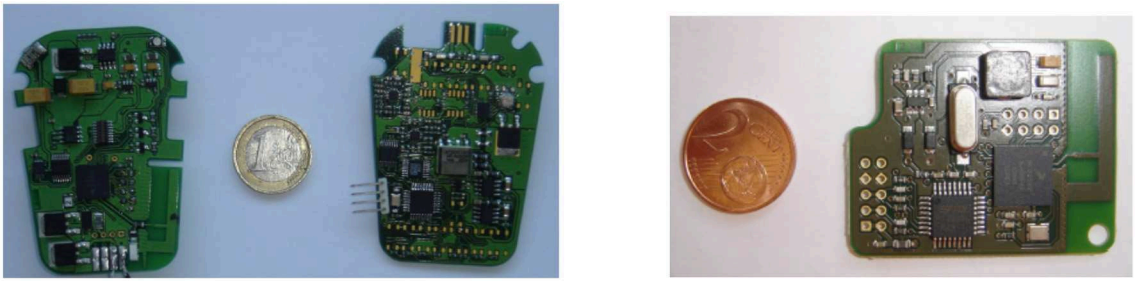

FIGURE 1 | (Left) A distributed stimulation unit is composed of a communication-dedicated board and a stimulation one. **(Right)** The controller board manages the wireless network and the real-time application.

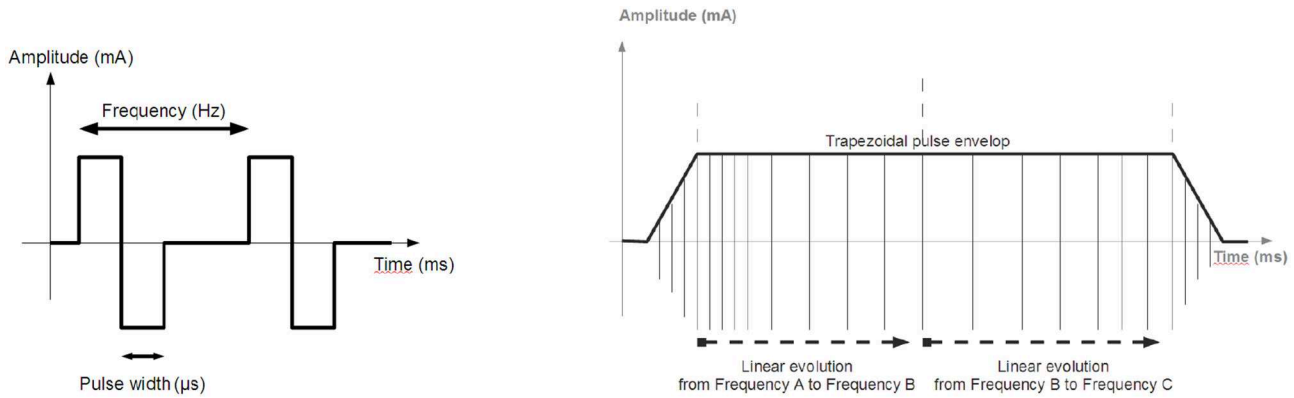

FIGURE 2 | Stimulation: **(Left)** Biphasic pulses stimulation profile generated by the distributed stimulation unit. **(Right)** Envelope of the pulse train.

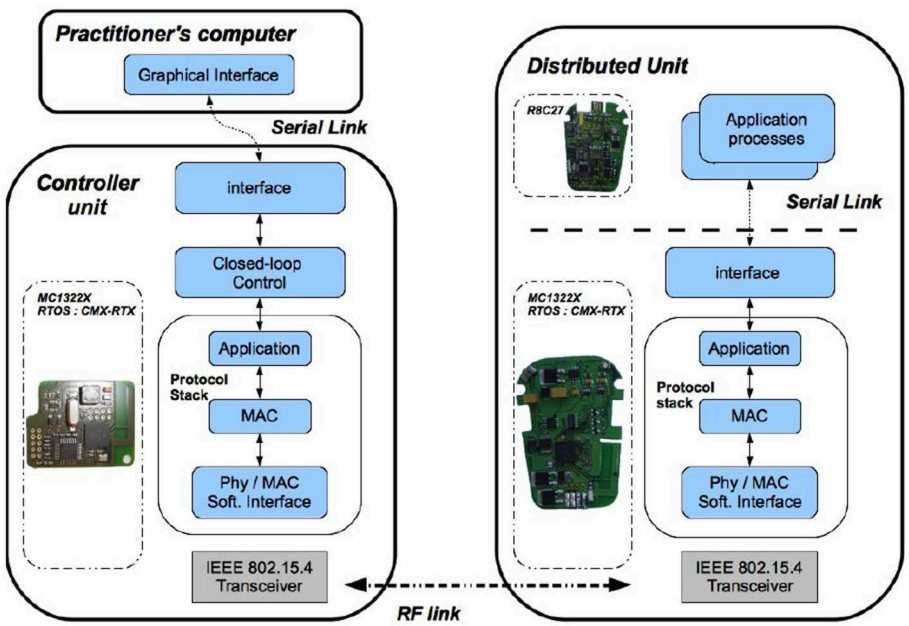

FIGURE 3 | Software modules deployment **(Left)** On the control unit board, embedded real-time software architecture manages both the wireless communication and the closed loop control. **(Right)** On the distributed unit board, the embedded micro-controller runs the real-time communication stack and controls the stimulation process.

the CU periodically checks if the DU is still communicating by means of presence test requests (section 3). Absence of DU acknowledgment can have several causes: communication (unreachable node), software application (DU locally stopped), and insufficient power. If the DU does not acknowledge a defined number of successive presence tests then the CU notifies the user, stops the application and goes in a predefined safe mode. On the DU side, the same safety check is performed: if the DU does not receive presence test requests for 3 s, then it stops its activity and shuts down itself in a predefined safe mode.

2.3.5. Power Issues

Each DU is powered by a rechargeable battery (3.7 *Wh*, 1,000 *mAh*). Measured power consumption of a DSU, including communication, is 2 W (260 *mA*, 7.4 *V*) with stimulation parameters being: 20 *mA* amplitude, 400 μs pulse width, and 100 *Hz* frequency on both channels. Considering the battery capacity, the autonomy is about 4 h. For standard stimulation with parameters set to 20 mA amplitude, 200 μs width, and 50 *Hz* frequency, the autonomy would be more than 11 h.

3. RESULTS

Advanced rehabilitation protocols would benefit from closed loop control but it requires determinism, time performances and safety. The results show the capabilities of our architecture and its devices to fulfill these requirements. We first defined a proof-of-concept experimental setup to characterize the performance of the system, based on a homogeneous architecture (i.e., implying only CU, DSUs, and DMUs). Then, this open wireless architecture has been extended to a heterogeneous version with a wearable controller and several wired and wireless sensors, and used in the context of a clinical protocol: FES-based control of knee joint to reduce stance phase asymmetry in post-stroke gait.

3.1. Proof-of-Concept Experimental Tests

We defined an experimental setup that includes a goniometer—1 DMU—for measuring a joint angle. It controls the contraction of 2 antagonist muscles acting on this joint—2 DSU. We observed the system outputs (both stimulation patterns) on a dummy load (**Figure 4**). This control scheme is not evaluated *per se*, but the whole system is provided to assess the following features: (i) wireless link properties in particular linked to the original MAC protocol we designed, (ii) real-time performances in particular timing and synchronization allowed by our original architecture associated with MAC protocol.

The control scheme is based on proportional gain while stimulating either the agonist or antagonist muscle according to the sign of tracking error (**Figure 4**).

Besides, in a closed loop control scheme, as muscles time response is around 100 ms (Vette et al., 2008) and stimulation period around 40 ms, the sampling period of the command is set to 40 ms without any loss of controllability. The proportional gains are $Kp = 0.5$ and $Kc = 1$ and include voltage to angle conversion. There is a saturation between the proportional error output and the actual stimulation intensity acting on muscles to avoid over stimulation of muscles. These maximum amplitudes are set for each muscle *a priori*, within safe limits.

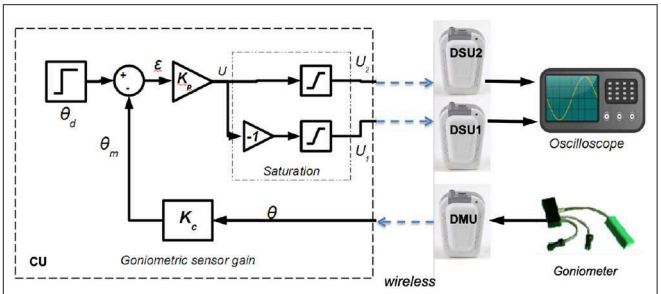

FIGURE 4 | Multiple muscle contraction control scheme based on proportional gain using 3 distributed units and 1 control unit.

3.1.1. Wireless Link Performances

In this characterization, the CU is responsible for dating events and collecting transmission parameters: time stamping requests and corresponding acknowledgments to calculate the round-trip time (RTT) between CU and DU communications, collecting the link quality indicator (LQI, measuring the signal quality level of the frame reception) and determination of frame losses (number of non-received acknowledgments) among 5,000 dummy frames exchange (100 bytes long).

3.1.1.1. Performances of the physical layer

Frame losses are due to collisions of frames or perturbations which can occur when other wireless technologies are used in the same environment around the 2.4 GHz RF band as local area networks (Wi-Fi IEEE802.11), wireless personal area networks (Bluetooth IEEE802.15.1) and Zigbee (IEEE802.15.4).

At power on, the CU and DUs are configured with a default channel. After having determined the least occupied channel from the 16 available ones, the CU indicates to all DUs the channel selected to communicate safely, i.e., with the least disturbances from other wireless technologies.

Moreover, as soon as a frame is received the physical coupler supplies a measure of the received RF signal power. This LQI is between –15 dBm for a good reception quality to –100 dBm for a bad reception quality. The CU observes the LQI evolution to detect any potential impact of the environment on the received signal power, since it can induce frame losses. In the worst case, CU connected to a computer and DUs worn by the patient, LQI is about –75 dBm in case of body opposition: with more than 10,000 exchanges composed of 2 frames each, only 3 DMU and 7 DSU frames were lost in such case. This loss rate can easily be managed by the CU / DU safety procedures without any functional impact, and no frame loss occurs when both CU and DU are worn by the patient.

As physical transmission impacts closed-loop control design, we perform RTT measurements at the physical layer (RTT_{PHY}), i.e., directly from the software interface of the physical layer that

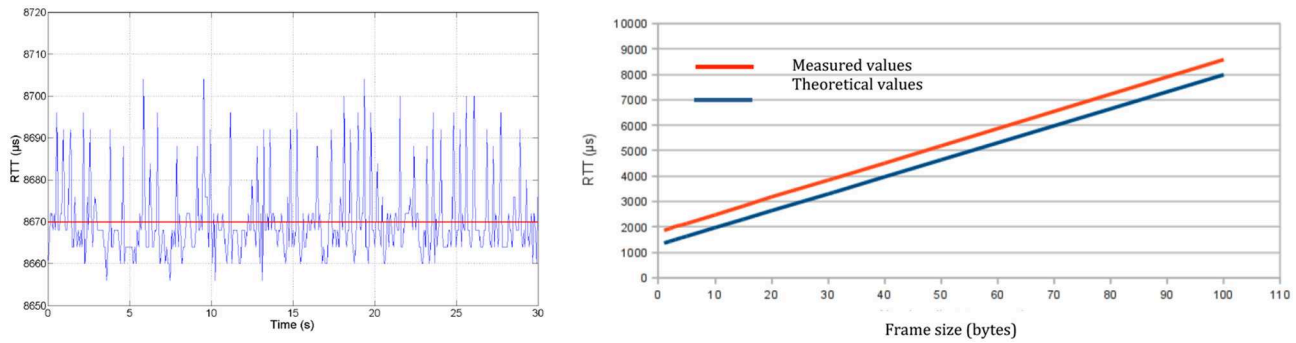

FIGURE 5 | Round-trip time at physical layer (RTT_{PHY}): **(Left)** Evolution with time of 100-byte frame transmission—mean RTT_{PHY} of 8,670 μs with a standard deviation of 9 μs. **(Right)** Evolution of the transmission time according to frame size.

pilots the radio transceiver (**Figure 5**, left). Experiments show that transmission durations increase linearly with the number of transmitted bytes (**Figure 5**, right). Thus, a minimum RTT_{PHY} can be estimated knowing the number of bytes exchanged, allowing to set some closed-loop control parameters. Moreover, RTT_{PHY} is needed to set the time-slot duration of the STIMAP protocol (see **Appendix**) and set the timeout for monitoring CU to DUs communications.

3.1.1.2. Performances of the MAC layer

As mentioned in section 2, the CU is in charge of configuring groups of DUs (group size, priority, time-slot, etc.). RTT_{MAC} are measured at MAC layer within the protocol stack, meaning that both MAC software module and physical layer interface software module are taken into account. First, individual (unicast) communications are evaluated for requests like node configuration (MAC parameters setting) and test of presence (similar to the ping protocol). The smallest RTT_{MAC} is for a test of presence request (2.850 ms) and the highest is for the node configuration (3.080 ms). Then, group based communications are evaluated to verify time-slot positioning at MAC layer since it is essential to ensure the absence of collision (no time-slot overlap) in this context of real-time control: such deterministic MAC protocol ensures an optimized balance between reactivity and time slot occupation (Godary et al., 2007; Andreu et al., 2009).

3.1.1.3. Performances at application layer

The application layer of a DU, executed on the communication board, is in charge of extracting and decoding data from application request sent by the CU. However, the operating mode is not always the same depending on the application, i.e., stimulation or acquisition. Let's first consider the stimulation case. The CU initiated a stimulation sequence by a configuration request sent to the DSU, defining default stimulation parameters as: pulse pattern (**Figure 2**, left), pulse amplitude, pulse width and frequency. Then the stimulation sequence is enabled by a start request sent to the DSU. Locally the DSU executes an amplitude or a frequency modulation (**Figure 2**, right) without any other communication. However, during the stimulation sequence execution, the CU can remotely modify the frequency, the pulse width and the current amplitude. So RTT_{APP} of each operation (**Table 1**) is evaluated since these values must be taken into account in the design of the FES closed-loop control scheme.

TABLE 1 | Round-trip time at application layer (RTT_{APP}) for stimulation operations.

Operation	Mean RTT_{APP} (ms)	Std deviation (ms)
Configuration	12.19	0.016
Stimulation start	5.92	0.011
Amplitude modulation	6.178	0.018
Pulse width modulation	6.012	0.015
Stimulation stop	5.99	0.009

Regarding acquisition operation, the DMU dedicated to goniometers is able to store in a circular buffer up to the last 150 data samples. The measured mean RTT_{APP} for one data sample gathering is 3.023 ms with a standard deviation of 15 μs. For goniometers the sampling period is equal to the command sampling period, i.e., 40 ms. For EMG, if we want to transmit the envelope, the sampled signal is filtered on the specific board (cut-off frequency is set to 5 Hz) avoiding raw data transmission. This drastically decreases the data rate transfer over the network down to a sample each 40 ms requiring a useful data throughput of 300 bs^{-1} instead of 30 kbs^{-1}. The difference between performances of stimulation vs. acquisition requests comes from the local operating modes: regarding acquisition data are periodically transmitted to the CU (data acquisition and data gathering are independent processes), while concerning stimulation the modulation is effective when applied by the DSU stimulation board (and not only once the message has been received by the DSU).

3.1.2. Distributed Stimulation Synchronization Performances

To evaluate the accuracy of synchronization process at the network level, we estimate the time lag between different stimulations induced when simultaneously starting two DSUs. They may be placed to different sites actuating joints simultaneously by a coordinated stimulation of a 2 pairs of

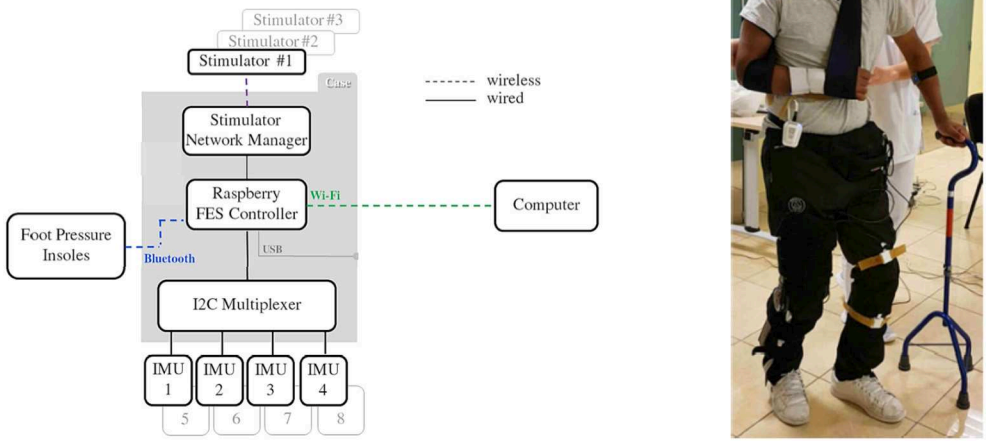

FIGURE 6 | Architecture used for knee control. Subject equipped with inertial measurement unit sensors, stimulator and controller (© Inria / Photo L. Jacq).

agonist and antagonist muscles (wrist for instance). Tests were performed using two DSUs configured with the same stimulation profile and associated to the same DSU group. Then, they have been started through a group-addressed request. The measured time lag between the 2 first pulses generated by each DSU is 16 μs. This impact is negligible compared to the closed-loop control period and the muscle bandwidth (section 3.1) and demonstrate the accuracy of the protocol stack timing for advanced stimulation synchronization over the network.

3.2. Results With FES-Based Knee Joint Control

We developed a closed-loop architecture for FES-based control of knee joint to reduce stance phase asymmetry in post-stroke gait (Sijobert, 2018). We do not present the clinical results but the closed loop performances of the system. However, in few words, the clinical rationale was that the process of gait recovery in patients with severe post-stroke hemiplegia does not only require the control of the foot dorsiflexion but also that of the knee joint. Indeed, it greatly impacts the entire gait cycle and notably the support phase quality. Usual disorders are knee hyperextension during the stance phase (genu recurvatum) and flexed knees (crouch gait). FES is an effective alternative to fixed orthoses to produce appropriately timed knee flexion or extension.

The designed closed loop system aimed at ensuring a safe knee joint lock to allow patients to rely on their paretic leg and transfer their weight onto it during the stance phase. Quadriceps and hamstring are electrically stimulated to ensure that knee extension and flexion are restricted to a safe and physiological range of motion, depending on the gait phase. To do so, a set of sensors is used to detect the gait phases and knee angle evolution, according to which stimulation levels are modulated.

The corresponding protocol was approved by a national ethical committee and participants have signed an informed consent. 11 participants have been included.

3.2.1. Knee Joint Control Experimental Setup

The heterogeneous architecture developed for this FES based knee joint control protocol is described in **Figure 6**. Wireless and wired sensors feed the Raspberry (wearable controller) running a porportional (P) controller, wirelessly connected to one DSU by means of the CU which acts as the DSU network manager. A computer is used to remotely configure and then start or stop the closed-loop process that is running on the wearable controller without any other communication with the computer.

The closed-loop control relies on 4 sensors: 2 foot pressure insoles that communicate through a Bluetooth 4.0 BLE protocol (FeetMe©, France) with the wearable controller and 2 wired IMU (Bosch© BNO055) that directly provide quaternion estimation. Stimulation is sent via a two-channel DSU to the quadriceps (channel #1) and hamstrings (channel #2) via pairs of surface electrodes located on the skin over the target muscle.

Powered by a commercial USB power bank, a dedicated 3D-printed case (strapped around the waist of the subjects, **Figure 6**) was designed to host the Raspberry card, the CU acting as a gateway with stimulators' network and the I2C multiplexer used for wired IMU sensors. With up to 8 h of battery life, the FES controller case weighs less than 130 g and measures 9 (length) x 6 (width) x 4 (depth) cm.

Data from IMUs and pressure insoles were periodically acquired and processed online on the controller. Insoles data were used to analyze paretic foot support (PFS) in order to discriminate between stance and swing phases. Stimulation could also be delivered just before initial contact (IC) at the end of the swing phase, in order to anticipate a possible genu recurvatum or

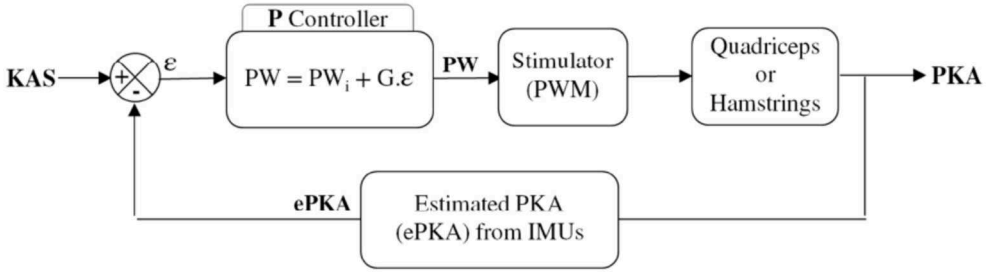

FIGURE 7 | Closed loop control scheme.

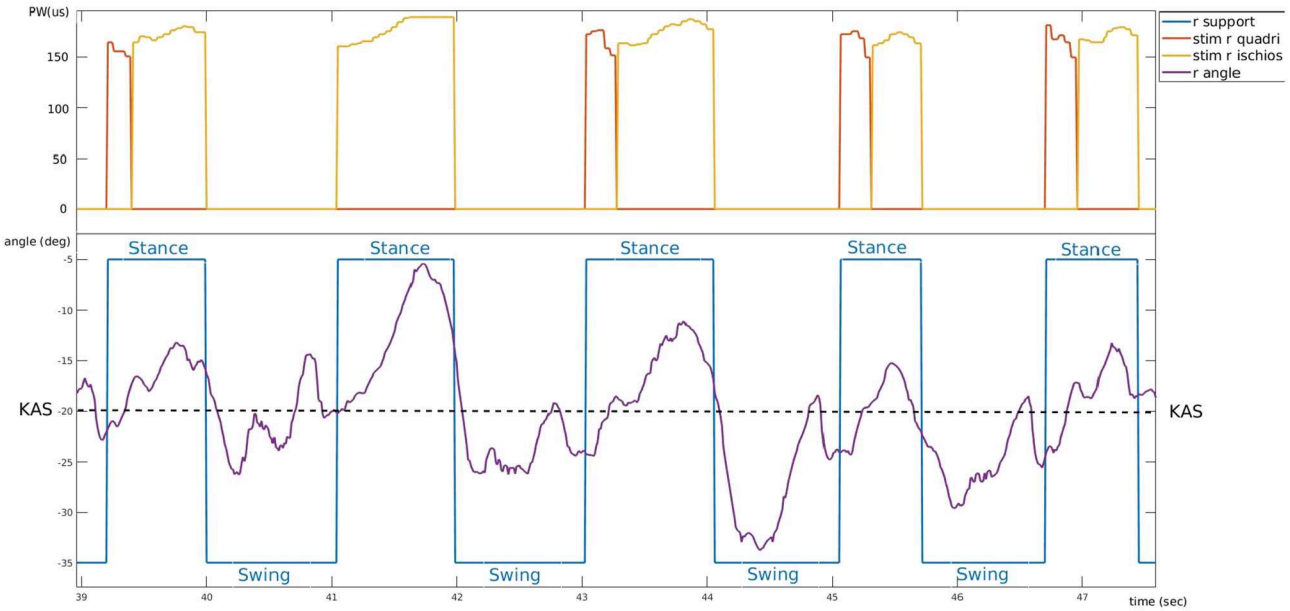

FIGURE 8 | Typical controller behavior. Example of experimental data from participant 3 who suffers a right hemiplegia (trial 4). Bottom: evolution of the right knee angle (purple) around knee angle set-point value (dashed line) and corresponding support phase (blue). Top: electrical stimulation pulse width of right quadriceps (red) and right hamstring (yellow).

crouch gait in stance phase and compensate muscular activation latency. When required and depending on the participant's gait pattern, this "pre-stance" stimulation could be triggered either via an online detection of peak knee flexion or when the sagittal angular speed recorded via the gyroscope crossed zero. In stance phase, stimulation was triggered ($F = 30$ Hz, $I = 50$ mA) either to quadriceps or hamstrings, depending on the paretic knee angle (PKA) estimation relatively to the knee angle set-point (KAS) defined by the practitioner as the optimal flexion during stance phase (around 5°). the P controller adjusted the pulse width (**Figure 9**) depending on the error ϵ between PKA and KAS (**Figure 7**).

3.2.2. Knee Joint Real-Time Control in Stance Phase

A typical control of the system is shown on **Figure 8**. 5 gait cycles of participant 3 are plotted. During stance phase (blue), stimulation of hamstrings (yellow) is delivered when PKA (purple line) is higher than the predefined KAS value (dashed line) and stimulation of quadriceps (red) is delivered when PKA is lower than KAS. Stimulation pulse width is adjusted via the P controller depending on the error between PKA and KAS (**Figure 9**).

The **Figure 9** corresponds to a zoom on the time window from 32.04 to 32.18 s of the same trial. We observe more precisely the modulation of the pulse width performed by the closed-loop controller: the pulse-width modulation update at the stimulator output is performed in due time i.e., according to the stimulation frequency.

We checked the latency of the system from the sensor input at the wearable controller level to the actual output of the channel #1 of the DSU. To do so, acquired data were recorded and then played again with a higher stimulation frequency (F increased from 30 to 100 Hz) to allow for a more accurate evaluation of the delay. Results are shown on

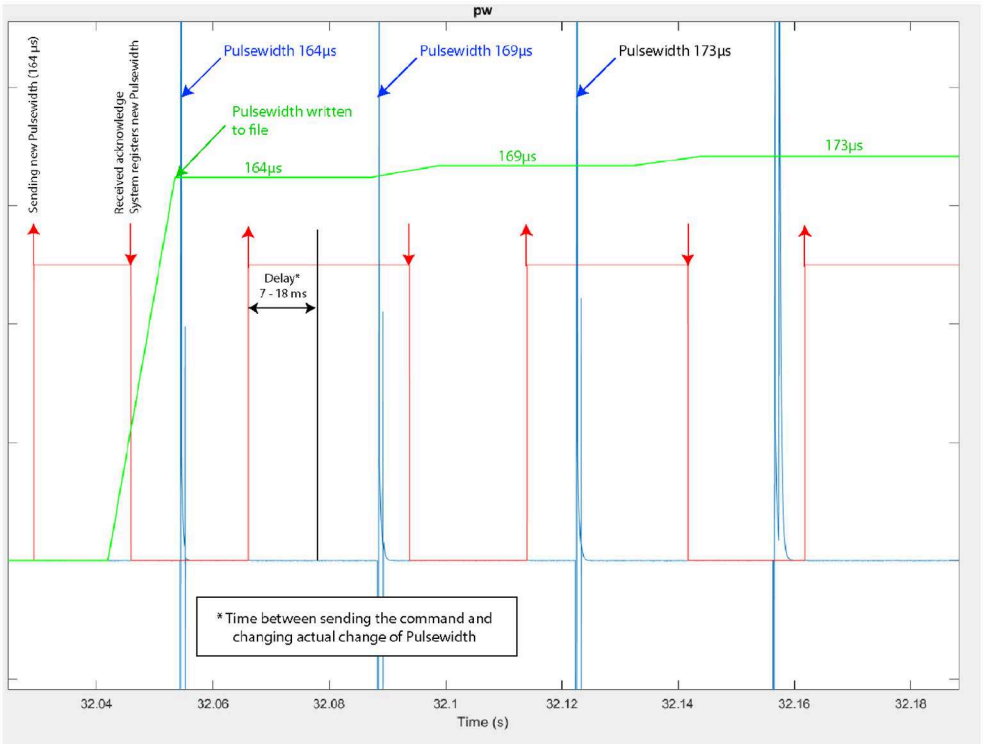

FIGURE 9 | Modulation of the stimulus pulse width during knee joint control (Participant 3–trial 4). In red: time at which a pulse-width modulation request is sent by the controller, indicating also the modulated pulse width value (e.g., 164 μs), in blue: actual pulse-width measured at the stimulator's output, with its current value.

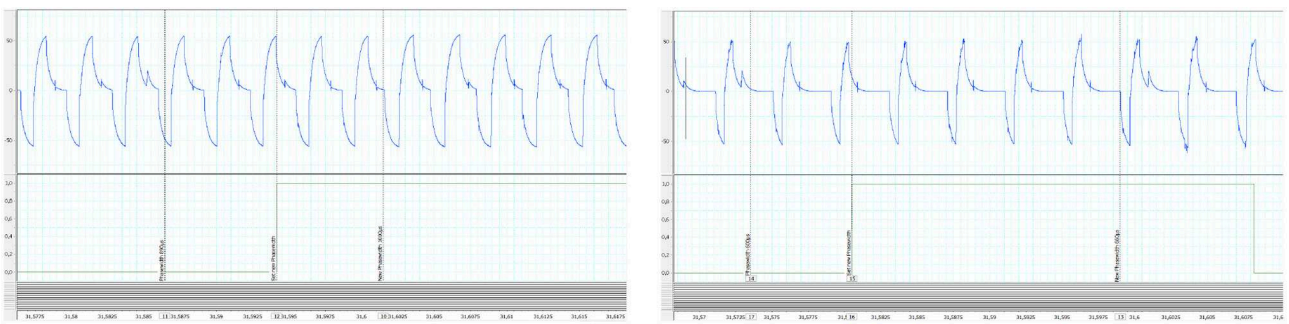

FIGURE 10 | Control latency evaluation from replay (100 Hz) of recorded experimental data: **(Left)** shortest measured latency **(Right)** largest measured latency. In abscissa time is in seconds. Y-Axis are in volt.

Figure 10: the maximal measured latency was 18.4 ms and the shortest 7.3 ms. Even in the worst case (due to the fact that the controller must communicate with the CU to control the DSU), this latency is compatible with the dynamics of FES muscle control.

4. DISCUSSION AND CONCLUSION

We developed a wireless FES architecture based on a set of distributed stimulation and measurement units managed by a wearable controller. We characterized the performances of the RF network we designed in the proposed distributed FES architecture. The network QoS was observed measuring RTT at every protocol stack layer, as well as LQI and frame loss rate. Time performances reported by RTT measures are highly stable, and medium access is deterministic. This proves that this wireless architecture, with its original STIMAP MAC protocol, is a suitable framework for the deployment of safe closed loop control. The link quality of the 2.4 GHz wireless technology is sensitive to human body attenuation. However, the placement of DUs on the body showed that even in the worst case, frame losses are not critical at all and can be easily avoided. In any case, the CU permanently monitors QoS and both wireless link failure monitoring and safety procedures are implemented on the CU and DUs.

The deterministic and collision free features were demonstrated. Moreover, the accuracy of the timing, linked to the optimization of the STIMAP protocol, shows impressive results with only few μs of delay synchronization error between 2 DSUs simultaneously started through the network.

We assessed the performances of this technology for both open and closed-loop control schemes through a proof-of-concept experimental setup and several applications including the one presented regarding knee joint control in post-stroke patients. A real-time control of the stimulation was also demonstrated using EMG as inputs and the same DSU architecture (Zhan et al., 2018).

The main contribution of this work concerns the design and development of a wireless FES architecture based on dedicated MAC and application layers protocol together with an optimized distribution of the software on DUs. It ensures the flexibility, reliability, and accuracy of this innovative system: adapted to patient / pathology (as regards numbers of DUs), wireless and controllable in closed loop for surface FES with guaranteed timings and safe implementation.

Through this open wearable FES architecture, a scalable hardware solution has been achieved, adaptable to the needs of different FES applications, environments, and pathologies. It is now used by our research team for other applications (Sijobert et al., 2017; Zhan et al., 2018), enabling clinicians to explore novel directions and study new hypotheses.

DATA AVAILABILITY STATEMENT

All datasets generated and analyzed for this study are included in the article/supplementary material.

ETHICS STATEMENT

The studies involving human participants were reviewed and approved by CPP Nord Ouest I Ethics committee (Trial #017-A03611-52). The patients/participants provided their written informed consent to participate in this study.

AUTHOR CONTRIBUTIONS

DA, DG, and MT drafted the manuscript. CA-C and DG supervised the researches. DA and MT Developed the hardware solution. DG had the initial idea of distributed FES concept. CA-C and CF designed the clinical trial. CA-C, CF, and BS participated to the clinical trial.

FUNDING

This work was supported by Association Nationale de la Recherche et de la Technologie, Grant Number 526/2007. We thank Ronan Le Guillou for the technical help with the system.

REFERENCES

Andreu, D., Guiraud D., and Souquet, G. (2009). A distributed architecture for activating the peripheral nervous system. *J. Neural Eng.* 6:026001. doi: 10.1088/1741-2560/6/2/026001

Angeli, C. A., Boakye, M., Morton, R. A., Vogt, J., Benton, K., Chen, Y., et al. (2018). Recovery of over-ground walking after chronic motor complete spinal cord injury. *New Engl. J. Med.* 379, 1344–1250. doi: 10.1056/NEJMoa1803588

Baker, S. D., and Hoglund, D. H. (2008). Medical-grade, mission-critical wireless networks. *IEEE Eng. Med. Biol. Mag.* 27, 86–95. doi: 10.1109/EMB.2008.915498

Broderick, B., Breen, P., and Ölaighin, G. (2008). Electronic stimulators for surface neural prosthesis. *J. Autom. Control* 18, 25–33. doi: 10.2298/JAC0802025B

Chae, J., Sheffler, L., and Knutson, J. (2008). Neuromuscular electrical stimulation for motor restoration in hemiplegia. *Top. Stroke Rehabil.* 15, 412–426. doi: 10.1310/tsr1505-412

Davis, R., Houdayer, T., Andrews, B., Emmons, S., and Patrick, J. (1997). Paraplegia: prolonged closed-loop standing with implanted nucleus FES-22 stimulator and Andrews' foot-ankle orthosis. *Stereotact. Funct. Neurosurg.* 69, 281–287. doi: 10.1159/000099889

Dunning, K., Black, K., Harrison, A., McBride, K., and Israel, S. (2009). Electrical stimulation in the acute inpatient rehabilitation setting : a case series. *Phys. Ther.* 89, 499–506. doi: 10.2522/ptj.20080241

Godary, K., Andreu D., and Souquet, G. (2007). "Sliding Time Interval based MAC Protocol and its Temporal Validation," in *7th IFAC International Conference on Fieldbuses & Networks in Industrial & Embedded Systems (FET'07)* (Toulouse).

Godary-Dejean, K., and Andreu, D. (2013). Formal validation of a deterministic MAC protocol. *ACM Trans. Embedded Comput. Syst.* 12, 6:1–6:23. doi: 10.1145/2406336.2406342

Guiraud, D., Stieglitz, T., Koch, K. P., Divoux, J. L., and Rabischong, P. (2006b). An implantable neuroprosthesis for standing and walking in paraplegia: 5-year patient follow-up. *J. Neural Eng.* 3, 268–275. doi: 10.1088/1741-2560/3/4/003

Guiraud, D., Stieglitz, T., Taroni, G., and Divoux J. L. (2006a). Original electronic design to perform epimysial and neural stimulation in paraplegia. *J. Neural Eng.* 3, 276–286. doi: 10.1088/1741-2560/3/4/004

Harkema, S., Gerasimenko, Y., Hodes, J., Burdick, J., Angeli, C., Chen, Y., et al. (2011). Effect of epidural stimulation of the lumbosacral spinal cord on voluntary movement, standing, and assisted stepping after motor complete paraplegia: a case study. *Lancet* 377, 1938–1947. doi: 10.1016/S0140-6736(11)60547-3

Hausdorff, J. M., and Ring, H. (2008). Effects of a new radio frequency-controlled neuroprosthesis on gait symmetry and rhythmicity in patients with chronic hemiparesis. *Am. J. Phys. Med. Rehabil.* 87, 4–13. doi: 10.1097/PHM.0b013e31815e6680

Jovicic, N., Saranovac, L., and Popovic, D. (2012). Wireless distributed functional electrical stimulation system. *J. Neuroeng. Rehabil.* 1, 54–58. doi: 10.1186/1743-0003-9-54

Kobetic, R., Triolo, R. J., and Marsolais, E. B. (1997). Muscle selection and walking performance of multichannel FES systems for ambulation in paraplegia. *IEEE Trans. Rehabil. Eng.* 5, 23–29. doi: 10.1109/86.559346

Kobetic, R., Triolo, R. J., Uhlir, J. P., Bieri, C., Wibowo, M., Polando, G., et al. (1999). Implanted functional electrical stimulation system for mobility in paraplegia: a follow-up case report. *IEEE Trans. Rehabil. Eng.* 7, 390–398. doi: 10.1109/86.808942

Kralj, A., and Bajd, T. (1989). *Functional Electrical Stimulation: Standing and Walking After Spinal Cord Injury*. Boca Raton, FL: CRC Press Inc.

Laufer, Y., Ring, H., Sprecher, E., and Hausdorff, J. M. (2009). Gait in individuals with chronic hemiparesis : one-year follow-up of the effects of a neuroprosthesis that ameliorates foot drop. *J. Neurol. Phys. Ther.* 33, 104–110. doi: 10.1097/NPT.0b013e3181a33624

Liberson, W. T., Holmquest, H. J., Scot, D., and Dow, M. (1961). Functional electrotherapy: stimulation of the peroneal nerve synchronized with the swing phase of the gait of hemiplegic patients. *Arch. Phys. Med. Rehabil.* 42, 101–105.

Loeb, G. E., Peck, R. A., Moore, W. H., and Hood, K. (2001). BIONtm system for distributed neural prosthetic interfaces. *Med. Eng. Phys.* 23, 9–18. doi: 10.1016/S1350-4533(01)00011-X

Panescu, D. (2008). Wireless communication systems for implantable medical devices. *IEEE Eng. Med. Biol. Mag.* 27, 96–101. doi: 10.1109/EMB.2008.915488

Possover, M., Schurch, B., and Henle K.P. (2010). New strategies of pelvic nerves stimulation for recovery of pelvic visceral functions and locomotion in paraplegics. *Neurourol. Urodyn.* 29, 1433–1438. doi: 10.1002/nau.20897

Rijkhoff N. J. M. (2004). Neuroprostheses to treat neurogenic bladder dysfunction: current status and future perspectives. *Childs Nerv. Syst.* 20, 75–86. doi: 10.1007/s00381-003-0859-1

Sijobert, B. (2018). *Assistive control of motion in sensorimotor impairments based on functional electrical stimulation* (Ph.D. Thesis). University Montpellier, Montpellier, France.

Sijobert, B., Azevedo, C., Andreu, D., Verna, C., and Geny, C. (2017). Effects of sensitive electrical stimulation-based somatosensory cueing in Parkinson's disease gait and freezing of gait assessment. *Artif. Organs.* 41, E222–E232. doi: 10.1111/aor.13059

Smith, B., Zhengnian, T., Johnson, M. W., Pourmehdi, S., Gazdik, M. M., Buckett J. R., et al. (1998). An externally powered, multichannel, implantable stimulator-telemeter for control of paralyzed muscle. *IEEE Trans. Biomed. Eng.* 45, 463–475. doi: 10.1109/10.664202

Vette A. H., Masani, K., and Popovic, M. R. (2008). "Time delay from muscle activation to torque generation during quiet stance: implications for closed-loop control via FES," in *13th Annual Conference of the IFES Society*, (Freiburg) 423–425.

Wagner, F. B., Mignardot, J. B., Le Goff-Mignardot, C. G., Demesmaeker, R., Komi, S., Capogrosso, M., et al. (2018). Targeted neurotechnology restores walking in humans with spinal cord injury. *Nature* 563, 1476–4687. doi: 10.1038/s41586-018-0649-2

Weber, D. J., Stein, R. B., Chan, K. M., Loeb, G., Richmond, F., Rolf, R., et al. (2005). BIONic WalkAide for correcting foot drop. *IEEE Trans. Neural Syst. Rehabil. Eng.* 13, 242–246. doi: 10.1109/TNSRE.2005.847385

Zhan, L., Guiraud, D., Andreu, D., Gelis, A., Fattal, C., and Hayashibe, M. (2018). Real-time closed-loop functional electrical stimulation control of muscle activation with evoked electromyography feedback for spinal cord injured patients. *Int. J. Neural Syst.* 28:17 50063.

Conflict of Interest: MT was employed by the company Vivaltis.

The remaining authors declare that the research was conducted in the absence of any commercial or financial relationships that could be construed as a potential conflict of interest.

APPENDIX

STIMAP is a MAC protocol based on the master/slaves model and dynamic TDMA (details in Andreu et al., 2009). Dynamic TDMA is used dealing with medium access for a group of units (**Figure A1**). TDMA relies on the allocation of one time-slot of duration D to each member of the group. The time-slot duration D is the same for all the members of the group. The time-slot duration is dynamically set by the CU (the master) depending on the type of request it sends to the group (the slaves). This means that the CU can define D at each group-based communication it induces. For example, a slave needs less time to reply to a test of presence (a simple acknowledgment) than to send back data samples, since the frame sizes are different. So the CU has to adapt D to each of these requests. Let's consider a group G of N_G members. Each member has a membership number in this group given by P_G. The CU sends a request to this group G, indicating through its request the time-slot duration D and the number of the membership that must start replying, thereafter called starting priority SP.

Knowing its membership number in the group, the group size and the starting priority, each member of the group determines itself the position of its time-slot. This position is given by the variable Pos_{P_G}, which corresponds to the position of the member P_G in the communication round.

$$Pos_{P_G} = P_G - SP + \alpha_P \times N_G \tag{A1}$$

where:

- P_G is the membership number (priority from 0 to $N_G - 1$),
- SP is the priority number of the member that must first reply,
- N_G is the G group size,

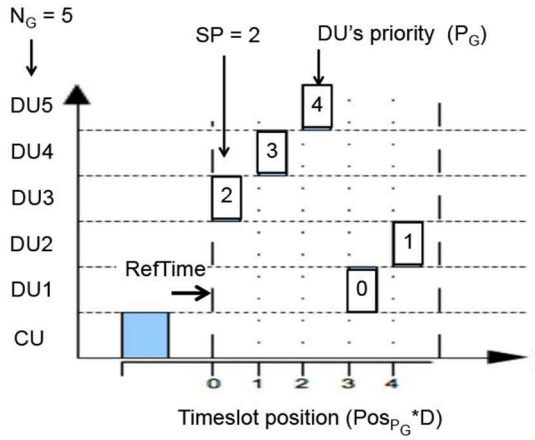

FIGURE A1 | Schematic representation of STIMAP TDMA.

- and $\alpha_p = 1$ if $P_G < SP$ else $\alpha_p = 0$.

And then, from a time point of view, the time-slot position of member P_G is given by:

$$TimeSlotPosition_{P_G} = RefTime_{P_G} + Pos_{P_G} \times D \tag{A2}$$

where:

- D is the dynamically set time-slot duration,
- and $RefTime_{P_G}$ corresponds to the reference instant of time for member P_G. This reference time being defined by:

$$RefTime_{P_G} = \frac{D}{2} - \frac{RTT_{P_G}}{2} \tag{A3}$$

frontiers in Neuroscience

ORIGINAL RESEARCH
published: 26 March 2020
doi: 10.3389/fnins.2020.00263

Mechanotactile Sensory Feedback Improves Embodiment of a Prosthetic Hand During Active Use

*Ahmed W. Shehata[1], Mayank Rehani[1], Zaheera E. Jassat[1,2] and Jacqueline S. Hebert[1,2]**

[1] Division of Physical Medicine and Rehabilitation, Department of Medicine, Faculty of Medicine and Dentistry, University of Alberta, Edmonton, AB, Canada, [2] Glenrose Rehabilitation Hospital, Alberta Health Services, Edmonton, AB, Canada

There have been several advancements in the field of myoelectric prostheses to improve dexterity and restore hand grasp patterns for persons with upper limb loss, including robust control strategies, novel sensory feedback, and multifunction prosthetic terminal devices. Although these advancements have shown to improve prosthesis performance, a key element that may further improve acceptance is often overlooked. Embodiment, which encompasses the feeling of owning, controlling and locating the device without the need to constantly look at it, has been shown to be affected by sensory feedback. However, the specific aspects of embodiment that are influenced are not clearly understood, particularly when a prosthesis is actively controlled. In this work, we used a sensorized simulated prosthesis in able-bodied participants to investigate the contribution of sensory feedback, active motor control, and the combination of both to the components of embodiment; using a common methodology in the literature, namely the rubber hand illusion (RHI). Our results indicate that (1) the sensorized simulated prosthesis may be embodied by able-bodied users in a similar fashion as prosthetic devices embodied by persons with upper limb amputation, and (2) mechanotactile sensory feedback might not only be useful for improving certain aspects of embodiment, i.e., ownership and location, but also may have a modulating effect on other aspects, namely sense of agency, when provided asynchronously during active motor control tasks. This work may allow us to further investigate and manipulate factors contributing to the complex phenomenon of embodiment in relation to active motor control of a device, enabling future study of more precise quantitative measures of embodiment that do not rely as much on subjective perception.

Keywords: rubber hand illusion, prosthetics, sensory feedback, embodiment, motor learning, electromyography, simulated prosthesis

OPEN ACCESS

Edited by:
Max Ortiz-Catalan, Chalmers University of Technology, Sweden

Reviewed by:
Giovanni Di Pino, Campus Bio-Medico University, Italy
Francesco Clemente, Scuola Superiore Sant'Anna, Italy

***Correspondence:**
Jacqueline S. Hebert
jhebert@ualberta.ca

Specialty section:
This article was submitted to Neural Technology, a section of the journal Frontiers in Neuroscience

Received: *20 November 2019*
Accepted: *09 March 2020*
Published: *26 March 2020*

Citation:
Shehata AW, Rehani M, Jassat ZE and Hebert JS (2020) Mechanotactile Sensory Feedback Improves Embodiment of a Prosthetic Hand During Active Use. Front. Neurosci. 14:263. doi: 10.3389/fnins.2020.00263

INTRODUCTION

Persons with upper limb amputation face significant limitations in performing activities of daily living. Myoelectric prosthesis, controlled by electrical signals extracted from residual limb muscles, provide a potentially feasible solution (Belter et al., 2013; van der Riet et al., 2013; Geethanjali, 2016), however, dissatisfaction and rejection of the prosthesis remains high, with some studies

Abbreviations: RHI, rubber hand illusion; SB, synchronous brushing; AB, asynchronous brushing; ST, synchronous tapping; AT, asynchronous tapping.

reporting up to 75% of myoelectric prosthesis users abandoning their device (Biddiss and Chau, 2007). Although there have been several advancements to improve dexterity and restore hand grasp patterns (Gallagher, 1986; Murray, 2004; Giummarra et al., 2008), myoelectric prostheses do not provide continuous feedback to allow real-time regulation of muscle contraction. The lack of feedback poses a significant challenge to the prosthesis user; without such sensory feedback, the prosthesis needs near-constant visual attention and mental concentration to operate (Sobuh et al., 2014; Hebert et al., 2019).

Sensory feedback has thus been highlighted as a possible missing element for improving the acceptance of upper limb prosthetic devices (Ehrsson et al., 2004; Longo et al., 2008). One hypothesis is that sensory feedback will restore the feeling of ownership of the prosthesis as part of the body, by facilitating integration of the prosthesis into the body representation (Gallagher, 1986; Murray, 2004). Although ownership can be induced by providing sensory input matched to natural sensation, i.e., pressure proportionally matching touch sensation, in an expected location and orientation (Giummarra et al., 2008), embodiment is likely a more complex phenomenon. Embodiment is thought to involve sub-components of ownership (the feeling that the hand is actually a part of the body), location (the sensation that the hand is in an appropriate area and that a relationship exists between what is seen in that area and where it is felt on the hand) and agency (a feeling of control over the actions of the hand) (Ehrsson et al., 2004; Longo et al., 2008). These items interrelate and may result in a foreign object, such as the prosthetic hand, being integrated into the body schema (Gallagher and Cole, 1995), which may increase acceptance and use of the prosthesis.

Prior research has used an experimental paradigm called the rubber hand illusion (RHI) to elicit the sense of embodiment by applying synchronous stimulation to a rubber hand and the participant's hand, demonstrating that the sense of body ownership is closely associated with cutaneous touch (Botvinick and Cohen, 1998; Ehrsson et al., 2004; Tsakiris and Haggard, 2005; Longo et al., 2008). The RHI is a robust phenomenon and appears to be sensitive to the relative strength of the tactile input (Ehrsson et al., 2008). Tactile input has been shown to induce this illusion even if it is modality mismatched (D'Alonzo and Cipriani, 2012), however, the input needs to be delivered synchronously in order to preserve the illusion (Armel and Ramachandran, 2003; Ehrsson et al., 2004; D'Alonzo and Cipriani, 2012). In persons with upper limb amputation who have undergone the targeted reinnervation procedure, the provision of direct cutaneous touch feedback to the residual limb has been reported to create a vivid illusion of ownership of a passive prosthetic hand (Marasco et al., 2011), similar to other populations with upper limb amputation when synchronous touches were applied to their residual limb and a rubber hand (Ehrsson et al., 2008) or a robotic hand (Rosen et al., 2009).

Adding active control of the hand has been shown to enhance the experience of the RHI; both able-bodied and participants with amputation have been shown to experience a sense of ownership over the robotic hand when they were remotely controlling the robotic movements (Rosen et al., 2009; Sato et al., 2018). In fact, active motor control of a congruent movement was shown to induce both ownership and agency, without a significant effect of additional brushing feedback (Sato et al., 2018). Studies in participants with amputation have further shown that embodiment responses can be positive with motor control alone as well as with sensory feedback provided by peripheral intraneural stimulation (Graczyk et al., 2018; Page et al., 2018), and that the naturalness of the tactile sensation elicited by nerve stimulation may affect embodiment responses (Valle et al., 2018). Furthermore, in other participants with wearable closed-loop control prosthetic systems, it has been shown that kinesthetic feedback enhances agency but not ownership (Marasco et al., 2018).

There is, therefore, building evidence that multisensory inputs of both sensation and motoric cues can enhance the sense of ownership (Kalckert and Ehrsson, 2014). However, there remains some inconsistency in the literature regarding the relative contribution of active motor control with or without concordant sensory stimulation to agency and ownership. The ability to further investigate these factors is limited by the small number of participants with bidirectional sensory feedback systems and the limitations of altering their sensory feedback parameters to explore the impact of feedback type.

A common technique used to study myoelectric prosthesis function is the use of simulated devices on able-bodied research participants as an approximation to prostheses used by persons with upper-limb amputation (Panarese et al., 2009; Amsuess et al., 2016; Johansen et al., 2016; Clemente et al., 2017; White et al., 2017). We designed such a device to allow the manipulation of sensory feedback during motor control (Kuus et al., 2017), to investigate the factors of ownership, location, and agency in a wearable prosthesis. The objective of the current work was to assess the embodiment responses of participants using a wearable simulated prosthesis platform providing mechanotactile feedback during active motor control. In order to ascertain the validity of this approach in comparison to the classic RHI, we first had to determine the influence of type of feedback (mechanotactile tapping versus brushing) in a passive condition with the worn prosthesis simulator (the "passive prosthesis test"), followed by investigation of the contributions of active motor control to the embodiment phenomenon (the "active prosthesis test").

MATERIALS AND METHODS

In this study, we used a simulated prosthesis that allows the integration of sensors and mechanotactile feedback tactors (Kuus et al., 2017). The study was divided into two test phases – passive prosthesis test and active prosthesis test.

Study Participants

Twenty-one able-bodied individuals were recruited to participate in this study [12 females; age: 31.9 ± 9.3 (mean ± SD); 3 left-hand dominant]. All participants were over 18 years old with no upper limb dysfunction (no muscular or neurological dysfunction, no sensory deficit in the hand), normal or corrected to normal vision, and no upper limb surgery in the past year.

Only 1 participant had previous experience operating a simulated prosthesis. Written informed consent according to the University of Alberta Health Research Ethics Board was obtained from all participants before conducting the experiment (Pro00057340).

Experimental Setup

Participants sat comfortably on a chair in front of a table and facing the experimenter. The height of the chair was adjusted to ensure that the participant's arm was resting on the table. A black sheet was placed over the participant's shoulder to ensure that their arm was completely obscured. Noise-canceling headphones were placed over the participant's ears during testing but were removed during instruction phases and setup.

Device Setup and Control Parameters

The participant's right arm was secured in an adjustable brace that comfortably restricted wrist movement. A prosthetic hand was secured to the brace such that it was oriented beneath the participant's right hand, similar to the specifications outlined by Kuus et al. (2017) with adjustments of the strapping to allow access to the participant's hand. The prosthetic hand was controlled using two-cite proportional myoelectric control (Battye et al., 1955) with one of the electromyography (EMG) sensors placed on the wrist extensor muscle and the other placed on the wrist flexor muscle. Muscle contractions at these sites were mapped to the velocity of the opening and closing of the single degree of freedom prosthetic hand. EMG sensor gains were adjusted to ensure easy and reliable control of the prosthetic hand. The participant was free to move around with the brace attached during training to use the device, but the testing occurred in a seated position resting the device on the table.

Tactor Setup

Three mechanotactile tactors integrated into the brace were aligned to stimulate the thumb, index, and middle fingers of the participant to relay tactile feedback to participants. These tactors pushed on the participant's fingers by converting rotational motion from a motor using rack and pinion gears to linear motion (Figure 6a in Schoepp et al., 2018). The linear displacement of these actuators on the fingertips was mapped proportionally to the force sensed using force-sensitive resistor sensors that were placed on the corresponding thumb, index, and middle fingers of the prosthetic hand (Saunders and Vijayakumar, 2011). This system had an average delay in response of 92 ± 16 ms, which is below the recommended threshold to evoke embodiment (Ismail and Shimada, 2016).

Experimental Protocol

In the first portion of this study, we investigated the effect of receiving two types of feedback (brushing and tapping) with and without delay (asynchronous and synchronous, respectively) on the sense of embodiment of the prosthetic hand while wearing the device during a Passive Prosthesis Test. We then investigated the effect of providing no feedback, synchronous tapping feedback, or asynchronous (delayed) tapping feedback during an Active Prosthesis Test. After each test and for each feedback condition, participants were asked to perform an assessment of proprioceptive drift followed by filling out a questionnaire. An overview of the experimental protocol is provided in **Figure 1**.

Passive Prosthesis Test

A box that was accessible from both the front and back sides was placed on the table in front of the participant. This box was placed over the participant's right arm between the brace and the prosthetic hand (**Figure 2**). The black sheet that was covering the participant's arm and shoulder was adjusted if needed. In this manner, the participant could see only the prosthetic hand and forearm section, but not their real hand or forearm. The experimenter administered various conditions of feedback stimuli to the participant's obscured right hand and to the visible prosthetic hand.

The combination of two different feedback types (brushing and tapping) and two different feedback timing (synchronous and asynchronous) yielded four different conditions of feedback stimuli. These conditions were: Synchronous Brushing (SB), Asynchronous Brushing (AB), Synchronous Tapping (ST), and Asynchronous Tapping (AT) (described in **Table 1**). A single trial block for each condition consisted of the experimenter applying the feedback stimulus, followed by the participant performing an assessment of proprioceptive drift and then filling out a questionnaire (**Appendix A**).

Participants were randomized into one of ten predetermined randomization sequences (**Figure 1A**). Each of these sequences consisted of 2 repetitions of each of the 4 conditions, presented in a random order for a total of 8 trial blocks (2×4).

Active Prosthesis Test

Participants had active motor control of the prosthetic hand, as per device setup 2.2.1. The participants were provided with a period of functional task training, wherein they used the simulated prosthesis to grasp and move objects with the prosthetic hand in a structured environment. They were encouraged to grasp and release a variety of objects of different sizes and densities (soft balls, blocks, plastic cups) to ensure adequate control and to experience the sensory feedback. Objects were then presented in a predetermined order, and participants were instructed to move the object to different positions or to stack them. Participants were asked to be as precise as possible and told that the time taken for each manipulation was not going to be considered, so that they would focus on the sensory experience and control rather than speed of moving the objects. Once they completed the object manipulation sequence, the participant would immediately rest their arm and device on the table.

For this test, three feedback conditions were tested, namely ST, AT, and no feedback. For all conditions, the participants had the same active motor control of the prosthetic hand. A trial block consisted of the participant actively using the prosthesis for grasp activities with one of the feedback conditions, followed by an assessment of proprioceptive drift, and then filling out the questionnaire. Participants were randomized to one of ten randomized sequences (**Figure 1B**). Each of these sequences consisted of two repetitions of each of the six conditions, presented in a random order for a total of six trial blocks.

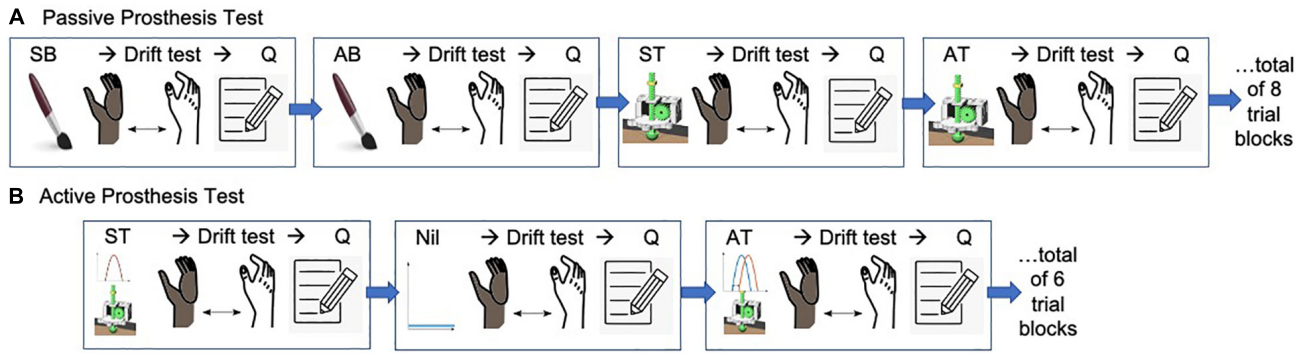

FIGURE 1 | Overview of experimental protocol. **(A)** A representative randomization sequence for the Passive Prosthesis Test. There were 4 feedback conditions tested: Synchronous Brushing (SB), Asynchronous Brushing (AB), Synchronous Tapping (ST), and Asynchronous Tapping (AT). A single trial block consisted of the experimenter applying one of the feedback conditions, followed by the participant performing the drift test, and then filling out the questionnaire (Q). Participants were randomized into one of ten predetermined randomization sequences, each consisting of 2 repetitions of each of the 4 conditions, presented in a random order for a total of 8 trial blocks. **(B)** A representative randomization sequence for the Active Prosthesis Test. For this test, the participant actively controlled the prosthesis in 3 feedback conditions: Synchronous Tapping (ST), Asynchronous Tapping (AT), and no feedback (Nil), for which the tactors were turned off. A trial block consisted of the participant actively using the prosthesis for grasp activities with one of the feedback conditions, followed by an assessment of proprioceptive drift, and then filling out the questionnaire. Participants were randomized to one of ten randomized sequences, consisting of 2 repetitions of each of the 3 conditions, presented in a random order for a total of 6 trial blocks.

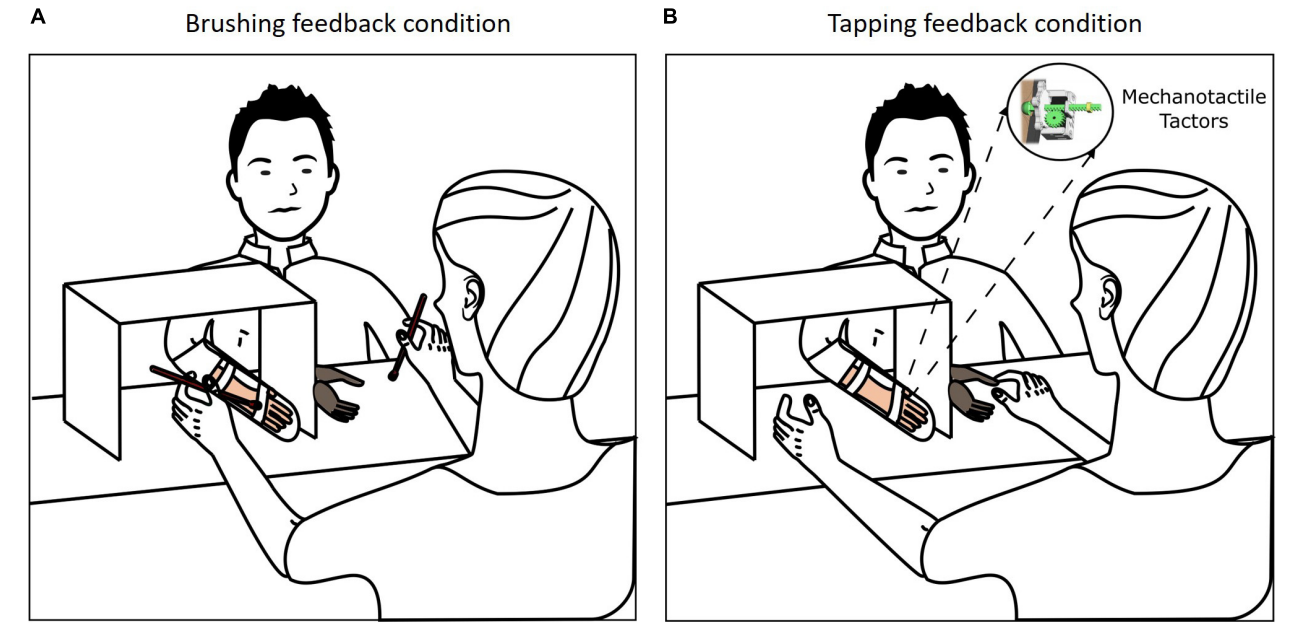

FIGURE 2 | Experimental setup for Passive Prosthesis Test. **(A)** Brushing feedback condition. The brushing stimulation was administered by the experimenter to the prosthetic hand and to the participant's hand with two paintbrushes. **(B)** Tapping feedback condition. Three mechanotactile tactors placed on the thumb, index and middle fingers of the participant delivered a mechanotactile stimulus when the experimenter applied pressure to the corresponding sensors on the fingertips of the prosthetic hand.

During ST condition block, participants felt the mechanotactile tactor push on their right-hand thumb, index, and middle fingers when using the prosthetic hand to grasp objects. Ismail and Shimada (Ismail and Shimada, 2016) showed that participants felt significant weaker sense of agency with temporal delays of 240–490 ms; therefore, for the AT condition block, the mechanotactile tactors were delayed by 500 ms, and for the no feedback condition the tactors were switched off. For all conditions, the participants had the same active motor control of the prosthetic hand.

Outcome Measures

Following each testing condition, participants were asked to (a) with vision obscured, point with their left index finger on the board where they thought the tip of their actual index finger was (to measure proprioceptive drift) and (b) rate their agreement

TABLE 1 | Feedback stimuli provided to the participant in random order during the passive prosthesis test.

Feedback stimulus	Description
Synchronous brushing (SB)	Both the prosthetic hand (in view of the participant) and the obscured participant's right hand were stroked with a paintbrush at the same time, location, and duration. Stimulation was delivered randomly to each location with varying durations (**Figure 1A**)
Asynchronous brushing (AB)	The prosthetic hand was stroked with a paintbrush at the same location as the participant's hand, but at a different time and duration. Stimulation was delivered randomly to different locations with varying durations.
Synchronous tapping (ST)	The sensorized fingers of the prosthetic hand were pressed resulting in the mechanotactile tactor applying pressure on the corresponding finger of the participant. Stimulation was delivered randomly to each finger with varying durations and pressures (**Figure 1B**)
Asynchronous tapping (AT)	A time delay was introduced into the mechanotactile tactor program resulting in a delayed response of 500 ms to pressure applied on the sensorized prosthetic finger. The sensorized fingers of the prosthetic hand were pressed resulting in the mechanotactile tactor applying a 500 ms delayed pressure on the corresponding finger of the participant. Stimulation was delivered randomly to each finger with varying durations and pressures.

with 10 questions in the embodiment survey using a visual analog scale, adapted from previous work in this area (Ehrsson et al., 2008; Longo et al., 2008).

Proprioceptive Drift

The proprioceptive drift, outlined by Tsakiris et al. (2005), was calculated by measuring the difference between the points at which the participant indicated the position of their index finger pre- and post-test. With eyes closed, participants were instructed to point with their left index finger where they thought the tip of their finger was before and after a test. A positive result (positive drift) was indicative of the participant locating their hand toward the prosthetic hand. A negative result (negative drift) indicated that the participant had located their hand further away from the prosthetic hand.

Embodiment Questionnaire

Ten questions (five control and five related to embodiment) were adapted from Ehrsson et al. (2008) and Longo et al. (2008) (see **Supplementary Table S1**) (Ehrsson et al., 2004; Longo et al., 2008), similar to modifications used by prior authors for closed loop prosthetic control (Marasco et al., 2011; Graczyk et al., 2018; Page et al., 2018; Valle et al., 2018). The control statements were included to assess suggestibility and the embodiment statements were included to assess perception of key components of embodiment which are location, ownership, and agency. Additional questions on agency and "loss of hand" were included as potential components of the RHI, modified from Longo et al. (2008). Four versions of this questionnaire with a randomized order of the questions were developed, and a randomly selected version of the questionnaire was administered after each condition. The participant was asked to rate the strength of their agreement or disagreement for each question by pointing on the Visual Analog Scale with their left index finger. The scale was graded from 0 mm (strongly disagree) to 100 mm (strongly agree), and the distance was measured in millimeters. Higher grades on the embodiment questions indicated a greater sense of embodiment.

Statistical Analysis

Normality was assessed using Levene's test. A paired sampled t-test was conducted to assess if there was a difference between the means of embodiment questions (Q1–Q5) and control questions (Q6–Q10) for each condition, to determine suggestibility.

A repeated measures Analysis of Variance (ANOVA) with Bonferroni correction was used on the average score of the embodiment questions. The factors for the ANOVA were Feedback Type and Feedback Condition, and levels of the factors were Brushing/Tapping and Synchronous/Asynchronous, respectively. The *F*-test of significance was used to assess the effects of the different independent variables. If significance was found, pairwise comparisons were made to assess where the differences lie. An α of 0.05 was used for all comparisons, and Bonferroni correction for multiple comparisons was utilized.

If a significant difference was detected between conditions on the average embodiment scores, then repeated measures ANOVA was run on the VAS response to each embodiment question (Q1–5) across conditions to determine if we could further detect differences among the responses to individual questions.

RESULTS

Passive Prosthesis Embodiment

Responses to the questionnaire show that there was a statistically significant difference between the responses to embodiment items (Q1–Q5) and control items (Q6–Q10) for synchronous brushing feedback condition, as determined by paired sample *t*-test [$t(20) = 5.1$, $p < 0.001$]. Conversely, there was no statistically significant difference between participant's responses to embodiment items and control items for the asynchronous brushing feedback condition; paired sample *t*-test [$t(20) = 1.8$, $p = 0.095$; **Supplementary Table S2**]. Both of these findings confirm that participants were not suggestible.

Participants' responses to embodiment questions (Q1–Q5) were statistically significantly different between all tested conditions as determined by repeated measures ANOVA [$F(3, 60) = 9.8$, $p < 0.001$]; *post hoc* analysis indicated all comparisons were significantly different, except for SB vs. ST (**Supplementary Figure S1** and **Supplementary Table S3**). Further analysis of the responses to individual questions indicated that providing users with synchronous brushing feedback prompted a significantly higher sense of embodiment on 4 out 5 of the embodiment questions than when providing users with asynchronous brushing feedback (Q 1, 2, 3, and 5, Bonferroni *post hoc* test, $p < 0.05$). The only question that did not evoke a significantly stronger response with synchronous brushing was the agency question (Q4) (**Figure 3**).

Results from the proprioceptive drift test showed a significant difference between testing conditions as determined by repeated measures ANOVA [$F(3, 60) = 3.02$, $p = 0.036$;

Supplementary Table S3]. Bonferroni *post hoc* analysis showed that participants had statistically significantly higher drift toward the prosthesis after receiving synchronous brushing feedback (14 ± 5.8 mm) or synchronous tapping feedback (6 ± 5.5 mm) compared to asynchronous tapping feedback (-13 ± 5.9 mm) (p = 0.014 and p = 0.018, respectively; **Figure 4**). Temporal manipulation of the brushing feedback (AB) did not result in a statistically significant difference in proprioceptive drift compared to the synchronous conditions, although the trend was to drift away from the prosthesis (−4 ± 6.0 mm).

To ensure that the mechanotactile system described in this work would have similar positive effects on prosthesis embodiment to brushing feedback, we also compared individual questionnaire responses for mechanotactile ST feedback to SB feedback (**Figure 5**). There was no statistically significant difference in responses to the embodiment statements between synchronous brushing and synchronous tapping conditions as determined by paired sample t-test [$t(4)$ = 2.78, p = 0.26]. A Pearson product-moment correlation was performed to determine the relationship between responses to the questionnaire after receiving SB feedback and after receiving ST feedback in the passive prosthesis test. There was a strong, positive correlation between SB and ST, which was statistically significant (r = 0.919, n = 10, p = 0.00017).

It is worth noting that, although not statistically significant, brushing feedback tended to evoke more positive responses on the first three embodiment statements than the tapping feedback (**Figure 5**). Similarly, participants had a trend toward greater proprioceptive drift toward the prosthetic hand when provided with synchronous brushing feedback than when provided with

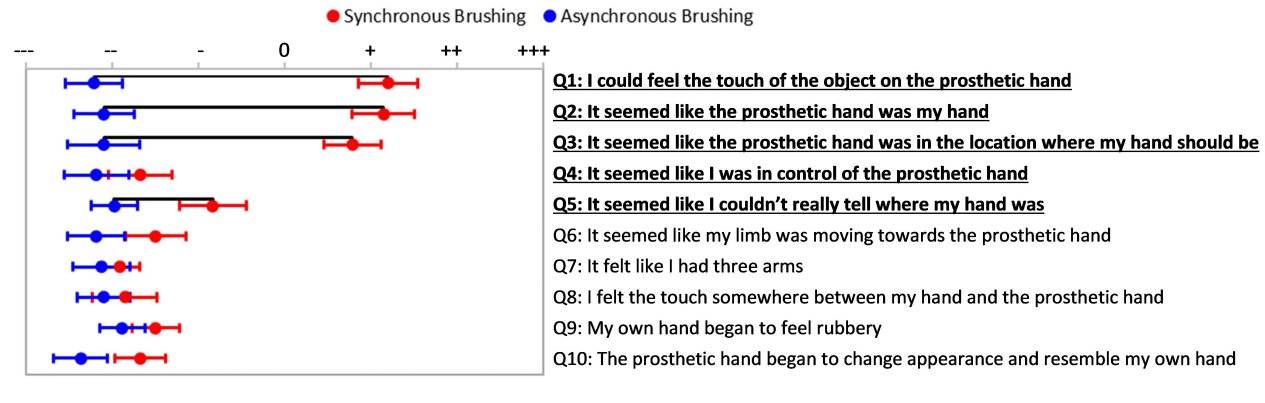

FIGURE 3 | Passive Prosthesis Test: Questionnaire results for synchronous and asynchronous brushing. The questionnaire included these 10 statements, presented randomly. Statements 1–5 were used to describe aspects of the embodiment phenomena (Longo et al., 2008). Subjects indicated their response on a visual analog scale ranging from strongly disagree to strongly agree. Red points indicate mean responses for synchronous brushing condition and blue points indicate mean responses for asynchronous brushing condition. Bars extending from these points indicate standard error of the mean (SEM) response. Horizontal black lines indicate statistically significant tendency to evoke affirmative responses ($p < 0.05$).

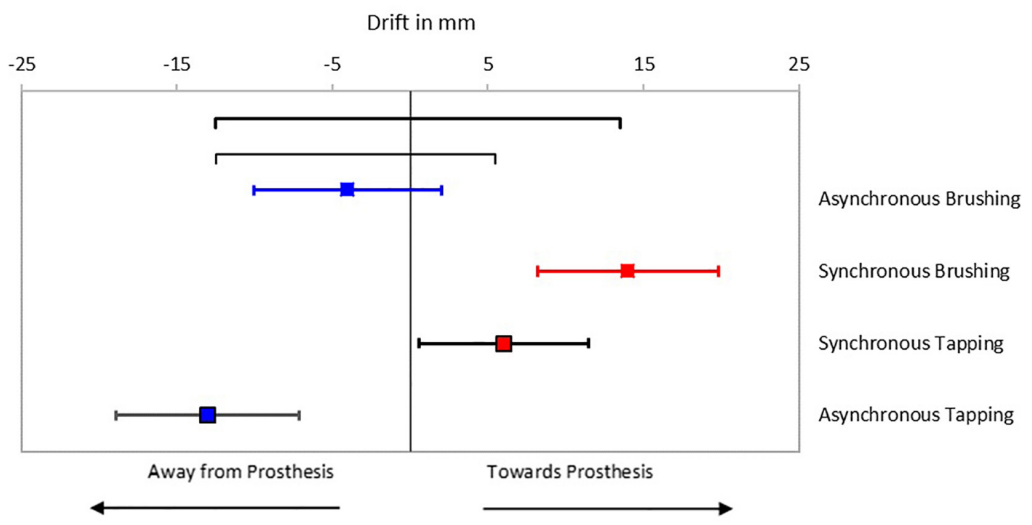

FIGURE 4 | Passive Prosthesis Test: Mean proprioceptive drifts toward the prosthetic hand for each of the conditions. Error bars indicate standard error of the mean. Black horizontal lines indicate statistical significance at $p < 0.05$. Red blocks indicate synchronous feedback, and blue blocks indicate asynchronous feedback.

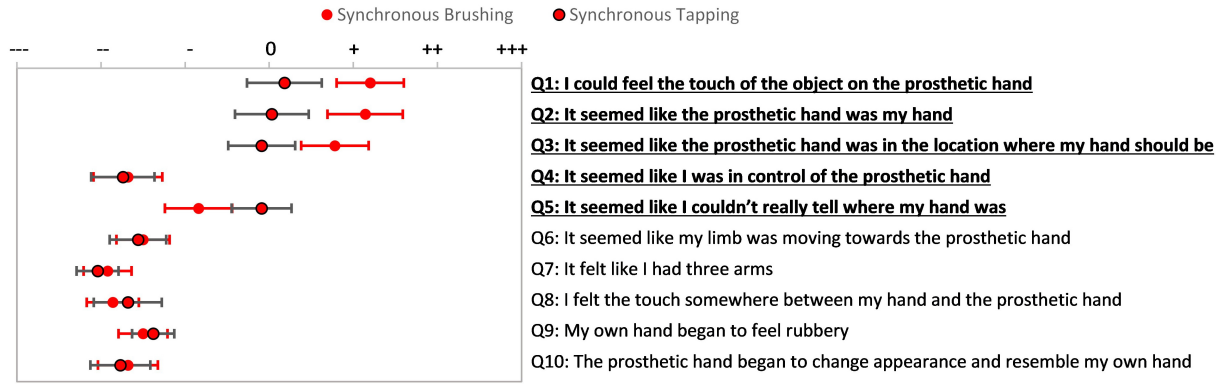

FIGURE 5 | Passive Prosthesis Test: Questionnaire results for synchronous feedback conditions. Participants' responses on statements 1–4 for synchronous brushing were higher than their corresponding responses for synchronous tapping. No statistically significant difference was found between both feedback types. Red points indicate mean responses for synchronous brushing condition and red with black outline dots indicate mean responses for synchronous tapping condition. Bars extending from these points indicate standard error of the mean (SEM) response.

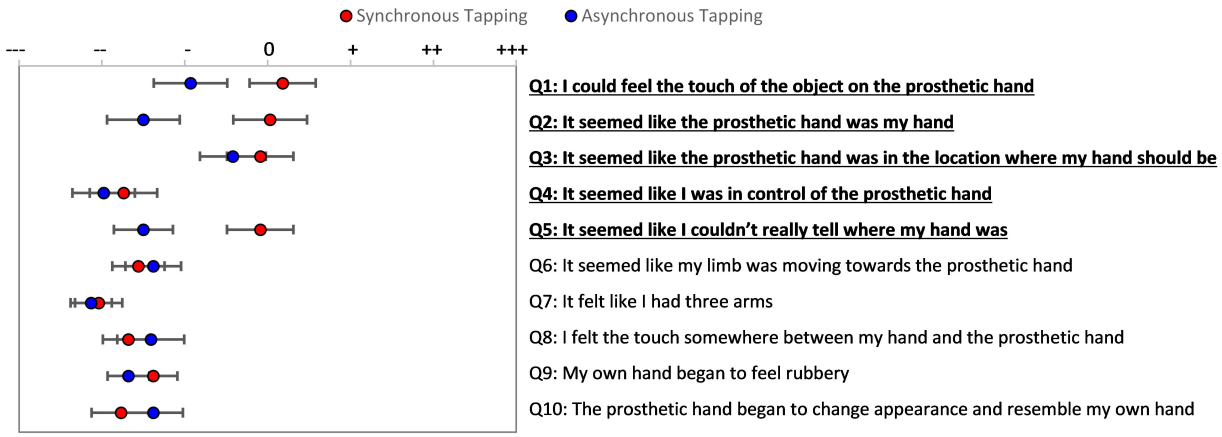

FIGURE 6 | Passive Prosthesis Test: Questionnaire results for synchronous and asynchronous tapping feedback conditions. Subjects indicated their response on a visual analog scale ranging from strongly disagree to strongly agree. Red with black outline points indicate mean responses for synchronous tapping condition and blue with black outline points indicate mean responses for asynchronous tapping condition. Bars extending from these points indicate standard error of the mean (SEM) response.

synchronous tapping feedback (see **Figure 4**), however this was not statistically significant.

Similar to the brushing condition, comparing the embodiment items to the control items for each tapping condition confirmed that participants were not suggestible, with a significant difference for the synchronous tapping condition [$t(20) = 3.8$, $p = 0.001$], but not for asynchronous tapping [$t(20) = 2.0$, $p = 0.06$]. The average of the embodiment question scores were statistically significantly different between synchronous and asynchronous conditions of the tapping feedback on Bonferroni *post hoc* analysis ($p = 0.02$; **Supplementary Table S3**). When examining individual questions, there was a trend for the temporal delay of the mechanotactile tapping feedback (AT) to negatively affect participants' responses to embodiment statements in the questionnaire (**Figure 6**), although no statistically significant differences were found in responses to individual questions ($p > 0.05$).

Active Prosthesis Embodiment

Having determined that tapping feedback using mechanotactile tactors promotes the embodiment of the prosthesis in a passive condition similar to brushing with the hand and forearm constrained in the brace, we next compared participants' responses after actively controlling the prosthetic device with synchronous mechanotactile tapping feedback, delayed tapping feedback, and without tapping feedback. Responses to the questionnaire show that there was a statistically significant difference between the responses to embodiment items (Q1–Q5) and control items (Q6–Q10) within each condition, as determined by paired sample *t*-test [ST: $t(18) = 5.5$, $p < 0.001$; AT: $t(18) = 4.0$, $p = 0.001$; no feedback: $t(18) = 2.6$, $p = 0.02$; **Supplementary Table S4**].

There was a significant difference in embodiment responses during the active prosthesis test with synchronous mechanotactile tapping feedback, delayed feedback, and

no feedback as determined by repeated measures ANOVA [$F(2, 36) = 7.2$, $p = 0.002$]; **Supplementary Figure S2** and **Supplementary Table S5**. Bonferroni *Post hoc* analysis showed that providing synchronous mechanotactile tapping feedback to participants while controlling the simulated prosthesis promoted statistically significant higher average responses to the embodiment questions than either asynchronous ($p = 0.003$) or no feedback ($p = 0.003$). When examining responses to individual embodiment questions, there was a significantly higher response to embodiment statement 1 with synchronous feedback compared to the response to the same statement when provided with no feedback ($p = 0.004$) (**Figure 7**). In contrast to the passive prosthesis experiment, high responses were seen on the agency question (Q4) for both the synchronous and no feedback conditions, with asynchronous tapping showing a non-significant trend of negatively affecting agency.

Results from the proprioceptive drift task in the Active Prosthesis Test showed all conditions resulted in some shift toward the prosthetic hand with a trend to higher proprioceptive drift for the synchronous tapping condition (shown in **Figure 8**), although not statistically significant (**Supplementary Table S5**).

DISCUSSION

Simulated upper-limb prosthesis systems are commonly used as an approximation to prostheses used by persons with upper-limb amputation, as a method of allowing able-bodied participants to actively control a prosthetic hand in a situation more similar to actual prosthesis use. Researchers have used various versions of simulated prostheses to investigate the performance of commercial prosthetic hands (Kyberd, 2011), performance of novel control strategies (Johansen et al., 2016; Shehata et al., 2018a), kinematic movement trajectories when using prosthetic hands (Williams et al., 2019), and, recently, the effect of providing sensory feedback to users on performance in functional tasks (Wilson et al., 2017; Engels et al., 2019). In this work, we used a sensorized simulated prosthesis to investigate the contribution of sensory feedback to the embodiment phenomenon during active motor control of the prosthesis, utilizing a common methodology in the literature, namely the RHI (Longo et al., 2008).

Passive RHI

Wearing a simulated prosthesis in a passive situation evoked similar embodiment responses to prior work with the RHI. Specifically, we found that similar to other studies (Botvinick and Cohen, 1998; Tsakiris et al., 2005), participants tended to embody the prosthesis in the passive synchronous brushing condition as indicated by their positive responses to location and ownership statements on the questionnaire (particularly Q1–Q3) and high proprioceptive drift toward the device (Tsakiris et al., 2005). This finding was important, as the tactile contact of the brace on the skin of the intact forearm and hand may have presented a distracting stimulus that could alter the embodiment experience (Parmentier et al., 2011). However, brushing stimulation is not common in prosthesis user applications. In previous work (Marasco et al., 2011; Hebert et al., 2014), researchers relayed tactile feedback to persons with upper-limb loss by placing tactors on reinnervated skin areas; therefore, returning physiologically appropriate touch and pressure feedback from the prosthesis to the user through skin indentation. Implantable peripheral nerve interface approaches also most commonly report and utilize touch and pressure feedback corresponding to the digits (Wendelken et al., 2017; Schiefer et al., 2018; George et al., 2019). We, therefore, investigated the effect of using a mechanotactile stimulation of touch and pressure to provide the sensory information (Schoepp et al., 2018), to investigate its effect on simulated prosthesis embodiment. We found that synchronous touch and pressure stimulation evoked similar embodiment responses as brushing (no significant differences and strong positive correlation), although responses were blunted, consistent with prior literature (D'Alonzo and Cipriani, 2012). This finding was not surprising given that stroking a brush is known to evoke higher emotional affective responses (Crucianelli et al., 2013), and affect has also been considered an influential component of embodiment (Longo et al., 2008). The proprioceptive drift results confirmed that the synchronous stimulation conditions evoked higher displacement toward the prosthetic hand compared to the asynchronous tapping condition.

Similar to work in participants with amputation (Ehrsson et al., 2008; Marasco et al., 2011; Schmalzl et al., 2014), in our study, ownership and location aspects of embodiment were affected by the synchronicity of the feedback in the passive condition, however, the agency question was not affected by either synchronous or asynchronous brushing and tapping. This would be expected since participants did not have any control over the device during the first testing phase and therefore did not develop any sense of agency over the device. Our results for the passive (no voluntary control) test, therefore, showed that wearing a sensorized simulated prosthesis with integrated mechanotactile feedback can drive the perceptual shift of certain aspects of embodiment, namely ownership and location.

Active Task

For the active prosthesis experiments, we found that active motor control induced a form of agency, reflected in the agency question and the proprioceptive drift, even for the no feedback condition. These results were consistent with prior findings in able-bodied subjects (Dummer et al., 2009) and those with limb amputation (Ehrsson et al., 2008; Sato et al., 2018). Having control over visualized movements of a robotic hand has been theorized to allow embodiment due to implicit knowledge of a kinesthetic sense, which contributes to making the experience personal (Dummer et al., 2009). The prosthesis user study by Marasco et al. (2018) examined the effect of restoring the kinesthetic sense of hand movement during an active grasping task on embodiment of a prosthetic hand. Results showed that providing kinesthetic feedback conferred a significantly greater sense of agency, but did not affect statements of limb ownership. Our findings support that the sense of agency can be induced by the use of the inherent kinesthetic sense associated with muscle contraction matched to active robotic control in our intact able-bodied participants (Kalckert and Ehrsson, 2012; Marotta et al., 2017), consistent with the restored kinesthesia and sense of agency in those with limb amputation (Marasco et al., 2018).

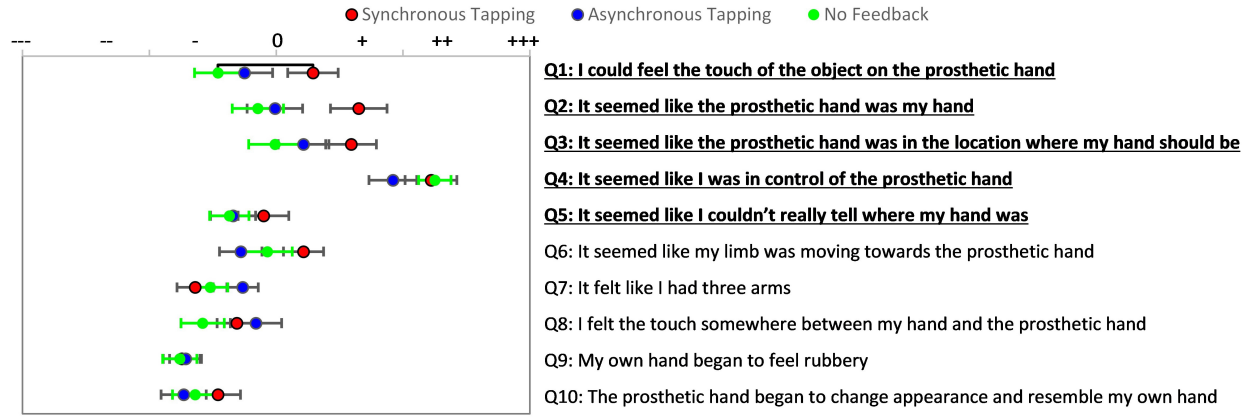

FIGURE 7 | Active Prosthesis Test: Questionnaire results for controlling a prosthesis while receiving three feedback conditions. Participants' responses on statements 1–5 for synchronous tapping were higher than responses for no feedback condition. Red with black outline points indicate mean responses for synchronous tapping condition, blue with black outline dots indicate mean responses for asynchronous tapping condition, and green dots indicate mean responses for no feedback condition. Bars extending from these points indicate standard error of the mean (SEM) response. Horizontal black line indicates statistically significant tendency to evoke affirmative responses ($p < 0.05$).

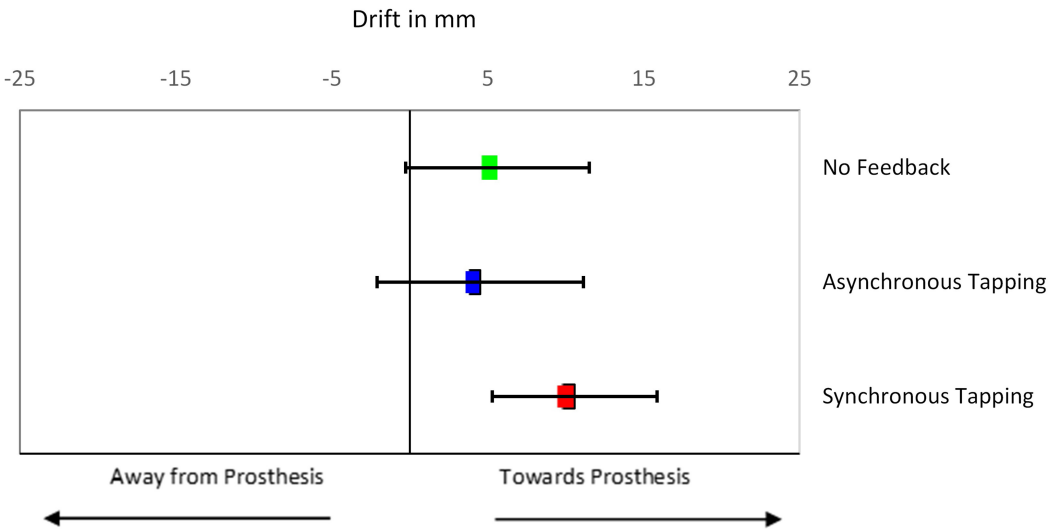

FIGURE 8 | Active Prosthesis Test: Mean proprioceptive drifts toward the prosthetic hand after actively controlling it while receiving three types of feedback. Error bars indicate standard error of the mean. Red with black outline bar indicates synchronous tapping feedback, blue with black outline bar indicates asynchronous tapping feedback, and green bar indicates no feedback condition.

Adding synchronous tactile feedback to the active task enhanced embodiment responses compared to asynchronous or no feedback, when the average score of all embodiment questions were considered. Examining responses to individual questions revealed that synchronous tapping tended to result in the highest embodiment responses particularly for the first three questions, with no feedback resulting in the least amount of embodiment (see **Figure 7**). These findings are consistent with Graczyk et al. (2018), who reported positive responses to embodiment questions in participants with implantable neural interfaces after a sensory-enabled take-home trial; although, this embodiment did persist to the subsequent non-sensory enabled trial. Page et al. (2018) also found that providing sensory feedback to their participants with a neural interface in a passive condition significantly induced embodiment compared to the motor control only condition, however, there was no additional advantage of closed-loop control in enhancing the embodiment response. However, these studies did not conduct a deeper investigation of the sense of agency, which may, in fact, potentiate embodiment (Sato et al., 2018).

In our active prosthesis control experiment, although the addition of synchronous feedback added to specific aspects of embodiment, i.e., ownership and location (as represented by the first three questions), it did not affect agency. Agency was high with active control and not changed with adding synchronous feedback; however, asynchronous feedback tended to result in the

lowest response to the agency question. This possible influence of asynchronous tapping raises an intriguing possibility for a potential mechanism to separate agency from ownership. Given that this finding was based on a single question, additional and more sensitive measures of agency would be helpful to test this hypothesis in future studies.

In the active prosthesis test, in addition to the high positive responses to the sense of agency statement on the questionnaire, participants demonstrated proprioceptive drift toward the simulated prosthesis for all conditions. This finding was unexpected as we hypothesized asynchronous tapping would cause a drift away from the prosthesis, as evidenced in the passive experiment. A possible influencing factor within our set up was that the asynchronous stimulation was provided at a fixed time delay, and the participant may have learned to incorporate that feedback, even though delayed (Blustein et al., 2018). Exploring the effect of timing of delayed feedback on feedback incorporation and real-time control may be an important area of future study.

Others have also noted a discrepancy between drift and subjective ownership responses in passive conditions of synchronous and asynchronous stroking (Rohde et al., 2011). In our work, participants were controlling a simulated prosthesis that was attached to their forearms to grasp and move objects. We propose that our participants utilized the kinesthetic sense of contracting their muscles to control the prosthesis to achieve the sense of agency over hand grasp. The proprioceptive senses associated with more proximal intact sensory organs around the shoulder and elbow could have affected the observed proprioceptive drift (Proske and Gandevia, 2012). There is also evidence that proprioceptive drift and agency may respond similarly (Tajima et al., 2015) and be task dependent (Shibuya et al., 2017). Proprioceptive drift may, therefore, be expected to differ between passive and active conditions, such that there is a stronger influence of motor control on this measurement of embodiment specifically.

Limitations

There are limited opportunities to access participants with bidirectional sensory feedback systems and further limitations in manipulating sensory experiences to explore the impact of feedback type. We, therefore, chose to use able-bodied participants using a simulated prosthesis to determine if their embodiment responses would be similar to those with limb amputation, and potentially modifiable. However, it must be kept in mind that the inherent neurophysiological structures have not been interrupted as in those with limb amputation (Knecht et al., 1996), therefore, these participants are a proxy at best. These preliminary results suggest that the use of a sensory simulated prosthesis can induce embodiment responses (ownership and location) and may separately affect the construct of agency, even with the limited subjective measures employed. This approach opens an avenue for more in-depth exploration of this phenomenon that may then be applied to the sample of individuals with sensory-enabled upper limb prosthesis systems.

We used three traditional embodiment statements commonly cited in the literature, and included additional questions on agency and loss of own hand. The questions, originally derived from Botvinick and Cohen (Botvinick and Cohen, 1998) and modified by other authors (Ehrsson et al., 2008; Longo et al., 2008) were based on experiments designed for a passive experience rather than an active control situation, and may need to be further refined and validated for new experimental paradigms (Gonzalez-Franco and Peck, 2018). Other authors have similarly used analysis of three modified embodiment statements (Graczyk et al., 2018; Page et al., 2018; Valle et al., 2018), as well as answers to individual questions (Marasco et al., 2011; Valle et al., 2018) to interpret embodiment in close-loop prosthetic control conditions. A lack of multiple quantitative measures to assess embodiment and the related phenomenon (such as agency, location, and proprioception) is a clear limitation of this work. The use of subjective questionnaire ratings generally limits the interpretation of the findings and highlights the crucial lack of quantitative measures to address outstanding questions on the components of embodiment such as agency. More recent work on quantitative measures of agency and ownership, including intentional binding paradigms, incorporation measures, and internal model (Haggard et al., 2002; Moore and Obhi, 2012; Kühn et al., 2013; Blustein et al., 2018; Shehata et al., 2018b) may allow future work to more adequately parse out the contributions of sensory feedback and active motor control in an active prosthesis control situation.

CONCLUSION

We have shown that a simulated prosthesis actively used for functional control activities may be embodied by able-bodied users (Ehrsson et al., 2008; Marasco et al., 2011; Schmalzl et al., 2014). In addition, we verified that mechanotactile sensory feedback might not only be useful for improving sense of ownership and location but also may have a modulating effect on the sense of agency when provided asynchronously during active motor control tasks. The simulated sensory-motor prosthesis system may allow us to manipulate the factors contributing to the complex phenomenon of embodiment, enabling future study of more precise quantitative measures of embodiment that do not rely as much on subjective perception, which will be crucial to advancing knowledge in this field.

DATA AVAILABILITY STATEMENT

The raw data supporting the conclusions of this article will be made available upon reasonable request, without undue reservation, to any qualified researcher.

ETHICS STATEMENT

Written informed consent according to the University of Alberta Health Research Ethics Board was obtained from all participants before conducting the experiments (Pro00057340). This work is not a clinical trial. All experiments were conducted with able-bodied participants in a lab setting and not in a clinic.

AUTHOR CONTRIBUTIONS

JSH and ZEJ conceived the idea and designed the study. ZEJ conducted the experiments, summarized the data, and contributed to the manuscript draft. MR and AWS analyzed the data. AWS, MR, and JSH wrote and contributed to manuscript revisions. All authors approved the submitted version.

FUNDING

Open access publication fees supported by the University of Alberta (JSH).

ACKNOWLEDGMENTS

We thank the volunteer participants in this study, the staff, and students at the Bionic Limbs for Improved Natural Control (BLINC) Lab for their help and support, and Tarvo Kuus for assistance with experimental setup and data collection.

SUPPLEMENTARY MATERIAL

The Supplementary Material for this article can be found online at: https://www.frontiersin.org/articles/10.3389/fnins.2020.00263/full#supplementary-material

REFERENCES

Amsuess, S., Vujaklija, I., Goebel, P., Roche, A. D., Graimann, B., Aszmann, O. C., et al. (2016). Context-dependent upper limb prosthesis control for natural and robust use. *IEEE Trans. Neural Syst. Rehabil. Eng.* 24, 744–753. doi: 10.1109/TNSRE.2015.2454240

Armel, K. C., and Ramachandran, V. S. (2003). Projecting sensations to external objects: evidence from skin conductance response. *Proc. Biol. Sci.* 270, 1499–1506. doi: 10.1098/rspb.2003.2364

Battye, C. K., Nightingale, A., and Whillis, J. (1955). The use of myo-electric currents in the operation of prostheses. *J. Bone Joint Surg. Br.* 37-B, 506–510. doi: 10.1302/0301-620X.37B3.506

Belter, J. T., Segil, J. L., Dollar, A. M., and Weir, R. F. (2013). Mechanical design and performance specifications of anthropomorphic prosthetic hands: a review. *J. Rehabil. Res. Dev.* 50, 599–618.

Biddiss, E., and Chau, T. (2007). Upper limb prosthesis use and abandonment: a survey of the last 25 years. *Prosthet. Orthot. Int.* 31, 236–257. doi: 10.1080/03093640600994581

Blustein, D., Wilson, A., and Sensinger, J. (2018). Assessing the quality of supplementary sensory feedback using the crossmodal congruency task. *Sci. Rep.* 8:6203. doi: 10.1038/s41598-018-24560-24563

Botvinick, M., and Cohen, J. (1998). Rubber hands "feel" touch that eyes see. *Nature* 391:756. doi: 10.1038/35784

Clemente, F., Dosen, S., Lonini, L., Markovic, M., Farina, D., and Cipriani, C. (2017). Humans can integrate augmented reality feedback in their sensorimotor control of a robotic hand. *IEEE Trans. Hum. Machine Syst.* 47, 583–589. doi: 10.1109/THMS.2016.2611998

Crucianelli, L., Metcalf, N., Fotopoulou, A. K., and Jenkinson, P. (2013). Bodily pleasure matters: velocity of touch modulates body ownership during the rubber hand illusion. *Front. Psychol.* 4:703. doi: 10.3389/fpsyg.2013.00703

D'Alonzo, M., and Cipriani, C. (2012). Vibrotactile sensory substitution elicits feeling of ownership of an alien hand. *PLoS One* 7:e50756. doi: 10.1371/journal.pone.0050756

Dummer, T., Picot-Annand, A., Neal, T., and Moore, C. (2009). Movement and the rubber hand illusion. *Perception* 38, 271–280. doi: 10.1068/p5921

Ehrsson, H. H., Rosen, B., Stockselius, A., Ragno, C., Kohler, P., and Lundborg, G. (2008). Upper limb amputees can be induced to experience a rubber hand as their own. *Brain* 131, 3443–3452. doi: 10.1093/brain/awn297

Ehrsson, H. H., Spence, C., and Passingham, R. E. (2004). That's my hand! Activity in premotor cortex reflects feeling of ownership of a limb. *Science* 305, 875–877. doi: 10.1126/science.1097011

Engels, L. F., Shehata, A. W., Scheme, E. J., Sensinger, J. W., and Cipriani, C. (2019). When less is more – discrete tactile feedback dominates continuous audio biofeedback in the integrated percept while controlling a myoelectric prosthetic hand. *Front. Neurosci.* 13:578. doi: 10.3389/fnins.2019.00578

Gallagher, S. (1986). Body image and body schema: a conceptual clarification. *J. Mind Behav.* 7, 541–554.

Gallagher, S., and Cole, J. (1995). Body image and body schema in a deafferented subject. *J. Mind Behav.* 16, 369–389.

Geethanjali, P. (2016). Myoelectric control of prosthetic hands: state-of-the-art review. *Med. Devices* 9, 247–255. doi: 10.2147/MDER.S91102

George, J. A., Kluger, D. T., Davis, T. S., Wendelken, S. M., Okorokova, E. V., He, Q., et al. (2019). Biomimetic sensory feedback through peripheral nerve stimulation improves dexterous use of a bionic hand. *Sci. Robot.* 4:eaax2352. doi: 10.1126/scirobotics.aax2352

Giummarra, M. J., Gibson, S. J., Georgiou-Karistianis, N., and Bradshaw, J. L. (2008). Mechanisms underlying embodiment, disembodiment and loss of embodiment. *Neurosci. Biobehav. Rev.* 32, 143–160. doi: 10.1016/j.neubiorev.2007.07.001

Gonzalez-Franco, M., and Peck, T. C. (2018). Avatar embodiment. towards a standardized questionnaire. *Front. Robot.* AI 5:74. doi: 10.3389/frobt.2018.00074

Graczyk, E. L., Resnik, L., Schiefer, M. A., Schmitt, M. S., and Tyler, D. J. (2018). Home use of a neural-connected sensory prosthesis provides the functional and psychosocial experience of having a hand again. *Sci. Rep.* 8:9866. doi: 10.1038/s41598-018-26952-x

Haggard, P., Clark, S., and Kalogeras, J. (2002). Voluntary action and conscious awareness. *Nat. Neurosci.* 5, 382–385. doi: 10.1038/nn827

Hebert, J., Boser, Q., Valevicius, A., Tanikawa, H., Lavoie, E., Vette, A., et al. (2019). Quantitative gaze and movement differences in visuomotor adaptations of upper extremity prosthesis users to varying task demands. *JAMA Netw. Open* 2:e1911197. doi: 10.1001/jamanetworkopen.2019.11197

Hebert, J. S., Olson, J. L., Morhart, M. J., Dawson, M. R., Marasco, P. D., Kuiken, T. A., et al. (2014). Novel targeted sensory reinnervation technique to restore functional hand sensation after transhumeral amputation. *IEEE Trans. Neural Syst. Rehabil. Eng.* 22, 765–773. doi: 10.1109/TNSRE.2013.2294907

Ismail, M. A. F., and Shimada, S. (2016). 'Robot' hand illusion under delayed visual feedback: relationship between the senses of ownership and agency. *PLoS One* 11:e0159619. doi: 10.1371/journal.pone.0159619

Johansen, D., Cipriani, C., Popovic, D. B., and Struijk, L. N. S. A. (2016). Control of a robotic hand using a tongue control system-a prosthesis application. *IEEE Trans. Biomed. Eng.* 63, 1368–1376. doi: 10.1109/tbme.2016.2517742

Kalckert, A., and Ehrsson, H. H. (2012). Moving a rubber hand that feels like your own: a dissociation of ownership and agency. *Front. Hum. Neurosci.* 6:40. doi: 10.3389/fnhum.2012.00040

Kalckert, A., and Ehrsson, H. H. (2014). The moving rubber hand illusion revisited: comparing movements and visuotactile stimulation to induce illusory ownership. *Conscious. Cogn.* 26, 117–132. doi: 10.1016/j.concog.2014.02.003

Knecht, S., Henningsen, H., Elbert, T., Flor, H., Hohling, C., Pantev, C., et al. (1996). Reorganizational and perceptional changes after amputation. *Brain* 119(Pt 4), 1213–1219. doi: 10.1093/brain/119.4.1213

Kühn, S., Brass, M., and Haggard, P. (2013). Feeling in control: neural correlates of experience of agency. *Cortex* 49, 1935–1942. doi: 10.1016/j.cortex.2012.09.002

Kuus, T., Dawson, M. R., Schoepp, K., Carey, J. P., and Hebert, J. S. (2017). "Development of a simulated sensory motor prosthesis: a device to research prosthetic sensory feedback using able-bodied individuals," in *Proceedings of the Myoelectric Controls Symposium*, Fredericton.

Kyberd, P. J. (2011). The influence of control format and hand design in single axis myoelectric hands: assessment of functionality of prosthetic hands using the

Southampton hand assessment procedure. *Prosthet. Orthot. Int.* 35, 285–293. doi: 10.1177/0309364611418554

Longo, M. R., Schuur, F., Kammers, M. P. M., Tsakiris, M., and Haggard, P. (2008). What is embodiment? a psychometric approach. *Cognition* 107, 978–998. doi: 10.1016/j.cognition.2007.12.004

Marasco, P. D., Hebert, J. S., Sensinger, J. W., Shell, C. E., Schofield, J. S., Thumser, Z. C., et al. (2018). Illusory movement perception improves motor control for prosthetic hands. *Sci. Transl. Med.* 10:eaao6990. doi: 10.1126/scitranslmed.aao6990

Marasco, P. D., Kim, K., Colgate, J. E., Peshkin, M. A., and Kuiken, T. A. (2011). Robotic touch shifts perception of embodiment to a prosthesis in targeted reinnervation amputees. *Brain* 134, 747–758. doi: 10.1093/brain/awq361

Marotta, A., Bombieri, F., Zampini, M., Schena, F., Dallocchio, C., Fiorio, M., et al. (2017). The moving rubber hand illusion reveals that explicit sense of agency for tapping movements is preserved in functional movement disorders. *Front. Hum. Neurosci.* 11:291. doi: 10.3389/fnhum.2017.00291

Moore, J. W., and Obhi, S. S. (2012). Intentional binding and the sense of agency: a review. *Conscious. Cogn.* 21, 546–561. doi: 10.1016/j.concog.2011.12.002

Murray, C. D. (2004). An interpretative phenomenological analysis of the embodiment of artificial limbs. *Disabil. Rehabil.* 26, 963–973. doi: 10.1080/09638280410001696764

Page, D. M., George, J. A., Kluger, D. T., Duncan, C., Wendelken, S., Davis, T., et al. (2018). Motor control and sensory feedback enhance prosthesis embodiment and reduce phantom pain after long-term hand amputation. *Front. Hum. Neurosci.* 12:352. doi: 10.3389/fnhum.2018.00352

Panarese, A., Edin, B. B., Vecchi, F., Carrozza, M. C., and Johansson, R. S. (2009). Humans can integrate force feedback to toes in their sensorimotor control of a robotic hand. *IEEE Trans. Neural Syst. Rehabil. Eng.* 17, 560–567. doi: 10.1109/TNSRE.2009.2021689

Parmentier, F. B. R., Ljungberg, J. K., Elsley, J. V., and Lindkvist, M. (2011). A behavioral study of distraction by vibrotactile novelty. *J. Exp. Psychol. Hum. Percept. Perform.* 37, 1134–1139. doi: 10.1037/a0021931

Proske, U., and Gandevia, S. C. (2012). The proprioceptive senses: their roles in signaling body shape, body position and movement, and muscle force. *Physiol. Rev.* 92, 1651–1697. doi: 10.1152/physrev.00048.2011

Rohde, M., Di Luca, M., and Ernst, M. O. (2011). The rubber hand illusion: feeling of ownership and proprioceptive drift do not go hand in hand. *PLoS One* 6:e21659. doi: 10.1371/journal.pone.0021659

Rosen, B., Ehrsson, H. H., Antfolk, C., Cipriani, C., Sebelius, F., and Lundborg, G. (2009). Referral of sensation to an advanced humanoid robotic hand prosthesis. *Scand. J. Plast. Reconstr. Surg. hand Surg.* 43, 260–266. doi: 10.3109/02844310903113107

Sato, Y., Kawase, T., Takano, K., Spence, C., and Kansaku, K. (2018). Body ownership and agency altered by an electromyographically controlled robotic arm. *R. Soc. Open Sci.* 5:172170. doi: 10.1098/rsos.172170

Saunders, I., and Vijayakumar, S. (2011). The role of feed-forward and feedback processes for closed-loop prosthesis control. *J. Neuroeng. Rehabil.* 8:60. doi: 10.1186/1743-0003-8-60

Schiefer, M. A., Graczyk, E. L., Sidik, S. M., Tan, D. W., and Tyler, D. J. (2018). Artificial tactile and proprioceptive feedback improves performance and confidence on object identification tasks. *PLoS One* 13:e0207659. doi: 10.1371/journal.pone.0207659

Schmalzl, L., Kalckert, A., Ragnö, C., and Ehrsson, H. H. (2014). Neural correlates of the rubber hand illusion in amputees: A report of two cases. *Neurocase* 20, 407–420. doi: 10.1080/13554794.2013.791861

Schoepp, K. R., Dawson, M. R., Schofield, J. S., Carey, J. P., and Hebert, J. S. (2018). Design and integration of an inexpensive wearable mechanotactile feedback system for myoelectric prostheses. *IEEE J. Transl. Eng. Heal. Med.* 6:2100711. doi: 10.1109/JTEHM.2018.2866105

Shehata, A. W., Engels, L. F., Controzzi, M., Cipriani, C., Scheme, E. J., and Sensinger, J. W. (2018a). Improving internal model strength and performance of prosthetic hands using augmented feedback. *J. Neuroeng. Rehabil.* 15:70. doi: 10.1186/s12984-018-0417-414

Shehata, A. W., Scheme, E. J., and Sensinger, J. W. (2018b). Evaluating internal model strength and performance of myoelectric prosthesis control strategies. *IEEE Trans. Neural Syst. Rehabil. Eng.* 26, 1046–1055. doi: 10.1109/TNSRE.2018.2826981

Shibuya, S., Unenaka, S., and Ohki, Y. (2017). Body ownership and agency: task-dependent effects of the virtual hand illusion on proprioceptive drift. *Exp. Brain Res.* 235, 121–134. doi: 10.1007/s00221-016-4777-4773

Sobuh, M. M. D., Kenney, L. P. J., Galpin, A. J., Thies, S. B., McLaughlin, J., Kulkarni, J., et al. (2014). Visuomotor behaviours when using a myoelectric prosthesis. *J. Neuroeng. Rehabil.* 11:72. doi: 10.1186/1743-0003-11-72

Tajima, D., Mizuno, T., Kume, Y., and Yoshida, T. (2015). The mirror illusion: does proprioceptive drift go hand in hand with sense of agency? *Front. Psychol.* 6:200. doi: 10.3389/fpsyg.2015.00200

Tsakiris, M., and Haggard, P. (2005). The rubber hand illusion revisited: visuotactile integration and self-attribution. *J. Exp. Psychol. Hum. Percept. Perform.* 31, 80–91. doi: 10.1037/0096-1523.31.1.80

Tsakiris, M., Haggard, P., Franck, N., Mainy, N., and Sirigu, A. (2005). A specific role for efferent information in self-recognition. *Cognition* 96, 215–231. doi: 10.1016/J.COGNITION.2004.08.002

Valle, G., Mazzoni, A., Iberite, F., D'Anna, E., Strauss, I., Granata, G., et al. (2018). Biomimetic intraneural sensory feedback enhances sensation naturalness, tactile sensitivity, and manual dexterity in a bidirectional prosthesis. *Neuron* 100, 37.e–45.e. doi: 10.1016/j.neuron.2018.08.033

van der Riet, D., Stopforth, R., Bright, G., and Diegel, O. (2013). "An overview and comparison of upper limb prosthetics," in *Proceedings of the IEEE AFRICON Conference*, Mauritius.

Wendelken, S., Page, D. M., Davis, T., Wark, H. A. C., Kluger, D. T., Duncan, C., et al. (2017). Restoration of motor control and proprioceptive and cutaneous sensation in humans with prior upper-limb amputation via multiple Utah Slanted Electrode Arrays (USEAs) implanted in residual peripheral arm nerves. *J. Neuroeng. Rehabil.* 14:121. doi: 10.1186/s12984-017-0320-324

White, M. M., Zhang, W., Winslow, A. T., Zahabi, M., Zhang, F., Huang, H., et al. (2017). Usability comparison of conventional direct control versus pattern recognition control of transradial prostheses. *IEEE Trans. Hum. Machine Syst.* 47, 1146–1157. doi: 10.1109/THMS.2017.2759762

Williams, H. E., Boser, Q. A., Pilarski, P. M., Chapman, C. S., Vette, A. H., and Hebert, J. S. (2019). Hand function kinematics when using a simulated myoelectric prosthesis. *IEEE Int. Conf. Rehabil. Robot.* 2019, 169–174. doi: 10.1109/ICORR.2019.8779443

Wilson, A. W., Blustein, D. H., and Sensinger, J. W. (2017). A third arm – design of a bypass prosthesis enabling incorporation. *IEEE Int. Conf. Rehabil. Robot.* 2017, 1381–1386. doi: 10.1109/ICORR.2017.8009441

Conflict of Interest: The authors declare that the research was conducted in the absence of any commercial or financial relationships that could be construed as a potential conflict of interest.

frontiers in Neuroscience

ORIGINAL RESEARCH
published: 27 April 2020
doi: 10.3389/fnins.2020.00348

Tactile Feedback in Closed-Loop Control of Myoelectric Hand Grasping: Conveying Information of Multiple Sensors Simultaneously via a Single Feedback Channel

Raphael M. Mayer[1], Ricardo Garcia-Rosas[1], Alireza Mohammadi[1], Ying Tan[1], Gursel Alici[2,3], Peter Choong[3,4] and Denny Oetomo[1,3]*

[1] Human Robotics Laboratory, Department of Mechanical Engineering, The University of Melbourne, Parkville, VIC, Australia, [2] School of Mechanical, Materials, Mechatronic and Biomedical Engineering, University of Wollongong, Wollongong, NSW, Australia, [3] ARC Centre of Excellence for Electromaterials Science, Wollongong, NSW, Australia, [4] Department of Surgery, St. Vincent's Hospital, The University of Melbourne, Parkville, VIC, Australia

OPEN ACCESS

Edited by:
Loredana Zollo,
Campus Bio-Medico University, Italy

Reviewed by:
Marco D'Alonzo,
Campus Bio-Medico University, Italy
Marko Markovic,
Otto Bock HealthCare GmbH, Germany
Maurizio Valle,
University of Genoa, Italy
Giorgio Grioli,
Italian Institute of Technology (IIT), Italy

***Correspondence:**
Raphael M. Mayer
r.mayer@student.unimelb.edu.au

Specialty section:
This article was submitted to Neural Technology, a section of the journal Frontiers in Neuroscience

Received: 10 September 2019
Accepted: 23 March 2020
Published: 27 April 2020

Citation:
Mayer RM, Garcia-Rosas R, Mohammadi A, Tan Y, Alici G, Choong P and Oetomo D (2020) Tactile Feedback in Closed-Loop Control of Myoelectric Hand Grasping: Conveying Information of Multiple Sensors Simultaneously via a Single Feedback Channel. Front. Neurosci. 14:348. doi: 10.3389/fnins.2020.00348

The appropriate sensory information feedback is important for the success of an object grasping and manipulation task. In many scenarios, the need arises for multiple feedback information to be conveyed to a prosthetic hand user simultaneously. The multiple sets of information may either (1) directly contribute to the performance of the grasping or object manipulation task, such as the feedback of the grasping force, or (2) simply form additional independent set(s) of information. In this paper, the efficacy of simultaneously conveying two independent sets of sensor information (the grasp force and a secondary set of information) through a single channel of feedback stimulation (vibrotactile via bone conduction) to the human user in a prosthetic application is investigated. The performance of the grasping task is not dependent to the second set of information in this study. Subject performance in two tasks: regulating the grasp force and identifying the secondary information, were evaluated when provided with either one corresponding information or both sets of feedback information. Visual feedback is involved in the training stage. The proposed approach is validated on human-subject experiments using a vibrotactile transducer worn on the elbow bony landmark (to realize a non-invasive bone conduction interface) carried out in a virtual reality environment to perform a closed-loop object grasping task. The experimental results show that the performance of the human subjects on either task, whilst perceiving two sets of sensory information, is not inferior to that when receiving only one set of corresponding sensory information, demonstrating the potential of conveying a second set of information through a bone conduction interface in an upper limb prosthetic task.

Keywords: neuroprostheses, sensory feedback restoration, human-robot interaction, tactile feedback, bone conduction

1. INTRODUCTION

It is well-established that the performance of grasping and object manipulation task relies heavily on the appropriate feedback. This is established in human grasping with or without using prostheses (Childress, 1980; Augurelle et al., 2003) and in robotic grasping algorithms (Dahiya et al., 2009; Shaw-Cortez et al., 2018, 2019). Within prosthetic applications, such feedback allows effective closed-loop control of the prostheses by the human user (Saunders and Vijayakumar, 2011; Antfolk et al., 2013; Markovic et al., 2018; Stephens-Fripp et al., 2018). To date, prosthetic hand users rely on visual and incidental feedback for the closed-loop control of hand prosthesis (Markovic et al., 2018), as explicit feedback mechanisms are not prevalent in commercial prostheses (Cordella et al., 2016). Incidental feedback can be obtained from vibrations transmitted through the socket (Svensson et al., 2017), proprioceptive information from the muscles (Antfolk et al., 2013), sound from the motor (Markovic et al., 2018), or the reaction forces transmitted by the actuating cable in body-powered prostheses (Shehata et al., 2018). Visual feedback has been the baseline feedback mechanism in prosthetic grasping exercises as it is the only feedback available naturally to all commercial hand prostheses (Saunders and Vijayakumar, 2011; Ninu et al., 2014).

It is also established that a combination of feedback information is required—and required simultaneously—for effective grasping and manipulation to be realized. In Westling and Johansson (1984) and Augurelle et al. (2003), it was demonstrated that the maintenance of grip force as a function of the measured load in a vertical lifting scenario is accompanied by their slip detection function. It was argued that in the scenarios of moving a hand-held object, accidental slips rarely occur because "the grip force exceeds the minimal force required" by a safety margin factor. No exceedingly high values of grip force are obtained due to a mechanism measuring the frictional condition using skin mechanoreceptors (Westling and Johansson, 1984). This argues for the use of two sets of information during the operation, namely the feedback of the grip force as well as the information of the object slippage and friction, even if it is to update an internal feed-forward model (Johansson and Westling, 1987). Other examples include an exercise in "sense and explore" where the proprioception information is required along with the tactile information relevant to the object/environment being explored. Information on temperature in addition to the proprioception and tactile could also be needed in specific applications to indicate dangerous temperature, for example when drinking hot beverage using a prosthetic hand—the user may not feel the temperature of the cup until it reaches the lips and causes a burn (Lederman and Klatzky, 1987).

Investigations in the prosthetic literature have so far focused on conveying each independent sensor information to the human user through a single transducer. The feedback is either continuous (Chaubey et al., 2014) or event driven (Clemente et al., 2017) and multiple transducers have been deployed via high density electrotactile arrays (Franceschi et al., 2017). The number of feedback transducers that can be deployed on the human is limited due to the physiology and the available space. Physiologically, the minimum spatial resolution is determined by the two point discrimination that can be discerned on the skin. The minimum spatial resolution is 40 mm for mechanotactile and vibrotactile feedback (on the forearm) and 9 mm for electrotactile feedback (Svensson et al., 2017). An improved result was shown in D'Alonzo et al. (2014), colocating the vibrotactile and electrotactile transducers on the surface of the skin. Spatially, the number of transducers that can be fitted in a transhumeral or transradial socket is limited by the available space within the socket and the contact surface with the residual limb. The limitation of the available stimulation points is even more compelling when using bone conduction for vibrotactile sensation. For osseointegrated implants there is only one rigid abutment point (Clemente et al., 2017; Li and Brånemark, 2017) and for non-invasive bone conduction there are 2–3 usable bony landmarks near the elbow (Mayer et al., 2019). In all these experiments, each sensory information is still conveyed by one dedicated feedback channel.

A few studies have recognized the need for the more efficient use of the feedback channels and proposed the use of multiple sensor information via a single feedback channel. Multiple sets of information have been transmitted in a sequential manner (Ninu et al., 2014), event triggered (Clemente et al., 2016), or representing only a discrete combination of the information from two sensors (Choi et al., 2016, 2017). Time sequential (Ninu et al., 2014) or event triggered feedback (Clemente et al., 2016) can be used for tasks or events where the need for each sensing information can be decoupled over the subsequent events, therefore do not address the need described above for simultaneous feedback information.

Of the many facets of the challenges in closing the prosthetic control loop through the provision of effective feedback, we seek in this paper to improve the information density that can be conveyed through a single stimulation transducer to deliver multiple sets of feedback information simultaneously to the prosthetic user. Specifically, the amplitude and the frequency of the stimulus signal are used to convey different information. This concept was observed in Dosen et al. (2016), where a vibrotactile transducer was designed to produce independent control of the amplitude and the frequency of the stimulation signal. It was reported that a psychophysical experiment on four healthy subjects found 400 stimulation settings (a combination of amplitude and frequency of the stimulus signal—each termed a "vixel") distinguishable by the subjects.

In this paper, the efficacy of this concept is further investigated on a closed-loop operation of a hand prosthesis in virtual reality. One set of information, the grasp force, is used in the closed-loop application, providing sensory feedback on the grasp force regulated by the motor input via surface electromyography (sEMG). The second set provides an additional secondary information. Note that a closed-loop operation differs from psychometric evaluation as the sensory excitation is a function of the voluntary user effort in the given task. This study is investigated within the context of non-invasive bone conduction interface, where the need for higher information bandwidth is

compelling due to the spatial limitations in the placement of feedback transducer to the human user. It should be noted that the purpose of the study in this paper is to establish the ability for a second piece of information to be perceived. Once this is established, the second set of information may be used to (1) perceive an independent set of information, such as the temperature of the object grasped, or (2) improve the performance of the primary task with additional information. In this paper, the second set of information is not expected to improve the performance of the primary task, which is the closed loop object grasping task.

It was found that the human subjects were able to discern the two sets of information even when applied simultaneously. The baseline for comparison is the case where only one set of sensor information was directly conveyed as feedback to the human user. Comparing the proposed technique to the baseline, a comparable performance in regulating the grasp force of the prosthesis (accuracy and repeatability) and in correctly identifying the secondary information (low, medium, or high) was achieved.

2. CONVEYING MULTI-SENSOR INFORMATION VIA FEWER FEEDBACK CHANNELS

We define the sensor information as $\mathbf{y} \in R^N$, where N is the number of independent sets of sensor information, where the measurements can be continuous-time signals or discrete events. The feedback stimulation to the prosthetic user is defined as $\mathbf{x} \in R^M$, where M is the number of channels (transducers) employed to provide the feedback stimulation. The scenario being addressed in this paper is that where $N > M$. The relationship between measurement $\mathbf{y}$ and the feedback stimulation $\mathbf{x}$ can be written as

$$\mathbf{x} = \phi(\mathbf{y}) \tag{1}$$

where $\phi : R^N \rightarrow R^M$.

2.1. Sensor Information y

Four major sensing modalities are generally present in the upper limbs: touch, proprioception, pain, and temperature. The touch modality is further made up of a combination of information: contact, normal and shear force/pressure, vibration, and texture (Antfolk et al., 2013). To achieve a robust execution of grasping and object manipulation task, only a subset of these sensing modalities are used as feedback. Recent studies have further isolated the types of feedback modalities and information that would be pertinent to an effective object grasping and manipulation, such as grip force and skin-object friction force (de Freitasnzo et al., 2009; Ninu et al., 2014). Furthermore, literature has explicitly determined that such combination of feedback information is required simultaneously for an effective grasping and manipulation (Westling and Johansson, 1984; Augurelle et al., 2003). In the context of an upper limb prosthesis, it is possible to equip a prosthetic hand with a large number of sensors (Kim et al., 2014; Mohammadi et al., 2019) so that $N > M$. It should be noted that the N sets of independent information can be constructed out of any number of sensing modalities, such as force sensing, grasp velocity sensing, tactile information e.g., for object roughness. It may even contain estimated quantities that cannot be directly measured by sensors, for example: object stiffness may require the measurements of contact force and displacement.

2.2. Feedback Stimulation x

The state of the art of non-invasive feedback in prosthetic technology generally utilizes electrotactile (ET), vibrotactile (VT), and mechanotactile (MT) modalities, placed in contact with the skin as a way to deliver the sensation (Stephens-Fripp et al., 2019). More novel feedback mechanisms have also been explored, such as using augmented reality (Markovic et al., 2014). Of these modalities, ET and VT present the challenges of a varying stimulation perception with location of application, VT also presents the challenge where its perception is static-force dependent (i.e., it depends on how hard the VT transducer is pressed against the skin) while MT is often bulky, with high power consumption (Svensson et al., 2017; Stephens-Fripp et al., 2018).

It was shown, however, that VT applied over bony landmarks does not suffer from the static force dependency (Mayer et al., 2018), is compact and does not suffer from high power consumption (Mayer et al., 2019). It does, however, restrict the locations that this technique can be applied to on the upper limb, as there are relatively fewer bony landmarks on the upper limb than skin surface. A psychophysical evaluation in Mayer et al. (2019) demonstrates comparable results in non-invasive vibrotactile feedback on the bone to the invasive (osseointegrated) study in Clemente et al. (2017). It is highlighted that personalization is required for the perception threshold in order to be used as an interface. A higher sensitivity has been reported for frequencies in the range of 100–200 Hz where lower stimulation forces are required. This allows the use of more compact transducers with lower power consumption (Mayer et al., 2019).

2.3. Specific Sensor Information and Feedback Stimulation Utilized

In order to demonstrate the concept of conveying multi-sensor information via fewer feedback channels, this paper uses one feedback channel to convey two sets of independent sensor information, namely the grasp force f_g and a secondary information s, which could be e.g., skin-object friction, temperature. That is,

$$\mathbf{y} = \begin{bmatrix} f_g \\ s \end{bmatrix} \in R^2, \tag{2}$$

where f_g represents a continuous-time signal of the grasp force and s is a discrete class of the secondary information. The primary information, the grasp force, is used as a feedback to the task of regulating the object grasp force. The secondary information does not directly contribute to the task of regulating the grasp force.

VT via bone conduction is selected as the feedback stimulation, applied on the elbow bony landmark. The sinusoidal waveform applied as the vibrotactile stimulus is:

$$x(t) = a(t)\sin(2\pi f(t)t), \tag{3}$$

where the amplitude $a(t)$ is modulated as a linear function of the continuous-time grasp force signal $f_g(t)$:

$$a(t) = a_0 + k_a f_g(t). \tag{4}$$

while the frequency $f(t)$ is modulated as a linear function of the secondary information $s(t)$

$$f(t) = f_0 + k_s s(t), \tag{5}$$

where $s(t) \in \{S1, S2, S3\}$ is a discrete set describing the secondary information at time t. The offset a_0 and f_0 denote the minimum amplitude and frequency detectable by human bone conduction perception. The constants k_a and k_s are positive.

3. METHODOLOGY

The proposed approach is validated in a human-subject experiment using a VT transducer worn on the elbow bony landmark to provide the feedback and a virtual reality based environment to simulate the grasping task, as shown in **Figure 1A**. This experiment seeks to verify that subjects can differentiate two encoded sensory information conveyed via one bone conduction channel. This is done by firstly, comparing the performance of the proposed approach against the baseline of carrying out the same task with only one set of information conveyed through the feedback channel. Secondly, the performance with and without the addition of visual feedback was compared.

The experiment consists of three parts:

(1) A pre-evaluation of the psychophysics of the interface;
(2) Obtaining the bone conduction perception threshold at the ulnar olecranon for individual subjects;
(3) Evaluating the performance of the human subject in the task of grasping within a virtual reality environment.

The experiment was conducted on 10 able-bodied subjects (2 female, 8 male; age 28.7 ± 4 years). Informed consent was received from all subjects in the study. The experimental procedure was approved by the University of Melbourne Human Research Ethics Committee, project numbers 1852875.2 and 1750711.1.

3.1. Psychophysics

This subsection performs the psychophysical evaluation of the bone conduction interface as sensory feedback. This is done to ensure that subjects can discriminate between the given stimulation frequencies and amplitudes chosen in the later for the Grasp Force Regulation and Secondary Information Classification Task (see section 3.3). Therefore the minimum noticeable difference for subjects, later referred to as "just noticeable difference" (JND), is obtained to quantify the capabilities of the bone conduction interface in frequency and amplitude domain.

3.1.1. Setup

3.1.1.1. Orthosis

A custom elbow orthosis with adjustable bone conduction transducers was fitted to the subjects dominant hand for the experiment as shown in **Figure 1A**. The orthosis (O) was fixed to the upper and lower arm of the subject through adjustable velcro straps. The vibrotactile transducer (VT) position was adjusted by a breadboard-style variable mounting in order to align and

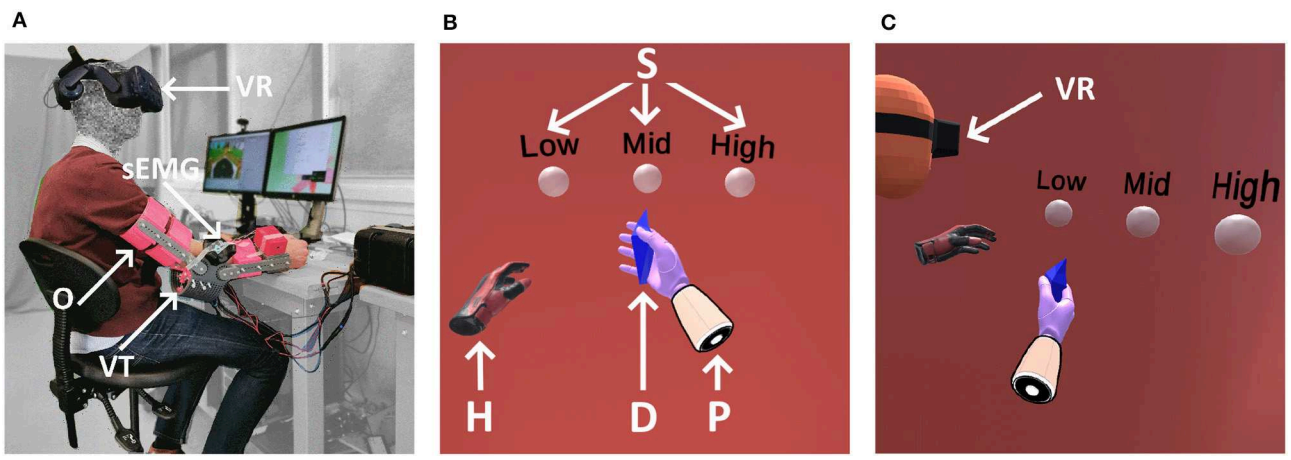

FIGURE 1 | The setup of the grasp task in virtual reality is shown in **(A)** where the subject is seated with the arm placed in the orthoses (O) onto the table. The vibrotactile transducer (VT) is mounted onto the ulnar olecranon; the EMG electrodes (sEMG) onto the forearm and the virtual reality headset (VR) placed on the subjects head. The subjects first person view in virtual reality in **(B)** shows the prosthetic (P); the grasped object (D); the non-dominant hand (H) for commands as activating/deactivating EMG or touching the sphere (S) for reporting the secondary information class and to advance to the next task; **(C)** shows the top person view of the virtual reality setup.

be in contact with the ulnar olecranon, which is the proximal end of the ulna located at the elbow. The VT is adjusted using two screws to ensure good contact with the bony landmark. The orthosis is placed on the desk (see **Figure 1A**), and kept static during the experiments.

3.1.1.2. Bone conduction

The setup consists of a B81 transducer (RadioEar Corporation, USA), calibrated using an Artificial Mastoid Type 4930 (Brüel & Kjære, Denmark) at the static force of 5.4 N. The stimulation signals were updated at 90 Hz and amplified using a 15 W Public Address amplifier Type A4017 (Redback Inc., Australia) having a suitable $4 - 16\Omega$ output to drive the 8Ω B81 transducers and a suitable low harmonic distortion of $< 3\%$ at 1 kHz. Calibrated force sensitive resistor (FSR) (Interlink Electronics 402 Round Short Tail), placed between the transducer and the mounting plate, were used to measure the applied force using a force sensitive area of $A = 1.33cm^2$. The calibration was done using three different weights [0.2, 0.5, 0.7] kg measuring five repetitions and applying a linear interpolation to obtain the force/voltage relationship. The achieved force/voltage relationship has a variance of 5.4 ± 0.37N. The stimulation signal was generated using a National Instruments NI USB-6343 connected to a Windows Surface Book 2 (Intel Core i7-8, 16GB RAM, Windows 10^{TM}) as control unit. A MATLAB® GUI was used to guide the user through the psychophysics and perception threshold experiment. The computer was connected via a Wi-Fi hotspot through a UDP connection to the head mounted virtual reality system for the experiment tasks.

3.1.2. Protocol

It is noted that the JND of frequency (JND_f) as well as the JND of amplitude (JND_a) are different for each person (Dosen et al., 2016). Therefore, a sample of five subjects are employed to evaluate JND_f and JND_a to show that the subjects can discriminate between the given stimulation frequencies and amplitudes. The JND_f is measured for three frequencies $f_{ref} \in [100, 400, 750]$ Hz and three amplitudes $a_{ref} \in [0.1, 0.3, 0.5]V$, giving the permutation of the nine different combinations. For each combination, a standard two-interval forced-choice (2IFC) threshold procedure is used. For the 2IFC, the reference stimulus f_{ref} is selected out of the three predetermined frequencies and the target stimulus f_t was varied in a stochastic approximation staircase (SAS) manner, where the variation is based on the report of the subjects of the perceived stimulus (Clemente et al., 2017). Therefore,

$$f_{t_{n+1}} = f_{t_n} - \frac{1.5 f_{ref}}{(2+m)}(Z_n - 0.85), \tag{6}$$

where f_{t_n} is the target stimulus during the previous trial, $f_{t_{n+1}}$ is the upcoming trial, m is the number of reversals showing how many times the answers change from wrong to right, Z_n is set to 1 for correct answer and 0 for an incorrect answer, and f_{t_n} is initialized with 1.5 times the reference stimulus. The trials are stopped after 50 iterations and the value $f_{t_{51}}$ for the 51st trial is taken as the perception threshold (Clemente et al., 2017; Mayer et al., 2019).

The JND_a is obtained similar to the JND_f where the target amplitude $a_{t_{n+1}}$ is now varied in a SAS manner and the reference stimulus a_{ref} is chosen out of the given amplitudes.

3.2. Perception Threshold

The objective of this subsection is to determine the minimum stimulation amplitude a_0 from which subjects could perceive a given stimulation frequency f. This will be referred to as "perception threshold" henceforth. For any given frequency, the amplitude thresholds change and are different for each person, thus it is necessary to be identified (Mayer et al., 2019).

3.2.1. Setup

The same setup as for the psychophysical evaluation was used which is explained in section 3.1.1.

3.2.2. Protocol

The perception threshold is obtained using a method of adjustment test (Kingdom and Prins, 2016, Chapter 3). The subjects are presented $n = 10$ times with each frequency $f \in [100, 200, 400, 750, 1500, 3000, 6000]$ Hz. At each iteration, the amplitude is adjusted by the subject to the lowest perceived stimulation. The subject can adjust the amplitude in small $\Delta U_{small} = 0.005V$ and large $\Delta U_{large} = 0.05V$ increments. The frequencies were presented in a randomized order.

The obtained perception threshold value a_0 for each subject is set in the bone conduction stimulation signal (Equation 4). The experiment then proceeded to the virtual reality based grasping tasks.

3.3. Grasp Force Regulation and Object Classification

Subjects were asked to perform a set of grasp force regulation and secondary information classification tasks with a virtual prosthetic hand. The tasks involved regulating the grasp force of the virtual reality prosthetic hand through the use of a sEMG-based control interface and classifying the secondary information. Different combinations of feedback modalities [visual feedback (V), grasp force (F), and the secondary information (S)] were presented, as shown in **Table 1**.

Three grasping tasks were tested in each group (**Table 1**). "Grasp Force Regulation Task" consisted purely of applying a grasp force to an object in-hand, this task is detailed in section 3.3.3.1. "Secondary Information Classification Task" consisted of classifying the secondary information, with no grasp force involved, this task is detailed in section 3.3.2.2. "Mixed Task" was a combination of "Grasp Force Regulation Task" and "Secondary Information Classification Task," where subjects required to apply a given grasp force and classify the secondary information, this task is detailed in section 3.3.2.3. Tasks VF and VS were considered as training for the users to familiarize themselves with the sEMG control interface and the feedback. Tasks VFS, F, S, and FS were used to show if subjects can differentiate multiple sensory feedback encoded in one channel with and without visual feedback. The tasks are detailed in the following subsections.

TABLE 1 | Experimental cases tested: encoding two sets of information onto the amplitude and frequency of the vibrotactile stimulation as the feedback to the subject through bone conduction.

	Task	V	F	S
VF	Grasp force	x	x	
VS	Secondary information	x		x
VFS	Mixed	x	x	x
F	Grasp force		x	
S	Secondary information			x
FS	Mixed		x	x

The role of visual feedback is also compared as a baseline.
The efficacy of this concept is further investigated on a closed-loop operation of a hand prosthesis.

3.3.1. Setup

3.3.1.1. Orthoses and bone conduction

The same setup as for the psychophysical evaluation was used, as explained in section 3.1.1.

3.3.1.2. sEMG

MyoWare sensors with Ag-AgCl electrodes were used for sEMG data gathering. Data gathering and virtual reality update were performed at 90 Hz.

3.3.1.3. Virtual reality

The virtual reality component of the experiment was performed on an HTC Vive Pro HMD with the application developed in Unity3D. The experimental platform runs on an Intel Core i7-8700K processor at 3.7 GHz, with 32 GB RAM, and GeForce GTX 1080Ti video card with 11 GB GDDR5. An HTC Vive Controller was used for tracking the non-dominant hand of the subject and to interact with the virtual reality application. The subjects report on the secondary information and navigate through the experiment with the non-dominant hand. An HTC Vive Tracker was used to determine the location of the dominant hand of the subject to determine the location of the virtual prosthesis. The application used for the experiment can be downloaded from https://github.com/Rigaro/VRProEP.

An average time latency of a touch event generated in virtual reality and the activation of the feedback stimulus of $t_{latency} = 66$ ms was estimated by measuring the single time latency's involved. The total delay results from the time delay of sending a command from the virtual reality setup via a UDP connection to the stimulation control unit $t_{UDP} = 65$ ms (measured) and the delay of sending the stimulation command to the NI USB-6343 $t_{NI} = 1$ ms (datasheet).

3.3.2. Protocol

Subjects performed a set of grasping and secondary information classification tasks in the virtual reality environment. The tasks were separated into two blocks (see **Table 1**) with a 2 min break between them. An HTC Vive Pro Head Mounted Display (HMD) was used to display the virtual reality environment to subjects. The virtual reality set-up is shown in **Figure 1A** while the subject's first person view in virtual reality is shown in **Figure 1B** and a top person view in **Figure 1C**. A Vive Controller was held by the subject on their non-dominant hand and was used to enable the EMG interface by a button press and to select the secondary information class in the classification task. A standard dual-site differential surface EMG proportional prosthetic interface was used to command the prosthetic hand closing velocity (Fougner et al., 2012). Muscle activation was gathered using sEMG electrodes placed on the forearm targeting wrist flexor and extensor muscles for hand closing and opening, respectively.

3.3.2.1. Grasp force regulation task

In the grasp force task, subjects were asked to use the sEMG control interface to regulate the grasp force to grip objects with a certain grasp force level. A fixed stimulation frequency was used, in line with the result of the psychophysical evaluation, while the amplitude $a(t)$ is used to provide feedback on the grasp force produced by the human subject as determined by Equation (4).

The grasp force f_g was calculated from the sEMG signal magnitude. Therefore, the sEMG signal magnitude u_{EMG} is integrated in a recursive discrete manner, as given by

$$\begin{aligned} -100 \leq u_{EMG}(k) \leq 100, \\ f_g(k+1) = f_g(k) + \Delta f_g u_{EMG}(k), \\ 0 \leq f_g(k+1) \leq 1, \end{aligned} \tag{7}$$

where $u_{EMG}(k)$ is the sEMG input amplification adjusted per subject to range from [−100, 100]; $\Delta f_g = 0.005$ is the scaling factor to convert sEMG signal magnitude to a force rate of change. The grasp force f_g is bounded to [0, 1]. The recursion is updated at 90 Hz.

The grasp tasks were grouped in two parts (see **Table 1**). In the first part (VF), visual feedback related to the grasp force was given to the subjects and is considered as training. The visual feedback consisted of the grasped object changing color in a gradient depending on the applied grasp force $f_g(k)$. In the second part (F), no visual feedback was provided. Three different target grasp force levels were used for the task and each was repeated five times in a randomized manner. The target grasp force levels were [0.3, 0.5, 0.8]. The object starting color represented the target grasp force level, however, subjects did not explicitly know the exact target force.

3.3.2.2. Secondary information classification task

In the secondary information classification task, subjects were asked to report on which of the three different classes they perceived by touching one of three spheres in front of them representing each of the classes. The classes (s) were low, mid, and high, which translated to the following frequencies [100, 400, 750] Hz. The grasp force was set to constant at $f_g = 0.8$ resulting in a constant amplitude $a(t)$ in the feedback stimulus to the subject for this task. In other words, it is not regulated based on the subject sEMG involvement. Each class was presented 5 times in a randomized manner. The secondary information classification tasks were grouped in two parts (see **Table 1**). In the first part (VS), visual feedback related to the correct class was shown to the subject through the color of

the classification spheres whilst presenting the stimuli and is therefore considered as training. In the second part (S), no visual feedback was provided.

3.3.2.3. Mixed task

The mixed task combines both the grasp force regulation and secondary information classification tasks simultaneously, such that the grasp force regulation had to be executed and the subjects were then asked to report on which secondary information class they perceived. This means that the stimulation provided to the subjects had the grasp force $f_g(k)$ encoded in its amplitude $a(t)$ and the secondary information class s encoded in its frequency f, simultaneously. A permutation of all force levels and secondary information classes was presented and each combination was repeated five times in a randomized manner. Force levels are [0.3, 0.5, 0.8] and secondary information classes are [100, 400, 750] Hz. The mixed tasks were grouped in two parts (see **Table 1**). In the first part (VFS), visual feedback related to the grasp force was given to the subjects. No visual feedback was given for the secondary information feedback. In the second part (FS), no visual feedback was provided.

3.3.3. Data Gathering and Performance Measure

The grasp force f_g (as calculated in Equation 7) and the actual sEMG activation levels were continuously recorded for all trials for the duration of each task, along with the desired force target. The subject's answer for the Secondary Information Classification Task was recorded for tasks "Secondary Information Classification Task" and "Mixed Task," along with the correct class.

The following performance measures were used:

Normalized Grasp Force: is the normalized grasp force $f_g(k_f)$ at the time k_f, where k_f is the time the subjects finalize the force adjustment by disabling the EMG interface by a button press. The mean and standard deviation is calculated over the repetitions of each task regulating the grasp force and represents the accuracy and repeatability of the grasp force regulation exercise.

Secondary Information Classification Rate: The rate with which the subject identifies the correct secondary information class was used as the performance measure in the secondary information classification task.

The achieved results of perception threshold, secondary information classification rate and normalized grasp force are visually presented using boxplots, showing the median, 25th and 75th percentiles and the whiskers indicating the most extreme points not considered outliers. Any outliers are plotted using the "+" symbol.

For statistical analysis a non-parametric ANOVA like analysis, specifically a Friedman test was applied (Daniel, 1990) as an ANOVA due to non normal distributed data (Shapiro–Wilk test) was not suitable. This was followed up by a *post-hoc* analysis via Wilcoxon signed rank test (Wilcoxon, 1945). The obtained p values are given as well as the statistical significance indicated in the plots.

4. RESULTS

Before using the VT bone conduction feedback interface, a pre-evaluation of the psychophysics of this interface is conducted and the perception threshold of each subject determined.

4.1. Psychophysics

Figures 2A,B show the obtained mean and standard deviation for the JND_a and JND_f. In **Figure 2C**, the mean of both JND_a and JND_f are plotted together to show the resolution of the proposed interface. The black dots in **Figure 2C** denote the reference stimulus of the SAS approach and the red and blue dots show the obtained mean value of the JND. Therefore, this plot shows the next closest noticeable stimulation point (frequency or amplitude).

The results in **Figure 2C** show that the JND_a is the smallest for lower frequencies except at 100 Hz and 0.3 V reference stimulus. Hence, the fixed frequency of the grasp force regulation task, as discussed in section 3.3.2, was set to 100 Hz since subjects had the best amplitude discrimination. Comparing the results obtained for VT on skin in Dosen et al. (2016), **Figures 2A,B** show similar behavior where the JND is increasing linearly with increasing amplitude and frequency. The lower value for JND_a at 100 Hz indicates better sensitivity at lower frequencies for higher stimulation amplitudes in case of bone conduction.

4.2. Perception Threshold

Before applying VT bone conduction feedback, the lowest perceived stimulation at the given frequencies was found using a method of adjustment. This threshold a_0 was used in Equation (4) to fit the linear relation. The maximum was set to half of the maximum transducer voltage of 0.5 V. **Figure 2D** shows the obtained perception threshold for all subjects.

4.3. Grasp and Object Classification

In the following subsections, the performance of the Mixed Task, representing the proposed concept of conveying two sets of information simultaneously via one feedback channel to the human subject, is compared to the baseline performance of the Grasp Force Regulation Task and the Secondary Information Classification Task, using the defined performance measures.

4.3.1. Secondary Information Classification Rate

The obtained secondary information classification rates are shown in the boxplot of **Figure 3A** for the VFS, S, and FS tasks. VS and VF are the training tasks and therefore the obtained data is not considered in the plots. In VS, the subjects received visual feedback for the correct answer in order to learn how to interpret the secondary information feedback and therefore reached 100% secondary information classification rate. In S, only secondary information feedback via bone conduction is provided without visual feedback. In FS, the grasp force level has to be adjusted and the correct secondary information class chosen afterwards, with both grasp force and secondary information feedback provided simultaneously via the bone conduction mechanism.

A mean secondary information classification rate of 86.22 ± 18.17% for VFS (visual, force, and secondary information feedback), 92.00±16.57% for S (secondary information feedback)

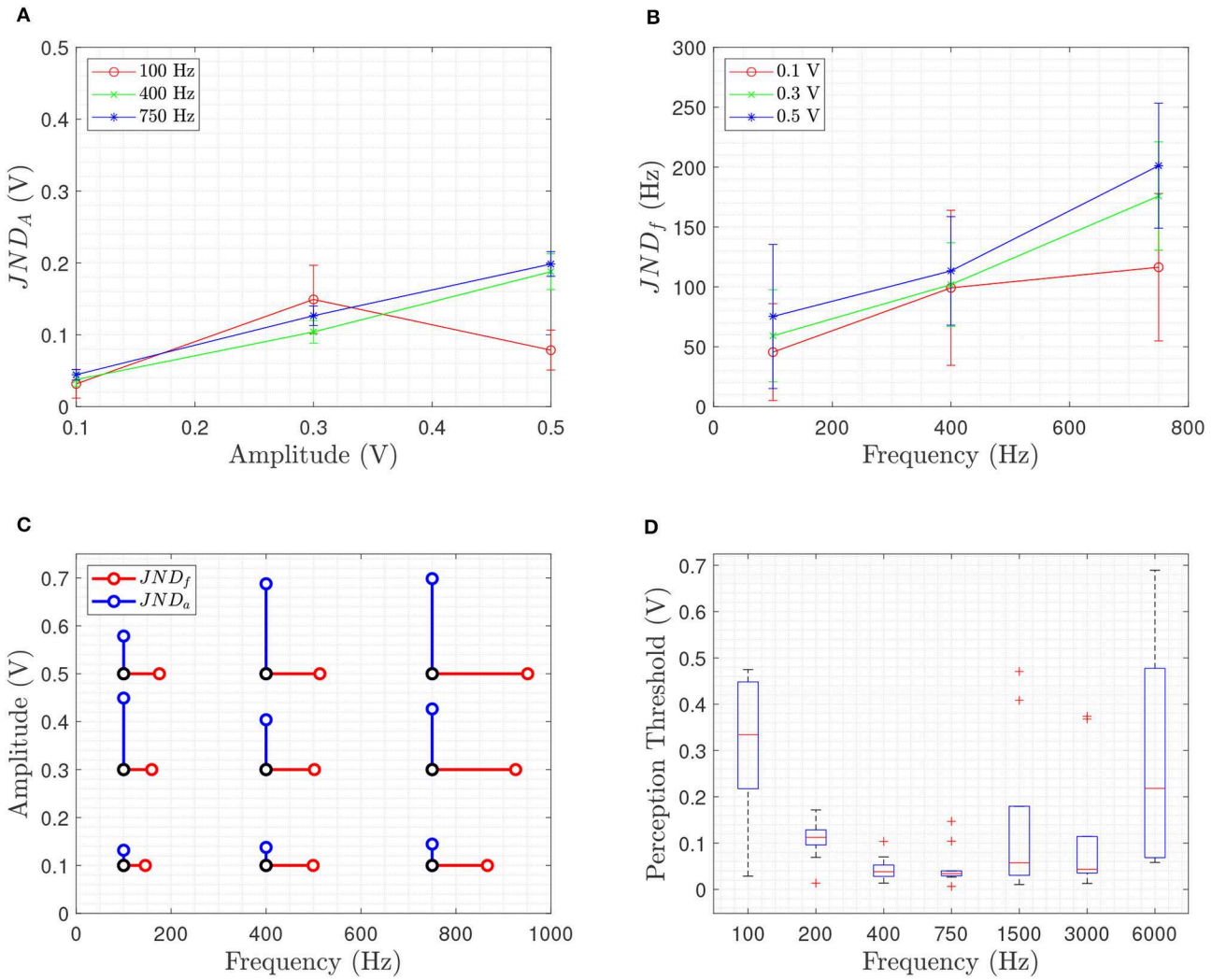

FIGURE 2 | Results of the psychophysical evaluation of five subjects show the mean and standard deviation of the **(A)** JND_a giving the amplitude resolution for three different frequencies at three different amplitudes and **(B)** JND_f giving the frequency resolution for three different amplitudes at three different frequencies while **(C)** shows a summary plot of the obtained mean value of JND_a (blue) and JND_f (red) at each reference stimulus (black). In **(D)**, the identified perception threshold value a_0 at the frequencies [100, 200, 400, 750, 1500, 3000, 6000] Hz for 10 subjects, is shown.

and 89.11 ± 16.16% for FS (force and secondary information feedback) has been observed. The mean secondary information classification rate and standard deviation for each class (low, medium, high) for the three different tasks are given in **Table 2** and the boxplot shown in **Figure 3A**. A Friedman test (VFS, S, FS) for secondary information classification rate resulted in a statistical significance for the medium secondary information class classification (see **Table 3**).

For low and high secondary information class, no statistical significance could be found, suggesting the data is compatible with all groups having the same distribution. For medium secondary information class a Wilcoxon signed rank test is applied as *post-hoc* test and results are shown in **Table 4**. A statistical significance could be found for VFS vs. S, but not for VFS vs. FS and S vs. FS suggesting the data is compatible with all groups having the same distribution.

4.3.2. Normalized Grasp Force

Figure 3B shows the boxplot of the achieved grasp force by the subjects during VFS, F, and FS. In VF, the subjects received visual feedback for the applied grasp force to learn how to associate grasp force to visual feedback as well as tactile feedback. In all cases, grasp force feedback is present, while visual feedback is present only in VFS (see **Table 1**). The result of each force level and each trial is given in **Table 2**.

The obtained results for the Friedman Test (VFS, F, FS) of all force levels are shown in **Table 5** and no statistical significance could be found suggesting the data is compatible with all groups having the same distribution.

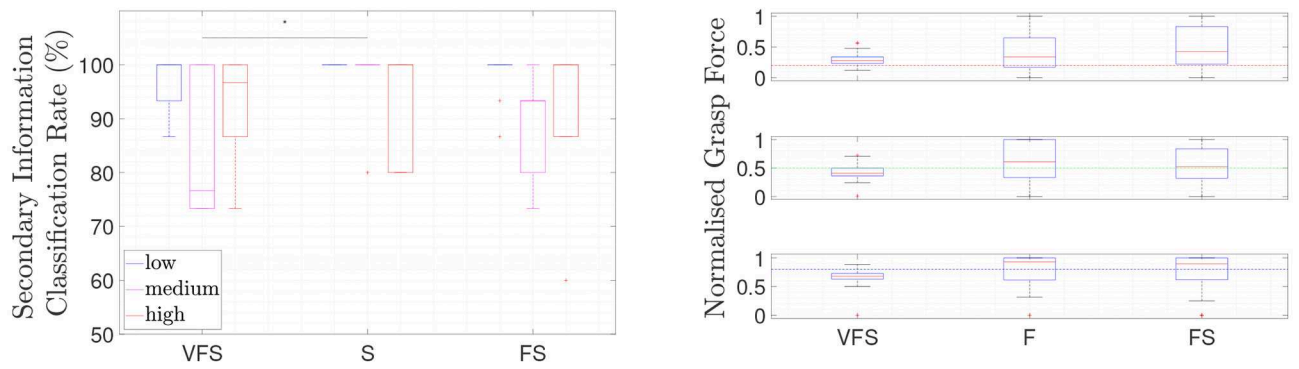

FIGURE 3 | Boxplots of the obtained results of the **(A)** secondary information classification task, subdivided into the three secondary information classes, and in **(B)** the achieved grasp force, subdivide into the three target grasp force levels, is shown for 10 subjects. *Asterisk indicates statistical difference by *post-hoc* analysis $p < 0.05$.

TABLE 2 | Shows the mean and standard deviation of the obtained results for secondary information classification rate and normalized grasp force for the 4 tasks for 10 subjects.

	Level	*VFS*	*F*	*S*	*FS*
Secondary information	Low	97.33 ± 4.66	–	100.00 ± 0.00	98.00 ± 4.50
Classification rate (%)	Medium	76.67 ± 25.19	–	90.00 ± 25.38	84.67 ± 19.89
	High	84.67 ± 30.96	–	86.00 ± 25.03	84.67 ± 28.12
Normalized grasp force	0.2	0.29 ± 0.08	0.45 ± 0.33	–	0.50 ± 0.33
	0.5	0.43 ± 0.11	0.60 ± 0.35	–	0.56 ± 0.29
	0.8	0.68 ± 0.09	0.80 ± 0.24	–	0.80 ± 0.24

TABLE 3 | The *p*-values of the Friedman test for the secondary information classification rate for the three different classes.

	Secondary information class		
	Low	**Medium**	**High**
p value	0.174	0.031	0.717

A significance level of $p < 0.05$ was used.

TABLE 4 | The *p*-values of the *post-hoc* Wilcoxon signed rank test for medium class of the mean secondary information classification rate.

	Task		
	VFS* vs.*S	***VFS* vs.*FS***	***S* vs. *FS***
p value	0.024	0.062	0.255

A significance level of $p < 0.05$ was used.

5. DISCUSSION

5.1. Conveying Multi-Sensor Information

5.1.1. Secondary Information Classification

In this subsection, we discuss the performance of the subjects in Tasks FS compared to S. The role of visual feedback (Task VFS) is discussed separately in the following subsection 5.2. **Table 3** indicates a statistical difference for the performance in recognizing the medium secondary information class but not for low and high. However, the *post-hoc* test, **Table 4**, provides more details by showing no significant difference between the performance in Tasks S vs. FS for detecting the medium secondary information class. Therefore, no statistically significant difference is found between conveying two sets of information simultaneously through the single bone conduction channel in the context of recognizing the secondary information compared to conveying one set of information.

5.1.2. Normalized Grasp Force

The Friedman test for the performance of the subjects in the grasp force regulation task as shown in **Table 5** does not show any statistically significant difference across the cases of F, FS, and VFS. This is found consistently across the three levels of grasp force. Therefore, no statistically significant reduction in performance is found in the proposed approach against the baseline in the context of grasp force regulation, leading us to conclude that adding a second set of sensor information does not influence the ability to use the first set of sensor

TABLE 5 | The *p*-values of the Friedman test for the Normalized Grasp Force for the different target levels.

	Target grasp force		
	0.2	**0.5**	**0.8**
p value	0.150	0.407	0.150

A significance level of $p < 0.05$ was used.

information in a closed-loop manner. The standard deviation is qualitatively decreasing for increasing force levels indicating a better repeatability for higher force levels in the case of no visual feedback (F and FS).

It should be noted that the grasping task for F is carried out at the stimulation frequency of 100 Hz, as justified by the psychophysical evaluation. In the case of VFS and FS, the subject also had the chance to carry out the task of regulating grasp force alongside the secondary information classification exercises, which were conducted at [100, 400, 750]Hz. This difference did not significantly influence the ability to control the grasp force.

5.2. Role of Visual Feedback

As visual feedback is present in a prosthetic system next to incidental feedback, the influence of visual feedback is investigated while incidental feedback is avoided by using a virtual reality setup. To investigate the influence of visual feedback, whilst feeding back two sets of information, the grasp force has been feed back as a color gradient of the grasped object. Though this is not a real case scenario it contains the same underlying set of information.

5.2.1. Secondary Information Classification

Comparing VFS to S showed a statistically significant increase in the secondary information classification rate in the absence of visual feedback (see **Table 4**), for the medium secondary information class, but not for low and high. It should be noted that the visual feedback was representing grasp force information and not the secondary information. Comparing VFS to FS does not yield any statistically significant difference in performance (see **Tables 3**, **4**). Several explanations are possible. It could suggest that the subjects were able to learn the meaning of the feedback and perform better or that the reduced cognitive effort increased performance. However, the data collected in this study did not permit the authors to draw further conclusions.

5.2.2. Normalized Grasp Force

The obtained normalized grasp force performance shows no statistically significant difference between the tasks involving visual feedback VFS compared to those with no visual feedback (F and FS). A smaller variance of the normalized grasp force is obtained for VFS compared to F and FS. It should be noted that VFS adds visual feedback for the same sensory information, namely the grasp force. A similar observation was reported in Patterson and Katz (1992) stating that the primary advantage of supplemental feedback is to reduce the variability of responses. This decrease can not be observed for F compared to FS as it does not add more feedback of the same sensory information but rather superimposes other types of sensory information.

It should be noted that the results are obtained using a virtual reality setup. This allows the control of the provision of visual feedback while guiding the subjects through the grasp task experiment. Admittedly it abstracts the experiment from a practical grasping task. However, it does not take away the main premise from the study, which is to understand how well two sets of information can be conveyed in this novel manner.

6. CONCLUSION

This study investigated the efficacy of conveying multi-sensor information via fewer feedback channels in a prosthetics context. Two sets of sensor information: grasp force and a secondary information, are conveyed simultaneously to human users through one feedback channel (a vibrotactile transducer on bone conduction). Human subject experiment was conducted using physical vibrotactile transducers on the elbow bony landmark and virtual reality environment to simulate the prosthetic grasping force regulation and secondary information classification tasks. It was found that the subjects were able to discern the two sets of feedback information, sufficient to perform the grasping and secondary information classification tasks to a performance not inferior to that when carried out with only one set of feedback information. The addition of visual feedback, a common feedback mechanism present in prostheses, was found to improve the repeatability of grasp force regulation as reported in literature.

It is expected that the result is generalizable to other types of information and modalities (not limited to grasp force and bone conduction stimulation) and more freedom in the selection of the number of independent sets of sensor information N and feedback stimulation channel M, as long as $N > M$. The second set of information was generalized and labeled secondary information but can be multiple in a real world application e.g., temperature, friction.

It should be noted that in this experiment, one set of sensor information was used explicitly in the closed-loop performance of grasp force regulation, while the other set constitutes additional information. Future work will investigate other modulation techniques to encode the multi-sets of information into the one feedback stimulation channel and algorithms to find an optimal matching between sensory information and provided feedback.

DATA AVAILABILITY STATEMENT

The datasets generated for this study are available on request to the corresponding author.

ETHICS STATEMENT

The studies involving human participants were reviewed and approved by Ethics Committee of the University of

Melbourne. Project numbers are 1852875.2 and 1750711.1. The patients/participants provided their written informed consent to participate in this study.

AUTHOR CONTRIBUTIONS

RM, RG-R, AM, YT, and DO: literature, experiment, data analysis, and paper. GA and PC: paper design, experiment design, and paper review.

FUNDING

This project was funded by the Valma Angliss Trust and the University of Melbourne.

ACKNOWLEDGMENTS

The authors acknowledge the assistance in the statistical analysis of the data in this paper by Cameron Patrick from the Statistical Consulting Centre at The University of Melbourne.

REFERENCES

Antfolk, C., D'alonzo, M., Rosén, B., Lundborg, G., Sebelius, F., and Cipriani, C. (2013). Sensory feedback in upper limb prosthetics. *Expert Rev. Med. Dev.* 10, 45–54. doi: 10.1586/erd.12.68

Augurelle, A.-S., Smith, A. M., Lejeune, T., and Thonnard, J.-L. (2003). Importance of cutaneous feedback in maintaining a secure grip during manipulation of hand-held objects. *J. Neurophysiol.* 89, 665–671. doi: 10.1152/jn.00249.2002

Chaubey, P., Rosenbaum-Chou, T., Daly, W., and Boone, D. (2014). Closed-loop vibratory haptic feedback in upper-limb prosthetic users. *J. Prosthet. Orthot.* 26, 120–127. doi: 10.1097/JPO.0000000000000030

Childress, D. S. (1980). Closed-loop control in prosthetic systems: historical perspective. *Ann. Biomed. Eng.* 8, 293–303.

Choi, K., Kim, P., Kim, K. S., and Kim, S. (2016). "Two-channel electrotactile stimulation for sensory feedback of fingers of prosthesis," in *IEEE International Conference on Intelligent Robots and Systems* (Daejeon), 1133–1138.

Choi, K., Kim, P., Kim, K. S., and Kim, S. (2017). Mixed-modality stimulation to evoke two modalities simultaneously in one channel for electrocutaneous sensory feedback. *IEEE Trans. Neural Syst. Rehabil. Eng.* 25, 2258–2269. doi: 10.1109/TNSRE.2017.2730856

Clemente, F., D'Alonzo, M., Controzzi, M., Edin, B. B., and Cipriani, C. (2016). Non-invasive, temporally discrete feedback of object contact and release improves grasp control of closed-loop myoelectric transradial prostheses. *IEEE Trans. Neural Syst. Rehabil. Eng.* 24, 1314–1322. doi: 10.1109/TNSRE.2015.2500586

Clemente, F., Håkansson, B., Cipriani, C., Wessberg, J., Kulbacka-Ortiz, K., Brånemark, R., et al. (2017). Touch and hearing mediate osseoperception. *Sci. Rep.* 7:45363. doi: 10.1038/srep45363

Cordella, F., Ciancio, A. L., Sacchetti, R., Davalli, A., Cutti, A. G., Guglielmelli, E., et al. (2016). Literature review on needs of upper limb prosthesis users. *Front. Neurosci.* 10:209. doi: 10.3389/fnins.2016.00209

Dahiya, R. S., Metta, G., Valle, M., and Sandini, G. (2009). Tactile sensing - from humans to humanoids. *IEEE Trans. Robot.* 26, 1–20. doi: 10.1109/TRO.2009.2033627

D'Alonzo, M., Dosen, S., Cipriani, C., and Farina, D. (2014). HyVE: Hybrid vibro-electrotactile stimulation for sensory feedback and substitution in rehabilitation. *IEEE Trans. Neural Syst. Rehabil. Eng.* 22, 290–301. doi: 10.1109/TNSRE.2013.2266482

Daniel, W. W. (1990). *Applied Nonparametric Statistics, 2nd Edn.* Boston, MA: PWS-KENT Pub.

de Freitas, P. B., Uygur, M., and Jaric, S. (2009). Grip force adaptation in manipulation activities performed under different coating and grasping conditions. *Neurosci. Lett.* 457, 16–20. doi: 10.1016/j.neulet.2009.03.108

Dosen, S., Ninu, A., Yakimovich, T., Dietl, H., and Farina, D. (2016). A novel method to generate amplitude-frequency modulated vibrotactile stimulation. *IEEE Trans. Haptics* 9, 3–12. doi: 10.1109/TOH.2015.2497229

Fougner, A., Stavdahl, O., Kyberd, P. J., Losier, Y. G., and Parker, P. A. (2012). Control of upper limb prostheses: terminology and proportional myoelectric controla review. *IEEE Trans. Neural Syst. Rehabil. Eng.* 20, 663–677. doi: 10.1109/TNSRE.2012.2196711

Franceschi, M., Seminara, L., Dosen, S., Strbac, M., Valle, M., and Farina, D. (2017). A system for electrotactile feedback using electronic skin and flexible matrix electrodes: experimental evaluation. *IEEE Trans. Haptics* 10, 162–172. doi: 10.1109/TOH.2016.2618377

Johansson, R., and Westling, G. (1987). Signals in tactile afferents from the fingers eliciting adaptive motor responses during precision grip. *Exp. Brain Res.* 66, 141–154. doi: 10.1007/BF00236210

Kim, J., Lee, M., Shim, H. J., Ghaffari, R., Cho, H. R., Son, D., et al. (2014). Stretchable silicon nanoribbon electronics for skin prosthesis. *Nat. Commun.* 5:5747. doi: 10.1038/ncomms6747

Kingdom, F. A. A., and Prins, N. (2016). "Psychophysics," in *Science Direct 2nd Edn.*. doi: 10.1016/C2012-0-01278-1

Lederman, S. J., and Klatzky, R. L. (1987). Hand movements : a window into haptic object recognition. *Cogn. Psychol.* 19, 342–368. doi: 10.1016/0010-0285(87)90008-9

Li, Y., and Brånemark, R. (2017). Osseointegrated prostheses for rehabilitation following amputation. *Der Unfallchirurg* 120, 285–292. doi: 10.1007/s00113-017-0331-4

Markovic, M., Dosen, S., Cipriani, C., Popovic, D., and Farina, D. (2014). Stereovision and augmented reality for closed-loop control of grasping in hand prostheses. *J. Neural Eng.* 11:046001. doi: 10.1088/1741-2560/11/4/046001

Markovic, M., Schweisfurth, M. A., Engels, L. F., Farina, D., and Dosen, S. (2018). Myocontrol is closed-loop control : incidental feedback is sufficient for scaling the prosthesis force in routine grasping. *J. Neuroeng. Rehabil.* 15:81. doi: 10.1186/s12984-018-0422-7

Mayer, R. M., Mohammadi, A., Alici, G., Choong, P., and Oetomo, D. (2018). "Static force dependency of bone conduction transducer as sensory feedback for stump-socket based prosthesis," in *ACRA 2018 Proceedings* (Lincoln).

Mayer, R. M., Mohammadi, A., Alici, G., Choong, P., and Oetomo, D. (2019). "Bone conduction as sensory feedback interface : a preliminary study," in *Engineering in Medicine and Biology (EMBC)* (Berlin).

Mohammadi, A., Xu, Y., Tan, Y., Choong, P., and Oetomo, D. (2019). Magnetic-based soft tactile sensors with deformable continuous force transfer medium for resolving contact locations in robotic grasping and manipulation. *Sensors* 19:4925. doi: 10.3390/s19224925

Ninu, A., Dosen, S., Muceli, S., Rattay, F., Dietl, H., and Farina, D. (2014). Closed-loop control of grasping with a myoelectric hand prosthesis: which are the relevant feedback variables for force control? *IEEE Trans. Neural Syst. Rehabil. Eng.* 22, 1041–1052. doi: 10.1109/TNSRE.2014.2318431

Patterson, P. E., and Katz, J. A. (1992). Design and evaluation of a sensory feedback system that provides grasping pressure in a myoelectric hand. *J. Rehabil. Res. Dev.* 29, 1–8. doi: 10.1682/JRRD.1992.01.0001

Saunders, I., and Vijayakumar, S. (2011). The role of feed-forward and feedback processes for closed-loop prosthesis control. *J. NeuroEng. Rehabil.* 8:60. doi: 10.1186/1743-0003-8-60

Shaw-Cortez, W., Oetomo, D., Manzie, C., and Choong, P. (2018). Tactile-based blind grasping: a discrete-time object manipulation controller for robotic hands. *IEEE Robot. Autom. Lett.* 3, 1064–1071. doi: 10.1109/LRA.2020.2977585

Shaw-Cortez, W., Oetomo, D., Manzie, C., and Choong, P. (2019). Robust object manipulation for tactile-based blind grasping. *Control Eng. Pract.* 92:104136. doi: 10.1016/j.conengprac.2019.104136

Shehata, A. W., Scheme, E. J., and Sensinger, J. W. (2018). Audible feedback improves internal model strength and performance of myoelectric prosthesis control. *Sci. Rep.* 8:8541. doi: 10.1038/s41598-018-26810-w

Stephens-Fripp, B., Alici, G., and Mutlu, R. (2018). A review of non-invasive sensory feedback methods for transradial prosthetic hands. *IEEE Access* 6, 6878–6899. doi: 10.1109/ACCESS.2018.2791583

Stephens-Fripp, B., Mutlu, R., and Alici, G. (2019). A comparison of recognition and sensitivity in the upper arm and lower arm to mechanotactile stimulation. *IEEE Trans. Med. Robot. Bion.* 2, 76–85. doi: 10.1109/TMRB.2019.2956231

Svensson, P., Wijk, U., Björkman, A., and Antfolk, C. (2017). A review of invasive and non-invasive sensory feedback in upper limb prostheses. *Expert Rev. Med. Dev.* 14, 439–447. doi: 10.1080/17434440.2017.1332989

Westling, G., and Johansson, R. (1984). Factors influencing the force control during precision grip. *Exp. Brain Res.* 53, 277–284.

Wilcoxon, F. (1945). Individual comparisons by ranking methods. *Biometr. Bull.* 1, 80–83. doi: 10.2307/3001968

Conflict of Interest: The authors declare that the research was conducted in the absence of any commercial or financial relationships that could be construed as a potential conflict of interest.

frontiers in Neuroscience

TECHNOLOGY AND CODE
published: 30 April 2020
doi: 10.3389/fnins.2020.00408

Modular Current Stimulation System for Pre-clinical Studies

Soheil Mottaghi[1,2,3], Niloofar Afshari[1], Oliver Buchholz[1], Samuel Liebana[4] and Ulrich G. Hofmann[1,2,3]*

[1] Section for Neuroelectronic Systems, Department of Neurosurgery, Medical Center University of Freiburg, Freiburg, Germany, [2] Faculty of Medicine, University of Freiburg, Freiburg, Germany, [3] Technical Faculty, University of Freiburg, Freiburg, Germany, [4] Department of Engineering, University of Cambridge, Cambridge, United Kingdom

Electric stimulators with precise and reliable outputs are an indispensable part of electrophysiological research. From single cells to deep brain or neuromuscular tissue, there are diverse targets for electrical stimulation. Even though commercial systems are available, we state the need for a low-cost, high precision, functional, and modular (hardware, firmware, and software) current stimulation system with the capacity to generate stable and complex waveforms for pre-clinical research. The system presented in this study is a USB controlled 4-channel modular current stimulator that can be expanded and generate biphasic arbitrary waveforms with 16-bit resolution, high temporal precision (μs), and passive charge balancing: the NES STiM (Neuro Electronic Systems Stimulator). We present a detailed description of the system's structural design, the controlling software, reliability test, and the pre-clinical studies [deep brain stimulation (DBS) in hemi-PD rat model] in which it was utilized. The NES STiM has been tested with MacOS and Windows operating systems. Interfaces to MATLAB source codes are provided. The system is inexpensive, relatively easy to build and can be assembled quickly. We hope that the NES STiM will be used in a wide variety of neurological applications such as Functional Electrical Stimulation (FES), DBS and closed loop neurophysiological research.

Keywords: Modular current source, current stimulation, biphasic stimulation, deep brain stimulation, arbitrary waveform

OPEN ACCESS

Edited by:
Max Ortiz-Catalan, Chalmers University of Technology, Sweden

Reviewed by:
Massimo Barbaro, University of Cagliari, Italy
Danny Eytan, Technion Israel Institute of Technology, Israel

****Correspondence:***
Soheil Mottaghi
soheil.mottaghi@uniklinik-freiburg.de; soheilmottaghi@gmail.com

Specialty section:
This article was submitted to Neural Technology, a section of the journal Frontiers in Neuroscience

Received: *14 January 2020*
Accepted: *03 April 2020*
Published: *30 April 2020*

Citation:
Mottaghi S, Afshari N, Buchholz O, Liebana S and Hofmann UG (2020) Modular Current Stimulation System for Pre-clinical Studies. Front. Neurosci. 14:408. doi: 10.3389/fnins.2020.00408

INTRODUCTION

Electrical stimulation was recommended in ancient Roman medical scriptures to treat severe headaches using the electric discharges of atlantic torpedo rays (Largus, 1983). Medically relevant beneficial electrical stimulation has since then, and particularly in the last few decades, come a very long way in the biomedical field, as well as in rehabilitation and sports medicine (Petrofsky and Phillips, 1984; Wu et al., 2002; Hamid and Hayek, 2008; Maffiuletti, 2010; Brinton et al., 2014; Bin Altaf et al., 2015). Today, electrical stimulation of the brain can achieve reliable mitigation of the symptoms of neurological diseases such as Parkinson's disease (PD) or dystonia (Benabid et al., 2002; Tronnier et al., 2002; Vidailhet et al., 2005; Hardesty and Sackeim, 2007; de Hemptinne et al., 2015; Tronnier et al., 2015), can reduce chronic pain (Russo and Sheth, 2015), and reduce seizure incidents in epileptics (Velasco et al., 2000; Vonck et al., 2002). Most recently, advances regarding psychiatric disorders like obsessive compulsive disorder (OCD; Alonso et al., 2015) or

major depression disorder (Schlaepfer et al., 2013) have also introduced electrical stimulation as an effective treatment.

In all of these applications, electrical stimulation is delivered as either current or voltage driven charge injection into brain tissue through small noble metal electrodes (Tehovnik, 2006; Rattay et al., 2012). In the case of voltage driven charge injection, the transferrable charge is sometimes hindered by a time-varying impedance of the interface between electrode and tissue (McConnell et al., 2009; Sooksood et al., 2010; Karumbaiah et al., 2013; Nag et al., 2013; Washburn et al., 2014; Ramirez De Noriega et al., 2015). Due to biotic factors such as tissue reaction, glial encapsulation at the electrode-tissue interface and electrochemical factors, voltage stimulation frequently needs to be performed regardless of this limitation (Biran et al., 2005; Gimsa et al., 2005). In contrast, current stimulation delivers the desired charge reliably over time but is inconvenienced by its more complex electronic setup (Nag et al., 2013; Washburn et al., 2014; Ramirez De Noriega et al., 2015).

In light of the growing interest in bioelectronic medicine, there is a need for user-friendly, affordable, and standalone yet precise stimulators coping with changing requirements in stimulation paradigms (Sahin and Tie, 2007; Jezernik et al., 2010; Wongsarnpigoon et al., 2010; Foutz and McIntyre, 2010; Schor and Nelson, 2019). These needs can only partially be satisfied by any of the multiple commercially available stimulation devices. Cost, proprietary firmware, dependence on electrophysiological recording setups, and companies' policies can be prohibitive for customization and improvement research. Consequently, there are various custom-designed electrical stimulation systems which are tailored to the requirements of targets such as cardiac tissue (Tandon et al., 2011), cell cultures (Yuan and Silberstein, 2016), brain slices (Li et al., 2015), deep brain areas (Gong et al., 2015), and muscles (Wang et al., 2015; Stewart et al., 2016) in closed-loop and other electrophysiological applications (Sanders and Kepecs, 2014). In this paper, we introduce a low cost (see **Appendix A** for details) modular electrical current stimulation system that can be used in all of the above-mentioned applications. We hope to encourage researchers not to limit themselves to cloning the system, but to improve and develop it further. A thorough and detailed demonstration of the system's elements, including links to the downloadable documents, is given in the Materials and Methods section. The implementation and characterization of the system, as well as its application, are presented in the Results section. Finally, we compare the Neuro Electronic Systems Stimulator (NES STiM) to two commercially available stimulators, presented in the Discussion.

MATERIALS AND METHODS

The NES STiM consists of four modular 16-bit current stimulation units, which can generate arbitrary biphasic current pulses. It is compatible with MacOS and Windows and can be used as a standalone unit. All the technical details of the system, from electronic schematics, printed circuit board (PCB) drawings, drivers, and firmware to software interfaces for MATLAB are available in our repository (Mottaghi et al., 2020). The instructions on how-to setup a NES STiM, are provided in the repository called (HowTo).

The NES STiM can be used in standalone or PC mode. In the standalone mode, all parameters should be predefined in the device and activate the output by external trigger. in PC mode all stimulation parameters can be defined by the MATLAB function or graphical user interface (GUI) before generating the output pulses.

The NES STiM's power unit provides low noise, medical standard $\pm$15 V and 5 V outputs to be used by the main board subunits. TEL 3-2023 and TMA 1205D, two medical grade isolated DC/DC converters (Traco Electronic AG., Switzerland) were integrated to supply the required power. The essential components of the power unit are depicted in **Figure 1B**.

The processing module also regulates the power consumption of the system by monitoring the system's state using optical switches IS7000X (ISOCOM, United States) (**Appendix A**) and connecting or disconnecting the power supply to the main board accordingly. The NES STiM features two BNC ports (one for the input trigger and one for the output) in case synchronization with other instruments is needed. Moreover, each channel has a specific LED, indicating whether the channel is active or not. Both port triggering and LED activation are also controlled by the processing unit (see **Appendix A**).

The mbed LPC1768, a prototyping module with a 32-Bit ARM Cortex-M3 microcontroller (NXP semiconductors, Netherlands), 30 input/output (I/O) ports and two integrated Serial-Peripheral-Interface (SPI) units, was selected for the processing module (see **Appendix A**). It benefits from a lightweight online C++ compiler and drag-*n*-drop programming which makes developing the system relatively easy. In PC mode, LPC1768 receives the desired parameters and start/stop commands via a mini USB-B port from the host PC. A serial port is assigned to the LPC1768 and all communications between the PC and NES STiM are conducted through this port (see the serial port setup procedure in the C code in the **Supplementary Material**).

The LPC 1768 transfers the stimulation parameters for each channel via SPI. The SPI data is placed on the data-bus (DO), but only the stimulation modules which have their chip-select pin (CS) activated, receive the data. 16-bit digital-to-analog DAC8831 converters receive the data as the first stage of the stimulation module and produce an amplified analog voltage between $-$2.5 V to +2.5 V (see **Appendix A**). The DAC's analog output voltage is converted into current using a voltage controlled current source (modified Howland current pump) (Stitt, 1990) (see **Figure 1A**). Four pulse waveshapes [rectangle, sinusoidal, triangle, and linear decay (sawtooth)] are pre-defined in the C code of the LPC1768, which can be customized when needed. The stimulation pulses can be either generated for a defined number of pulses or continuously until the stop command is sent from the PC.

Safety

To protect the tissue from excessive charge accumulation, a passive charge balancing mechanism was implemented (Sooksood et al., 2009; Sooksood et al., 2010). A 1 μF capacitor was mounted in series with the load (electrode) to prevent a net DC current, which could result in pH change and potential

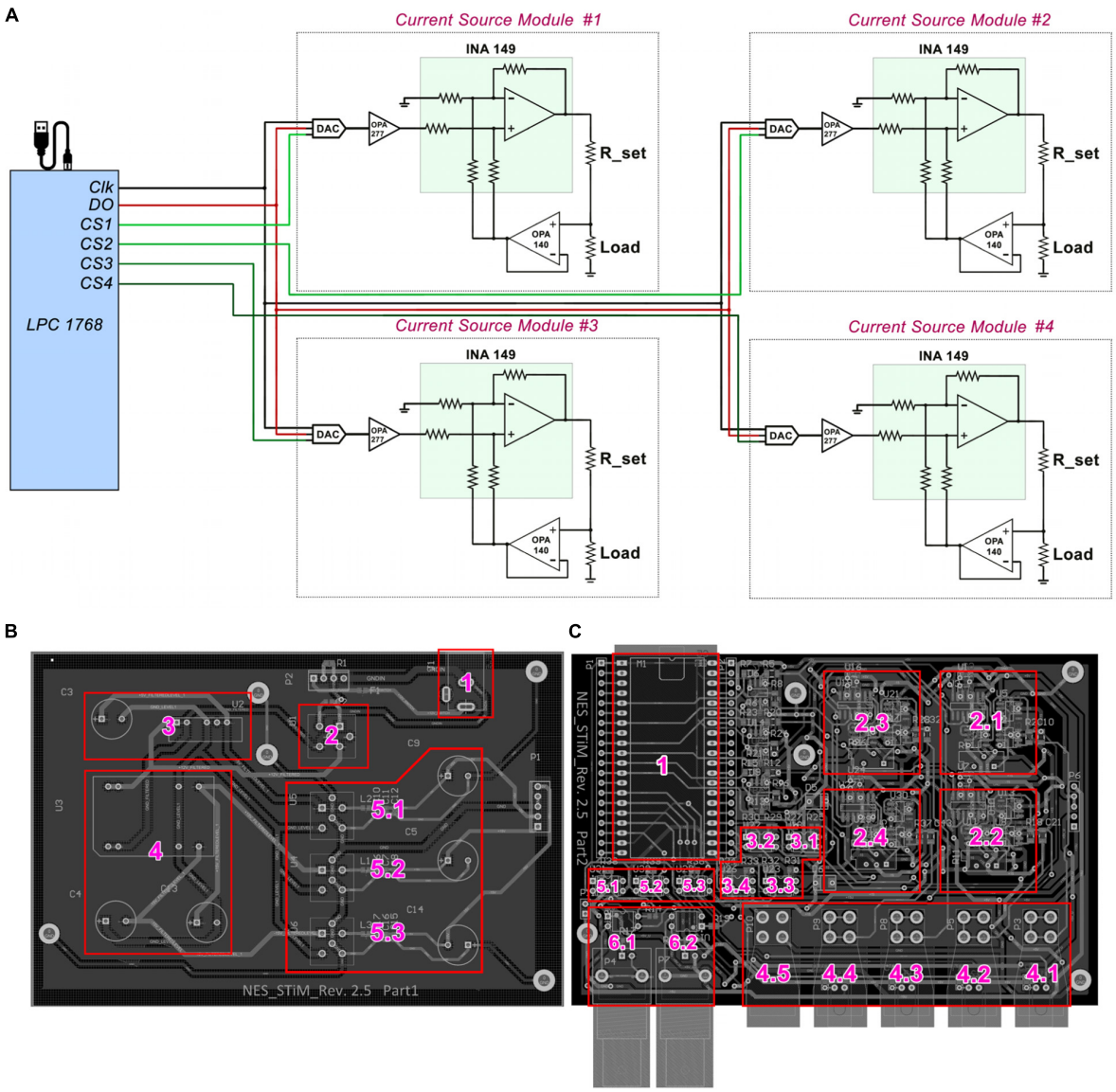

FIGURE 1 | Schematic drawing of NES STiM system. **(A)** LPC1768 activates desired channels via their chip select (CS) pins, and places the SPI binary streams on the data bus (DO). With each clock signal, one bit is received by the DAC8831. **(B)** Essential units of the power unit are labled with numbers; 1) Input power socket receives +12 V power supply, which is filtered by the unit 2. The clean and filtered +12 V is fed to the units 3 and 4 in order to produce +5 and ±15 V, respectively. The generated +5 and ±15 V are then filtered by 5.1–5.3 and provided to the main board. **(C)** The input powers received from the power unit are only connected to the main board's subunits only when the LPC1768 (unit 1) activates three ISO7000X optical switches (5.1–5.3), which is only done before the stimulation activation. Units 2.1–2.4 are the stimulation modules for corresponding to the channels 1–4, respectively. Charge balancing optical switches (3.1–3.4), current outputs for channes 1–4 (4.1–4.5), the ground connector (4.5), and digital input/output triggers (6.1–6.2) are labeled as well.

tissue damages. It has been shown that the charge density safe threshold for microelectrodes is between 100–200 $\mu C\ cm^{-2}$ and around 30 $\mu C\ cm^{-2}$ for macroelectrodes used clinically (McCreery et al., 1990). A warning pop-up window with the "USE AT YOUR OWN RISK" message appears when the user runs the GUI. Since the surface area of the electrode that the user utilizes determines the stimulation amplitude and pulse-width limits per phase, a highlighted note at the beginning of all the codes (MATLAB and C) is added as a warning before the experiment can be started. Additionally, the LPC1768 discharges the electrode potentials in interpulse intervals via activating optical switches (ISO7000x, ISOCOM, United States) (see **Appendix A**). The main subsections of the mainboard design are depicted in **Figure 1C**.

Animal Experiments

Every procedure involving animal experiments was conducted in accordance with the guidelines of the German Council on Animal Protection. The protocols were approved by the Animal Care Committee of the University of Freiburg under

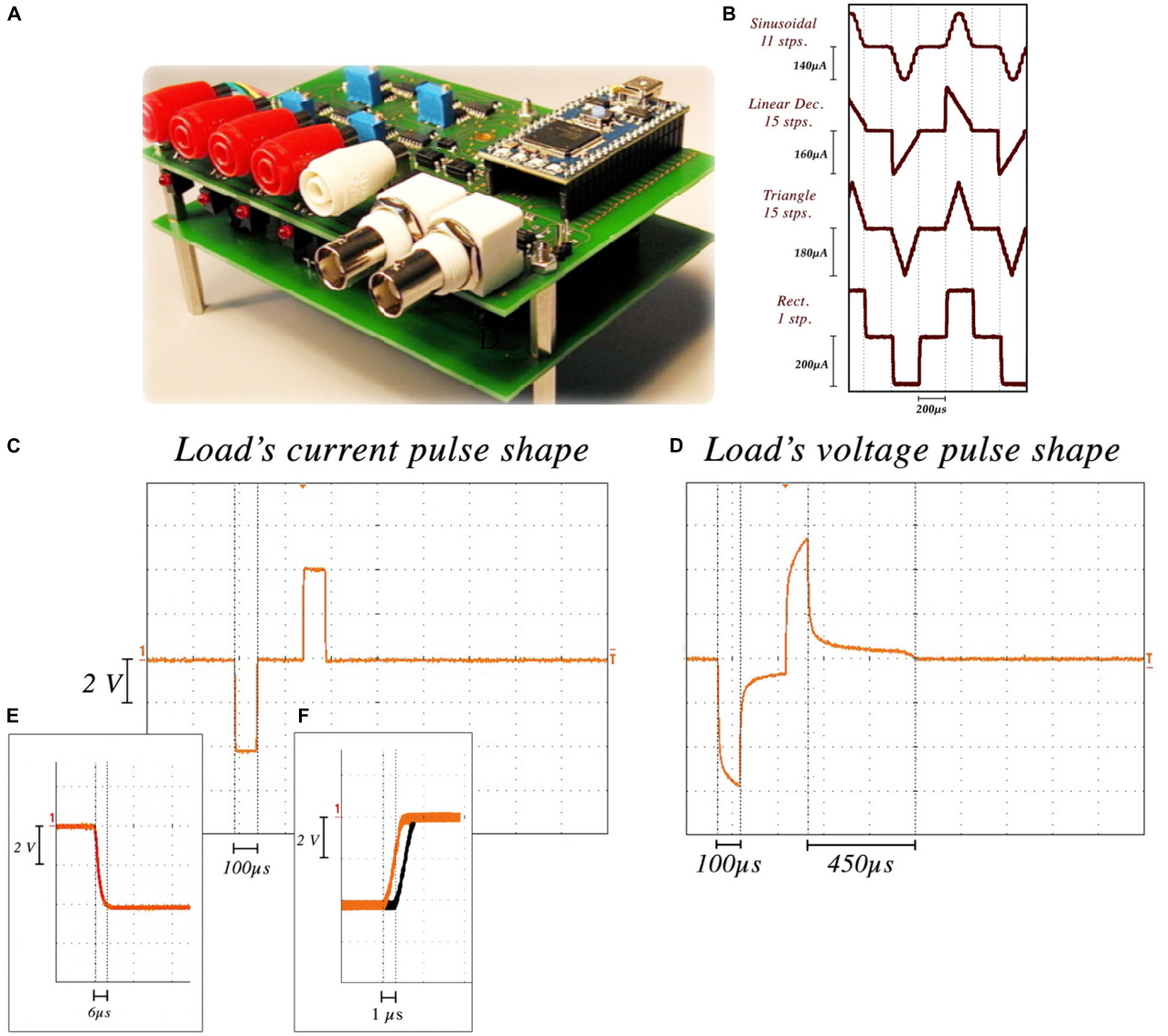

FIGURE 2 | NES STiM characterization. **(A)** the NES STiM system. **(B)** Comparison between sinusoidal (11 steps), linear decreasing (15 steps), triangle (15 steps), and standard rectangular (1 step) pulses. **(C)** Current pulse measured from an 80 W resistor placed in series with the electrode. **(D)** Electrode potential of the same pulse, showing the duration of the passive charge balancing required for the potential to reach the pre-pulse value. **(E)** Rise and fall time of each step ≈6 μs. **(F)** The latency between first and last channel outputs.

the responsible supervision of the Regierungspräsidium Freiburg (approval G15/031) in accordance with the guidelines of the European Union Directive 2010/63/UE.

All the rodents, to be experimented on, were handled for several days in order to habituate to the new environment and experimenter. Female Sprague-Dawley rats (n = 21) underwent stereotactic surgery for unilateral 6-hydroxydopamine (6-OHDA) lesioning. They were anesthetized initially with 5% isoflurane and oxygen (0.15 l/min). Isoflurane concentration was lowered to 1.5% after fixing the animal in the stereotactic frame (David Kopf, United States). Animal reflexes, breathing and anesthesia depth were monitored throughout all the surgeries. Freshly prepared 6-OHDA neurotoxin solution (3.6 mg 6-OHDA dissolved in 1 ml of 20 mg ascorbic acid and 10 ml 0.9% NaCl solution) was prepared before each surgery and kept on ice and away from direct light throughout the surgical procedure (Sigma-Aldrich Chemie GmbH, Germany). 6-OHDA solution (3.3 μl) was administered using a microinjection pump UMP3 UltraMicroPump (World Precision Instruments, United States) either to the substantia nigra pars compacta (SNc; AP = −3.2 mm, ML = −1.5 mm from bregma, and DV = −7.2 mm from dura) with an injection speed of 0.5 μl/min or to the medial forebrain bundle (MFB; AP = −4.4, −4.0 mm, ML = −1.2, −0.8 mm from bregma, and DV = −7.8, −7.2 mm from dura) with an injection speed of 1 μl/min. The needle was left in the brain for 5 min after the injection to allow the brain to absorb the neurotoxin. The drill

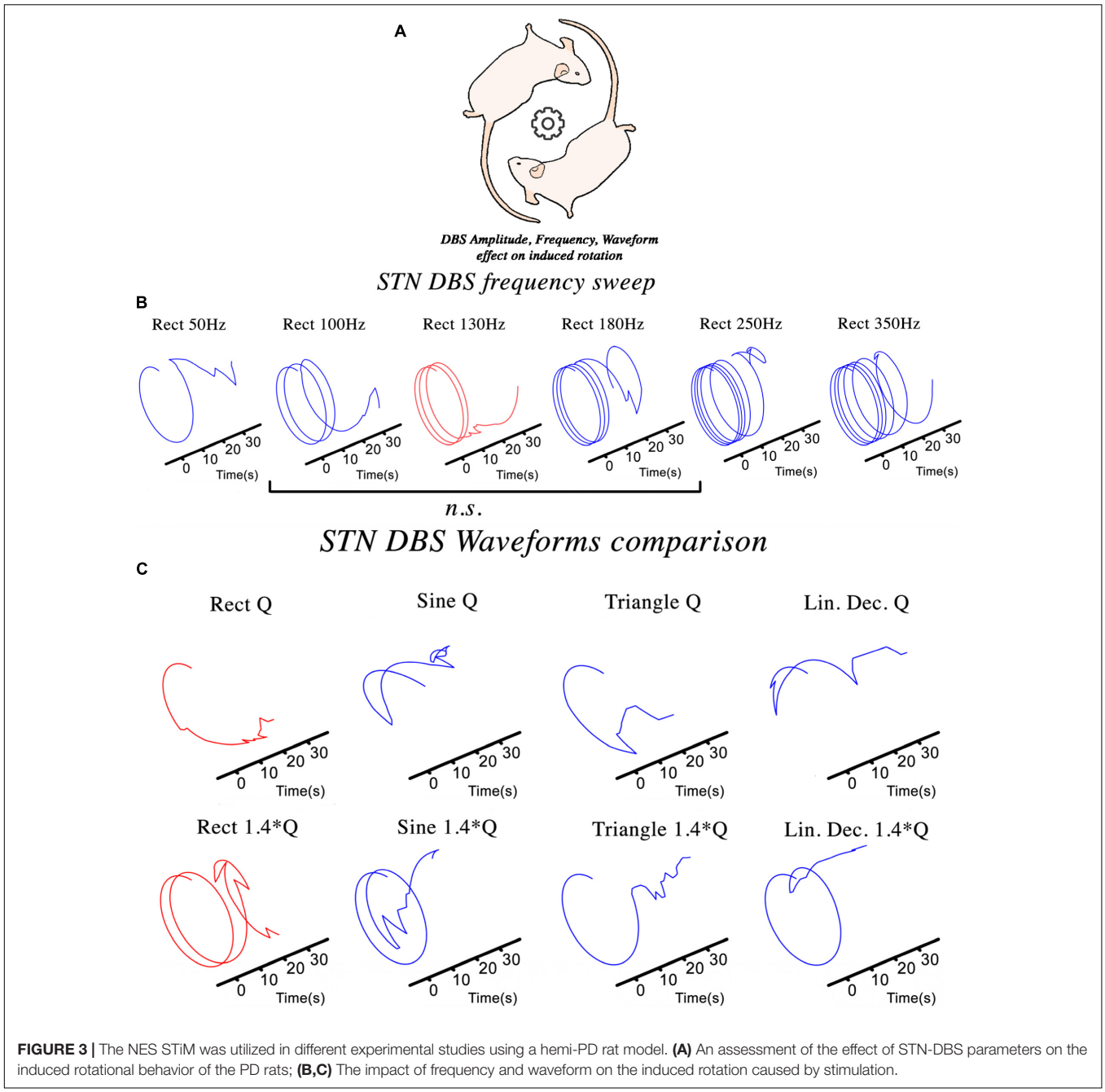

FIGURE 3 | The NES STiM was utilized in different experimental studies using a hemi-PD rat model. **(A)** An assessment of the effect of STN-DBS parameters on the induced rotational behavior of the PD rats; **(B,C)** The impact of frequency and waveform on the induced rotation caused by stimulation.

hole was filled with bone wax and the scalp then carefully stitched. Animals were given 14 days of recovery after lesioning.

All animals were tested using an Apomorphine test (Ungerstedt and Arbuthnott, 1970) in order to assess the success of the lesioning surgery. This test challenges the severity of dopamine depletion using a subcutaneous apomorphine solution injection (1 mg apomorphine, 2 mg ascorbic acid, 20 ml NaCl; 0.1 ml/100 gr of rat body weight, Sigma-Aldrich Chemie GmbH, Germany) to induce counter-clockwise rotations relative to the lesioned hemisphere. The rats showing an average of at least 3 counter-clockwise rotations per minute over a 30-min interval were categorized as the PD group.

In a separate stereotactic surgery, PD animals were implanted with stimulation electrodes positioned in the subthalamic nucleus (STN; AP = −3.6 mm, ML = −2.5 mm from bregma, and DV = −7.8 mm from dura) ipsilateral to the lesioned hemisphere. Bipolar stimulation electrodes consisting of two intertwining 50 μm coated Platinum/Iridium microwires (Science Products GmbH, Germany) were used in the course of this study. Stimulation electrodes with impedances <20 kΩ

were selected for implantation. The animals were given 1 week of recovery after surgery.

Accuracy and Reliability Assessment

To evaluate the precision of the NES STiM, several parameters relevant to neurophysiological applications were tested. These tests were all performed on a single NES StiM and on two computers with Windows and MacOS operating systems.

The NES STiM's reliability and precision characterization (**Figures 2A,B**) was performed using the aforementioned stimulation electrodes immersed in 0.9% saline. We performed 12-h tests which measured the current from a channel stimulating with a standard rectangular high frequency stimulation (HFS) waveform with 250 μA amplitude, 100 μs PW, 100 μs interphase interval, and 130 Hz frequency. The injected current was measured by the potential difference over an 80Ω resistor placed in series with the electrode. Due to the electrode tissue interface (ETI) and the capacitive characteristic of the ETI (Merrill et al., 2005), the electrode potential is smoothed (**Figures 2C,D**). The average rise and fall time for 100,000 pulses was 6.2 ± 1.3 μs. The passive charge balancing mechanism required 455 ± 32 μs, on average yielding a maximum tolerable frequency of 1.27 kHz.

Waveform shape was shown to impact the injected charge and energy-efficiency of the stimulation (Brocker and Grill, 2013). Digital arbitrary waveforms are composed of multiple discrete steps with different values and timings. **Figure 2E** shows four different waveforms (sinusoidal, linear decay, symmetric triangular, and rectangular) generated using this technique. Waveform resolution can be controlled by changing the number of discrete steps per phase. More steps in each phase results in a smoother waveform, while taking more time in total per phase. There is hence a trade-off between the minimum PW of a waveform and the number of steps in each phase (i.e., resolution). As an example, if we assume a single step requires 6 μs, 60 μs is the minimum time needed to produce a 10-step pulse.

Temporal latencies between channel outputs was another feature to test. Similar stimulation parameters were set for all channels and the delay between the outputs of the first and last channel was measured. As shown in **Figure 2F**, a 1.3 ± 0.18 μs delay was observed on average.

Applications

High frequency DBS (>100 Hz) has been shown to be effective in treating movement disorders like those of PD patients. It alleviates motor symptoms such as tremor, rigidity, and akinesia (Lanotte et al., 2002; Brocker and Grill, 2013). The therapeutic frequency window is reported to be 100 Hz $< f <$ 180 Hz with ceiling and floor limits of 250 Hz and 50 Hz, respectively (Moro et al., 2002).

The hemi-PD rat model is a well-established pre-clinical platform for testing novel stimulation paradigms not easily examined in patients. The NES STiM was used to apply four different waveforms (rectangular, sinusoidal, symmetric triangular, and linear decay) to hemi-PD rats and compare the induced contralateral rotation as in the frequency sweep test (**Figure 3B**). The evaluation of DBS in a hemi-PD rat model was the original reason for designing and developing the NES STiM. This device has been tested in various experimental paradigms related to the mentioned PD model. Examples are the impact of frequency and waveform on the effectiveness of DBS (see **Figure 3**), as well as implementing closed-loop DBS (Castaño-Candamil et al., 2017).

To test the effect of varying stimulation frequency on the hemi-PD rat model, we quantified the contralateral (to the lesion) rotational effect caused by biphasic rectangular electrical stimulation (So et al., 2017). Each animal was placed and habituated for >7 days in a large cornerless, semi-spherical bowl before being tested. DBS was then applied with increasing stimulation frequencies for 30 s at each value with a 45 s pause between different frequencies (see **Figure 3B**). Statistical evaluation of the observed rotational effect showed smaller Euclidean Distance (ED) for biphasic rectangular stimulation with frequencies between 100 and 180 Hz, whereas smaller (50 Hz) or higher stimulation frequencies (250 and 350 Hz) showed significantly higher ED values ($ED_{130Hz.vs.100-180Hz}$ = 2.62 ± 0.22, $ED_{130Hz.vs.50Hz}$ = 4.08 ± 0.17 and $ED_{130Hz.vs.250-350Hz}$ = 12.89 ± 4.43).

Another essential aspect of electrical stimulation is the waveform. Studies on tissue damage (Yuen et al., 1981; McCreery

TABLE 1 | Specification overview between the NES STiM and two commercially available stimulation devices (Plexon Stim, and AlphaLab SnR).

Model name	NES STiM	Plexon Stim	AlphaLab SnR
Output channels	4	16	8
Current modules	4	16	3
Output voltage	±13.5 V	±10 V	60 V
Polarity	Anod./ Cathod. First	Anod./ Cathod. First	Anod./ Cathod. First
Output current	1 μA–2500 μA, 1 μA increment	1 μA–1000 μA 1 μA increment	2 μA–3500 μA
Stimulation frequency	0.005 Hz–25 kHz	0.008 Hz–100 kHz	1–300 Hz
Pulse width	40 μS–65535 μs	5 μS–65535 μs	10–1000 μs
Inter-phase intervals	2 μS–Inf μs	5 μS–65535 μs	0–1000 μs
PC hardware interface	Mini USB B	Mini USB B	Ethernet
Stim manager PC Software compatibility	Windows Mac	Windows	Windows
API	Matlab, C++	C/C++ and Matlab	X86 / x64 library version
Analog resolution	16 bits	16 bits	16 bits
Dependency	–	–	AlphaSNR

et al., 1990; Shannon et al., 1995), power efficiency (Bin-Mahfoodh et al., 2003; Anheim et al., 2007), and DBS energy efficiency (Foutz and McIntyre, 2010; Brocker and Grill, 2013) are all valuable examples of the importance of waveform shape. We depict in **Figure 3C** the rotational effects induced by different waveforms, but comparable charge injections. Charge injection (Q) is normalized to the usual biphasic rectangular 130 Hz stimulation and alternated between the waveforms described in **Figure 2E**.

The history of closed-loop DBS goes back to (Osorio et al., 2001), where it aimed to control DBS by seizure detection. An invaluable closed-loop DBS study was performed using a primate model of PD (Rosin et al., 2011), which showed potential superiority over conventional open-loop DBS. This investigation inspired several studies assessing the method for human patients (Little et al., 2013, 2016). In these studies, beta oscillatory activities from local field potential (LFP) recordings were used to control the DBS. Consequently, the third test conducted using the NES STiM was a closed-loop DBS study on the hemi-PD rat model. In this study, beta band power was used to trigger the DBS in rats. Preliminary results from the study were published in (Castaño-Candamil et al., 2017).

DISCUSSION

Electrical stimulation and DBS studies in animal models will benefit from a robust, precise, yet modular electrical stimulation device augmenting available access to well-made commercial devices such as Plexon Stim (Plexon, United States) and AlphaSnR (AlphaOmega, Israel). Challenges in adjusting the latter to our research requirements motivated us to design and build the NES STiM.

In order to use the AlphaSnR stimulation device, a complex electrophysiological set-up has to be employed. This makes it rather prohibitive for a broad use and too expensive for many users. Plexon Stim can be used in standalone mode, but low compliance voltages make it difficult to stimulate using high impedance microelectrodes: output voltage reaches saturation fast and causes the output current to decline. A comparison of the specifications of the NES STiM and the two mentioned commercial devices is summarized in **Table 1**.

An important difficulty concerns any customization which may be required for specific experimental paradigms. Since the technical designs of the commercial devices are not public, if at all possible, it would be cumbersome to arrange these customizations relying on the technical support from these companies. For instance, eventhough the NES STiM has 4 channels, however, the number of channels can be expanded by adding stimulation modules. In the current setup, in addition to the shared DO and Clk pins, each channel needs a CS and two pins for LED and charge balancing switch (one for each). LPC1768 has nine unused I/O ports which can support another 3 channels (7 channels in total). If more channels are still needed, replacing the LPC1768 by more capable products such as STM32F429I-DISC1 that contains 144 I/O ports could be an alternative.

Another customization for the NES STiM, is to add the bootstrapping mechanism explained (Mottaghi et al., 2015) to increase the compliance voltage to a desired level, while keeping rest of the components as they are in NES STiM. In order to challenge the device and high compliance voltages, up to 2000 $\mu C\ cm^{-2}$ charge density was tested in flexible microelectrodes (Mottaghi et al., 2015). The NES STiM's design is instead modular and it has been used as a stimulation device in a variety of experiments successfully. Details of said experiments will be published elsewhere and exceed the scope of this presentation of our modular NES STiM. We hope that this device will be cloned, customized and improved by other groups, engineers and researchers.

CONCLUSION

Neuro Electronic Systems Stimulator is a modular electrical stimulation system for electrophysiological applications. The system has four channels, with a dedicated current source for each channel. It can be controlled from the PC via a USB connection or operate in standalone mode. Schematics and drawings of the electronics are available online together with the MATLAB and C++ control programs. Although stimulation parameters such as amplitude, frequency, pulse shape, and pulse width can be actively selected NES STiM does fit in a closed loop stimulation experiment as well (Castaño-Candamil et al., 2017).

ETHICS STATEMENT

The animal study was reviewed and approved by University medical Freiburg, G15/031.

AUTHOR CONTRIBUTIONS

SM, NA, and UH contributed conception and design of the study. SM organized the work. SM performed the precision tests. SM wrote the first draft of the manuscript. SM, SL, OB, and UH wrote sections of the manuscript. All authors contributed to manuscript revision, read and approved the submitted version.

FUNDING

This work is partially supported by the BrainLinks-BrainToolsCluster of Excellence funded by the German Research Foundation (DGF, grant number EXC 1086).

SUPPLEMENTARY MATERIAL

The Supplementary Material for this article can be found online at: https://www.frontiersin.org/articles/10.3389/fnins.2020.00408/full#supplementary-material

REFERENCES

Alonso, P., Cuadras, D., Gabriells, L., Denys, D., Goodman, W., Greenberg, B. D., et al. (2015). Deep brain stimulation for obsessive-compulsive disorder: a meta-analysis of treatment outcome and predictors of response. *PLoS One* 10: e013359. doi: 10.1371/journal.pone.0133591

Anheim, M., Fraix, V., Chabardès, S., Krack, P., Benabid, A. L., and Pollak, P. (2007). Lifetime of Itrel II pulse generators for subthalamic nucleus stimulation in Parkinson's disease. *Mov. Disord.* 22, 2436–2439. doi: 10.1002/mds.21726

Benabid, A. L., Benazzous, A., and Pollak, P. (2002). Mechanisms of deep brain stimulation. *Mov. Disord.* 115, 19–38. doi: 10.1002/mds.10145

Bin Altaf, M. A., Zhang, C., and Yoo, J. (2015). A 16-channel patient-specific seizure onset and termination detection soc with impedance-adaptive transcranial electrical stimulator. *IEEE J. Solid State Circ.* 50, 2728–2740. doi: 10.1109/JSSC.2015.2482498

Bin-Mahfoodh, M., Hamani, C., Sime, E., and Lozano, A. M. (2003). Longevity of batteries in internal pulse generators used for deep brain stimulation. *Stereotactic Funct. Neurosurg.* 80, 56–60. doi: 10.1159/00007 5161

Biran, R., Martin, D. C., and Tresco, P. A. (2005). Neuronal cell loss accompanies the brain tissue response to chronically implanted silicon microelectrode arrays. *Exp. Neurol.* 195, 115–126. doi: 10.1016/j.expneurol.2005.04.020

Brinton, M. R., Mandel, Y., Dalal, R., and Palanker, D. (2014). Miniature electrical stimulator for hemorrhage control. *IEEE Trans. Biomed. Eng.* 61, 1765–1771. doi: 10.1109/TBME.2014.2306672

Brocker, D. T., and Grill, W. M. (2013). "Principles of electrical stimulation of neural tissue," in *Handbook of Clinical Neurology*, Vol. 116, eds P. J. Vinken and G. W. Bruyn (Amsterdam: Elsevier), 3–18.

Castaño-Candamil, S., Mottaghi, S., Coenen, V. A., Hofmann, U. G., and Tangermann, M. (2017). "closed-loop deep brain stimulation system for an animal model of parkinson's disease: a pilot study," in *Proceedings of the 7th Graz Brain-Computer Interface Conference 2017*, Graz.

de Hemptinne, C., Swann, N. C., Ostrem, J. L., Ryapolova-Webb, E. S., San Luciano, M., Galifianakis, N. B., et al. (2015). Therapeutic deep brain stimulation reduces cortical phase-amplitude coupling in Parkinson's disease. *Nat. Neurosci.* 18, 779–786. doi: 10.1038/nn.3997

Foutz, T. J., and McIntyre, C. C. (2010). Evaluation of novel stimulus waveforms for deep brain stimulation. *J. Neural Eng.* 7:066008. doi: 10.1088/1741-2560/7/ 6/066008

Gimsa, J., Habel, B., Schreiber, U., Rienen, U., Van, Strauss, U., et al. (2005). Choosing electrodes for deep brain stimulation experiments-electrochemical considerations. *J. Neurosci. Methods* 142, 251–265. doi: 10.1016/j.jneumeth. 2004.09.001

Gong, C. S. A., Lai, H. Y., Huang, S. H., Lo, Y. C., Lee, N., Chen, P. Y., et al. (2015). A programmable high-voltage compliance neural stimulator for deep brain stimulation in vivo. *Sensors* 15, 12700–12719. doi: 10.3390/s15061 2700

Hamid, S., and Hayek, R. (2008). Role of electrical stimulation for rehabilitation and regeneration after spinal cord injury: an overview. *Eur. Spine J.* 17, 1256–1269. doi: 10.1007/s00586-008-0729-3

Hardesty, D. E., and Sackeim, H. A. (2007). Deep brain stimulation in movement and psychiatric disorders. *Biol. Psychiatry* 61, 831–835. doi: 10.1016/j.biopsych. 2006.08.028

Jezernik, S., Sinkjaer, T., and Morari, M. (2010). Charge and energy minimization in electrical/magnetic stimulation of nervous tissue. *J. Neural Eng.* 7:046004. doi: 10.1088/1741-2560/7/4/046004

Karumbaiah, L., Saxena, T., Carlson, D., Patil, K., Patkar, R., Gaupp, E. A., et al. (2013). Relationship between intracortical electrode design and chronic recording function. *Biomaterials* 34, 8061–8074. doi: 10.1016/j.biomaterials. 2013.07.016

Lanotte, M. M., Rizzone, M., Bergamasco, B., Faccani, G., Melcarne, A., and Lopiano, L. (2002). Deep brain stimulation of the subthalamic nucleus: anatomical, neurophysiological, and outcome correlations with the effects of stimulation. *J. Neurol. Neurosurg. Psychiatry* 72, 53–58.

Largus, S. (1983). *Compositiones, in Scribonii Largi*. Leipzig: Teubner.

Li, Y., Li, H., Wang, Y., and Bi, G. (2015). A multichannel waveform generator for spatiotemporal stimulation of dissociated neuronal network on MEA. *J. Med. Bioeng.* 4, 105–109. doi: 10.12720/jomb.4.2.105-109

Little, S., Beudel, M., Zrinzo, L., Foltynie, T., Limousin, P., Hariz, M., et al. (2016). Bilateral adaptive deep brain stimulation is effective in Parkinson's disease. *J. Neurol. Neurosurg. Psychiatry* 87, 717–721. doi: 10.1136/jnnp-2015-31 0972

Little, S., Pogosyan, A., Neal, S., Zavala, B., Zrinzo, L., Hariz, M., et al. (2013). Adaptive deep brain stimulation in advanced Parkinson disease. *Ann. Neurol.* 74, 449–457. doi: 10.1002/ana.23951

Maffiuletti, N. A. (2010). Physiological and methodological considerations for the use of neuromuscular electrical stimulation. *Eur. J. Appl. Physiol.* 110, 223–234. doi: 10.1007/s00421-010-1502-y

McConnell, G. C., Butera, R. J., and Bellamkonda, R. V. (2009). Bioimpedance modeling to monitor astrocytic response to chronically implanted electrodes. *J. Neural Eng.* 6:055005. doi: 10.1088/1741-2560/6/5/055005

McCreery, D. B., Agnew, W. F., Yuen, T. G., and Bullara, L. (1990). Charge density and charge per phase as cofactors in neural injury induced by electrical stimulation. *IEEE Trans. Biomed. Eng.* 37, 996–1001.

Merrill, D. R., Bikson, M., and Jefferys, J. G. R. (2005). Electrical stimulation of excitable tissue: design of efficacious and safe protocols. *J. Neurosci. Methods* 141, 171–198. doi: 10.1016/j.jneumeth.2004.10.020

Moro, E., Esselink, R. J. A., Xie, J., Hommel, M., Benabid, A. L., and Pollak, P. (2002). The impact on Parkinson's disease of electrical parameter settings in STN stimulation. *Neurology* 59, 706–713. doi: 10.1212/WNL.59.5.706

Mottaghi, S., Afshari, N., Buchholz, O., Liebana, S., and Hofmann, U. G. (2020). NES stim ressources. *Figshare*.

Mottaghi, S., Pinnell, R., and Hofmann, U. G. (2015). "A 16-bit High-Voltage Digital Charge-Control Electrical Stimulator BT -," in *World Congress on Medical Physics and Biomedical Engineering*, Toronto.

Nag, S., Jia, X., Thakor, N. V., and Sharma, D. (2013). Flexible charge balanced stimulator with 5.6 fC accuracy for 140 nC injections. *IEEE Trans. Biomed. Circ. Syst.* 7, 266–275. doi: 10.1109/TBCAS.2012.2205574

Osorio, I., Frei, M. G., Manly, B. F. J., Sunderam, S., Bhavaraju, N. C., and Wilkinson, S. B. (2001). An introduction to contingent (closed-loop) brain electrical stimulation for seizure blockage, to ultra-short-term clinical trials, and to multidimensional statistical analysis of therapeutic efficacy. *J. Clin. Neurophysiol.* 18, 533–544. doi: 10.1097/00004691-200111000-00003

Petrofsky, J. S., and Phillips, C. A. (1984). The use of functional electrical stimulation for rehabilitation of spinal cord injured patients. *Central Nervous Syst. Trauma* 1, 57–73.

Ramirez De Noriega, F., Eitan, R., Marmor, O., Lavi, A., Linetzky, E., et al. (2015). Constant current versus constant voltage subthalamic nucleus deep brain stimulation in parkinson's disease. *Stereotactic Funct. Neurosurg.* 93, 114–121. doi: 10.1159/000368443

Rattay, F., Paredes, L. P., and Leao, R. N. (2012). Strength-duration relationship for intra- versus extracellular stimulation with microelectrodes. *Neuroscience* 214, 1–13. doi: 10.1016/j.neuroscience.2012.04.004

Rosin, B., Slovik, M., Mitelman, R., Rivlin-Etzion, M., Haber, S. N., Israel, Z., et al. (2011). Closed-loop deep brain stimulation is superior in ameliorating parkinsonism. *Neuron* 72, 370–384. doi: 10.1016/j.neuron.2011. 08.023

Russo, J. F., and Sheth, S. (2015). Deep brain stimulation of the dorsal anterior cingulate cortex for the treatment of chronic neuropathic pain. *Neurosurg. Focus* 38, 1–11. doi: 10.3171/2015.3.FOCUS1543.Disclosure

Sahin, M., and Tie, Y. (2007). Non-rectangular waveforms for neural stimulation with practical electrodes. *J. Neural Eng.* 4, 227–233. doi: 10.1088/1741-2560/4/ 3/008

Sanders, J. I., and Kepecs, A. (2014). A low-cost programmable pulse generator for physiology and behavior. *Front. Neuroeng.* 7:43. doi: 10.3389/fneng.2014. 00043

Schlaepfer, T. E., Bewernick, B. H., Kayser, S., Mädler, B., and Coenen, V. A. (2013). Rapid effects of deep brain stimulation for treatment-resistant major depression. *Biol. Psychiatry* 73, 1204–1212. doi: 10.1016/j.biopsych.2013.01.034

Schor, J. S., and Nelson, A. B. (2019). Multiple stimulation parameters influence efficacy of deep brain stimulation in parkinsonian mice. *J. Clin. Invest.* 130, 3833–3838. doi: 10.1172/JCI122390

Shannon, R. V., Zeng, F. G., Kamath, V., Wygonski, J., and Ekelid, M. (1995). Speech recognition with primarily temporal cues. *Science* 270, 303–304.

So, R. Q., McConnell, G. C., and Grill, W. M. (2017). Frequency-dependent, transient effects of subthalamic nucleus deep brain stimulation on

methamphetamine-induced circling and neuronal activity in the hemiparkinsonian rat. *Behav. Brain Res.* 320, 119–127. doi: 10.1016/j.bbr.2016.12.003

Sooksood, K., Stieglitz, T., and Ortmanns, M. (2009). An experimental study on passive charge balancing. *Adv. Radio Sci.* 7, 197–200. doi: 10.5194/ars-7-197-2009

Sooksood, K., Stieglitz, T., and Ortmanns, M. (2010). An active approach for charge balancing in functional electrical stimulation. *IEEE Trans. Biomed. Circ. Syst.* 4, 162–170. doi: 10.1109/TBCAS.2010.2040277

Stewart, F., Gameiro, O. L. F., El Dib, R., Gameiro, M. O., Kapoor, A., and Amaro, J. L. (2016). Electrical stimulation with non-implanted electrodes for overactive bladder in adults. *Cochrane Database Syst Rev.* 12:CD010098. doi: 10.1002/14651858.CD010098.pub4

Stitt, R. M. (1990). Implementation and applications of current sources and current receivers. *Burr-Brown Application Bulletin*, 1–30. Available online at: http://www.ti.com/lit/an/sboa046/sboa046.pdf

Tandon, N., Cannizzaro, C., Chao, P.-H. G., Maidhof, R., Marsano, A., Au, H. T. H., et al. (2009). Electrical stimulation systems for cardiac tissue engineering. *Nat. Protocol.* 4, 155–173. doi: 10.1038/nprot.2008.183

Tehovnik, E. J. (2006). Direct and indirect activation of cortical neurons by electrical microstimulation. *J. Neurophysiol.* 96, 512–521. doi: 10.1152/jn.00126.2006

Tronnier, V. M., Domingo, A., Moll, C. K., Rasche, D., Mohr, C., Rosales, R., et al. (2015). Biochemical mechanisms of pallidal deep brain stimulation in X-linked dystonia parkinsonism. *Parkinsonism. Relat. Disord.* 21, 954–959. doi: 10.1016/j.parkreldis.2015.06.010

Tronnier, Volker, M., Fogel, W., Krause, M., Bonsanto, M. M., Tronnier, J., et al. (2002). High frequency stimulation of the basal ganglia for the treatment of movement disorders: current status and clinical results. *Minim. Invasive Neurosurg.* 45, 91–96. doi: 10.1055/s-2002-32495

Ungerstedt, U., and Arbuthnott, G. W. (1970). Quantitative recording of rotational behavior in rats after 6-hydroxy-dopamine lesions of the nigrostriatal dopamine system. *Brain Res.* 24, 485–493. doi: 10.1016/0006-8993(70)90187-3

Velasco, A. L., Velasco, M., Velasco, F., Menes, D., Gordon, F., Rocha, L., et al. (2000). Subacute and chronic electrical stimulation of the hippocampus on intractable temporal lobe seizures: preliminary report. *Arch. Med. Res.* 31, 316–328. doi: 10.1016/S0188-4409(00)00064-3

Vidailhet, M., Vercueil, L., Houeto, J.-L., Krystkowiak, P., Benabid, A.-L., Cornu, P., et al. (2005). Bilateral deep-brain stimulation of the globus pallidus in primary generalized dystonia. *N. Engl. J. Med.* 352, 459–467. doi: 10.1056/NEJMoa042187

Vonck, K., Boon, P., Achten, E., De Reuck, J., and Caemaert, J. (2002). Long-term amygdalohippocampal stimulation for refractory temporal lobe epilepsy. *Ann. Neurol.* 52, 556–565. doi: 10.1002/ana.10323

Wang, J. S., Lee, J. H., and Kim, N. J. (2015). Effects of neuromuscular electrical stimulation on masticatory muscles in elderly stroke patients. *J. Phys. Ther. Sci.* 27, 2767–2770. doi: 10.1589/jpts.27.2767

Washburn, S., Catlin, R., Bethel, K., and Canlas, B. (2014). Patient-perceived differences between constant current and constant voltage spinal cord stimulation systems. *Neuromodulation* 17, 28–35. doi: 10.1111/ner.12085

Wongsarnpigoon, A., Woock, J. P., and Grill, W. M. (2010). Efficiency analysis of waveform shape for electrical excitation of nerve fibers. *IEEE Trans. Neural Syst. Rehabil. Eng.* 18, 319–328. doi: 10.1109/TNSRE.2010.2047610

Wu, H. C., Young, S. T., and Kuo, T. S. (2002). A versatile multichannel direct-synthesized electrical stimulator for FES applications. *IEEE Trans. Instrum. Meas.* 51, 2–9. doi: 10.1109/19.989882

Yuan, H., and Silberstein, S. D. (2016). Vagus nerve and vagus nerve stimulation, a comprehensive review: part II. *Headache* 56, 259–266. doi: 10.1111/head.12650

Yuen, T. G. H., Agnew, W. F., Bullara, L. A., Jacques, S., and McCreery, D. B. (1981). Histological evaluation of neural damage from electrical stimulation: considerations for the selection of parameters for clinical application. *Neurosurgery* 9, 292–299. doi: 10.1227/00006123-198109000-00013

Conflict of Interest: The authors declare that the research was conducted in the absence of any commercial or financial relationships that could be construed as a potential conflict of interest.

frontiers in Neuroscience

ORIGINAL RESEARCH
published: 07 May 2020
doi: 10.3389/fnins.2020.00389

Sensory- and Action-Oriented Embodiment of Neurally-Interfaced Robotic Hand Prostheses

Giovanni Di Pino[1], Daniele Romano[2], Chiara Spaccasassi[2], Alessandro Mioli[1], Marco D'Alonzo[1], Rinaldo Sacchetti[3], Eugenio Guglielmelli[4], Loredana Zollo[4], Vincenzo Di Lazzaro[5], Vincenzo Denaro[6] and Angelo Maravita[2]*

[1] Research Unit of Neurophysiology and Neuroengineering of Human-Technology Interaction (NeXTlab), Università Campus Bio-Medico di Roma, Rome, Italy, [2] Psychology Department & NeuroMi, Milan Center for Neuroscience, University of Milan-Bicocca, Milan, Italy, [3] National Institute for Insurance Against Accidents at Work, Bologna, Italy, [4] Research Unit of Advanced Robotics and Human-Centred Technologies, Università Campus Bio-Medico di Roma, Rome, Italy, [5] Research Unit of Neurology, Neurophysiology, Neurobiology, Università Campus Bio-Medico di Roma, Rome, Italy, [6] Research Unit of Orthopedics and Traumatology, Università Campus Bio-Medico di Roma, Rome, Italy

OPEN ACCESS

Edited by:
Stefano Ferraina, Sapienza University of Rome, Italy

Reviewed by:
Brent Winslow, Design Interactive, United States
Solaiman Shokur, Federal Institute of Technology in Lausanne, Switzerland
Giacomo Valle, ETH Zürich, Switzerland

***Correspondence:**
Giovanni Di Pino
g.dipino@unicampus.it

Specialty section:
This article was submitted to Neural Technology, a section of the journal Frontiers in Neuroscience

Received: *10 January 2020*
Accepted: *30 March 2020*
Published: *07 May 2020*

Citation:
Di Pino G, Romano D, Spaccasassi C, Mioli A, D'Alonzo M, Sacchetti R, Guglielmelli E, Zollo L, Di Lazzaro V, Denaro V and Maravita A (2020) Sensory- and Action-Oriented Embodiment of Neurally-Interfaced Robotic Hand Prostheses. Front. Neurosci. 14:389. doi: 10.3389/fnins.2020.00389

Embodiment is the percept that something not originally belonging to the self becomes part of the body. Feeling embodiment for a prosthesis may counteract amputees' altered image of the body and increase prosthesis acceptability. Prosthesis embodiment has been studied longitudinally in an amputee receiving feedback through intraneural and perineural multichannel electrodes implanted in her stump. Three factors—invasive (vs non-invasive) stimulation, training, and anthropomorphism—have been tested through two multisensory integration tasks: visuo-tactile integration (VTI) and crossing-hand effect in temporal order judgment (TOJ), the former more sensible to an extension of a safe margin around the body and the latter to action-oriented remapping. Results from the amputee participant were compared with the ones from healthy controls. Testing the participant with intraneural stimulation produced an extension of peripersonal space, a sign of prosthesis embodiment. One-month training extended the peripersonal space selectively on the side wearing the prostheses. More and less-anthropomorphic prostheses benefited of intraneural feedback and extended the peripersonal space. However, the worsening of TOJ performance following arm crossing was present only wearing the more trained, despite less anthropomorphic, prosthesis, suggesting that training was critical for our participant to achieve operative tool-like embodiment.

Keywords: neural interface, sensory feedback, robotic hand prostheses, embodiment, multisensory integration

INTRODUCTION

Despite improved mechatronic features have made hand prostheses more dexterous, their abandonment exceeds 30% (Cordella et al., 2016). Besides high weight and cost, low life-like appearance, low comfort and dexterity (Biddiss and Chau, 2007), and difficult pre-prosthetic training (Peerdeman et al., 2011), what amputees claim as a main limitation is that, regardless of the level of prosthesis functionality, they perceive it as an "inert supplement" or an "extracorporeal structure" and not as part of their body (Scarry, 1994).

As a multipurpose tool allowing capabilities and conveying sensory inflows, the hand is located at the human-environment frontier and defines the boundary of the body, so that its loss greatly affects how amputees perceive themselves and their body (Drench, 1994; Flannery and Faria, 1999). Somatosensory feedback plays a key role in dexterous manipulation and boosts motor learning. Today, commercial hand prostheses do not offer sensory feedback, although position and force information from the prosthesis are identified as design priority for myoelectric devices, in order to increase acceptance (Biddiss and Chau, 2007).

Those reasons generated a strong research effort to develop and test prosthesis-user interfacing systems that, in parallel to a better motor control, can offer rich and pleasant feedback. Sensory feedback from hand prostheses have been delivered employing intraneural (Dhillon and Horch, 2005; Rossini et al., 2010; Page et al., 2018; Petrini et al., 2018) and perineural (Ortiz-Catalan et al., 2014; Tan et al., 2014) electrodes, targeted sensory reinnervation (Kuiken et al., 2007; Marasco et al., 2009; Vadalà et al., 2017), or non-invasive sensory substitution (Antfolk et al., 2013). Richer sensory feedback from the prosthesis showed to improve motor ability (Valle et al., 2018; Zollo et al., 2019), object features discrimination (Raspopovic et al., 2014), and to counteract amputation-induced maladaptive brain plasticity (Di Pino et al., 2014; Serino et al., 2017).

Convergent multisensory afference build the representation of the body in the brain, which has been shown to be flexible to the point of integrating external objects not belonging to the self; the perceptual process producing such integration is known as embodiment (Iriki et al., 1996; Maravita and Iriki, 2004). Thus, a prosthesis enabling a more physiological sensory feedback is expected to greatly improve its embodiment and acceptance (Murray, 2004; Svensson et al., 2017; Graczyk et al., 2019).

Few reports tested the embodiment of worn prostheses able to deliver sensory feedback in amputees with targeted sensory reinnervation (Marasco et al., 2018), perineural flat interface nerve electrodes (FINE) (Schiefer et al., 2016; Graczyk et al., 2018), and with intraneural electrodes (Page et al., 2018; Rognini et al., 2018; Valle et al., 2018). All of them employed the rubber hand illusion (RHI) paradigm (Botvinick and Cohen, 1998) or modified versions of it (Page et al., 2018; Rognini et al., 2018), or interviewed participants using questionnaires derived from the one typically employed in the RHI.

However, the translation of RHI findings to prosthesis embodiment in amputees is not free from possible pitfalls; RHI setup is very structured and artificial, the fake hand is not worn and typically cannot move, and the illusion is only temporary (D'Alonzo et al., 2020; Niedernhuber et al., 2018).

Easily gathered clues on embodiment also come from changes reported by the subject in the perceived length of the phantom limb (Rossini et al., 2010; Graczyk et al., 2018; Rognini et al., 2018; Valle et al., 2018). Still, body representation and phantom awareness are very likely different concepts, partly relying on different brain networks (Ehrsson et al., 2005; Flor et al., 2006; Reilly and Sirigu, 2008; Di Pino et al., 2009; Kikkert et al., 2019).

Any outer event is caught by different sensory modalities; their flow of information is integrated by our brain to have a high probability of experiencing the fact with accuracy. The way the brain integrates senses while experiencing an event depends on the relation of that event with our body. For instance, our brain integrates faster somatosensory and visual stimuli delivered close to the body, within the so-called peripersonal space (PPS) (Fogassi et al., 1996). PPS is the space around the body that can be directly acted upon by the body and where the analysis of external events is more critical to ensure efficient action and protection against threat (Clery et al., 2015b; de Vignemont and Iannetti, 2015). Hence, the embodiment of a body part modulates the way in which multisensory integration occurs around us, and, in turn, multisensory integration can be used to highlight the process of embodiment itself.

In the investigation of multisensory integration, the computation of sensory stimuli can be assessed in reference to the somatotopic map or in reference to the external, egocentric space. On one hand, the former can be achieved through visuo-tactile integration (VTI) tasks. In a VTI, the participant has to respond to a stimulus delivered to a limb, while a concurrent incoming visual stimulus is delivered at different distances. The closer to the body the visual stimulus is, the faster the reaction time (RT). Since VTI tests the area of visuo-tactile integration, which is extended by an embodied extracorporeal tool, it has been employed to assess embodiment in the animal and in humans (Iriki et al., 1996; Maravita and Iriki, 2004).

The same approach, albeit using audio-tactile stimuli, has been recently adopted to assess the extension of PPS as a proxy of tools (Canzoneri et al., 2012) and prosthesis embodiment (Canzoneri et al., 2013a). In these paradigms, an overall speeding up of RT expresses general better performance, while a variation of the shape of the RTs/distance curve is a clue of enlargement of peripersonal space (Spaccasassi et al., 2019) that may occur following tool/prosthesis embodiment.

On the other hand, the computation of sensory stimuli in reference to the external, egocentric space can be investigated through a temporal order judgment (TOJ) task (Yamamoto and Kitazawa, 2001a). In the TOJ, the participant states which one of two tactile stimuli, delivered to the upper limbs with variable asynchrony, is perceived first. When TOJ is tested with uncrossed hands, the right hand is in the right side of the environment and the judgment of which hand was stimulated first can rely only on somatosensory stimuli. When TOJ is tested with the hands crossed, the performance typically deteriorates because the tactile somatotopic spatial coordinates come in contrast with the visual external spatial coordinates conveyed by vision (Yamamoto and Kitazawa, 2001a; Schicke and Roder, 2006). The increase of RT is due to the time needed for the resolution of conflict between sensory modalities (Shore et al., 2002) or for their integration (Heed et al., 2015). Critically, the embodiment of tools (Yamamoto and Kitazawa, 2001b) and prostheses (Sato et al., 2017) is subjected to the same hand crossing effect, which has been taken as a hint to the embodiment of such bodily extensions.

In the present study, we recruited a chronic amputee volunteer and implanted intraneural and perineural multichannel electrodes on her stump to deliver sensory feedback from the prosthesis. After a period of training, she was able to perform

grasps and dexterous manipulation, thanks to a closed-loop control enabled by neural feedback (Zollo et al., 2019). In this volunteer, we longitudinally investigated prosthesis embodiment, using both VTI and TOJ tasks. Experiments have been designed to assess the impact of three factors on prosthesis embodiment: (i) type of stimulation (intraneural invasive vs non-invasive), (ii) training, and (iii) type of prostheses (anthropomorphic vs more trained).

Compared to previous work, this is the first study that longitudinally investigates multiple determinants of prosthesis embodiment through proxies of body representation not derived from the rubber hand illusion or telescoping assessments, but investigating how the relation that multisensory integration has with the body impacts on reaction time. This has been done in a participant naïve for active prosthesis use and in a context of ecologic continuative use of a worn and neurally interfaced hand prosthesis.

The impact of intraneural stimulation on embodiment was investigated because invasive stimulation showed to achieve a more physiological sensory feedback (Raspopovic et al., 2014; Ciancio et al., 2016; Oddo et al., 2016; Valle et al., 2018; Zollo et al., 2019), and the valence and features of sensory feedback are recognized as enabling factors of embodiment (Blanke, 2012; D'Alonzo et al., 2019). Moreover, protocols testing multisensory integration seem to be well-suited to assess the performance of intraneural stimulation conveying information from the hand. Indeed, in monkeys implanted with intracortical array (Dadarlat et al., 2015) and in an amputee volunteer implanted with intraneural electrodes (Risso et al., 2019), multichannel invasive sensory feedback was recently shown to be optimally integrated with visual information, enhancing the precision of the estimation of position and posture of the hand. Training was investigated because it has been shown to facilitate the embodiment process (Iriki et al., 1996; Maravita et al., 2002; Farne et al., 2005) and because its impact was previously showed in healthy subjects taught to use a mechanical hand (Marini et al., 2013). Embodiment was also assessed in relation to the anthropomorphism of the prosthesis, due to a reported stronger embodiment for more human-like non-corporeal objects (Tsakiris et al., 2010).

To evaluate statistical significance of the results achieved with our participant in both experiments, they were compared with the data coming from a group of healthy controls.

MATERIALS AND METHODS

Amputee Participant, Surgery, and Electrodes

The part of this study involving the amputee participant was conducted at Campus Bio-Medico University Hospital of Rome in accordance with the Declaration of Helsinki and following amendments, and it was approved by the local Ethics Committee and by the assigned office of the Italian Ministry of Health. The volunteer participant signed an informed consent form. She is a right-handed female, 40 years old at the time of the experiment. Almost 30 years before, she was exposed to an explosion that produced a transradial left upper limb amputation.

Surgery and Electrodes

The participant underwent a surgical procedure under general anesthesia where two intraneural multichannel electrodes (ds-FILEs) and one cuff electrode (Ardiem Medical Inc.) were implanted in the ulnar nerve trunk, and the same was done in the median nerve trunk (Micera et al., 2010; Di Pino et al., 2013), achieving a total of 64 intraneural plus 28 perineural channels of communication (**Figure 1**, upper row). Electrodes were removed 75 days after implantation to comply with the constraints of the obtained formal approval. Mild fibrotic reaction (Lotti et al., 2017) was found around the electrodes. For a full description of the surgical procedure and electrodes implanted, see Zollo et al. (2019).

Prosthesis and Training

The volunteer subject habitually wore a cosmetic prosthesis for her everyday life, both during working hours and in social circumstances. She was naïve, though, for active prosthesis use. For the experimental tasks, she was tested with a robotic hand research prototype (prosthesis **A:** IH2 Azzurra, Prensilia s.r.l.[1]) and with a more anthropomorphic commercial device (prosthesis **B:** RoboLimb, TouchBionics s.r.l. now commercialized by Ossur[2]). Prosthesis A is an optimal robotic hand research platform, mostly open and flexible to be utilized in different lab experiments on human grip and manipulation. Prosthesis B is designed for amputee end-users to be employed in their daily living tasks at home, and during their social activities. The shape of prosthesis B was closer to the one of the human hand (e.g., the proportion of finger lengths), and its weight and size were very similar to the ones of our participant contralateral healthy hand (**Table 1**).

During training, both prostheses were controlled through surface EMG sensors (Ottobock 13E200) embedded into the socket, while forces of interaction with objects were measured with force-sensing resistors (Interlink Electronics Inc.) embedded in both prostheses' fingers and fed back through neural interfaces.

An *ad hoc* developed algorithm based on non-linear logistic regression allowed to perform power, pinch, lateral grasps, rest, open the hand, and to apply three levels of force. Every time the participant manipulation was evaluated, she performed 24 repetitions of each of the following four tasks: (A) Lateral grasp of large and small objects; (B) pick and place of large objects with a power grasp; (C) pick and place of small objects with a precision grasp; and (D) manipulation tasks featuring: pouring water from a bottle to a cup and sorting cylindric and circular-shaped objects (Zollo et al., 2019). In all the training period, the participant learned to exploit neural feedback to control both prostheses during grasps and manipulation. During the training period, the participant trained about 4 h, six times per week,

[1]https://www.prensilia.com/portfolio/ih2-azzurra/

[2]https://www.ossur.com/en-us/prosthetics/arms/i-limb-access

FIGURE 1 | Upper row, from left to right: surgical field on the median aspect of the left severed arm and identification of median and ulnar nerves **(left)**; higher magnification of the perineural **(central up)** and one of the intraneural electrodes **(central down)** implanted in the nerves, participant during a blinded manipulation training session learning to exploit the neural sensory feedback to control the robotic prostheses **(right)**. **Lower row**, from left to right: the participant involved in a visuo-tactile integration (VTI) experimental session **(left)** and in a temporal order judgment (TOJ) experimental session with the arms crossed **(right)**.

TABLE 1 | Hand and prostheses size, weight, and shape.

	Hand weight (g)	Palm length (mm)	Palm width (mm)	Palm thickness (mm)	Palm and back shape	Fingers rest posture	I digit length (mm)	III digit length (mm)
Healthy hand	450*	100	83	34	Curved	Partly flexed	71	85
Prosthesis A	640	116	102	45	Flat	Fully extended	103	103
Prosthesis B	507	104	75	35	Curved	Partly flexed	78	87

The weight of the healthy hand is expressed considering a percentage of 0.66% of the whole-body weight (Tözeren, 1999).

while she did not use any active prosthesis in her everyday life. The improvement was monitored after the first week of training with the closed-loop control, in the middle of the training period, and at the end of the experimental study. It was assessed by means of instrumented objects and a purposely developed metrics (Zollo et al., 2019).

Due to time constraints connected with the clinical procedures, the training with prosthesis A lasted approximately 45 days, while training with prosthesis B only 20 days. Thus, prosthesis A was the less anthropomorphic and the more trained, while prosthesis B was the more anthropomorphic but the less trained.

Experimental Design

In both VTI and TOJ experiments, the participant was placed in a silent and dimly illuminated room and was acoustically shielded with white noise playing headphones to cover the noise produced by the tappers (**Figure 1**, lower row; **Figures 2**, **3**). Visual and tactile stimuli were presented by the open-source "OpenSesame" software v.3.1 (Mathôt et al., 2012).

In order to assess the achievement of proficiency due to the training, the participant was tested at three different time points (**Figure 4**):

- (*PRE*) Pre-training, non-invasive stimulation: baseline measure, taken when the electrodes were already implanted but the subject had not yet started the training with the prosthesis. Stimulation was delivered to the stump through mechanical tappers.
- (*POST_I*) Post-training, invasive stimulation: 50 days after *PRE* and after 30 days of training with the prostheses. Somatosensory stimulation was delivered to the severed limb through intraneural electrodes.
- (*POST_NI*) Post-training, non-invasive stimulation: after electrodes removal. Stimulation was delivered to the severed limb through mechanical tappers.

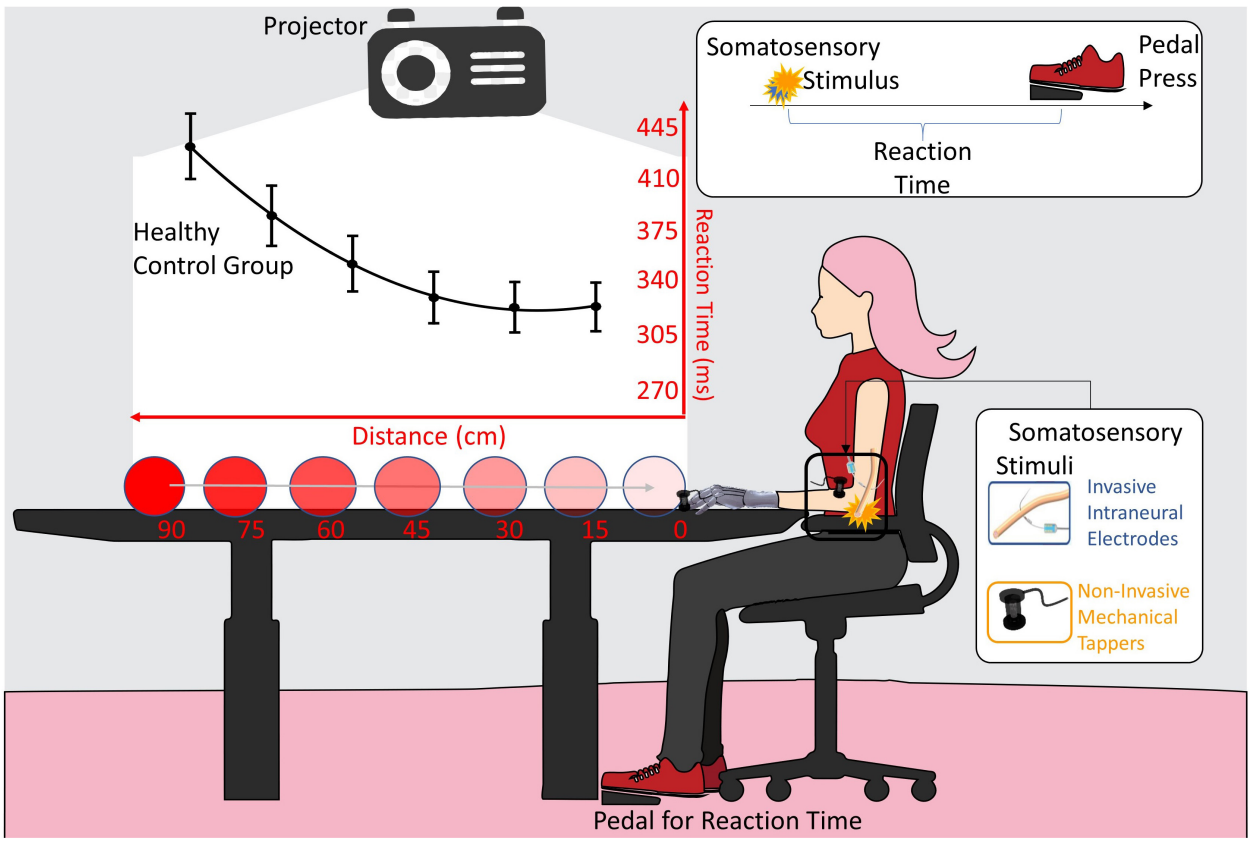

FIGURE 2 | VTI experimental setup. The somatosensory stimulation was delivered either invasively (blue) through intraneural electrodes, or non-invasively (orange) through mechanical tappers, when the visual stimulus, approaching the participant, was at six possible distances (90, 75, 60, 45, 30, 15 cm). Participant had to respond to somatosensory stimuli as fast as possible. Reaction time (RT) to the somatosensory stimulus was taken with a pedal. The black line is the RTs/distance curve (quadratic fitting function) of the healthy subjects control group. Values are means (dots) ± SEM (bars).

Visuo-somatic multisensory integration tasks were performed to assess the impact of the type of stimulation, training, and anthropomorphism on prosthesis embodiment (**Figure 4**).

(i) To test the impact of invasive stimulation on the achieved embodiment, the data from two sessions were compared: *POST_NI* (post_non invasive) collected after electrodes removal was compared with *POST_I* (post_invasive) performed while the participant still had the intraneural electrodes implanted. In both sessions, the healthy limb was stimulated non-invasively. In *POST_I* the stimulation was delivered intraneurally to the affected left limb. For a comprehensive description of the features and location of referred sensation, please see Zollo et al. (2019).

(ii) To investigate the impact of training on embodiment of neurally interfaced prosthesis, the participant, who was naïve for active prosthesis use, was tested non-invasively before (*PRE*), and after training (*POST_NI*).

(iii) To investigate embodiment in relation to the anthropomorphism of the prosthesis, in the *POST_I*, the participant was tested while wearing the two different prosthetic devices (Prosthesis **A** and Prosthesis **B**).

Two different groups of healthy subjects were enrolled as controls for the two experiments. Thirty-six participants (13 males, age = 24.11 years, SD = 4.15, range: 19–42) performed the VTI task and 11 participants (6 males, age = 26.36 years, SD = 3.34, range: 23–32) performed the TOJ. This research was approved by the local Ethics Committee of the Department of Psychology, University of Milano-Bicocca.

Somatosensory Stimulation

As mentioned in the previous paragraph, experiments were designed to deliver sensory stimuli on the fingertips of both hands' index finger and were of two types:

(i) Non-invasive tactile stimuli, administered by means of solenoid tappers (magnetic rod diameter: 4 mm) controlled by an *ad hoc* built relay box (Tactile Box, EMS, Bologna, Italy). Healthy participants, used as control groups, were always stimulated non-invasively. Non-invasive stimulation was also always used for stimulating amputee healthy right upper limb, as well as in *PRE* and *POST_NI* to stimulate her severed left limb. This was achieved by placing the tapper right upon the area of the skin that elicited, in the volunteer, the feeling of being

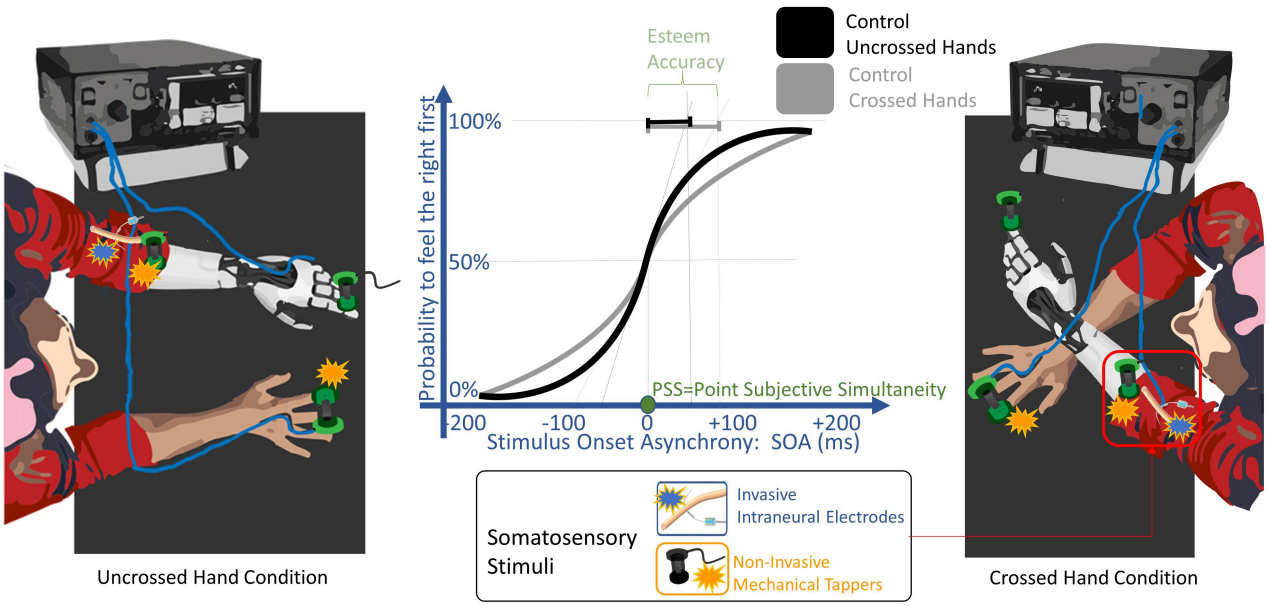

FIGURE 3 | TOJ experimental setup. A pair of somatosensory stimuli were delivered non-invasively (orange) through mechanical tappers, and only in the POST_I session to the left severed limb invasively (blue) through intraneural electrodes. Stimuli were delivered, one to each limb, with a stimulus onset asynchronies (SOA) randomly assigned from 15 to 200 ms. The participant had to discern in which limb the first stimulus was delivered. The task was performed either with uncrossed and with the crossed arms. The solid lines are the probability to feel the right limb stimulated first depending on the SOA, fitted with a sigmoid function, when the task was performed by a healthy subject control group with the arms uncrossed (black) and crossed (gray). The point of subjective simultaneity (PSS) is the SOA where both limbs have the same probability to be perceived as firstly stimulated. The decrease of the slope of the curve from uncrossed to the crossed condition represents the worsening of esteem accuracy typical of the arm crossing effect. The esteem accuracy (EA) is computed through the SOA corresponding to half of the inverse of its derivate for PSS (black and gray segments for uncrossed and crossed hands, respectively); thus, the shorter the EA value is, the higher the accuracy is.

touched on her phantom left index fingertip. The area where the fingers were reported to be was identified with two methods: firstly, by asking the subject where she felt a referred sensation of any digit, and secondly, by touching the skin of the stump until she referred to be touched on that finger. For all the fingers, the maps identified by the two methods were coherent. The skin area marked as digit II was employed as stimulation point. An inactive tapper was placed upon the prosthesis index finger to emulate the one placed on the healthy hand and to reinforce the perception in the volunteer that the stimulation was coming from the index finger on both sides.

(ii) Intraneural invasive stimulation was exploited in *POST_I* to stimulate the amputee participant severed left limb, employing parameters that induced a sensation that she referred to be closer to the one evoked by the mechanical tapper, in terms of intensity, modality, and referred territory. Indeed, after electrode implantation, a whole-contact psychophysical sensory mapping was performed to establish the match between stimulated contact, modality amplitude, and referred territory of the evoked sensation. Moreover, sensory mapping has been tested and retested day after day before *PRE* to have an estimation of the day-by-day reliability of the evoked sensations. The neural electrodes elicited sensations that the participant referred to 13 different locations of the anterior and the posterior parts of the phantom hand. The contacts that were used for the real-time closed-loop control of the prosthesis were chosen because they: (i) did not evoke muscle twitch at the beginning of the test period and (ii) changed over time the induced sensation from eliciting the sensation of movement to the sense of touch. In both tasks, invasive stimulation was delivered in the form of square pulse stimuli to the channel number 12 of the intraneural electrode (ds-FILE) positioned proximally within the median nerve (stimulus intensity 300 μA, duration 200 μs) (Intraneural Stimulator: Grass S88X, Astro-Med Inc., West Warwick, RI, United States). Stimulation parameters and channel were selected on the basis of the sensations reported by the participant in multiple assessment tests. For a comprehensive description of the features, stability, and location of referred sensations, please see Zollo et al. (2019).

VTI Task

In this experiment, a VTI task was carried out to assess the extent of the peripersonal space (PPS) in different conditions and at different time points.

Experimental Setup and Procedure

The participant was seated beside the wall with her tested upper limb resting on a table in a prone position (**Figure 1**, lower row; **Figure 2**). A PC-driven digital projector was set at a distance suited for projecting a video that covered a 100 × 75 cm surface

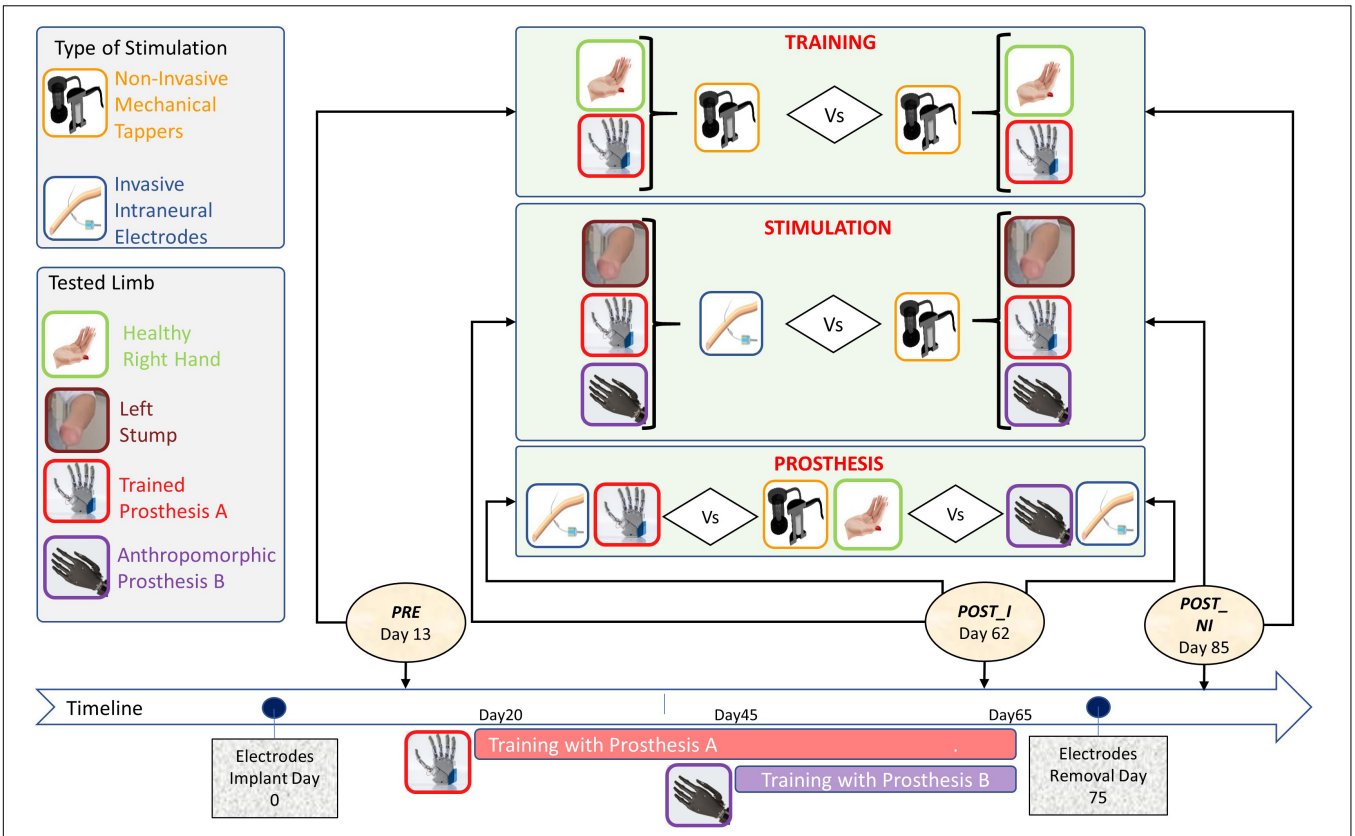

FIGURE 4 | Timeline and protocol design for the three tested factors: (i) Training, (ii) Stimulation, and (iii) Prosthesis, with the types of stimulation (left-up panel) and tested limbs/prostheses (left-center panel).

on the wall. The video showed a visual stimulus approaching the participant. Visual stimuli consisted of looming images on a white background covering a distance of 1 m on the bottom side of the projecting area and traveling at a constant speed of 66 cm/s.

On all testing sessions, the space of VTI was tested for the participant's right healthy limb, the severed left limb wearing prosthesis **A** and prosthesis **B** (in PRE session, prosthesis **B** was not available), and the bare stump. The participant's elbow was always kept at 42 cm from the limit of the projecting area. This resulted in a distance from the projecting area of 30 cm from the endpoint of the stump, while in all the other conditions, the extremity of the limb or the prosthesis was in contact with the limit of the projecting area.

Along with the visual stimulus, in 85% of the trials, a tactile stimulus was randomly delivered when the visual approaching stimulus was at one of six distance points (15, 30, 45, 60, 75, 90 cm) from the end of the projecting area. The participant was asked to press a pedal as soon as she perceived the tactile stimulus. The remaining 15% of the trials were "catch trials," where no tactile stimulus was administered and no response was expected.

The task lasted approximately 8 min, consisting in a total of 168 trials (24 repetitions per distance points and 24 catch trials) and 800 ms of inter-trial interval. A small training phase with 15 stimuli presentation preceded the experimental task.

Data Analysis

Data were analyzed by addressing the three experimental questions defined in the section "Introduction." Analysis was implemented in order to weigh different factors, while minimizing the total number of comparisons. The dependent variable which was taken into consideration was the RT in response to the tactile stimulus (Zangrandi et al., 2019). The factor *Distance* was computed as a continuous variable.

- STIMULATION. In order to assess the relative weight of the stimulation interface (*non-invasive* vs *intraneural*), we implemented a *linear mixed model* (*LMM*). The model was analyzed with an analysis of variance (ANOVA) with Satterthwaite approximation for degrees of freedom. We included as predictors the continuous factor *Distance* and the dichotomous factor *Stimulation* (*intraneural* vs *non-invasive*). The number of the trial was added as a random effect variable. The two levels of factor Stimulation have been implemented by pooling together all the conditions exploiting intraneural interface at *POST_I* (prosthesis **A** + prosthesis **B** + bare stump: level *intraneural)* tested against the same conditions recorded at *POST_NI* (level *non-invasive*). To maintain homogeneity of samples, data from *PRE* were not included because they lack prosthesis **B**. Before being available to perform the non-invasive

stimulation session, the participant had to go through all the activities linked with presurgical exams, surgery for electrode removal, and recovery after the surgery. Thus, *POST_NI* session was performed 22 days after the *POST_I* session. The time spent training with the prostheses between *POST_I* and *POST_NI* was marginal because the participant was involved in perioperative procedures; thus, the impact of any additional training between the two sessions should be considered negligible.

- TRAINING. In order to assess the relative weight of the training to control the prosthesis, we used the same approach of stimulation analysis. We employed a LMM, analyzed with an ANOVA with Satterthwaite approximation for degrees of freedom. The number of the trial was added as a random effect variable. Predictors were the continuous variable *Distance* and two dichotomous variables: *Hand* (prosthesis **A** vs healthy limb) and *Time* (*PRE* vs *POST_NI*). We have chosen these time points to avoid introducing noise in the data due to different types of stimulation (at *POST_I* stimulation was delivered intraneurally). Additionally, in order to highlight the effects of training on the performance of the task, we conducted two independent ANOVA with the predictors *Distance* and *Time* (*PRE* vs *POST_NI*).
- PROSTHESIS. In order to assess the relative weight of the employed prostheses, and whether they were embodied, we again employed a LMM, analyzed with an ANOVA with Satterthwaite approximation for degrees of freedom. The number of the trial was added as a random effect variable. Predictors were *Distance* and *Hand* (three levels: prosthesis **A**, prosthesis **B**, and healthy hand). The three levels of factor *Hand* have been implemented with data recorded at *POST_I*. *POST_I* has been chosen because it was the only time point when prosthesis feedback could have been done through intraneural stimulation, and because the proficiency with the prosthesis was already achieved. Additionally, we ran an analysis to evaluate the performance in the spatial transition from peripersonal to extrapersonal space. We selected the distances of 15 (near) and 45 (far) cm. When the participant was tested on the stump condition, thus not wearing any kind of prosthesis, the tip of the stump was 30 cm away of the tip of the prosthesis (e.g., closer to the trunk). By doing so, the same distances resulted in a 45 (near) and 75 (far) cm away, although the physical positions of both the visual stimulus and stump were exactly the same in both conditions. Thus, we adopted a LMM, analyzed with an ANOVA with Satterthwaite approximation for degrees of freedom including the number of trials as a random effect variable. The predictors were the *Distance* (near vs far) and *Hand* (prosthesis **A** vs stump).

TOJ Task

In this experiment, a TOJ of two stimuli delivered on the upper limb was carried out to investigate the participant's body awareness in different conditions and at different time points.

Experimental Setup and Procedure

The participant was seated in front of a table, with both her upper limbs lying on its surface in a prone position (**Figure 1**, lower row; **Figure 3**). Two tactile stimuli were delivered rapidly, one to each limb, with one of the following randomly assigned stimulus onset asynchronies (SOA): -200, -90, -55, -30, -15, 15, 30, 55, 90, 200 ms. Negative intervals indicate that the right limb was stimulated before the left limb and *vice versa*.

Each trial started with a visual cue (100 ms red LED light) which was followed, after 300 ms, by two tactile stimuli, delivered one to each limb. Before the experiment started, two colored stickers were applied to the participant's arms (the association between color and arms varied across the testing conditions) and they were used as a code to indicate the stimulated limb without referring to laterality tags (left/right).

Each experimental condition was tested with eight experimental blocks, four while the subject's hands were uncrossed (with a gap of 40 cm between her hands) and the other four when her hands were crossed. In the crossed conditions, in half of these blocks, the right limb was kept over the left limb and in the other half, the left limb was kept over the right limb. In four experimental blocks, the participant was asked to verbally report whether the first of the two stimuli was administered on the right or the left limb, while in the other four, on the contrary, she had to report where the second stimulus occurred.

Testing each condition, consisting in a total of 200 trials (20 repetitions per SOA) for the uncrossed limbs and the same amount of trials for the crossed limbs, lasted approximately 35 min. In *POST_I*, the task was repeated twice, using either prosthesis **A** or prosthesis **B.**

Data Analysis

The order judgment of the subject in each condition was plotted with the different "*stimulus onset asynchrony (SOA)*" as independent variable (x-axis) and "*the probability to judge the right limb as the one firstly stimulated*" as the dependent variable (y-axis). Then, data distribution was fitted with a psychophysics sigmoid function:

$$\mathrm{P}\,(\mathrm{SOA},\ \mathrm{PSS},\ \mathrm{EA}) = \frac{1}{1+\exp\left(-\frac{\mathrm{SOA}-\mathrm{PSS}}{0.5\times\mathrm{EA}}\right)}$$

where the two parameters PSS and EA represent:

Point of subjective simultaneity (PSS):

$$\mathrm{PSS} = \mathrm{SoA}|_{P_{0.5}}$$

This is the SOA value on the curve where the first stimulus had the same probability (p = 0.5) to be felt on the right and on the left limb. It testifies the laterality stimulation bias measured in milliseconds.

Esteem accuracy (EA):

$$\mathrm{EA} = \left(2 \times \frac{d\mathrm{P}}{d\mathrm{SOA}}\bigg|_{\mathrm{SOA}=\mathrm{PSS}}\right)^{-1}$$

This is the SOA needed for the line tangent to the curve at (p = 0.5) to reach the value p = 1. It is the inverse of the

slope of the curve multiplied by 0.5. The shorter it is, the more accurate the esteem.

Fitting TOJ data with the previous function gives back a value of PSS and EA for each tested condition. To give statistic relevance to those outputs, they were compared with the ones obtained by the control group of healthy subjects performing the same task, by means of Crawford *t*-tests.

The Crawford t-test, instead of comparing the performance with that of a large population with a normal distribution, matches the participant's score against a relatively small control group (i.e., frequently $N < 10$ and typically up to 30). The control group must have done exactly the same task of the single case participant, then a Student-*t* distribution was adopted for matching the participant's performance. Under simulations, the method proved to reliably keep under control the alpha error probability to the nominal value of.05 (Crawford and Garthwaite, 2007; Crawford et al., 2010). We also report the effect size (Z-CC), an index analogous to the Cohen's d and the limit of the credibility intervals (CI) of the effect size.

- STIMULATION: Pooling together the bare stump, prosthesis **A** and prosthesis **B**, two different pair of stimulations (in *POST_I*: right limb stimulated non-invasively and left limb stimulated invasively vs in *POST_NI* both limbs stimulated non-invasively) were compared through their PSS in the uncrossed condition. The uncrossed condition is the standard situation of the TOJ task, without conflicting information about laterality, thus results in the highest accuracy. Therefore, this is the best condition to evaluate any laterality temporal bias which may be only due to the type of stimulation.
- TRAINING: In *PRE* session, the participant was extremely inaccurate and variable in performing the crossed condition, so data have not been analyzed.
- PROSTHESIS: To assess embodiment of prostheses with intraneural sensory feedback, we evaluated in *POST_I* the worsening of Esteem Accuracy due to hand crossing, while the participant was wearing prosthesis **A** or prosthesis **B**.

RESULTS

Stimulation

The VTI experiment first replicated the well-known reduction of RT when the somatosensory stimulus was delivered while the visual stimulus was closer to the upper limb extremity, with a main effect of *Distance* [$F(1,766) = 47.758$, $p < 0.001$]. Critically, the participant accomplished the task differently according to the type of somatosensory stimulation, as shown by the main effect of *Stimulation* [$F(1,760) = 5.842$, $p = 0.016$]. Moreover, the type of stimulation affected the pattern of the RT/distance curve, as shown by the interaction *Distance* × *Stimulation* [$F(1,766) = 5.544$, $p = 0.019$] (**Figure 5**).

When the participant was stimulated non-invasively, the presence of clearly significant *Distance* × *Group* interaction (*amputee stimulated non-invasively* vs *Control*) [$F(1,5077) = 28.379$, $p < 0.001$] suggests that the participant behaved differently from the control healthy group. The same remarkable difference was not observed when the participant was stimulated invasively (*Distance* × *Group* – *amputee stimulated invasively* vs *Control*: [$F(1,5033) = 3.3954$, $p = 0.066$], showing a behavior similar to that of the control group (**Figure 5**). Having a similar RT/Distance pattern than healthy control is in favor of facilitation of prosthesis embodiment when this was tested with intraneural stimulation.

In the TOJ with uncrossed limbs, when the right limb was stimulated non-invasively and the left invasively, there was a significant right laterality bias, so that the participant perceived intraneural left stimulation with about 30 ms delay compared to the healthy limb [point of subjective simultaneity (PSS) = + 28.9, CI: (+14.8 ms, +42.5 ms)]. PSS was significantly different than the one of the control group only when the left limb was stimulated invasively [non-invasive/intraneural vs control: $t(10) = 2.582$, $p = 0.027$, Z-CC = 2.69 CI (1.37, 3.98); noninvasive/non-invasive vs control: $t(10) = 0.946$, $p = 0.336$)].

When the left limb was stimulated intraneurally and the right limb non-invasively, the performance of the task was not worse than when both limbs were stimulated non-invasively, despite the asymmetric stimulation. Indeed, both conditions had esteem accuracy (EA) not different than the one of the control group (non-invasive/intraneural vs control: $t = 1.011$, $p = 0.336$; non-invasive/non-invasive vs control: $t = -0.383$, $p = 0.71$) (**Figure 6**).

Training

The training changed the way the participant accomplishes the task, depending on the hand tested; this was suggested by the presence of significant *Hand* × *Time* [$F(1,537) = 8.166$, $p = 0.004$], *Distance* × *Time* [$F(1,549) = 5.965$, $p = 0.015$] and *Distance* × *Hand* × *Time* [$F(1,550) = 5.990$, $p = 0.015$] interactions. The training induced in the healthy limb a general speeding up of RTs for all distances, as suggested by the presence of main effect of *Time* [$F(1,271) = 5.523$, $p = 0.019$], but it did not change the pattern of the RT/distance; absence of *Distance* × *Time* interaction [$F(1,277) = 0.011$, $p = 0.916$]. Conversely, testing the prosthesis, the training changed the pattern of the RT/distance curve as shown by the presence of interaction *Distance* × *Time* [$F(1,277) = 10.764$, $p = 0.001$], besides the main effects of *Distance* [$F(1,277) = 8.780$, $p = 0.003$] and *Time* [$F(1,277) = 4.392$, $p = 0.037$]. Change of pattern, with a decrease of RTs in far space, going from 60 to 90 cm, suggested an extension of the PPS and it is in favor of a positive effect of training on the embodiment of the prosthesis (**Figure 7**).

The TOJ task did not give additional information on the effect of training since, in the PRE, the participant was extremely inaccurate and variable in performing the crossed hand condition (EA: uncrossed SOA = 70 ± 15 ms vs crossed SOA = 220 ± 140 ms) and data have not been analyzed.

Prosthesis

In the VTI task, the healthy limb was in general more rapid than both the tested prostheses, as suggested by the presence of a main effect of *Hand* [$F(2,338) = 4.136$, $p = 0.017$]. The direct comparison between the levels of the factor *Hand* showed that the healthy limb was different from both the prosthesis **A**

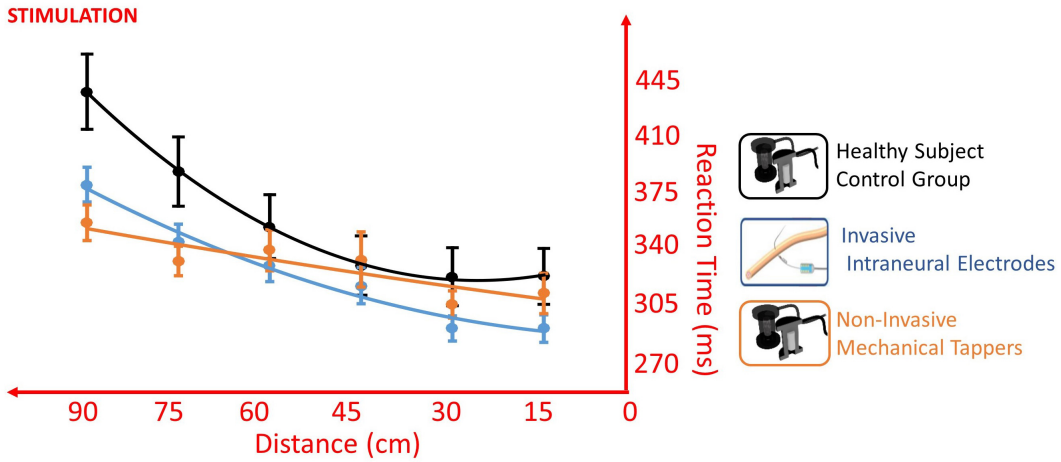

FIGURE 5 | Different RT/Distance curves (quadratic fitting function) in the VTI experiment of Invasive Intraneural Stimulation (blue) and Non-Invasive Stimulation (orange) compared to the pattern of the control group (black). Values are means (dots) ± SEM (bars). The absence of interaction between Intraneural and Control [$F(1,5033) = 3.3954$, $p = 0.066$], compared to the presence of interaction between Non-Invasive and Control [$F(1,5077) = 28.379$, $p < 0.001$], supports a facilitation of prosthesis embodiment when this was tested with intraneural stimulation.

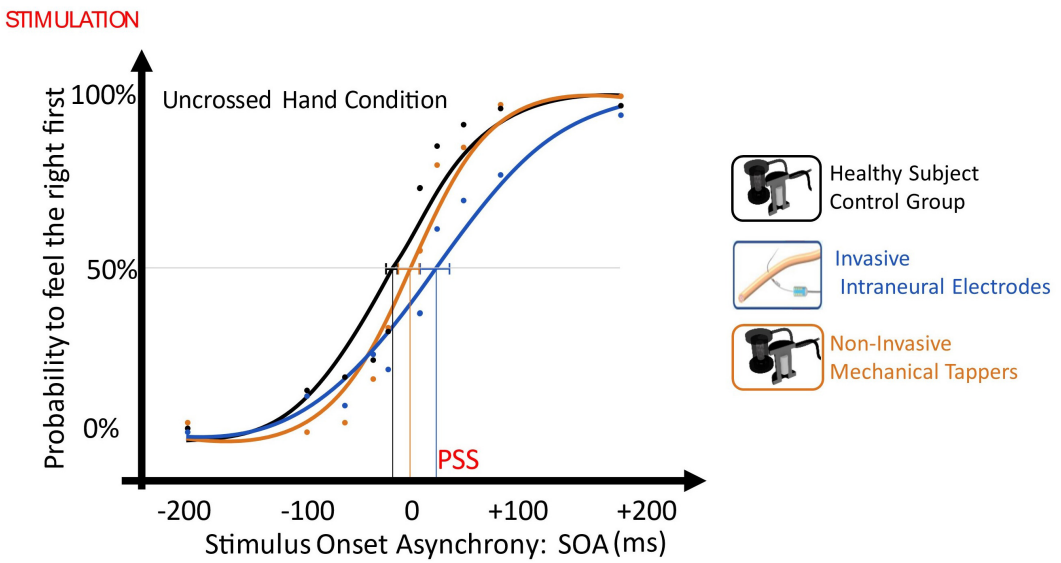

FIGURE 6 | Plot of uncrossed hand order judgment with the different SOAs as independent variable (x-axis, ms) and the probability to judge the right limb as the one stimulated first, as the dependent variable (y-axis). Then, data distribution was fitted with a sigmoid function, and the SOA value in the curve where the first stimulus had the same probability ($p = 0.5$) to be felt on right and on the left limb was defined as Point of Subjective Simultaneity (PSS) and it testifies the laterality stimulation bias. The dashed lines represent PSS 95% confidence intervals. Blue: Invasive vs Non-Invasive; Orange: Non-invasive vs Non-Invasive; Black: Control.

($p < 0.001$) and the prosthesis **B** ($p < 0.001$), while prosthesis **A** did not differ from prosthesis **B** ($p = 0.428$). Despite the different average RT, the two prostheses and the healthy limb did not show a statistically different pattern of response across the distances (*Distance* × *Hand* interaction: $F(2,351) = 1.180$, $p = 0.309$), suggesting that the stimuli approaching the prosthesis were processed similarly to those approaching the healthy limb. This is in favor of an embodiment of both prostheses (**Figure 8**).

Moreover, VTI gave an additional cue of prosthesis embodiment. The first and third distances, i.e., 15 and 45 cm from the prosthesis respectively corresponded to 45 and 75 cm from the stump, because the tip of the stump was 30 cm shorter than the tip of the prosthesis. Considering the bare stump, the shift from PPS to extrapersonal space would likely fall within a 45–75 cm range (Serino et al., 2015), so that when the stump was tested, there was an important decrease of RTs from the third distance (RT = 368) to first distance (RT = 314 ms). An embodied prosthesis would shift the boundary of peripersonal space, so that both first and third distances would fall within the PPS, because they correspond to 15 and 45 cm from the prosthesis

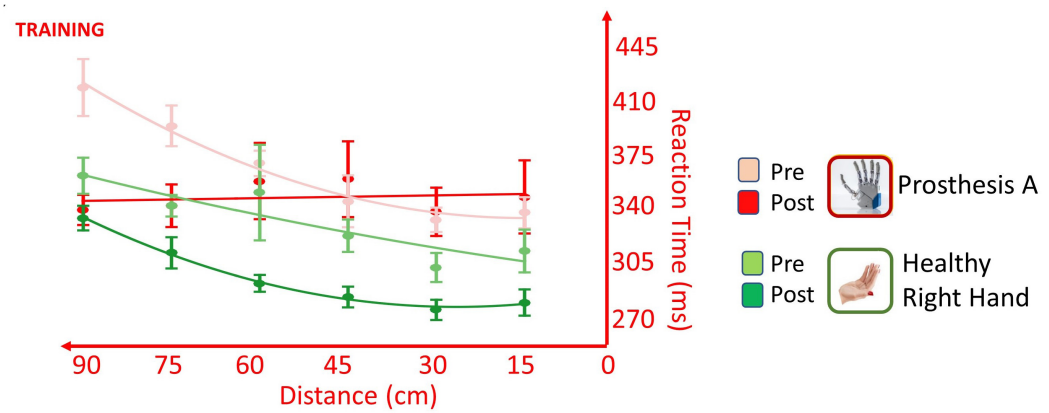

FIGURE 7 | Effect of training on RT/Distance curves (quadratic fitting function) in the VTI experiment, when the participant was tested with the healthy right limb (green) and with the more trained prosthesis (red) in the PRE session (lighter colors) and in the POST_NI session (darker colors). Somatosensory stimulation was always delivered non-invasively. Values are means (dots) ± SEM (bars). The healthy hand underwent a general speeding of RTs for all the tested distances yet maintaining a similar RT/Distance pattern, while the prosthesis changed the pattern of the RT/distance with a decrease of RTs in far space. This suggests an extension of the PPS induced by the embodiment of the prosthesis.

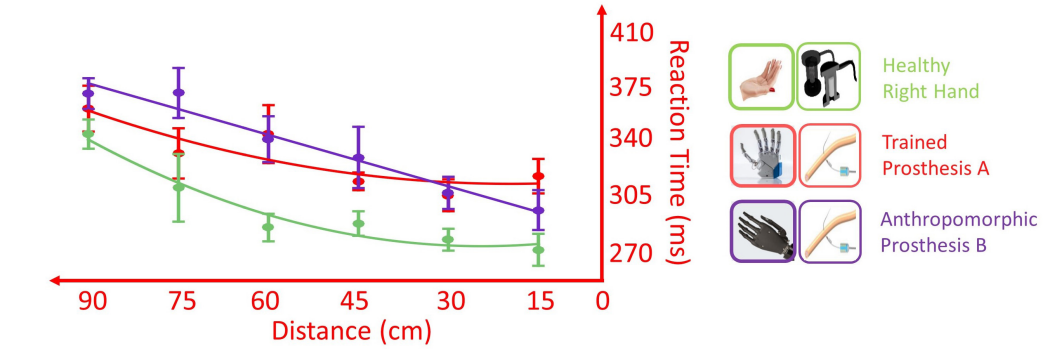

FIGURE 8 | Effect of different prostheses on RT/Distance curves (quadratic fitting function) in the VTI experiment. Values are means (dots) ± SEM (bars). In the POST_I session when the participant was tested with both the prostheses, she was slower for all the tested distances than when she was tested with the right healthy limb (green); however, the RT/Distance pattern was not different (Distance × Hand interaction $p = 0.309$), which is in favor of an embodiment of both prostheses.

(**Figure 9**). Indeed, when prostheses were tested, there was almost no RT difference (from 3rd = 335 to 1st = 330 ms). Prosthesis embodiment was statistically confirmed by the presence of a significant *Distance* (1st vs 3rd) × *Hand (stump vs prosthesis)* interaction [$F(1,256.92) = 8.3077$, $p = 0.004$].

So far, the VTI task showed that both prostheses tested with intraneural stimulation behaved as the healthy limb, thus suggesting their embodiment, while the TOJ gave contrasting results.

In the TOJ, the worsening of esteem accuracy going from the uncrossed to crossed hands, typical of healthy subjects (EA control group: 66.3 vs 97.2 ms), was present only for the less-anthropomorphic more-trained prosthesis **A** (EA: 55.9 vs 114.1 ms). Indeed, esteem accuracy with this prosthesis was not significantly different with the ones of the healthy subject control group, both in crossed [$t(10) = 0.480$, $p = 0.642$] and uncrossed hand [$t(10) = 0.432$, $p = 0.675$] conditions. By contrast, the crossed/uncrossed difference was absent for the more-anthropomorphic less-trained prosthesis **B** (EA: 121.7 vs 113.5 ms), where esteem accuracy was significantly different from controls in the uncrossed hand condition [$t(10) = 2.298$, $p = 0.044$, Z-CC = 2.39 CI (1.19, 3.57)] and not in the crossed hand condition [$t(10) = 0.463$, $p = 0.653$] (**Figure 10**).

DISCUSSION

This study was designed to investigate the embodiment achieved in a context of ecologic continuative use of a worn and neurally interfaced hand prosthesis. Embodiment was favored by the

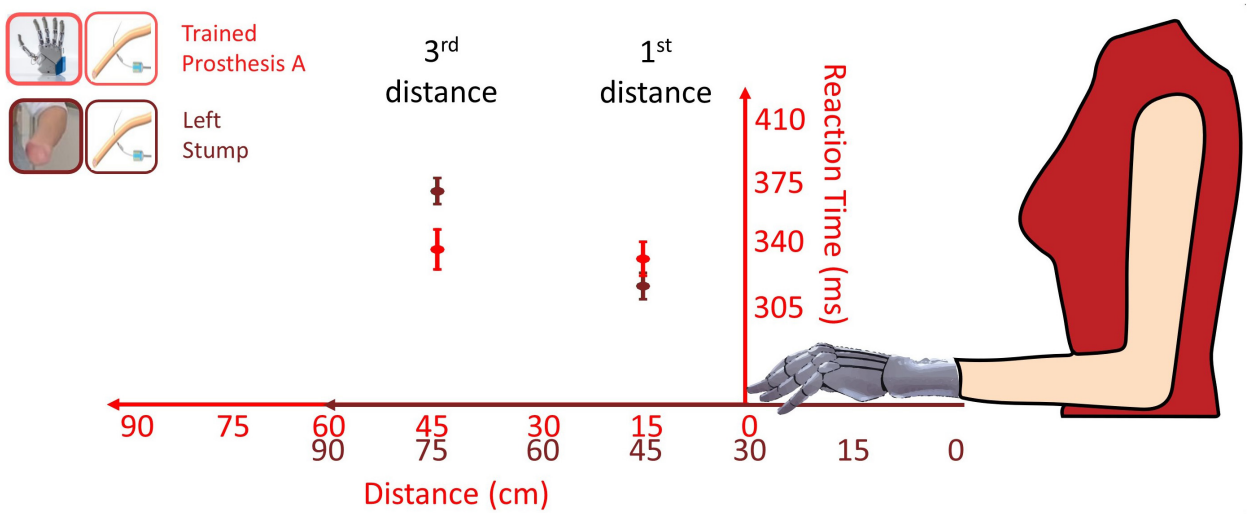

FIGURE 9 | Comparison of RTs (mean ± SEM) for the first and third distance tested with the more trained prosthesis (red) and with the bare stump (brown) in the POST_I session stimulating invasively through the intraneural interface. The red values correspond to the distances of the visual stimulus from the Prosthesis A; the brown values correspond to the distances of the visual stimulus from the bare stump. The passage between peripersonal to extrapersonal space, which seems to be between those distances, appears to shifted forward when the participant was tested with the prosthesis.

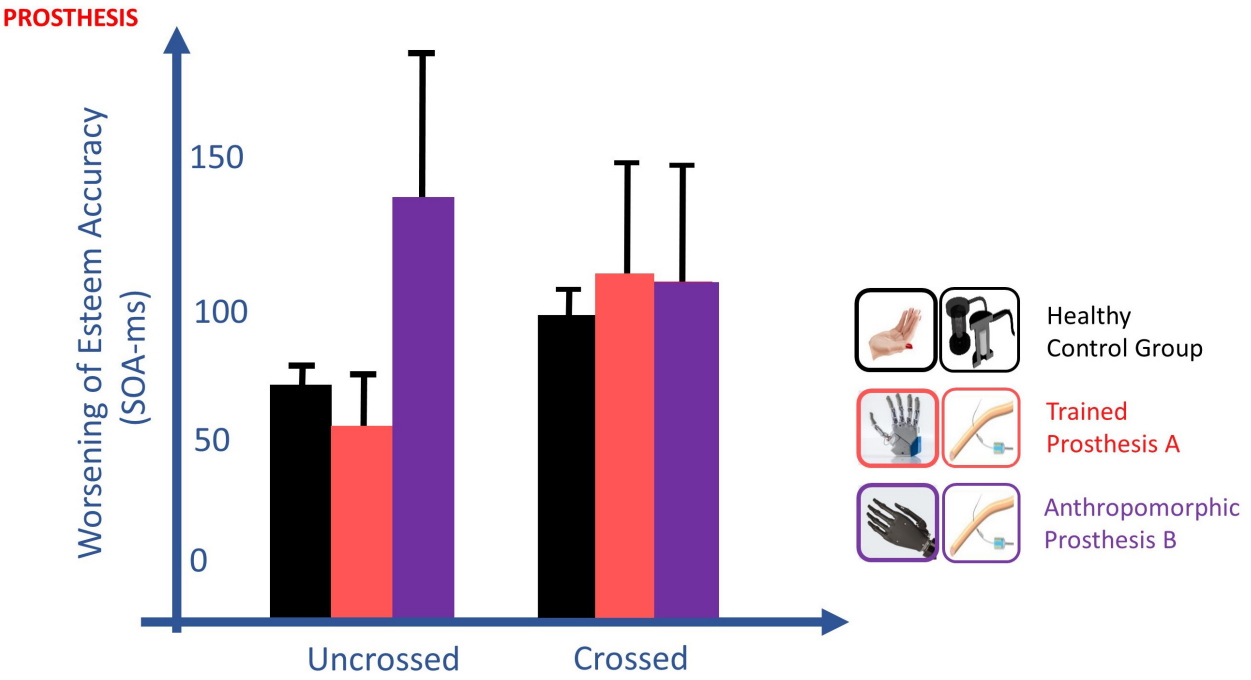

FIGURE 10 | Changes of esteem accuracy (EA) between uncrossed and crossed-arm TOJ in the POST_I session. EA is computed through the SOA corresponding to half of the inverse of its derivate for PSS; thus, the shorter the SOA, the better the accuracy is. The worsening of EA going from the uncrossed to crossed hands, typical of healthy subjects (black), was present only for the more-trained prosthesis (red) and absent for the more anthropomorphic (violet) prosthesis. TOJ crossing hand effect is in favor of the embodiment of only the more trained prosthesis.

closure of the sensorimotor control loop of the prosthesis, enabled by a more natural and rich sensory feedback delivered through multichannel neural interface.

It has peculiar features compared to the previous studies approaching prosthesis embodiment. We had the opportunity to test our subject longitudinally, before and after a one-month period when she achieved proficiency in controlling the prosthesis. Moreover, the studied subject had a stable chronic amputation; thus, at the time of the study, she was not going through any spontaneous recovery plasticity, and she had not

used active prostheses before the study, allowing us to have a clean measure of her baseline prosthesis embodiment at the beginning of the experiment.

Amputee subjects carrying intraneural electrodes implantation to receive prosthesis sensory feedback are still rare; thus, single-case studies are worth running to gather clues on the embodiment of neurally interfaced prostheses. To minimize possible biases linked with studying single cases, we decided not to rely on subjective and explicit statements, but to employ two implicit and objective paradigms, to test-retest the subject, and to statistically compare the results from the volunteer with those from a healthy subject control group.

The paradigms investigated prosthesis embodiment through the study of multisensory integration and spatial remapping; they were developed in healthy subjects (Yamamoto and Kitazawa, 2001a; Gray and Tan, 2002; Shore et al., 2002) and demonstrated to be sensible to the embodiment of tools (Yamamoto and Kitazawa, 2001b; Canzoneri et al., 2013b) and were already validated in amputees (Canzoneri et al., 2013a; Sato et al., 2017).

During the period of training, the participant used both prostheses, always receiving a rich tactile feedback related to manipulation activities made with the prosthesis through intraneural and perineural multichannel electrodes. However, when the participant was tested in the multisensory integration tasks, somatosensory stimuli were delivered in different sessions, either with non-invasive mechanical tappers or with invasive intraneural stimulation to highlight possible advantages of the latter on embodiment.

Intraneural stimulation did not speed VTI RT, and when TOJ was tested by stimulating the right limb non-invasively and the left limb invasively, there was a laterality bias toward the healthy right limb. Indeed, intraneural stimulation had to be delivered about 30 ms before the contralateral to have the same probability to be felt as the first. Since electrodes are implanted in the median nerve of the arm and since intraneural stimulation does not need mechanoreceptor transduction, the longer duration of the tapper stimulation (40 ms vs 200 μs) has likely hidden the perception of the intraneural stimulation.

Being the electrode implanted only in the left limb, we could not test TOJ performed with both sides stimulated intraneurally and demonstrate any improvement of performance due to intraneural stimulation. However, we could show that when stimulation was delivered non-invasively on the right and invasively on the left limb, TOJ performance did not become worse, despite the asymmetry of stimulation.

Even more importantly, VTI showed that with intraneural stimulation the RT/Distance pattern of the amputee wearing the prosthesis was more similar to the one of the healthy subject control group. This normalization of the relation between multisensory integration and distance from the body is in favor of a selective advantage of intraneural stimulation on prosthesis embodiment.

To the best of our knowledge, this is the first study that demonstrated in an amputee that training the control of the prosthesis favors the process of embodiment by testing-retesting the participant before and after the training period. To avoid any bias due to different stimulation, the effect of training was always tested with the same stimulation, i.e., non-invasively.

During the month of training, the participant was often involved in performing skilled bimanual tasks; thus, both limbs were trained. When the effect of training on the PPS expansion was assessed through the VTI task, we found a differential effect depending on the tested limb. The healthy limb showed an overall increase of performance, boosting up the effect of incoming visual stimuli on touch detection, thus decreasing RTs at all distances of the visual approaching stimulus. Notably, the affected limb showed a modification of the RT/Distance pattern, with a clear extension of the PPS, which is a strong clue of extracorporeal device embodiment (Maravita and Iriki, 2004). From the TOJ task, we could not gather additional information on the effect of training because the esteem accuracy in the crossed hand condition was extremely low and variable, probably due to the rarity of exploiting the stump to act and explore the contralateral side of the space.

In the VTI, prostheses recalibrated the PPS around the subject, as shown by the shift of the PPS/Extrapersonal boundary. Indeed, when the subject was tested with the bare stump, the boundary distanced between 30 and 60 cm from the stump, and when the subject was tested wearing the prosthesis, the boundary distanced more than 60 cm. This was in line with the previously demonstrated partial recovery of PPS shrank by the amputation (Canzoneri et al., 2013a). Moreover, the participant had a similar pattern of response across distances for her right healthy limb and both prostheses, suggesting that these were similarly able to determine the extension of VTI in the PPS. Conversely, only wearing the more trained, despite less anthropomorphic, prosthesis, the participant experienced the worsening of the TOJ performance following arm crossing, comparably to the control group.

Recently, it has been shown that even prostheses unable to give any sensory feedback were able to induce the crossing hand effect, typical of healthy limbs (Sato et al., 2017). It is worth noting that in that study, the three amputees were tested with their own, daily used (thus hypertrained) prosthesis. This suggests that using the prosthesis to act in external space provides enough clues to allow the remapping of its cortical representation, inducing the relocation of somatosensory stimuli in the contralateral side, thus explaining the detrimental effect on TOJ on arm crossing.

Notably, previous studies that reported the hand crossing effect on TOJ, always stimulated the tip of the hand, drumstick, or prosthesis, which could be relocated in the contralateral space quite far from the midsagittal plane in the limb/tool crossing. By contrast, intraneural stimulation was delivered to our participant through electrodes placed on the median portion of the arm, which even in the crossed condition remained in the same side of the space, as if electrodes were uncrossed. Thus, in our case, we had a dissociation between the side where the stimulation was physically delivered and the side where it was referred. Performance worsening occurred with uncrossed real stimulation which was perceived as crossed only because of the sensation remapping, emphasizing the link between prosthesis embodiment and hand crossing effect.

Both VTI and TOJ crossing hand effect are based upon multisensory integration. Somatosensory feedbacks, such as touch, proprioception, and the efference copy are coded in an egocentric reference frame, where they are compared to "where I am." Conversely, environmental feedbacks, such as sight and hearing, are coded in an allocentric reference frame, i.e., where the information is compared to the rest of the environment. To integrate information that does not share the same reference frame, a process of remapping is needed.

In sensory remapping, a sensory modality is not just recoded in the frame of another modality. Instead, it is recoded in a new space that mixes the spaces of the two modalities using weights in line with a policy based on Bayesian integration (Miyazaki et al., 2006; Heed et al., 2015) such as Kalman filter-like noise optimization of sensory fusion (Deneve et al., 2007). However, for the sake of simplicity, we will treat sensory remapping as a simple sequential transformation in the following discussion.

The knowledge of where the environment is in relation to the hand and the awareness of what the hand movement will affect are both needed to achieve an effective hand-environment interaction. Thus, a close sensorimotor control loop involves a double transformation: along the afferent branch, environmental information must be re-referenced in a bodily frame, while in the efferent branch, the knowledge of the body coordinates must be re-referenced in the allocentric frame of the environment.

In VTI and related acoustic-tactile integration tasks, environmental inputs collected by sight or hearing assume different valence, and are able to enhance the effect of touch, depending on where they are in respect to the body (Serino, 2019). This process subtends a re-referencing of environmental information in a bodily frame; thus, VTI tests the remapping typical of the afferent branch.

PPS is the space around the body where external events are considered more relevant. It has been suggested that we have a motor-based PPS that has the higher possibility to be directly acted upon by the body, and a defense-based PPS where external stimuli may be more effective upon the body (Clery et al., 2015b; de Vignemont and Iannetti, 2015).

In our VTI task, we tested fast approaching stimuli. Looming stimuli are potentially more dangerous than static, so that they induce a protection response with enhanced tactile sensitivity in their predicted time and site of impact (Gray and Tan, 2002; Clery et al., 2015a). It's likely that we tested the extension of a safe margin around the body, since training was less relevant than sensory feedback in determining VTI outcome.

In the uncrossed hand condition of the TOJ task, egocentric and allocentric reference frames are concordant and somatosensory stimuli are analyzed in their original bodily referenced frame. On the contrary, with crossed hands, the delivered somatosensory stimuli assume a different value depending on where they occur in the egocentric space; thus, the judgment subtends a compulsory remapping of the location of tactile stimuli in external world coordinates (Schicke and Roder, 2006). Accordingly, we think that the TOJ hand crossing effect tests the remapping typical of the efferent branch, which is more aimed to action.

Despite TOJ being a tactile task, several cues are in favor of a motor-based origin of the transformation it tests, because external spatial coordinates allow the movement toward the tactile event. Indeed, TOJ is modulated by hand movements, which are able to compress time interval (Tomassini et al., 2014). The crossing effect is also present behind the body where the space can be only coded by movement (Gillmeister and Forster, 2012), and may be due to the efference copy since it is present when the hands are uncrossed but a crossing movement is planned (Hermosillo et al., 2011). Moreover, the crossing effect sticks with the part where the motor operational ability is focused, while the position of the rest of the arm or of the tool is irrelevant, as showed by the absence of the effect when double crossing with drumsticks (Yamamoto and Kitazawa, 2001b) and its presence with L-shape sticks (Yamamoto et al., 2005).

The participant we tested could control both prostheses with an *ad hoc* developed EMG control and received tactile feedback from the prostheses related to dexterous manipulation and slippage through invasive nerve stimulation (Zollo et al., 2019). Hence, the control loop of both prostheses benefited of invasive feedback, and this may explain why both prostheses were embodied accordingly to the VTI. Both prostheses behaved as her right real hand because they were both able to trigger the remapping of visual stimuli into bodily coordinates.

The time our volunteer spent in training skilled manipulation with each of two prostheses was very different (45 days for prosthesis **A** vs 20 days for prosthesis **B**), and this may be the reason of a different embodiment of the two prostheses according to the TOJ. Only the more trained prosthesis, despite being less anthropomorphic, was able to trigger the bodily-into-environment remapping and to induce the hand crossing effect.

Training is needed by the plastic processes at the base of remapping and neurally interfaced hand prostheses have shown a strong ability to foster such plasticity. This has been widely demonstrated in primary sensorimotor cortices (Rossini et al., 2010) and in their interplay (Ferreri et al., 2014; Di Pino et al., 2012), but it failed to be shown in the fronto-parietal network (Mioli et al., 2018). In targeted muscle and sensory reinnervated patients, which benefit of high effective bidirectional interface with the prosthesis, M1 and S1 activity and connectivity were almost normal, but the interplay with the frontal and parietal areas was highly impaired (Serino et al., 2017). Is the induction of plasticity on that network still beyond the ability of highly interacting prostheses? The present study offers a behavioral demonstration of plasticity of the frontoparietal network induced by neurally interfaced prostheses.

Indeed, TOJ has been ascribed to the activity of parietal and prefrontal cortices and the crossing hand effect to their combination with multisensory perisylvian cortices coding the representation of motion (Takahashi et al., 2013). The multisensory integration at the base of VTI has been widely ascribed to fronto-parietal interplay (di Pellegrino and Ladavas, 2015) and TMS entrainment and disruption studies highlighted the importance of posterior parietal cortex in frame remapping

(Bolognini and Maravita, 2007; Konen and Haggard, 2014; Ruzzoli and Soto-Faraco, 2014). In monkey, two partly separated networks with bimodal visuotactile neurons are responsible for multisensory integration in the PPS. The VIP-F4 is more involved in coding a defense PPS around the vulnerable parts, especially hand and face (Graziano and Cooke, 2006) and is sensible to emotional and social aspects (Clery et al., 2015b), while the areas7b and AIP-F5, which are in charge of the visuomotor transformation needed for grasping objects in the environment (Rizzolatti and Luppino, 2001), code the motor PPS. We may speculate that prosthesis embodiment revealed by VTI relies more on the former and has been achieved in our subject with both prostheses, while embodiment revealed by TOJ relies more on the latter, and it has been achieved only with the more trained prosthesis.

In our participant, the continuative use of multichannel and multi-nerve intraneural stimulation, providing a richer and more pleasant sensory feedback, showed to induce prosthesis embodiment. More importantly, the acute employment of such feedback signals during the test induced an even deeper embodiment compared to non-invasive tactile substitution. However, a comprehensive analysis of both experiments suggests that sensory- and action-oriented embodiment may not always completely match. While the quality of sensory feedback and the degree of human-like appearance of the prosthesis are key factors to attain the former, an operative tool-like embodiment is only achieved through a learning process that leads to proficiency.

DATA AVAILABILITY STATEMENT

The raw data supporting the conclusions of this article will be made available by the authors, without undue reservation, to any qualified researcher.

ETHICS STATEMENT

The studies involving human participants were reviewed and approved by Campus Bio-Medico Ethics Committee and the Ethics Committee of University of Milano-Bicocca. The patients/participants provided their written informed consent to participate in this study. Written informed consent was obtained from the individual(s) for the publication of any potentially identifiable images or data included in this article.

AUTHOR CONTRIBUTIONS

GD, DR, and AMa designed the study, analyzed the data, and wrote the manuscript. CS, AMi, and MD'A performed the study, analyzed the data, and wrote the manuscript. VDe performed the surgery and collaborated during the experiments. VDi designed the study and collaborated during the experiments. RS and LZ collaborated during the experiments. EG supervised the experiments. All authors discussed the results and commented on the manuscript.

FUNDING

This work was supported by the European Research Council (ERC) Starting Grant 2015 RESHAPE "REstoring the Self with embodiable Hand ProsthesEs" (ERC-2015-STG, project no. 678908) and by INAIL with PPR2 project "Control of upper-limb prosthesis with neural invasive interfaces" (CUP:E58C13000990001).

ACKNOWLEDGMENTS

We are grateful to participant CP for her great commitment to the experiments.

REFERENCES

Antfolk, C., D'Alonzo, M., Controzzi, M., Lundborg, G., Rosen, B., Sebelius, F., et al. (2013). Artificial redirection of sensation from prosthetic fingers to the phantom hand map on transradial amputees: vibrotactile versus mechanotactile sensory feedback. *IEEE Trans. Neural Syst. Rehabil. Eng.* 21, 112–120. doi: 10.1109/TNSRE.2012.2217989

Biddiss, E. A., and Chau, T. T. (2007). Upper limb prosthesis use and abandonment: a survey of the last 25 years. *Prosthet. Orthotics Int.* 31, 236–257. doi: 10.1080/03093640600994581

Blanke, O. (2012). Multisensory brain mechanisms of bodily self-consciousness. *Nat. Rev. Neurosci.* 13, 556–571. doi: 10.1038/nrn3292

Bolognini, N., and Maravita, A. (2007). Proprioceptive alignment of visual and somatosensory maps in the posterior parietal cortex. *Curr. Biol.* 17, 1890–1895. doi: 10.1016/j.cub.2007.09.057

Botvinick, M., and Cohen, J. (1998). Rubber hands' feel'touch that eyes see. *Nature* 391, 756–756. doi: 10.1038/35784

Canzoneri, E., Magosso, E., and Serino, A. (2012). Dynamic sounds capture the boundaries of peripersonal space representation in humans. *PLoS One* 7:e44306. doi: 10.1371/journal.pone.0044306

Canzoneri, E., Marzolla, M., Amoresano, A., Verni, G., and Serino, A. (2013a). Amputation and prosthesis implantation shape body and peripersonal space representations. *Sci. Rep.* 3:2844. doi: 10.1038/srep02844

Canzoneri, E., Ubaldi, S., Rastelli, V., Finisguerra, A., Bassolino, M., and Serino, A. (2013b). Tool-use reshapes the boundaries of body and peripersonal space representations. *Exp. Brain Res.* 228, 25–42. doi: 10.1007/s00221-013-3532-2

Ciancio, A. L., Cordella, F., Barone, R., Romeo, R. A., Bellingegni, A. D., Sacchetti, R., et al. (2016). Control of prosthetic hands via the peripheral nervous system. *Front. Neurosci.* 10:116. doi: 10.3389/fnins.2016.00116

Clery, J., Guipponi, O., Odouard, S., Wardak, C., and Ben Hamed, S. (2015a). Impact prediction by looming visual stimuli enhances tactile detection. *J. Neurosci.* 35, 4179–4189. doi: 10.1523/JNEUROSCI.3031-14.2015

Clery, J., Guipponi, O., Wardak, C., and Ben Hamed, S. (2015b). Neuronal bases of peripersonal and extrapersonal spaces, their plasticity and their dynamics: knowns and unknowns. *Neuropsychologia* 70, 313–326. doi: 10.1016/j.neuropsychologia.2014.10.022

Cordella, F., Ciancio, A. L., Sacchetti, R., Davalli, A., Cutti, A. G., Guglielmelli, E., et al. (2016). Literature review on needs of upper limb prosthesis users. *Front. Neurosci.* 10:209. doi: 10.3389/fnins.2016.00209

Crawford, J. R., and Garthwaite, P. H. (2007). Comparison of a single case to a control or normative sample in neuropsychology: development of a Bayesian approach. *Cogn. Neuropsychol.* 24, 343–372. doi: 10.1080/02643290701290146

Crawford, J. R., Garthwaite, P. H., and Porter, S. (2010). Point and interval estimates of effect sizes for the case-controls design in neuropsychology: rationale, methods, implementations, and proposed reporting standards. *Cogn. Neuropsychol.* 27, 245–260. doi: 10.1080/02643294.2010.513967

Dadarlat, M. C., O'doherty, J. E., and Sabes, P. N. (2015). A learning-based approach to artificial sensory feedback leads to optimal integration. *Nat. Neurosci.* 18, 138–144. doi: 10.1038/nn.3883

D'Alonzo, M., Mioli, A., Formica, D., and Pino, G. D. (2020). Modulation of body representation impacts on efferent autonomic activity. *J. Cogn. Neurosci.* [Epub ahead of print]. doi: 10.1162/jocn_a_01532

D'Alonzo, M., Mioli, A., Formica, D., Vollero, L., and Di Pino, G. (2019). Different level of virtualization of sight and touch produces the uncanny valley of avatar's hand embodiment. *Sci. Rep.* 9:19030. doi: 10.1038/s41598-019-55478-z

de Vignemont, F., and Iannetti, G. D. (2015). How many peripersonal spaces? *Neuropsychologia* 70, 327–334. doi: 10.1016/j.neuropsychologia.2014.11.018

Deneve, S., Duhamel, J. R., and Pouget, A. (2007). Optimal sensorimotor integration in recurrent cortical networks: a neural implementation of Kalman filters. *J. Neurosci.* 27, 5744–5756.

Dhillon, G. S., and Horch, K. W. (2005). Direct neural sensory feedback and control of a prosthetic arm. *IEEE Trans. Neural Syst. Rehabil. Eng.* 13, 468–472. doi: 10.1109/TNSRE.2005.856072

di Pellegrino, G., and Ladavas, E. (2015). Peripersonal space in the brain. *Neuropsychologia* 66, 126–133.

Di Pino, G., Denaro, L., Vadala, G., Marinozzi, A., Tombini, M., Ferreri, F., et al. (2013). Invasive neural interfaces: the perspective of the surgeon. *J. Surg. Res.* 188, 77–87. doi: 10.1016/j.jss.2013.12.014

Di Pino, G., Guglielmelli, E., and Rossini, P. M. (2009). Neuroplasticity in amputees: main implications on bidirectional interfacing of cybernetic hand prostheses. *Prog. Neurobiol.* 88, 114–126. doi: 10.1016/j.pneurobio.2009.03.001

Di Pino, G., Maravita, A., Zollo, L., Guglielmelli, E., and Di Lazzaro, V. (2014). Augmentation-related brain plasticity. *Front. Syst. Neurosci.* 8:109. doi: 10.3389/fnsys.2014.00109

Di Pino, G., Porcaro, C., Tombini, M., Assenza, G., Pellegrino, G., Tecchio, F., et al. (2012). A neurally-interfaced hand prosthesis tuned inter-hemispheric communication. *Restor. Neurol. Neurosci.* 30, 407–418. doi: 10.3233/RNN-2012-120224

Drench, M. E. (1994). Changes in body image secondary to disease and injury. *Rehabil. Nurs.* 19, 31–36. doi: 10.1002/j.2048-7940.1994.tb01300.x

Ehrsson, H. H., Holmes, N. P., and Passingham, R. E. (2005). Touching a rubber hand: feeling of body ownership is associated with activity in multisensory brain areas. *J. Neurosci.* 25, 10564–10573. doi: 10.1523/JNEUROSCI.0800-05.2005

Farne, A., Iriki, A., and Ladavas, E. (2005). Shaping multisensory action-space with tools: evidence from patients with cross-modal extinction. *Neuropsychologia* 43, 238–248. doi: 10.1016/j.neuropsychologia.2004.11.010

Ferreri, F., Ponzo, D., Vollero, L., Guerra, A., Di Pino, G., Petrichella, S., et al. (2014). Does an intraneural interface short-term implant for robotic hand control modulate sensorimotor cortical integration? An EEG-TMS co-registration study on a human amputee. *Restor. Neurol. Neurosci.* 32, 281–292. doi: 10.3233/RNN-130347

Flannery, J. C., and Faria, S. H. (1999). Limb loss: Alterations in body image. *J. Vasc. Nurs.* 17, 100–106. doi: 10.1016/s1062-0303(99)90036-5

Flor, H., Nikolajsen, L., and Staehelin Jensen, T. (2006). Phantom limb pain: a case of maladaptive CNS plasticity? *Nat. Rev. Neurosci.* 7, 873–881. doi: 10.1038/nrn1991

Fogassi, L., Gallese, V., Fadiga, L., Luppino, G., Matelli, M., and Rizzolatti, G. (1996). Coding of peripersonal space in inferior premotor cortex (area F4). *J. Neurophysiol.* 76, 141–157. doi: 10.1152/jn.1996.76.1.141

Gillmeister, H., and Forster, B. (2012). Hands behind your back: effects of arm posture on tactile attention in the space behind the body. *Exp. Brain Res.* 216, 489–497. doi: 10.1007/s00221-011-2953-z

Graczyk, E. L., Gill, A., Tyler, D. J., and Resnik, L. J. (2019). The benefits of sensation on the experience of a hand: a qualitative case series. *PLoS One* 14:e0211469. doi: 10.1371/journal.pone.0211469

Graczyk, E. L., Resnik, L., Schiefer, M. A., Schmitt, M. S., and Tyler, D. J. (2018). Home use of a neural-connected sensory prosthesis provides the functional and psychosocial experience of having a hand again. *Sci. Rep.* 8:9866. doi: 10.1038/s41598-018-26952-x

Gray, R., and Tan, H. Z. (2002). Dynamic and predictive links between touch and vision. *Exp. Brain Res.* 145, 50–55. doi: 10.1007/s00221-002-1085-x

Graziano, M. S. A., and Cooke, D. F. (2006). Parieto-frontal interactions, personal space, and defensive behavior. *Neuropsychologia* 44, 2621–2635. doi: 10.1016/j.neuropsychologia.2005.09.011

Heed, T., Buchholz, V. N., Engel, A. K., and Röder, B. (2015). Tactile remapping: from coordinate transformation to integration in sensorimotor processing. *Trends Cogn. Sci.* 19, 251–258. doi: 10.1016/j.tics.2015.03.001

Hermosillo, R., Ritterband-Rosenbaum, A., and Van Donkelaar, P. (2011). Predicting future sensorimotor states influences current temporal decision making. *J. Neurosci.* 31, 10019–10022. doi: 10.1523/JNEUROSCI.0037-11.2011

Iriki, A., Tanaka, M., and Iwamura, Y. (1996). Coding of modified body schema during tool use by macaque postcentral neurones. *Neuroreport* 7, 2325–2330. doi: 10.1097/00001756-199610020-00010

Kikkert, S., Mezue, M., O'shea, J., Henderson Slater, D., Johansen-Berg, H., Tracey, I., et al. (2019). Neural basis of induced phantom limb pain relief. *Ann. Neurol.* 85, 59–73. doi: 10.1002/ana.25371

Konen, C. S., and Haggard, P. (2014). Multisensory parietal cortex contributes to visual enhancement of touch in humans: a single-pulse TMS study. *Cereb. Cortex* 24, 501–507. doi: 10.1093/cercor/bhs331

Kuiken, T. A., Marasco, P. D., Lock, B. A., Harden, R. N., and Dewald, J. P. (2007). Redirection of cutaneous sensation from the hand to the chest skin of human amputees with targeted reinnervation. *Proc. Natl. Acad. Sci. U.S.A.* 104, 20061–20066. doi: 10.1073/pnas.0706525104

Lotti, F., Ranieri, F., Vadalà, G., Zollo, L., and Di Pino, G. (2017). Invasive intraneural interfaces: foreign body reaction issues. *Front. Neurosci.* 11:497. doi: 10.3389/fnins.2017.00497

Marasco, P. D., Hebert, J. S., Sensinger, J. W., Shell, C. E., Schofield, J. S., Thumser, Z. C., et al. (2018). Illusory movement perception improves motor control for prosthetic hands. *Sci. Transl. Med.* 10:eaao6990. doi: 10.1126/scitranslmed.aao6990

Marasco, P. D., Schultz, A. E., and Kuiken, T. A. (2009). Sensory capacity of reinnervated skin after redirection of amputated upper limb nerves to the chest. *Brain* 132, 1441–1448. doi: 10.1093/brain/awp082

Maravita, A., and Iriki, A. (2004). Tools for the body (schema). *Trends Cogn. Sci.* 8, 79–86.

Maravita, A., Spence, C., Kennett, S., and Driver, J. (2002). Tool-use changes multimodal spatial interactions between vision and touch in normal humans. *Cognition* 83, B25–B34. doi: 10.1016/s0010-0277(02)00003-3

Marini, F., Tagliabue, C. F., Sposito, A. V., Hernandez-Arieta, A., Brugger, P., Estevez, N., et al. (2013). Crossmodal representation of a functional robotic hand arises after extensive training in healthy participants. *Neuropsychologia* 53, 178–186. doi: 10.1016/j.neuropsychologia.2013.11.017

Mathôt, S., Schreij, D., and Theeuwes, J. (2012). OpenSesame: an open-source, graphical experiment builder for the social sciences. *Behav. Res. Methods* 44, 314–324. doi: 10.3758/s13428-011-0168-7

Micera, S., Citi, L., Rigosa, J., Carpaneto, J., Raspopovic, S., Di Pino, G., et al. (2010). Decoding information from neural signals recorded using intraneural electrodes: towards the development of a neurocontrolled hand prosthesis. *Proc. IEEE* 98, 407–417. doi: 10.1186/1743-0003-8-53

Mioli, A., D'alonzo, M., Pellegrino, G., Formica, D., and Di Pino, G. (2018). Intermittent theta burst stimulation over ventral premotor cortex or inferior parietal lobule does not enhance the rubber hand illusion. *Front. Neurosci.* 12:870. doi: 10.3389/fnins.2018.00870

Miyazaki, M., Yamamoto, S., Uchida, S., and Kitazawa, S. (2006). Bayesian calibration of simultaneity in tactile temporal order judgment. *Nat. Neurosci.* 9, 875–877. doi: 10.1038/nn1712

Murray, C. D. (2004). An interpretative phenomenological analysis of the embodiment of artificial limbs. *Disabil. Rehabil.* 26, 963–973. doi: 10.1080/09638280410001696764

Niedernhuber, M., Barone, D. G., and Lenggenhager, B. (2018). Prostheses as extensions of the body: progress and challenges. *Neurosci. Biobehav. Rev.* 92, 1–6. doi: 10.1016/j.neubiorev.2018.04.020

Oddo, C. M., Raspopovic, S., Artoni, F., Mazzoni, A., Spigler, G., Petrini, F., et al. (2016). Intraneural stimulation elicits discrimination of textural features by

artificial fingertip in intact and amputee humans. *eLife* 5:e09148. doi: 10.7554/eLife.09148

Ortiz-Catalan, M., Håkansson, B., and Brånemark, R. (2014). An osseointegrated human-machine gateway for long-term sensory feedback and motor control of artificial limbs. *Sci. Transl. Med.* 6:257re6. doi: 10.1126/scitranslmed.3008933

Page, D. M., George, J. A., Kluger, D. T., Duncan, C., Wendelken, S., Davis, T., et al. (2018). Motor control and sensory feedback enhance prosthesis embodiment and reduce phantom pain after long-term hand amputation. *Front. Hum. Neurosci.* 12:352. doi: 10.3389/fnhum.2018.00352

Peerdeman, B., Boere, D., Witteveen, H., Hermens, H., Stramigioli, S., Rietman, H., et al. (2011). Myoelectric forearm prostheses: state of the art from a user-centered perspective. *J. Rehabil. Res. Dev.* 48, 719–737. doi: 10.1682/jrrd.2010.08.0161

Petrini, F. M., Valle, G., Strauss, I., Granata, G., Di Iorio, R., D'anna, E., et al. (2018). Six-months assessment of a hand prosthesis with intraneural tactile feedback. *Ann. Neurol.* 85, 137–154. doi: 10.1002/ana.25384

Raspopovic, S., Capogrosso, M., Petrini, F. M., Bonizzato, M., Rigosa, J., Di Pino, G., et al. (2014). Restoring natural sensory feedback in real-time bidirectional hand prostheses. *Sci. Transl. Med.* 6:222ra19. doi: 10.1126/scitranslmed.3006820

Reilly, K. T., and Sirigu, A. (2008). The motor cortex and its role in phantom limb phenomena. *Neuroscientist* 14, 195–202. doi: 10.1177/1073858407309466

Risso, G., Valle, G., Iberite, F., Strauss, I., Stieglitz, T., Controzzi, M., et al. (2019). Optimal integration of intraneural somatosensory feedback with visual information: a single-case study. *Sci. Rep.* 9:7916. doi: 10.1038/s41598-019-43815-1

Rizzolatti, G., and Luppino, G. (2001). The cortical motor system. *Neuron* 31, 889–901.

Rognini, G., Petrini, F. M., Raspopovic, S., Valle, G., Granata, G., Strauss, I., et al. (2018). Multisensory bionic limb to achieve prosthesis embodiment and reduce distorted phantom limb perceptions. *J. Neurol. Neurosurg. Psychiatry* 90, 833–836. doi: 10.1136/jnnp-2018-318570

Rossini, P. M., Micera, S., Benvenuto, A., Carpaneto, J., Cavallo, G., Citi, L., et al. (2010). Double nerve intraneural interface implant on a human amputee for robotic hand control. *Clin. Neurophysiol.* 121, 777–783. doi: 10.1016/j.clinph.2010.01.001

Ruzzoli, M., and Soto-Faraco, S. (2014). Alpha stimulation of the human parietal cortex attunes tactile perception to external space. *Curr. Biol.* 24, 329–332. doi: 10.1016/j.cub.2013.12.029

Sato, Y., Kawase, T., Takano, K., Spence, C., and Kansaku, K. (2017). Incorporation of prosthetic limbs into the body representation of amputees: evidence from the crossed hands temporal order illusion. *Prog. Brain Res.* 236, 225–241. doi: 10.1016/bs.pbr.2017.08.003

Scarry, E. (1994). "The merging of bodies and artifacts in the social contract," in *Culture on the Brink: Ideologies of Technology*, eds G. Bender and T. Druckrey (Seattle, WA: Bay Press), 85–97.

Schicke, T., and Roder, B. (2006). Spatial remapping of touch: confusion of perceived stimulus order across hand and foot. *Proc. Natl. Acad. Sci. U.S.A.* 103, 11808–11813. doi: 10.1073/pnas.0601486103

Schiefer, M., Tan, D., Sidek, S. M., and Tyler, D. J. (2016). Sensory feedback by peripheral nerve stimulation improves task performance in individuals with upper limb loss using a myoelectric prosthesis. *J. Neural Eng.* 13:016001. doi: 10.1088/1741-2560/13/1/016001

Serino, A. (2019). Peripersonal space (PPS) as a multisensory interface between the individual and the environment, defining the space of the self. *Neurosci. Biobehav. Rev.* 99, 138–159. doi: 10.1016/j.neubiorev.2019.01.016

Serino, A., Akselrod, M., Salomon, R., Martuzzi, R., Blefari, M. L., Canzoneri, E., et al. (2017). Upper limb cortical maps in amputees with targeted muscle and sensory reinnervation. *Brain* 140, 2993–3011. doi: 10.1093/brain/awx242

Serino, A., Noel, J. P., Galli, G., Canzoneri, E., Marmaroli, P., Lissek, H., et al. (2015). Body part-centered and full body-centered peripersonal space representations. *Sci. Rep.* 5:18603. doi: 10.1038/srep18603

Shore, D. I., Spry, E., and Spence, C. (2002). Confusing the mind by crossing the hands. *Brain Res. Cogn. Brain Res.* 14, 153–163. doi: 10.1016/s0926-6410(02)00070-8

Spaccasassi, C., Romano, D., and Maravita, A. (2019). Everything is worth when it is close to my body: how spatial proximity and stimulus valence affect visuo-tactile integration. *Acta Psychol.* 192, 42–51. doi: 10.1016/j.actpsy.2018.10.013

Svensson, P., Wijk, U., Björkman, A., and Antfolk, C. (2017). A review of invasive and non-invasive sensory feedback in upper limb prostheses. *Expert Rev. Med. Devices* 14, 439–447. doi: 10.1080/17434440.2017.1332989

Takahashi, T., Kansaku, K., Wada, M., Shibuya, S., and Kitazawa, S. (2013). Neural correlates of tactile temporal-order judgment in humans: an fMRI Study. *Cereb. Cortex* 23, 1952–1964. doi: 10.1093/cercor/bhs179

Tan, D. W., Schiefer, M. A., Keith, M. W., Anderson, J. R., Tyler, J., and Tyler, D. J. (2014). A neural interface provides long-term stable natural touch perception. *Sci. Transl. Med.* 6:257ra138. doi: 10.1126/scitranslmed.3008669

Tomassini, A., Gori, M., Baud-Bovy, G., Sandini, G., and Morrone, M. C. (2014). Motor commands induce time compression for tactile stimuli. *J. Neurosci.* 34, 9164–9172. doi: 10.1523/JNEUROSCI.2782-13.2014

Tözeren, A. (1999). *Human Body Dynamics: Classical Mechanics and Human Movement*. London: Springer Science & Business Media.

Tsakiris, M., Carpenter, L., James, D., and Fotopoulou, A. (2010). Hands only illusion: multisensory integration elicits sense of ownership for body parts but not for non-corporeal objects. *Exp. Brain Res.* 204, 343–352. doi: 10.1007/s00221-009-2039-3

Vadalà, G., Di Pino, G., Ambrosio, L., Diaz, B. L., and Denaro, V. (2017). Targeted muscle reinnervation for improved control of myoelectric upper limb prostheses. *J. Biol. Regul. Homeost. Agents* 31(4 Suppl. 1), 183–189.

Valle, G., Mazzoni, A., Iberite, F., D'anna, E., Strauss, I., Granata, G., et al. (2018). Biomimetic intraneural sensory feedback enhances sensation naturalness, tactile sensitivity, and manual dexterity in a bidirectional prosthesis. *Neuron* 100, 37–45.e7. doi: 10.1016/j.neuron.2018.08.033

Yamamoto, S., and Kitazawa, S. (2001a). Reversal of subjective temporal order due to arm crossing. *Nat. Neurosci.* 4, 759–765. doi: 10.1038/89559

Yamamoto, S., and Kitazawa, S. (2001b). Sensation at the tips of invisible tools. *Nat. Neurosci.* 4, 979–980. doi: 10.1038/nn721

Yamamoto, S., Moizumi, S., and Kitazawa, S. (2005). Referral of tactile sensation to the tips of L-shaped sticks. *J. Neurophysiol.* 93, 2856–2863. doi: 10.1152/jn.01015.2004

Zangrandi, A., Mioli, A., D'Alonzo, M., Formica, D., Pellegrino, G., and Di Pino, G. (2019). Conditioning transcranial magnetic stimulation of ventral premotor cortex shortens simple reaction time. *Cortex* 121, 322–331. doi: 10.1016/j.cortex.2019.09.006

Zollo, L., Di Pino, G., Ciancio, A. L., Ranieri, F., Cordella, F., Gentile, C., et al. (2019). Restoring tactile sensations via neural interfaces for real-time force-and-slippage closed-loop control of bionic hands. *Sci. Robot.* 4:eaau9924. doi: 10.1126/scirobotics.aau9924

Conflict of Interest: The authors declare that the research was conducted in the absence of any commercial or financial relationships that could be construed as a potential conflict of interest.

frontiers in Neuroscience

ORIGINAL RESEARCH
published: 19 May 2020
doi: 10.3389/fnins.2020.00499

A Framework for Adapting Deep Brain Stimulation Using Parkinsonian State Estimates

Ameer Mohammed[1,2], *Richard Bayford*[1,3] *and Andreas Demosthenous*[1*]

[1] *Department of Electronic and Electrical Engineering, University College London, London, United Kingdom,* [2] *Department of Mechatronic Engineering, Air Force Institute of Technology, Kaduna, Nigeria,* [3] *Department of Natural Sciences, Middlesex University, London, United Kingdom*

The mechanisms underlying the beneficial effects of deep brain stimulation (DBS) for Parkinson's disease (PD) remain poorly understood and are still under debate. This has hindered the development of adaptive DBS (aDBS). For further progress in aDBS, more insight into the dynamics of PD is needed, which can be obtained using machine learning models. This study presents an approach that uses generative and discriminative machine learning models to more accurately estimate the symptom severity of patients and adjust therapy accordingly. A support vector machine is used as the representative algorithm for discriminative machine learning models, and the Gaussian mixture model is used for the generative models. Therapy is effected using the state estimates obtained from the machine learning models together with a fuzzy controller in a *critic-actor* control approach. Both machine learning model configurations achieve PD suppression to desired state in 7 out of 9 cases; most of which settle in under 2 s.

Keywords: biomedical signal processing, deep brain stimulation (DBS), feature extraction, fuzzy control, Gaussian mixture models, support vector machine, Parkinson's disease, state estimator

OPEN ACCESS

Edited by:
Elsa Andrea Kirchner,
University of Bremen, Germany

Reviewed by:
Vassiliy Tsytsarev,
University of Maryland, College Park, United States
Xin Liu,
University of California, San Diego, United States

***Correspondence:**
Andreas Demosthenous
a.demosthenous@ucl.ac.uk

Specialty section:
This article was submitted to Neural Technology, a section of the journal Frontiers in Neuroscience

Received: *01 December 2019*
Accepted: *21 April 2020*
Published: *19 May 2020*

Citation:
Mohammed A, Bayford R and Demosthenous A (2020) A Framework for Adapting Deep Brain Stimulation Using Parkinsonian State Estimates. Front. Neurosci. 14:499. doi: 10.3389/fnins.2020.00499

INTRODUCTION

Continuous deep brain stimulation (DBS) for Parkinson's disease (PD) uses high frequency stimulation to ameliorate patient condition. However, this induces side effects in patients and shortens pacemaker battery life (Little et al., 2013). Both can be resolved using adaptive deep brain stimulation (aDBS). Adaptive DBS driven by feedback signals provides an approach that optimizes clinical benefits whilst minimizing side effects and battery depletion (Little et al., 2013; Arlotti et al., 2016). A commonly adopted feedback signal for aDBS are local field potentials (LFP) (Arlotti et al., 2018). LFP are used due to their correlation to patient clinical states and the ease with which they can be acquired (Priori et al., 2012; Little et al., 2016). In conventional DBS, programming of stimulation parameters are done by trained clinicians (Picillo et al., 2016). Thus, aDBS techniques that imitate human reasoning into decision making could be adopted—an example of which is fuzzy control.

Fuzzy control is found in numerous applications for closed loop therapy (Zarkogianni et al., 2011; Soltesz et al., 2013; Zavitsanou et al., 2016). It has the potential to achieve a level of expertise close to (and possibly better than) human expertise in therapy modulation (Barro and Marin, 2002). However, the capabilities of fuzzy control are dependent on the level of sophistication of its rules and input signal. In this paper, state estimates are used as input to a fuzzy controller to achieve a *critic-actor* control policy as shown in **Figure 1**. It leverages on a machine learning model

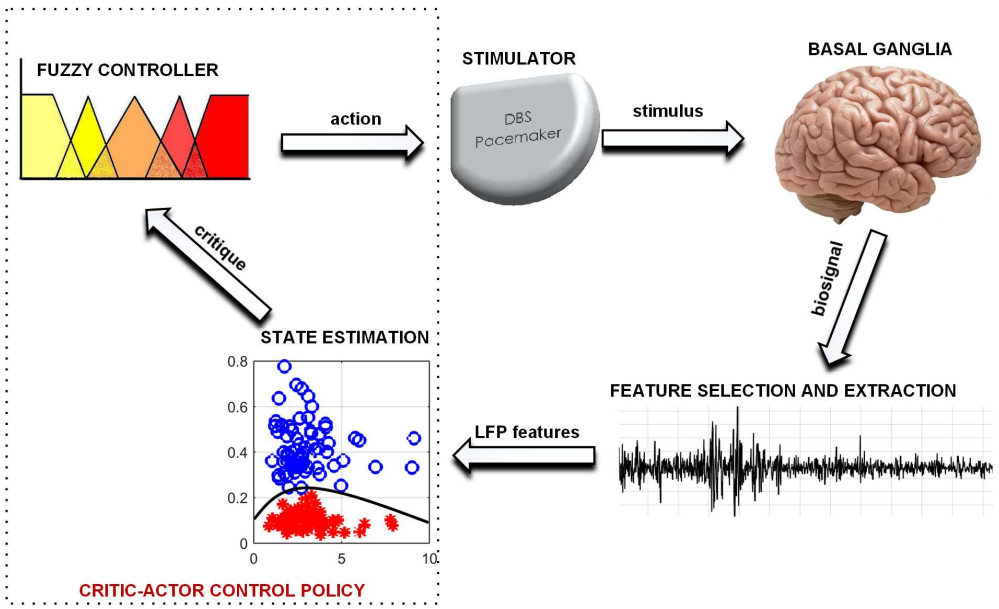

FIGURE 1 | A typical scheme for adapting DBS using PD state estimates.

as the *critic* and a fuzzy controller as the *actor*. This individualizes therapy by means of patient-specific state estimates which are obtained through the machine learning models. Machine learning models were selected because of their ability to create adaptable models for complex signals using statistical attributes from the signals (Sajda, 2006). The choice of fuzzy control was driven by their ability to provide computationally efficient and robust decision making. Consequently, as more knowledge on PD and DBS is gained, the fuzzy rules could be updated, which provides an adaptable control scheme. The scheme has the potential to be developed into a fully implantable closed-loop DBS system.

The rest of the paper is organized as follows. Section Machine Learning for Disease Tracking describes the methods adopted for disease tracking. Sections Models and Metrics and Fuzzy Controller Design describe the materials used for implementing the adopted methods. Section Performance Evaluation presents the results obtained. Sections Discussion and Conclusion present discussion and concluding remarks, respectively.

MACHINE LEARNING FOR DISEASE TRACKING

Disease tracking is important because dynamic changes in PD pathophysiology could help inform treatment strategies. This can be achieved using machine learning models as they provide insights on disease progression. In brain machine interface applications, machine learning provides the ability to notify caregivers of life-threatening events related to chronic disease diagnosis and management (Johnson et al., 2016; Mohammed and Demosthenous, 2018). Using closed-loop control strategies, this useful information can be used to generate actionable outputs—mostly from stimulation devices—to mitigate patient conditions (Csavoy et al., 2009). Machine learning models for disease tracking are intended to achieve one of two outcomes: prediction or state estimation. For optimal delivery of bio-electronic therapy, prediction is the most desirable outcome. Nevertheless, early and accurate state estimation can be used to adjust therapy to suit patients' needs. State estimation tracks fluctuations in PD symptom severity so that stimulation can be modulated correspondingly. Machine learning algorithms can be used to obtain state estimates. Generally, machine learning algorithms are classified into supervised (using labeled data), semi-supervised (using partly labeled data) and unsupervised (using unlabeled data) learning algorithms. This work will focus on the use of supervised learning algorithms.

Supervised Learning Algorithms

These algorithms are not only concerned with detecting patient states, but can also be used in understanding the evolution of the pathophysiological processes in patients; thus, modeling transitions between various states in a disease. Supervised learning algorithms are divided into discriminative and generative machine learning models. For both algorithms, the major pre-processing approach adopted before state estimation is scaling the features using mean normalization. This is represented mathematically as follows,

$$x_{j\_new}^{(i)} = \frac{x_j^{(i)} - \mu_j}{s_j} \tag{1}$$

where $\mu_j = \frac{1}{m}\sum_{i=1}^{m} x_j^{(i)}$ is the mean of feature j, $x_j^{(i)}$ is feature j of training example i (with a total of m training examples $x_1^{(i)}, x_2^{(i)}, \ldots x_m^{(i)}$) and s_j is the standard deviation of feature j.

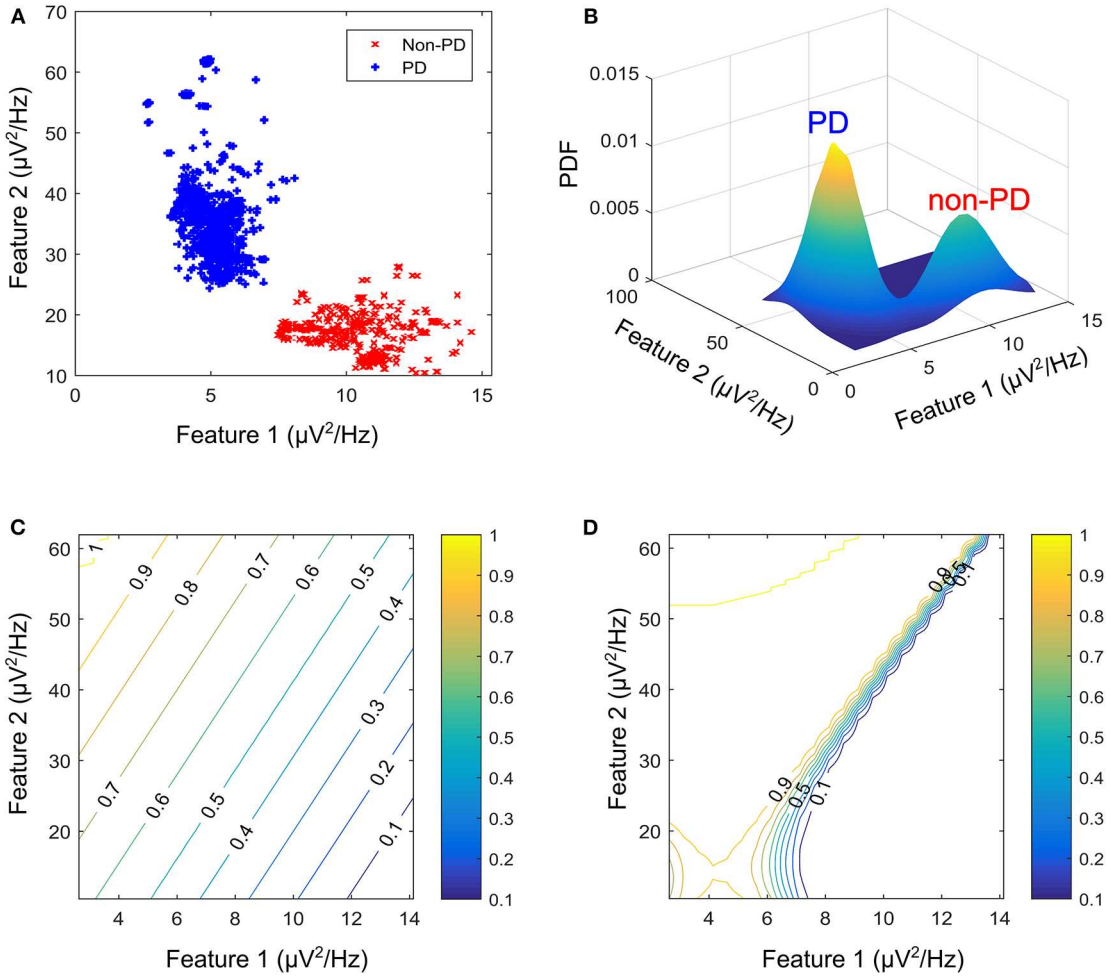

FIGURE 2 | Contour plot for state estimates over a feature space for the machine learning models. **(A)** Example feature space showing PD and non-PD examples for dataset C. **(B)** Probability density function (PDF) for PD and non-PD training examples in **(A)**. **(C)** Contour plot for state estimates using SVM, with a range from 0 to 1 representing levels of severity from non-PD to PD for **(A)**. **(D)** Contour plot for state estimates using GMM, with a range from 0 to 1 representing levels of severity from non-PD to PD for **(A)**. The two features are, Feature 1 (21–26 Hz band) and Feature 2 (18–23 Hz band).

Feature scaling using mean normalization scales features such that features have a comparable range of values.

Discriminative models focus on detecting disease or non-disease states, in this case PD and non- PD states. On the other hand, generative algorithms are particularly useful in applications were the sequence of transition between states is essential in determining future states, like in sleep-stage monitoring applications (Rossow et al., 2011). In aDBS, they can be principally useful in applications were stimulation parameters are defined by the evolution of the sensed neural potentials.

Representative State Estimators

Generative algorithms model the data based on the joint probability distributions between its classes (PD and non-PD) while discriminative algorithm models data based on their conditional probability distribution. One example in each of the two models was used to test the soundness of the proposed framework for aDBS. A linear kernel support vector machine (SVM) was selected as the representative algorithm for the discriminative models while the Gaussian mixture model (GMM) was selected for the generative algorithms. SVM and GMM were selected because of their computational efficiency compared to other similar algorithms. **Figure 2** shows the contour plot for features space using the conditional probability from the SVM as state estimate and the joint probability from the GMM as state estimate. PD regions are points on the plot where the probability is >0.5, while non-PD regions are those in which the probability is <0.5. Thus, from non-PD to severe PD is a transition in probability from 0 to 1.

The SVM uses the widest margin between differing states to discriminate. For a linear SVM kernel, the discriminating function $f_{\mathrm{SVM}}(x)$, used in classifying test cases is obtained using the training examples as in Cristianini and Shawe-Taylor (2000).

$$f_{\mathrm{SVM}}(\boldsymbol{x}) = \sum_{\mathrm{i}} y_i \alpha_{\mathrm{i}} (\boldsymbol{x}_{\mathrm{i}}, \boldsymbol{x}) + \boldsymbol{b} \tag{2}$$

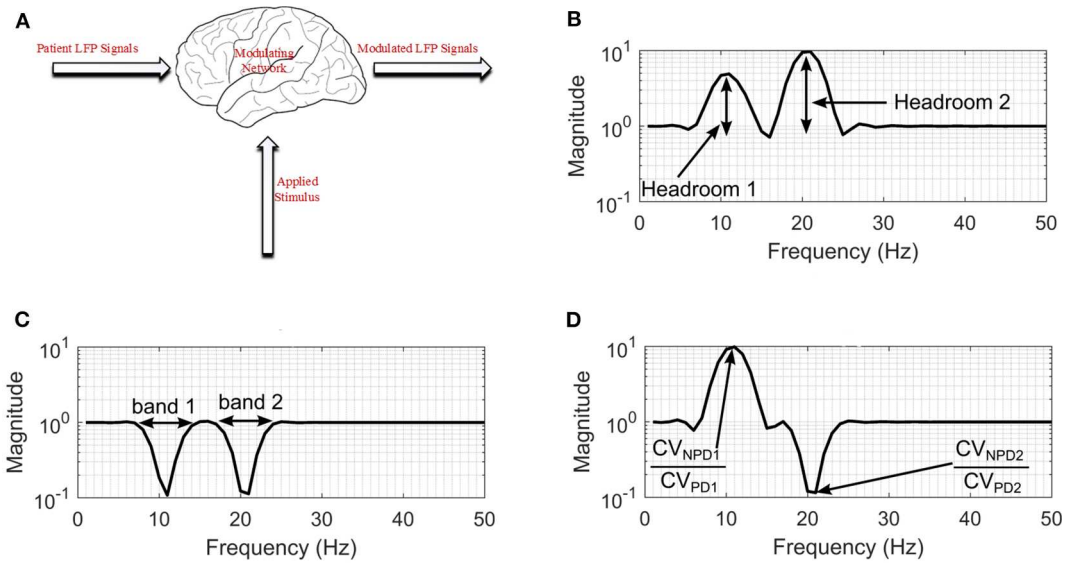

FIGURE 3 | Modulating network used to simulate the effect of DBS on neuronal signals. **(A)** Basal-ganglia network model. **(B)** Frequency response for configuration with non-PD having higher amplitude in both bands. **(C)** Frequency response for a configuration with PD having higher amplitude in both bands. **(D)** Frequency response for a configuration with non-PD having higher amplitude in band 1, and PD having higher amplitudes in band 2. CV_{NPD} is the coefficient of variation for non-PD LFP signal and CV_{PD} is the coefficient of variation for PD LFP signal.

where x_i are the support vectors and their labels y_i, x is the test case, (x_i, x) is the kernel transformation (linear kernel), α_i is a weight vector and b represents the classification threshold. **Figure 2C** depicts the state estimates obtained using SVM on the feature space in **Figure 2A**, whose probability density function (PDF) is shown in **Figure 2B**.

The GMM estimates conditional probability using a weighted sum of a number of PDFs. These PDFs are used to form the Gaussian models. The weighted Gaussian functions $f_{GMM}(x)$ modeling the underlying processes are

$$f_{\mathrm{GMM}}(\boldsymbol{x}) = \sum_{i=1}^{\mathrm{N}} \boldsymbol{w_i} \exp\left(-\left(\vec{\boldsymbol{x}} - \boldsymbol{\mu_i}\right)^{\mathrm{T}} \boldsymbol{\Lambda_i} \left(\vec{\boldsymbol{x}} - \boldsymbol{\mu_i}\right)\right) \quad (3)$$

where w_i is the weight assigned to a particular Gaussian model i, $\vec{x}$ is the input feature vector, μ_i is the mean vector and Λ_i is the covariance matrix. The major assumption employed in GMM is that the population of feature vectors can be represented by N Gaussian models. Thus, two Gaussian models are fitted in the training data, in order to represent each of the patient states (PD and non-PD). **Figure 2C** shows the state estimates obtained using SVM on the feature space in **Figure 2A**, whose PDF is shown in **Figure 2B**.

MODELS AND METRICS

The proposed model in **Figure 1** consists of a basal ganglia network, a feature extraction stage, a state estimation stage for diagnosing PD severity and an adaptive stimulator for delivering therapy. The basal ganglia network uses LFP recordings to mimic the underlying mechanism of PD. LFP signals from the basal ganglia model are applied to a feature processing stage, and the output from this stage is applied to a state estimation stage. Stimulation parameters are adjusted based on patient state estimates. The model was developed using custom SIMULINK blocks. The SIMULINK blocks were implemented using level-2 MATLAB S-functions. This was used to validate the complete aDBS system.

Basal-Ganglia Network Model

In order to validate these methods a basal ganglia model using LFP recordings obtained from measurements made on patients exhibiting a combination of bradykinesia and/or rigidity during the onset of PD, with less noticeable tremor was employed. The network which is shown in **Figure 3A**, consists of: patient LFP signals, modulating network and the modulated LFP signal.

Patient LFP Signals

These are LFP signals consisting of PD and non-PD periods synthesized from real-life LFP recordings. The LFP synthesis, involved fitting autoregressive moving average (ARMA) models to the LFP recordings to produce semi-synthetic LFP signals. Fitting an ARMA model provides the flexibility to manipulate the signal characteristics such that all underlying conditions can be represented. Also, it offers the opportunity to generate LFP signals consisting of PD and non-PD episodes of variable duration. The LFP dataset consists of LFP recording for nine patients. The recordings were obtained from the subthalamic nucleus (STN) of subjects exhibiting a combination of bradykinesia and/or rigidity during the onset of PD, with less noticeable tremor.

The permanent quadri-polar macro-electrode used was model 3,389 (Medtronic Neurologic Division, Minneapolis, MN) consisting of 4 platinum-iridium cylindrical contacts. Its contacts were numbered 0, 1, 2, and 3, with 0 being the most caudal and 3 being the most cranial for both right and left electrodes—making a total of eight monopolar channels for each patient. The recorded signals were amplified using a low-noise amplifier and band-pass filtered. **Figure 4** shows a snapshot of OFF and ON L-dopa recordings of the left DBS lead for patient/dataset A. The complete LFP data synthesis process and a detailed description of the LFP recordings are provided in Mohammed et al. (2017). For the basal-ganglia model in **Figure 3A**, the applied stimulus regulates the patient LFP signal such that the modulated LFP characteristics are restored to those resembling non-PD LFP. Stimulation is not applied on detecting patient LFP with non-PD characteristics.

Modulating Network and Modulated LFP Signals

The therapeutic mechanisms of DBS on neuronal activities is still not clear. Various studies suggest that it reduces neuronal activities (Kiss et al., 2002), while others claim that it increases neuronal activities (Carlson et al., 2010). Later studies provide other alternative explanations (Chiken and Nambu, 2016). Generally, studies show that the frequency settings of DBS of the STN influence the motor symptoms of PD. For example, the study in Su et al. (2018), observed that frequency-specific effects can ultimately inform the frequency programming of STN-DBS in the clinical use. From the studies, what is clear is that DBS has a multimodal and modulating effect on neuronal activities at the stimulation site (Hell et al., 2019). In addition, the various clinical aspects related to bradykinesia and other PD symptoms are still unclear (Bologna et al., 2020). As such, to model the effect of stimulation on patient LFP signals, a black-box approach was used as shown in **Figure 3A**.

For the black box model, changes in the coefficient of variation (CV) of neuronal signals during DBS supports the hypothesis that modulating LFP signals is one of the mechanisms that can lead to PD suppression (Birdno and Grill, 2008; Dorval et al., 2010). PD symptoms have been found to correlate with beta band LFPs (Little et al., 2012, 2013; Grant and Lowery, 2013); gamma (Brown and Williams, 2005; Little and Brown, 2012; Brittain and Brown, 2014); and tremor (Heida et al., 2013) bands. Hence, the neuromodulatory effect of DBS on PD occurs in multiple bands. This prompted the two-degrees-of-freedom (2-DOF) changes in CV applied by the modulating network as shown in **Figures 3B–D**. For 2-DOF modulation in CV, the modulating network varies the amplitude of patient LFP signals in the two bands with the most pronounced variation between non-PD and PD bands as shown in **Figure 3C**. For both bands, the headroom of variation for the magnitude of the filter response is between 1 and the ratio of CV for non-PD to PD (CV_{NPD}/CV_{PD}), as is shown in **Figure 3D**. **Figures 3B–D** show all the cases of CV ratio between PD and non-PD for 2-DOF variation. **Figure 3B** shows a situation where CV_{NPD} in both bands is greater than CV_{PD}. **Figure 3C** shows a situation where CV_{NPD} in both bands is less than CV_{PD}. Finally, **Figure 3D** shows a situation where CV_{NPD} in one of the bands is greater than CV_{PD}. This makes the modulating network unique for each patient since the frequency response of the modulating network is dependent on the relationship between PD and non-PD periods of each patient.

The modulated LFP signals are extracellular/LFP signals resulting from the modification of patient LFP signals by the modulating network. The modulated LFP signals are the signals monitored by aDBS in order to adjust the stimulation.

Feature Extraction and Selection

For feature extraction, the fast Fourier Transform (FFT) is used to obtain time-frequency data. This is achieved by dividing the signal into windows and applying FFT to each window (Prandoni and Vetterli, 2008). Mathematically STFT is given by

$$X_n\ [m;k] = \sum_{n=0}^{L-1} x\,[m+n]\ e^{-j\frac{2\pi}{L}nk} \tag{4}$$

where m is the discrete time index, L is the window length into which the signal is split and k is the discrete frequency index. For this application, the time-stamped measurements are split into 2 s overlapping epochs, with 50% overlap between epochs. In addition, the power bands (features) are divided into 5 Hz bands, with 3 Hz overlap between bands; 0 to 5, 3 to 8 Hz, … 45 to 50 Hz. This provides a total of 16 features. The window is chosen such that a balance between time and frequency resolution is obtained.

More so, feature selection involves reducing the number of features that will be used for state estimation. For this study, the maximum ratio method is used (Mohammed et al., 2017). It starts by identifying the channel having the two bands with the most pronounced variation in activity between PD and non-PD LFP signals. The goal is to obtain the frequency bands that make state estimation easier and computationally efficient. The maximum ratio method is a computationally simple method. A more detailed description is presented in Mohammed et al. (2017).

Stimulation Parameters

Stimulation is used to respond to fluctuations in the dynamics of patient LFP data. The estimated patient state is applied to the fuzzy controller and the fuzzy controller determines the appropriate stimulation parameters. The fuzzy controller is designed in section Fuzzy Controller Design. The poorly understood mechanisms for DBS makes the selection of stimulation parameters (i.e., amplitude, frequency and pulse duration) difficult (Kuncel and Grill, 2004). Experimental studies have been undertaken regarding the most beneficial stimulation parameter for reduction in motor symptoms. Some studies suggest that there are more noticeable improvements when stimulation frequency is adjusted (Moreau et al., 2008; Xie et al., 2012; Belasen et al., 2016). However, other studies maintain that stimulation amplitude is more critical (Moro et al., 2002; Eusebio et al., 2011; Whitmer et al., 2012). More research has focused on stimulation frequency alone (Birdno and Grill, 2008; Baker et al., 2011; Brocker et al., 2013). Varying the stimulation frequency is essential for the therapeutic effects of STN-DBS on motor symptoms in PD (Su et al., 2018). Nevertheless, the major

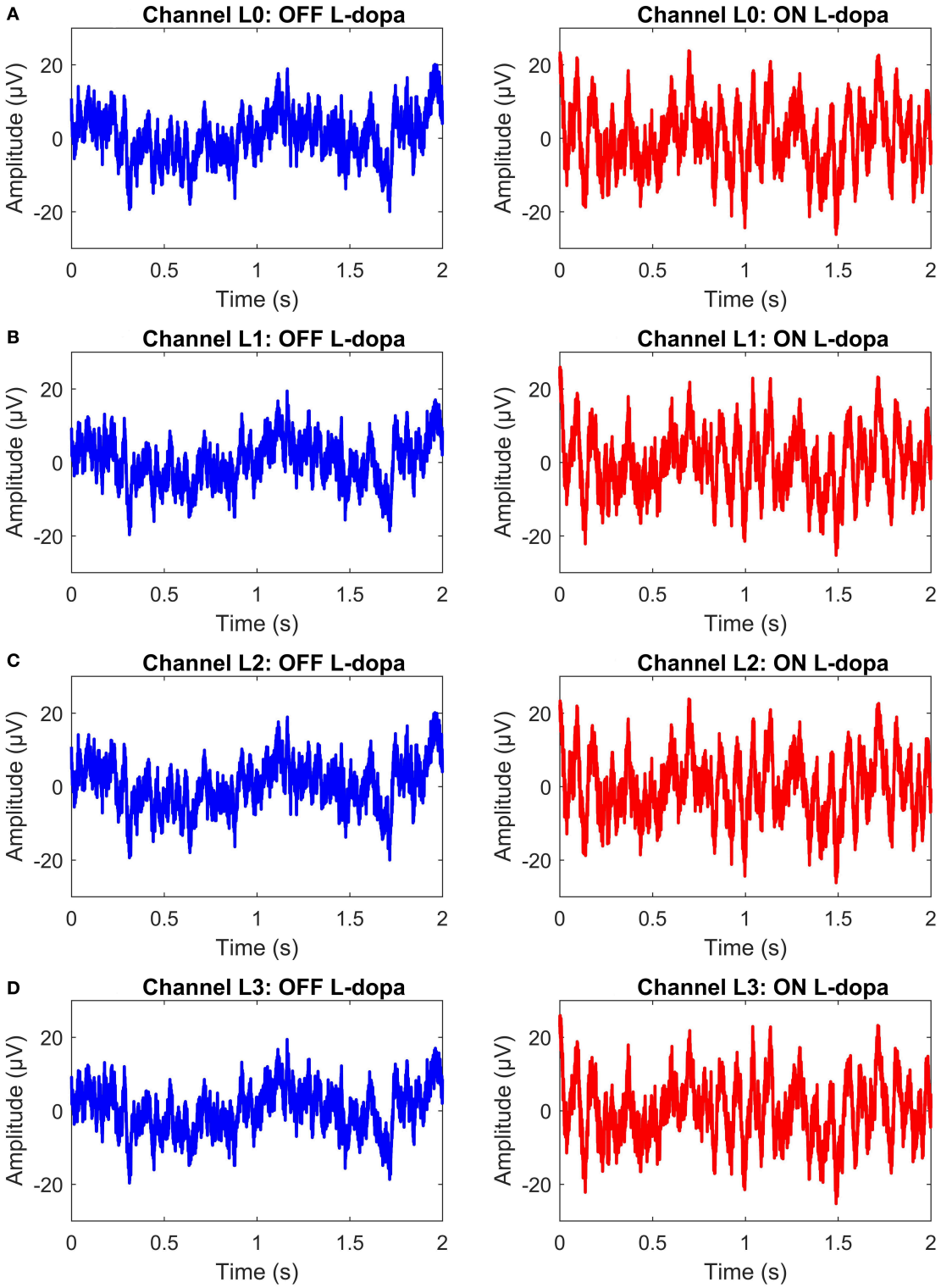

FIGURE 4 | A snapshot of OFF and ON L-dopa recordings (representing PD and non-PD LFP recordings) of the left DBS lead of dataset A. **(A)** OFF and ON L-dopa recordings of electrode L0. **(B)** OFF and ON L-dopa recordings of electrode L1. **(C)** OFF and ON L-dopa recordings of electrode L2. **(D)** OFF and ON L-dopa recordings of electrode L3.

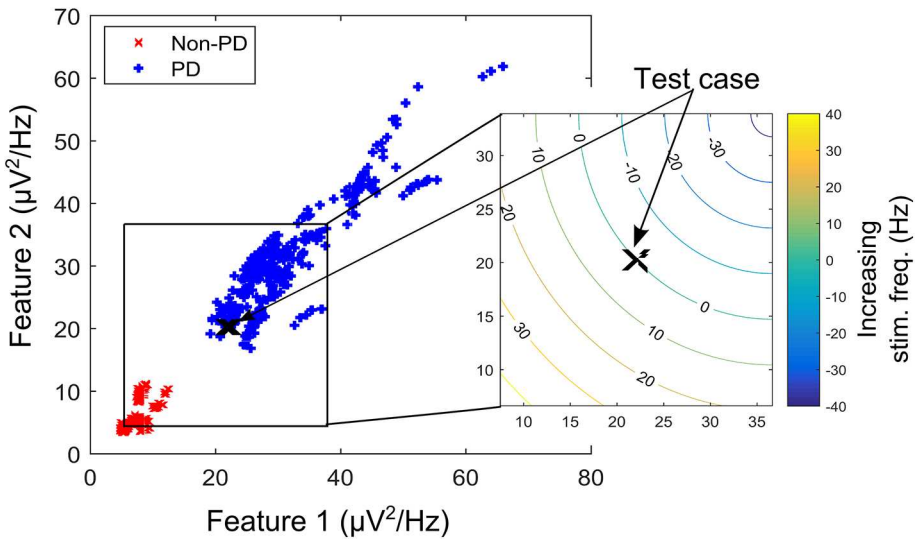

FIGURE 5 | A contour plot depicting the effect of increasing/decreasing stimulation frequency on the transition path of a test case (in the XY-location marked "X") over the feature space. Feature space is that of dataset B.

considerations in selecting stimulation parameters are patient responses to stimulation patterns and power consumption to conserve battery life (Kuncel and Grill, 2004). The consensus is that the most beneficial stimulation frequency occurs at 130 Hz (Birdno and Grill, 2008; Moreau et al., 2008; Vercruysse et al., 2014).

Based on the therapeutic benefits of varying the stimulation frequency, the fuzzy rules are designed to adjust the stimulation frequency. Adjusting the stimulation frequency modifies the modulating effect in a linear fashion as depicted in **Figure 5**. The headroom for the frequency response of the modulating network in **Figure 3** (i.e., a magnitude response of between 1 and CV_{NPD}/CV_{PD}) corresponds to a stimulation frequency ranging from 0 to 90 Hz. This is shown in the contour plot of **Figure 5**, where increasing the stimulation frequency by 45 Hz moves the test case from the point marked X to the center of the non-PD cluster, while a decrease of 45 Hz moves it to the center of the PD cluster. In theory, a 90 Hz increase/decrease in stimulation frequency maintained over 2 s can move a test case from the center of one cluster to the other (PD to non-PD cluster or vice versa). The range of stimulation frequency is between 0 and 180 Hz, which is within the limit for conventional DBS.

Evaluation Metrics

In assessing the performance of the different state estimator-based approaches, three measures that are indicative of accuracy, latency and computational complexity have been used.

Accuracy

The state estimators are evaluated using Mathews correlation coefficient (MCC) and weighted classification error (WCE). MCC and WCE are balanced measures used in assessing state estimator quality that can be used even for cases with skewed classes. MCC measures the correlation coefficient between the observed and predicted binary classifications. It has a range between −1 (total disagreement) and +1 (total agreement); with 0 representing a random prediction. Mathematically,

$$\mathbf{MCC} = \frac{(\mathbf{TP}\times\mathbf{TN}) - (\mathbf{FP}\times\mathbf{FN})}{\sqrt{(\mathbf{TP}+\mathbf{FN})\ (\mathbf{TP}+\mathbf{FP})\ (\mathbf{TN}+\mathbf{FP})\ (\mathbf{TN}+\mathbf{FN})}} \quad (5)$$

where TP are the true positives, FP the false positives, FN the false negatives and TN the true negatives. The major shortcoming of MCC is that it can only be used when one of the denominators TP + FN, TP + FP, TN + FP and TN + FN is not a zero. For WCE, it can be represented mathematically as,

$$\mathbf{WCE} = \frac{1}{2}\left(\frac{\mathbf{FP}}{\mathbf{FP}+\mathbf{TN}} + \frac{\mathbf{FN}}{\mathbf{TP}+\mathbf{FN}}\right). \quad (6)$$

The first part of Equation (5) represents type I error (false-positive rate), while the second part represents type II error (false-negative rate). In Equation (5), WCE uses equal weights to compute the average of type I and type II error.

Latency

Detection latency in this work, measures the total time required by the system (or controller) to settle to the modal state interval for non-PD defined by the fuzzy controller. For SVM driven control policy, the modal state interval is between 0.15 and 0.35, while for GMM, it is a state between 1×10^{-8} and 0.1. This were empirically obtained considering that from non-PD to severe PD is a transition from 0 to 1.

Computational Complexity

In this work, the primary concern is the computational cost of the critic-actor control algorithm consisting of the state estimator and the fuzzy controller. Computational cost consists of two components, number of operations (NOP) and

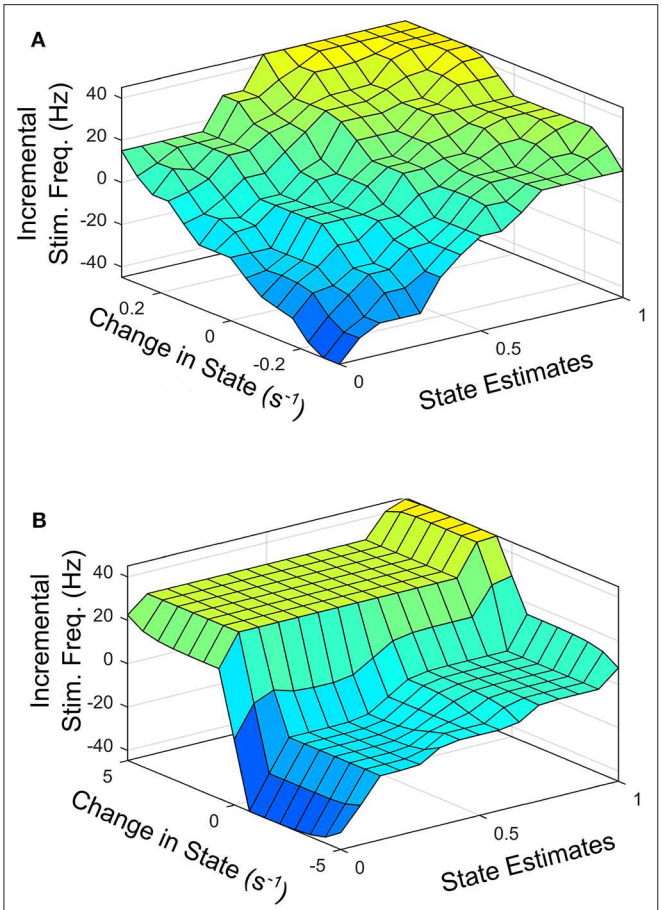

FIGURE 6 | Surface plot for input-output relationship for: **(A)** SVM based controller, **(B)** GMM based controller.

memory requirements. NOP is measured using the number of additions and number of multiplications. It can be represented mathematically as,

$$\mathbf{NOP} = N_{\mathbf{add(sub)}} + \mathbf{Res} \times N_{\mathbf{mult(div)}} \tag{7}$$

where $N_{\text{add(sub)}}$ is the number of 1-bit additions or subtractions; $N_{\text{mult(div)}}$ is the number of 1-bit multiplications and divisions; and Res is the resolution of the data converter used. For memory estimates, the number of 1-bit registers required are obtained.

FUZZY CONTROLLER DESIGN

Based on parkinsonian state estimates, fuzzy rules are defined to regulate stimulation. The fuzzy controller modifies the stimulation parameters applied to the modulating network to suppress PD-related oscillations. A fuzzy controller was chosen because it uses a reasoning which is similar to human reasoning and decision making. This makes it superior in handling non-linearity and uncertainty compared to schemes like proportional-integral-derivative controllers, lead-lag and state feedback control (Feng, 2006; Wu et al., 2017). Fuzzy controller design essentially involves the following:

- Choosing the fuzzy controller inputs and outputs.
- Choosing the pre-processing that is required for the controller inputs and the post-processing for the controller outputs.
- Designing the four components of the fuzzy controller (rule-table, inference mechanism, fuzzification and defuzzification).

To facilitate the design of the fuzzy controller, **Figures 6A,B** shows the desired average profile for the effect of incremental stimulation frequency for all possible input combinations for the SVM and GMM driven approaches, respectively.

Figure 6 represents the average 3-D profile that maps inputs (state estimates and change in state) to outputs (stimulation frequency). To obtain the profile or each patient dataset, training examples at discrete points on the feature space representing states estimates ranging from 0 to 1 in steps of 0.1 are identified. For training examples at each discrete point on the feature space, stimulation frequency is increased in steps from -45 *to* $+45$ Hz (in steps of 5 Hz). The corresponding rate of change in patient state is obtained for each discrete pair consisting of patient state estimate and applied stimulation frequency. This produces a mapping of three variables (patient state estimates, change in state and applied stimulation frequency). This means, for every patient state, there is an applied stimulation frequency that results in a specific rate of change in patient state. The process is repeated for all nine patient datasets and the average for the various profiles are obtained as **Figures 6A,B**. For the SVM based approach, **Figure 6A** represents the average 3-D profile that maps state estimates and change in state to stimulation frequency. This is represented by **Figure 6B** for the GMM based approach. The average profiles in **Figure 6** are used to guide the rule-tables for controlling PD suppression.

The profile for the change in state (measured in s^{-1}) targets a settling time of between 1 and 1.5 s from the center of the modal class of the PD state (with a probability 0.75 for SVM, and 0.9999 for GMM) to the center of the modal class of the non-PD state (with a probability 0.25 for SVM and 1×10^{-4} for GMM). From **Figure 6** it is obvious that from a PD state of 1, the SVM-driven approach has a more gradual descent, while the GMM has a sharper descent at the edges, plateaus for a range of input values in which change in input only causes a slight change in stimulation frequency before it finally descends steeply. This surface plot guided the choice of membership function and rule table for the fuzzy controller, which are normally chosen heuristically. The input-output relationship was obtained using the average profile for state estimate and incremental stimulation frequency which are depicted in **Figures 2**, **5**, respectively.

Fuzzification

This is the encoding step. It modifies the inputs so that they can be interpreted and compared to the rules in the rule-table. The controller inputs are converted to information usable by the inference mechanism. Obtaining a value for an input variable and finding the numeric values of the membership functions that are defined for that variable. It can also be seen as an encoding of the

TABLE 1 | Rule table for control policy using SVM for state estimation.

Incremental stimulation frequency		Change in state								
		B_{-4}	B_{-3}	B_{-2}	B_{-1}	B_0	B_1	B_2	B_3	B_4
State	A_0	C_{-3}	C_{-3}	C_{-2}	C_{-2}	C_{-1}	C_{-1}	C_{-0}	C_{-0}	C_1
	A_1	C_{-2}	C_{-2}	C_{-1}	C_{-1}	C_{-1}	C_{-0}	C_0	C_1	C_1
	A_2	C_{-2}	C_{-1}	C_{-1}	C_{-0}	C_{-0}	C_{-0}	C_1	C_1	C_1
	A_3	C_{-1}	C_{-1}	C_0	C_0	C_0	C_1	C_1	C_2	C_2
	A_4	C_0	C_0	C_0	C_0	C_1	C_1	C_2	C_2	C_2
	A_5	C_0	C_0	C_0	C_1	C_1	C_2	C_2	C_3	C_3
	A_6	C_0	C_1	C_1	C_1	C_2	C_2	C_3	C_3	C_3
	A_7	C_1	C_1	C_1	C_1	C_2	C_2	C_2	C_3	C_3
	A_8	C_1	C_1	C_1	C_2	C_2	C_2	C_3	C_3	C_3
	A_9	C_1	C_1	C_2	C_2	C_2	C_3	C_3	C_3	C_3
	A_{10}	C_1	C_2	C_2	C_2	C_2	C_3	C_3	C_3	C_3

fuzzy controller inputs. The encoded information is used in the fuzzy inference process that begins with matching.

Fuzzy Rules and Membership Functions

Fuzzy rules and membership functions are obtained by studying the plant dynamics (using modeling and simulation), based on these, a set of control rules that make sense are adopted. This makes fuzzy controller design subjective and dependent on expert designer (Passino and Yurkovich, 1998). In addition, the adaptable nature of a fuzzy controller makes a suitable candidate, since the mechanisms of DBS are still under debate. The control scheme uses a two-input one-output fuzzy controller. The inputs are PD state estimate and the rate of change in state. The state estimates and rate of change in state quantify the dynamics of the underlying process to enable control. State estimates are obtained using SVM and GMM. The output is the incremental stimulation frequency. Based on the contour plot of the state estimates in **Figures 2C,D**, and the contour plot depicting the effect of stimulation frequency in **Figure 5**, triangular membership functions were used for the inputs and output of the SVM driven approach. While for the GMM based approach, Gaussian functions were adopted. The rule table for the SVM-driven approach is shown in **Table 1**. It is obtained using the 3-D profile in **Figure 7A** representing the mapping between inputs (state estimates and change in state) and outputs (stimulation frequency). The input membership function for the rules in **Table 1** are summarized in **Figures 7A,B**. While the membership functions for the output (incremental stimulation frequency) is summarized in **Figure 7C**.

For the GMM-based control approach, its rule table is shown in **Table 2**. It uses Gaussian membership functions. Its input membership functions for the rules in **Table 2** are summarized in **Figures 8A,B**. While the membership functions for the output (incremental stimulation frequency) is shown in **Figure 8C**. The universe of discourse for the state estimates is [0, 1] as can be seen in **Figure 7A** and **Figure 8A** for the SVM and GMM, respectively. The input fuzzy sets for the SVM are represented by alphanumeric variables A_0 A_1 … A_{10}, and that of the GMM is D_0, D_1 … D_7. This means for state estimates, the SVM driven approach has eleven fuzzy sets and the GMM driven approach has eight fuzzy sets. The membership functions for the SVM and GMM driven controllers are summarized in **Figures 7**, **8**, respectively.

For the second input which is change in state, the fuzzy sets of the SVM driven approach are represented by alphanumeric variables B_{-4} … B_0 … B_4, making a total of nine fuzzy sets. Their membership functions are summarized in **Figure 7**. From **Figure 7**, it can be seen that negative subscripts represent a change from one toward zero (PD to non-PD) and positive subscripts represent a change from zero toward one (non-PD to PD). This is the same for the change in state of the GMM-driven approach with fuzzy sets represented by alphanumeric variables E_{-4} … E_0 … E_4, and their respective membership functions summarized in **Figure 8**. As summarized in **Figures 7**, **8**, the universe of discourse for the SVM-driven approach is [−0.31, 0.31] s^{-1} and that of the GMM-driven approach is [−5, 5] s^{-1}. The fuzzy sets representing the output (incremental stimulation frequency) are labeled C_{-3} … C_3, for the SVM approach and that of the GMM are labeled F_{-3} … F_3. Like in the fuzzy sets for the change in state, the negative subscripts represent an output representing a reduction in stimulation frequency, while a positive subscript represents an output resulting in an increase in stimulation frequency. Both have a universe of discourse of [−60, 60] Hz. Based on heuristics, the SVM rule-table has an 11 × 9 array making a total of 99 possible rules, which are summarized in **Table 1**. For the GMM rule-table in **Table 2**, it is made up of an 8 × 9 array making a total of 72 possible rules.

The desired fuzzy set for the SVM driven approach is shaded in **Figure 7**. The desired fuzzy set for state estimates is between the intervals 0.15 and 0.35 (represented by A_2 in **Figure 7A**). This represents the modal class for non-PD cases. In terms of the change in state, the desired interval is between −0.1 s^{-1} and 0.1 s^{-1} (represented by B_0 in **Figure 7B**). The modal class interval for the state estimate (A_2) was made not to overlap with other classes to avoid ambiguity in fuzzy quantification. The outermost membership functions for the inputs can be seen to saturate and values outside the range are grouped to their closest fuzzy set. However, this is not the case for the output, due to

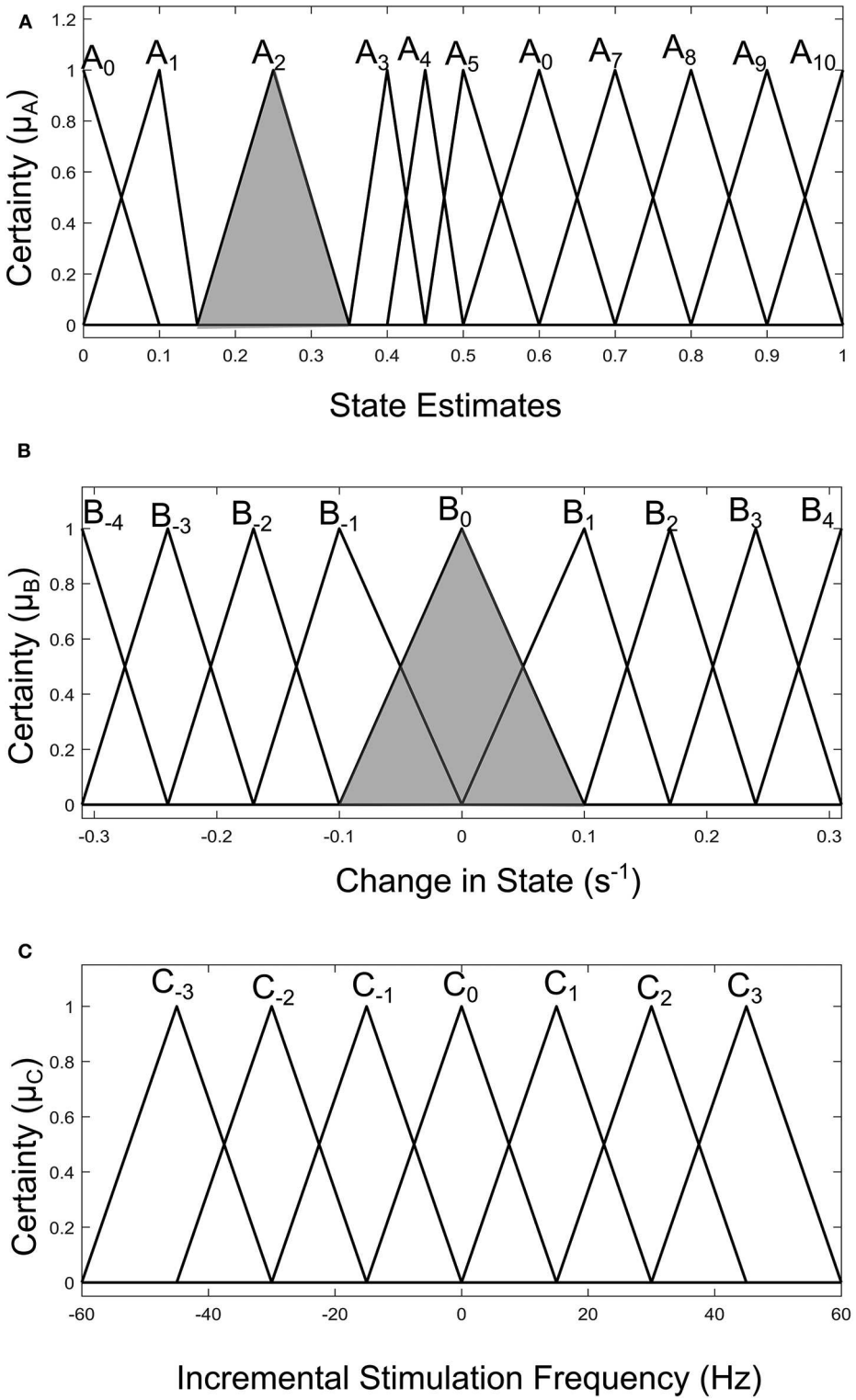

FIGURE 7 | Input-output membership functions for the fuzzy controller driven by SVM state estimates. **(A)** Membership functions for the state estimates. **(B)** Membership functions for the rate of change in state. **(C)** Membership function for the incremental stimulation frequency.

the requirement for a defined output value at any instant in time. For the GMM driven approach, the desired input values are: 1×10^{-8}—0.1 for state estimates (represented by D_2 in **Figure 8A**) and -5×10^{-14} s^{-1} to 5×10^{-14} s^{-1} for change in state (represented by E_0 in **Figure 8B**). Fuzzy rules and definition of membership function are subjective and are dependent on the

TABLE 2 | Rule table for control policy using GMM for state estimation.

Incremental stimulation frequency		Change in state								
		E_{-4}	E_{-3}	E_{-2}	E_{-1}	E_0	E_1	E_2	E_3	E_4
State	D_0	E_{-3}	E_{-3}	E_{-2}	E_{-1}	E_{-1}	E_{-1}	E_{-0}	E_{-0}	E_1
	D_1	E_{-2}	E_{-2}	E_{-1}	E_{-1}	E_{-1}	E_{-0}	E_0	E_1	E_1
	D_2	E_{-2}	E_{-1}	E_{-1}	E_{-0}	E_{-0}	E_{-0}	E_1	E_1	E_2
	D_3	E_{-1}	E_{-1}	E_0	E_0	E_0	E_1	E_1	E_2	E_2
	D_4	E_0	E_0	E_0	E_1	E_1	E_1	E_2	E_2	E_2
	D_5	E_0	E_0	E_1	E_1	E_2	E_2	E_2	E_2	E_3
	D_6	E_1	E_1	E_1	E_2	E_2	E_2	E_3	E_3	E_3
	D_7	E_1	E_1	E_2	E_2	E_2	E_3	E_3	E_3	E_3

expert designer. That is why a wide desired range was selected in both approaches to ensure convergence. In addition, the selected range represents the modal state for stable and non-disease conditions when projected to the patient feature space, which could be demonstrative of symptom severity. The membership functions and fuzzy rules were defined carefully based on the gradation of the state estimates on the patients feature space. This was to enable a gradual and deliberate PD suppression as against abrupt and jerky response.

Inference Mechanism

The inference mechanism generally involves two steps: premise quantification and determining conclusions. Premise quantification compares the premise of all rules to the controller inputs to determine which rules are applicable to the current situation. It involves determining the certainty with which rules apply. The recommendations from rules that we are more certain with are adopted. Next is the determination of conclusions. This decides the control action to take using the applicable rules at the current time instant. The conclusions are characterized with a fuzzy set that represents the certainty with which the input should take various values. Premise quantification using the minimum f the applicable rules is adopted, while conclusion determination is obtained by ANDing the applicable rules.

Defuzzification

This is the final operation of the fuzzy controller. It operates on implied fuzzy sets (output fuzzy sets) produced by the inference mechanism. It combines the effects of the various fuzzy sets to produce the "most certain" controller output (plant output). Defuzzification can be considered as decoding. As the fuzzy sets produced by the inferencing process (implied fuzzy sets) is converted to numerical controller outputs. The center of gravity (COG) method for combining recommendations was adopted. More detail of defuzzication is given in Passino and Yurkovich (1998). From both **Tables 1**, **2**, the pattern of rule consequents shows a certain symmetry. For states estimates approaching a state of 1 and having a positive rate of change in state (positive subscript i.e., moving from non-PD to PD), there is a positive increase in stimulation frequency (positive subscript). Similarly, for state estimates approaching 0 and having a negative rate of change in state (negative subscript i.e., moving from PD to non-PD), the incremental stimulation frequency is negative (negative subscript). Note, the diagonals of near zero for the incremental stimulation frequency from state A_0 to state A_6, for the SVM and A_0 to state A_5, for the GMM in **Tables 1**, **2**, respectively.

PERFORMANCE EVALUATION

PD Suppression

PD suppression is depicted in **Figure 9** using the GMM and SVM driven approaches. From **Figure 9A** which depicts SVM state estimation, it can be seen that the test case travels from the PD region and converges at the non-PD region as desired. It is also the case for the GMM approach in **Figure 7C**, but with a smoother trajectory. **Figures 9A,C** show the feature space profile and **Figures 9B,D** display the time profile. For the time profile, it can be seen that both cases cross the desired interval exactly after 2 s and both present the same settling profile. After settling, the SVM based approach has a mean PD state of 0.3137 and GMM-driven approach has a PD state of 1.3×10^{-2}, both of which fall within the desired range.

The stimulation profile for both cases is shown in **Figure 10**. Both cases present almost the same stepwise pattern, with the SVM having a more gradual ascent to the required stimulation frequency compared to the GMM which overshoots before finally settling. The settling stimulation frequency for both cases are not far apart. The feature space profile on the feature space and the time profile (both in **Figure 9**) display a stable PD suppression profile. In addition, the stimulation profile in **Figure 10** also displays a stable stimulation profile. Both of these are indicative of a stable PD suppression.

For the rest of the datasets, **Table 3** summarize their mean PD state and settling time. For the mean PD state in **Table 3**, the SVM has a lower quartile of 0.2514 and an upper quartile of 0.316, which both fall within the desired range (0.15–0.35). For the GMM, it has an upper quartile of 0.085 and a lower quartile of 2.5×10^{-4}, which are both within the desired range (1×10^{-8} −0.1). For the settling times in **Table 3**, the SVM-driven approach has a median of 1.5 s, lower quartile of 1.25 s and an upper quartile of 1.875 s. While for the GMM,

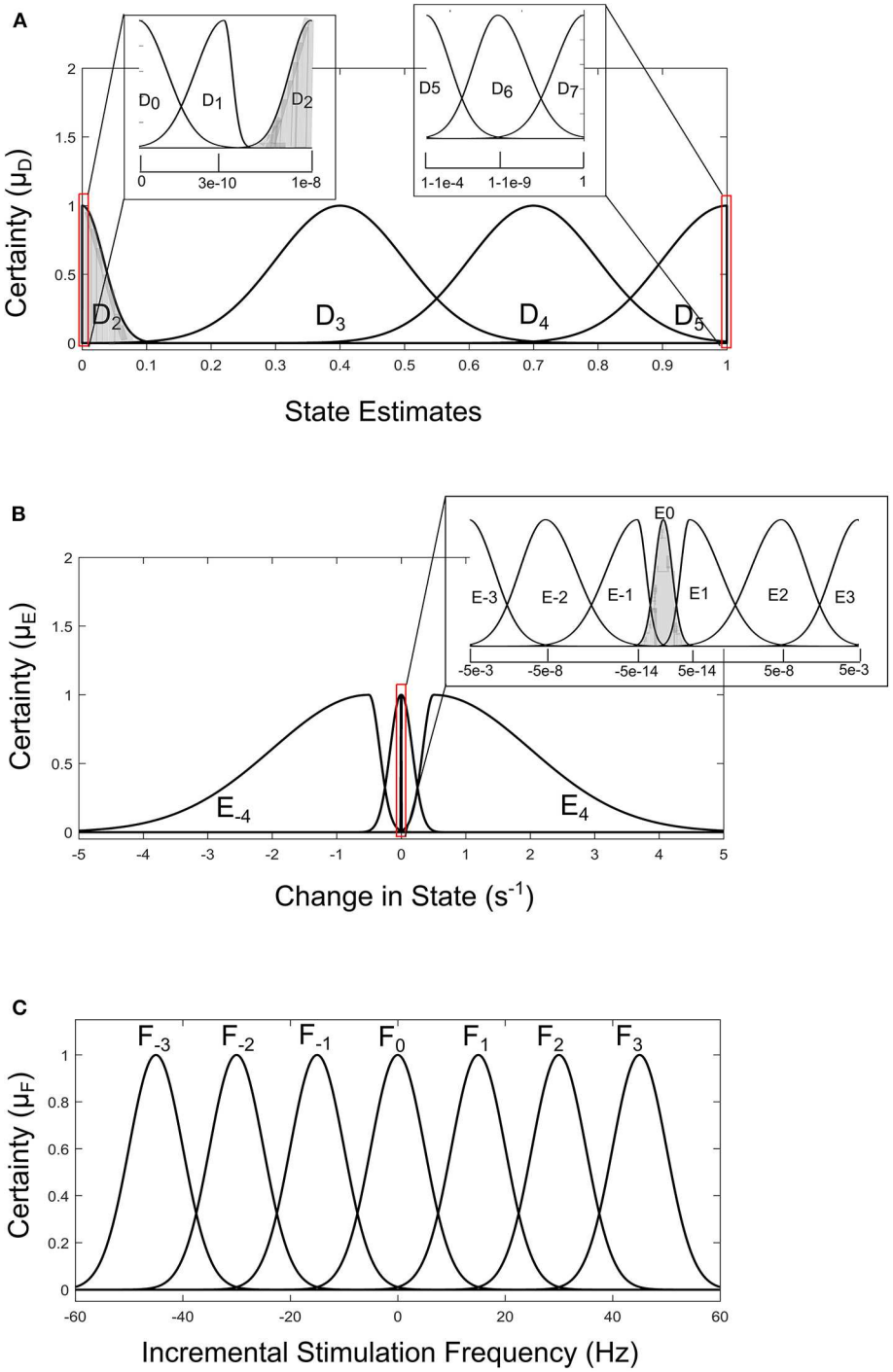

FIGURE 8 | Input-output membership functions for the fuzzy controller driven by GMM state estimates. **(A)** Membership functions for the state estimates. **(B)** Membership functions for the rate of change in state. **(C)** Membership function for the incremental stimulation frequency.

it has a median of 1.25 s, lower quartile of 0.25 and an upper quartile of 1.75 s. This shows that on average, the GMM based approach settles faster than the SVM based approach; however, the GMM has more variation in settling time as shown in **Table 3**.

Performance of State Estimators

To assess the quality of the SVM and GMM state estimators, the MCC and WCE which are skew insensitive measures were used. The MCC measured the correlation coefficient between the original dataset and the models fitted using each of the state

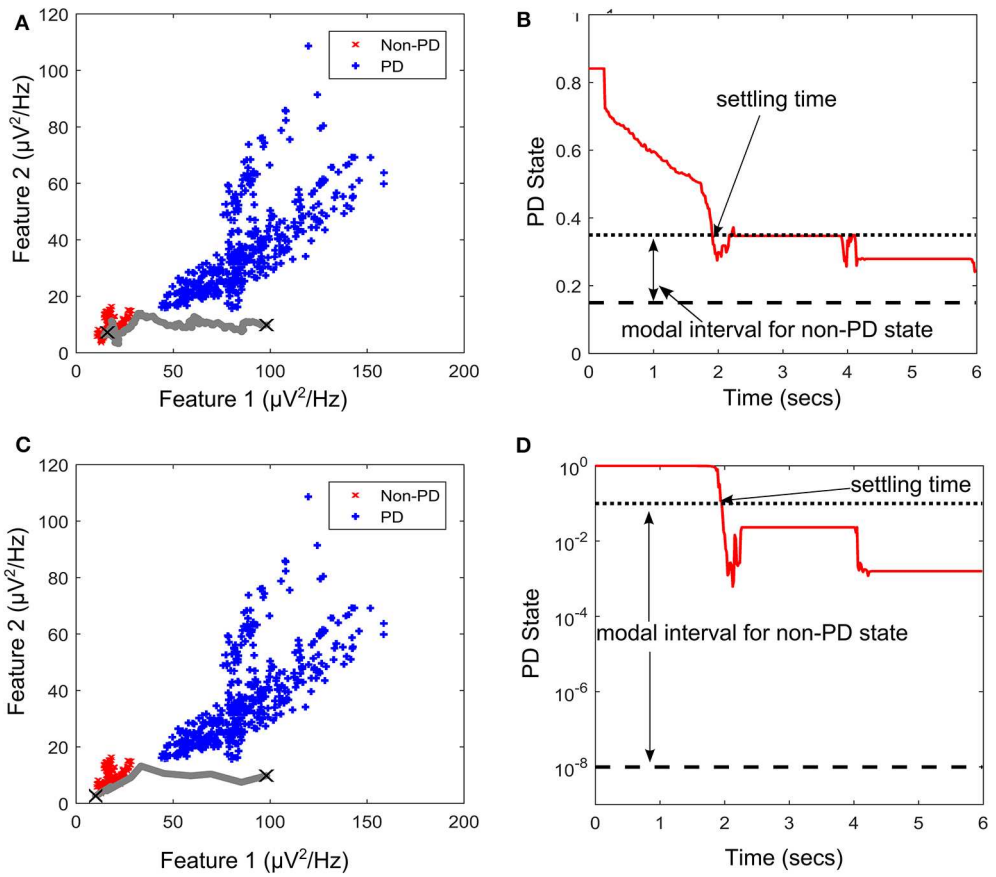

FIGURE 9 | State transition of PD suppression on feature space of patient/dataset E. **(A)** Showing PD state transition on a feature space using SVM for state estimation, with "X" markers showing start (from PD) and settling (non-PD) positions. The feature space trajectory is indicated in gray. **(B)** PD state profile for PD suppression using SVM to obtain state estimates. It depicts the modal interval for the non-PD state when SVM is used for state estimation. **(C)** Showing PD state transition on a feature space using GMM for state estimation, with "X" markers showing start (from PD) and settling (non-PD) positions. The feature space trajectory is indicated in gray. **(D)** PD state profile for PD suppression using GMM to obtain state estimates. It depicts the modal interval for the non-PD state when GMM is used for state estimation.

estimators. On the other hand, the WCE consisted of weightings of type I and type II error. This was because in aDBS, high false positive-rate will result in administering stimulation when it is not required, and this may lead to stimulation induced side effects (Baizabal-Carvallo and Jankovic, 2016). High false-negative rate will result in the non-administering of stimulation when it may be required, which could worsen patient condition (Hacker et al., 2015). The real-time detection performance of the state estimator was investigated. Both models used 128 training examples and PD events were detected from 2 s overlapping epochs (with 50% overlap). **Table 4** summarizes the average result obtained for each dataset for 100 Monte Carlo runs using 256 test cases (256 LFP epochs). For each of the nine test cases, there is a training (and hold-out/cross validation) phase then a test phase to validate the closed-loop architecture.

For MCC in **Table 4**, both state estimators present a positive correlation for all datasets, with the SVM having a median of 1 and the GMM with a median of 0.9433. Of the 9 cases, both SVM and GMM have 7 cases with strong positive correlation (MCC $\geq$ 0.5). Only the state estimates of dataset G have a weak positive correlation in both cases. This is due to the high overlap between its PD and non-PD clusters which makes it difficult to fit the classifier to the data. From the MCC results, it can be seen that SVM fits the data better than the GMM. Similarly, the WCE results present a superior performance of the SVM over the GMM. The SVM presents a mean and median WCE of 9.03 and 0%, respectively. While the GMM presents a mean and median of 11 and 1.98%, respectively. This further confirms the superiority of the SVM over the GMM in fitting the data.

Relative Complexity

To ensure that the approach is effective for real LFP recordings, the semi-synthetic LFP were made from real LFP recordings to mimic PD progression in real LFP recordings. In addition, state estimators that are size and power conscious were implemented. Complexity estimates for both approaches were obtained using 128 training examples were assumed to be used with 8-bit quantization (GMM inputs to fuzzy controller were assumed to

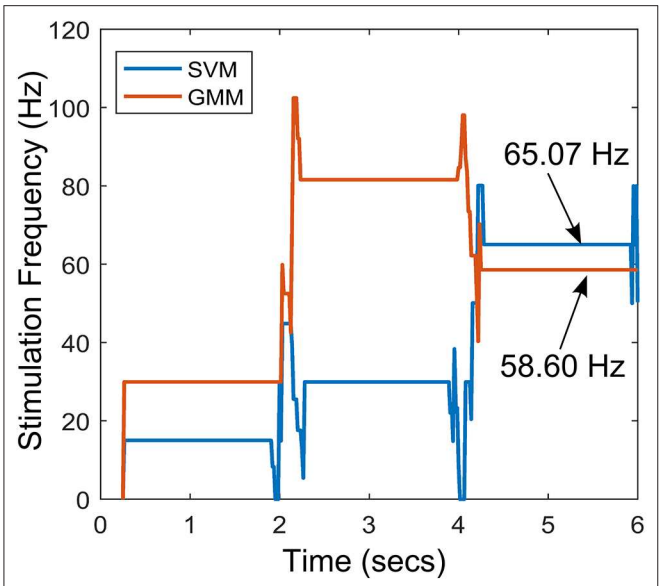

FIGURE 10 | Stimulation profile for the state transition shown in **Figure 9**.

have 32-bit quantization due to their resolution requirements) and 10% of the training examples were assumed to be support vectors of the SVM. The relative complexity between the SVM-driven and GMM-driven approach for each of the two stages of the critic-actor control policy are shown in **Figure 11**. From **Figure 11A**, it can be seen that at the state estimation stage the SVM-driven approach requires more NOP, with the GMM approach requiring only about 5% SVM NOP. At the state estimation stage, computation in the GMM is dominated by memory while for the SVM it is dominated by NOP. This is because the GMM is a population dependent algorithm, while the SVM only uses the footprint from the population to infer properties. In **Figure 11B**, the GMM requires a higher NOP for fuzzy inferencing due to its adoption of Gaussian functions as against the triangular function used by the SVM—where triangular COG is simpler to calculate. In terms of memory the GMM requires fewer rules compared to the SVM. It is clear that in the state estimation stage the GMM has less computation and more memory, while at the fuzzy control stage the reverse is the case.

TABLE 3 | Average settling time and settling state for various patient datasets.

Datasets	Average settling time (s)		Average settling state	
	SVM	GMM	SVM	GMM
A	1.25	0.50	0.3237	0.0034
B	1.50	1.75	0.2584	0.1640
C	1.50	1.25	0.2802	3.5×10^{-4}
D	1.25	0.25	0.2547	4.5×10^{-9}
E	1.75	1.75	0.3137	0.0130
F	1.75	1.75	0.2542	0.0720
G	2.25	2.25	0.4950	0.1245
H	2.25	0.25	0.1735	4.4×10^{-20}
I	0.50	0.25	0.2431	0.0042

TABLE 4 | State estimation performance of SVM and GMM on various patient data.

Datasets	MCC		WCE	
	SVM	GMM	SVM	GMM
A	0.3534	0.5273	0.3447	0.2204
B	1	0.8863	0	0.0771
C	1	1	0	0
D	1	0.9976	0	0.0016
E	1	1	0	0
F	0.9433	0.9433	0.0198	0.0198
G	0.4479	0.2347	0.3273	0.3757
H	1	0.9963	0	0.0012
I	0.7371	0.4343	0.1210	0.2943

DISCUSSION

Critic-Actor Control Policy

The *critic-actor* approach models the relationship between the physician and the automated neuromodulation system. The critic like the "trained clinician" assesses the state of the system based on a cost function (in this case state estimates) and provides the information to the actor. The actor provides control signal based on evaluation from the "informed critic." In this configuration the state estimator is the critic, while the fuzzy controller is the actor. The main motivation for adopting the critic-actor control policy is because PD suppression can be extremely difficult to achieve due to the limited understanding of the mechanisms underlying PD. This makes it difficult to produce an accurate model that could be used for controller development. It is for this reason that more heuristic methods are proposed. The adaptive scheme exhibits the ability to restore patient LFP characteristics to PD-free conditions for different patients without a change in controller parameters. Changing conditions were monitored through the state estimates, which was the feedback signal. The feedback-loop consists of parkinsonian state (representing symptom severity) determination and stimulation facilitated by the fuzzy controller. The control signal modulates the spectral features to match PD free conditions of each individual patient. The resulting spectral features show that the adaptive scheme has the capacity to restore PD signals to their primary oscillations present under PD-free conditions. More so, using fuzzy inference mechanisms to quantify the dynamics of PD can be very intuitive for modulating therapy. Since it uses rule-based decision making that combines human heuristics into decision making; these rules could be updated into the controller as more knowledge regarding PD is acquired. Effective fuzzy control can only be achieved by adopting the right input pre-processing, in this case state estimates and their rate of change over time were chosen. In the future, external signals e.g., accelerometry activity can be incorporated to produce comprehensive rules that cover an increased number of possible situations. As things stand, optimal control can only be achieved by having a deeper understanding of

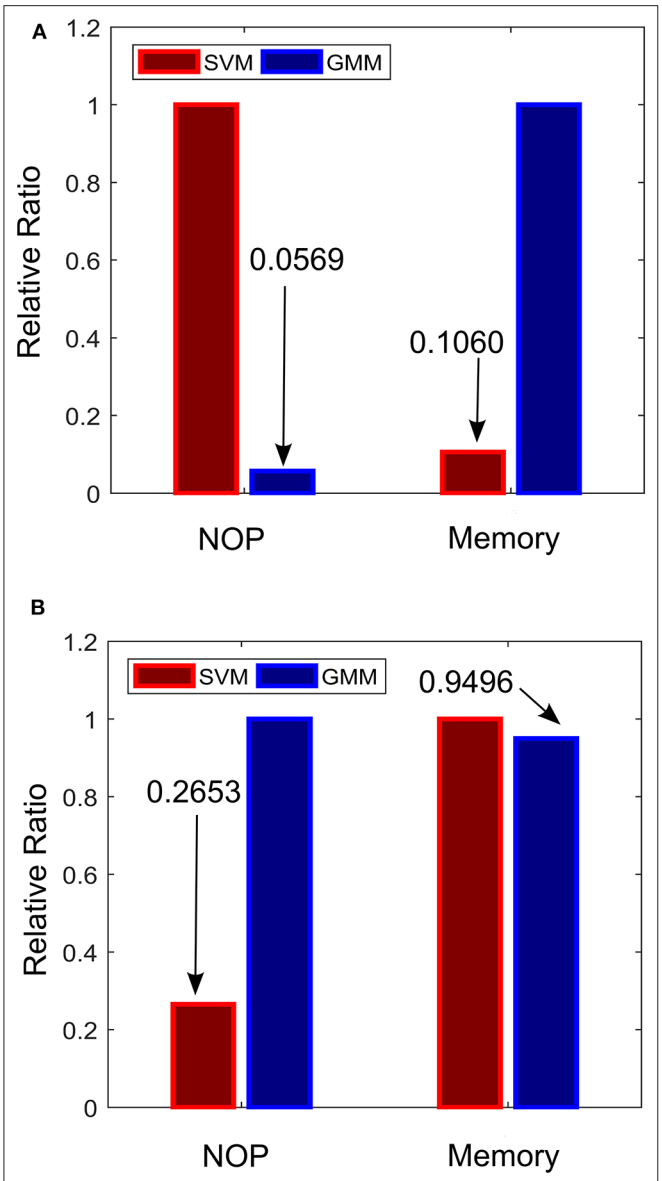

FIGURE 11 | Relative complexity of the critic-actor control driven by GMM and SVM. **(A)** Normalized complexity for the state estimation stage. **(B)** Normalized complexity for the fuzzy control stage. Normalized to the maximum for all cases (*maximum = 1*).

the underlying mechanisms of DBS and PD—which is more of a clinical challenge. Ultimately, this tool could provide a paradigm on which stimulation can be adapted. The study provides a scheme in which DBS can be adapted using heuristics. To validate the efficacy of the approach, state estimates were obtained using both generative and discriminative machine learning models. Both showed promising results, which are attributable to their self-adjusting nature due to periodic training.

Model Limitations

At present, a model representing all possible dynamics is far from being realized because there is insufficient knowledge to produce models which closely represent the expected behavior of the system. This is why PD symptom severity is represented by the probability that a patient LFP signal is a PD condition. Apart from clinically sound PD state estimates, several other issues are necessary in order to achieve efficient PD onset control, such as optimal stimulation parameters and how they vary across patients and time. More specifically, the study focused on modulating DBS frequency, it is still under debate which of the parameters (stimulation intensity, pulse width and frequency) is the most beneficial. Nevertheless, controlling one of the parameters could shed more light on how best to control therapy. Currently, a number of assumptions regarding the effect of stimulation on neuronal signals are used to create a stimulation model that draws on the common denominator in all of the theories in Kiss et al. (2002), Carlson et al. (2010), and Chiken and Nambu (2016); which suggest a modulating effect on neuronal signals. This model could be improved if more detailed information on experimental LFP data consisting of stimulation parameters and PD symptom severity are obtained.

Achieving significant progress in aDBS will depend on the correlation between patient state and LFP signal, as well as how stimulation modulates patient LFP. This would require a large set of LFP representing the effect of stimulation on the progression in PD symptoms for a wide range of patients. Presently, the major challenge in adaptive DBS is the difficulty in establishing a direct relationship between patient state and stimulation parameters. This is mainly due to the complexity of post-surgery programming of stimulation parameters by trained clinicians, which can take up to 6 months or more (Bronstein et al., 2011). Because of the limited availability of PD data incorporating the effects of stimulation, stimulation was modeled only by varying stimulation frequencies. This was chosen because stimulation frequency has proven to be more beneficial and reliable than other stimulation parameters (Birdno and Grill, 2008; Baker et al., 2011; Brocker et al., 2013; Su et al., 2018).

Finally, the control policy proposed tends to work better on cases with separable classes and clear states. A summary of the various transition profiles for PD suppression of datasets A to I is presented in the **Supplementary Material** of the paper. As presented in the **Supplementary Material**, for non-binary clusters (like the XOR classification problem) or binary clusters with large overlap, additional input information may be required to enable convergence. Convergence of the state estimates to the modal interval of the non-PD state can only be guaranteed for feature spaces with binary clusters and machine learning algorithms that produce an MCC >0.5.

CONCLUSION

The work provides theoretical evidence on the possibility of mitigating intractable Parkinsonism by adaptively regulating stimulation using recorded neurophysiological signals. It provides a framework for which if fine-tuned, could lead to the suppression of LFP characteristics in PD patients based on their state estimates (symptom severity) obtained using machine learning algorithms. The dynamic progression of neural signals

in PD patients necessitated the adoption of machine learning models for tracking PD. The fuzzy control approach was adopted for computational efficiency and robustness to non-linearity. This was done with hardware implementation in mind, so that the architecture can be deployed in fully implantable aDBS systems that automatically adjust stimulation parameters in real-time in response to changes neurophysiological signals.

DATA AVAILABILITY STATEMENT

The datasets generated for this study are available on request to the corresponding author.

AUTHOR CONTRIBUTIONS

AM performed simulations, analyzed the results, and wrote the manuscript. AD and RB supervised the work and reviewed the manuscript. All authors conceptualized the ideas and approved the manuscript.

SUPPLEMENTARY MATERIAL

The Supplementary Material for this article can be found online at: https://www.frontiersin.org/articles/10.3389/fnins.2020.00499/full#supplementary-material

REFERENCES

Arlotti, M., Marceglia, S., Foffani, G., Volkmann, J., Lozano, A. M., Moro, E., et al. (2018). Eight-hours adaptive deep brain stimulation in patients with Parkinson disease. *Neurology* 90, e971–e976. doi: 10.1212/WNL.0000000000005121

Arlotti, M., Rosa, M., Marceglia, S., Barbieri, S., and Priori, A. (2016). The adaptive deep brain stimulation challenge. *Parkinsonism Relat. Disord.* 28, 12–17. doi: 10.1016/j.parkreldis.2016.03.020

Baizabal-Carvallo, J. F., and Jankovic, J. (2016). Movement disorders induced by deep brain stimulation. *Parkinsonism Relat. Disord.* 25, 1–9. doi: 10.1016/j.parkreldis.2016.01.014

Baker, K. B., Zhang, J., and Vitek, J. L. (2011). Pallidal stimulation: effect of pattern and rate on bradykinesia in the non-human primate model of Parkinson's disease. *Exp. Neurol.* 231, 309–313. doi: 10.1016/j.expneurol.2011.06.012

Barro, S., and Marin, R. (Ed). (2002). *Fuzzy Logic in Medicine*. Heidelberg: Springer Science and Business Media.

Belasen, A., Rizvi, K., Gee, L. E., Yeung, P., Prusik, J., Ramirez-Zamora, A., et al. (2016). Effect of low-frequency deep brain stimulation on sensory thresholds in Parkinson's disease. *J. Neurosurg.* 126, 397–403. doi: 10.3171/2016.2.JNS152231

Birdno, M. J., and Grill, W. M. (2008). Mechanisms of deep brain stimulation in movement disorders as revealed by changes in stimulus frequency. *Neurotherapeutics* 5, 14–25. doi: 10.1016/j.nurt.2007.10.067

Bologna, M., Paparella, G., Fasano, A., Hallett, M., and Berardelli, A. (2020). Evolving concepts on bradykinesia. *Brain* 143, 727–750. doi: 10.1093/brain/awz344

Brittain, J.-S., and Brown, P. (2014). Oscillations and the basal ganglia: motor control and beyond. *Neuroimage* 85(Pt. 2), 637–647. doi: 10.1016/j.neuroimage.2013.05.084

Brocker, D. T., Swan, B. D., Turner, D. A., Gross, R. E., Tatter, S. B., Koop, M. M., et al. (2013). Improved efficacy of temporally non-regular deep brain stimulation in Parkinson's disease. *Exp. Neurol.* 239, 60–67. doi: 10.1016/j.expneurol.2012.09.008

Bronstein, J. M., Tagliati, M., Alterman, R. L., Lozano, A. M., Volkmann, J., Stefani, A., et al. (2011). Deep brain stimulation for Parkinson disease. *Arch. Neurol.* 68:165. doi: 10.1001/archneurol.2010.260

Brown, P., and Williams, D. (2005). Basal ganglia local field potential activity: character and functional significance in the human. *Clin. Neurophysiol.* 116, 2510–2519. doi: 10.1016/j.clinph.2005.05.009

Carlson, J. D., Cleary, D. R., Cetas, J. S., Heinricher, M. M., and Burchiel, K. J. (2010). Deep brain stimulation does not silence neurons in subthalamic nucleus in Parkinson's patients. *J. Neurophysiol.* 103, 962–967. doi: 10.1152/jn.00363.2009

Chiken, S., and Nambu, A. (2016). Mechanism of deep brain stimulation: inhibition, excitation, or disruption? *Neuroscience* 22, 313–322. doi: 10.1177/1073858415581986

Cristianini, N., and Shawe-Taylor, J. (2000). *An Introduction to Support Vector Machines and Other Kernel-based Learning Methods*. Cambridge: Cambridge University Press.

Csavoy, A., Molnar, G., and Denison, T. (2009). "Creating support circuits for the nervous system: considerations for 'brain-machine' interfacing," *in IEEE Symposium on VLSI Circuits* (Kyoto), 4–7.

Dorval, A. D., Kuncel, A. M., Birdno, M. J., Turner, D. A., and Grill, W. M. (2010). Deep brain stimulation alleviates parkinsonian bradykinesia by regularizing pallidal activity. *J. Neurophysiol.* 104, 911–921. doi: 10.1152/jn.00103.2010

Eusebio, A., Thevathasan, W., Doyle Gaynor, L., Pogosyan, A., Bye, E., Foltynie, T., et al. (2011). Deep brain stimulation can suppress pathological synchronisation in parkinsonian patients. *J. Neurol. Neurosurg. Psychiatry* 82, 569–573. doi: 10.1136/jnnp.2010.217489

Feng, G. (2006). A survey on analysis and design of model-based fuzzy control systems. *IEEE Trans. Fuzzy Syst.* 14, 676–697. doi: 10.1109/TFUZZ.2006.883415

Grant, P. F., and Lowery, M. M. (2013). Simulation of cortico-basal ganglia oscillations and their suppression by closed loop deep brain stimulation. *IEEE Trans. Neural Syst. Rehabil. Eng.* 21, 584–594. doi: 10.1109/TNSRE.2012.2202403

Hacker, M. L., Tonascia, J., Turchan, M., Currie, A., Heusinkveld, L., Konrad, P. E., et al. (2015). Deep brain stimulation may reduce the relative risk of clinically important worsening in early stage Parkinson's disease. *Parkinsonism Relat. Disord.* 21, 1177–1183. doi: 10.1016/j.parkreldis.2015.08.008

Heida, T., Wentink, E. C., and Marani, E. (2013). Power spectral density analysis of physiological, rest and action tremor in Parkinson's disease patients treated with deep brain stimulation. *J. Neuroeng. Rehabil.* 10:70. doi: 10.1186/1743-0003-10-70

Hell, F., Palleis, C., Mehrkens, J. H., Koeglsperger, T., and Bötzel, K. (2019). Deep brain stimulation programming 2.0: future perspectives for target identification and adaptive closed loop stimulation. *Front. Neurol.* 10:314. doi: 10.3389/fneur.2019.00314

Johnson, A. E., Ghassemi, M. M., Nemati, S., Niehaus, K. E., Clifton, D. A., and Clifford, G. D. (2016). Machine learning and decision support in critical care. *Proc. IEEE* 104, 444–466. doi: 10.1109/JPROC.2015.2501978

Kiss, Z. H., Mooney, D. M., Renaud, L., and Hu, B. (2002). Neuronal response to local electrical stimulation in rat thalamus: physiological implications for mechanisms of deep brain stimulation. *Neuroscience* 113, 137–143. doi: 10.1016/s0306-4522(02)00122-7

Kuncel, A. M., and Grill, W. M. (2004). Selection of stimulus parameters for deep brain stimulation. *Clin. Neurophysiol.* 115, 2431–2441. doi: 10.1016/j.clinph.2004.05.031

Little, S., Beudel, M., Zrinzo, L., Foltynie, T., Limousin, P., Hariz, M., et al. (2016). Bilateral adaptive deep brain stimulation is effective in Parkinson's disease. *J. Neurol. Neurosurg. Psychiatry*. 87, 717–721. doi: 10.1136/jnnp-2015-310972

Little, S., and Brown, P. (2012). What brain signals are suitable for feedback control of deep brain stimulation in Parkinson's disease? *Ann. N. Y. Acad. Sci.* 1, 9–24. doi: 10.1111/j.1749-6632.2012.06650.x

Little, S., Pogosyan, A., Kuhn, A. A., and Brown, P. (2012). β band stability over time correlates with Parkinsonian rigidity and bradykinesia. *Exp. Neurol.* 236, 383–388. doi: 10.1016/j.expneurol.2012.04.024

Little, S., Pogosyan, A., Neal, S., Zavala, B., Zrinzo, L., Hariz, M., et al. (2013). Adaptive deep brain stimulation in advanced Parkinson disease. *Ann. Neurol.* 74, 449–457. doi: 10.1002/ana.23951

Mohammed, A., and Demosthenous, A. (2018). Complementary detection for hardware efficient on-site monitoring of Parkinsonian progress. *IEEE J. Emerg. Sel. Top. Circuits Syst.* 8, 603–615. doi: 10.1109/JETCAS.2018.2830971

Mohammed, A., Zamani, M., Bayford, R., and Demosthenous, A. (2017). Toward on-demand deep brain stimulation using online Parkinson's disease prediction driven by dynamic detection. *IEEE Trans. Neural Syst. Rehabil. Eng.* 25, 2441–2452. doi: 10.1109/TNSRE.2017.2722986

Moreau, C., Defebvre, L., Destée, A., Bleuse, S., Clement, F., Blatt, J. L., et al. (2008). STN-DBS frequency effects on freezing of gait in advanced Parkinson disease. *Neurology* 71, 80–84. doi: 10.1212/01.wnl.0000303972.16279.46

Moro, E., Esselink, R. J., Xie, J., Hommel, M., Benabid, A. L., and Pollak, P. (2002). The impact on Parkinson's disease of electrical parameter settings in STN stimulation. *Neurology* 59, 706–713. doi: 10.1212/wnl.59.5.706

Passino, K., and Yurkovich, S. (1998). *Fuzzy Control,* 1st Edn. Boston, MA: Addison Wesley Publishing Company.

Picillo, M., Lozano, A. M., Kou, N., Puppi Munhoz, R., and Fasano, A. (2016). Programming deep brain stimulation for parkinson's disease: the Toronto western hospital algorithms. *Brain Stimul.* 9, 425–437. doi: 10.1016/j.brs.2016.02.004

Prandoni, P., and Vetterli, M. (2008). *Signal Processing for Communications,* 1t Edn. Boca Raton, FL: CRC Press.

Priori, A., Foffani, G., Rossi, L., and Marceglia, S. (2012). Adaptive deep brain stimulation (aDBS) controlled by local field potential oscillations. *Exp. Neurol.* 245, 77–86. doi: 10.1016/j.expneurol.2012.09.013

Rossow, A. B., Salles, E. O. T., and Coco, K. F. (2011). "Automatic sleep staging using a single-channel EEG modeling by Kalman filter and HMM," in *ISSNIP Biosignals and Biorobotics Conference* (Vitoria), 1–6.

Sajda, P. (2006). Machine learning for detection and diagnosis of disease. *Annu. Rev. Biomed. Eng.* 8, 537–565. doi: 10.1146/annurev.bioeng.8.061505.095802

Soltesz, K., Hahn, J. O., Hägglund, T., Dumont, G. A., and Ansermino, J. (2013). Individualized closed-loop control of propofol anesthesia: a preliminary study. *Biomed. Signal Process. Control.* 8, 500–508. doi: 10.1016/j.bspc.2013.04.005

Su, D., Chen, H., Hu, W., Liu, Y., Wang, Z., Wang, X., et al. (2018). Frequency-dependent effects of subthalamic deep brain stimulation on motor symptoms in Parkinson's disease: a meta-analysis of controlled trials. *Sci. Rep.* 8, 1–9. doi: 10.1038/s41598-018-32161-3

Vercruysse, S., Vandenberghe, W., Münks, L., Nuttin, B., Devos, H., and Nieuwboer, A. (2014). Effects of deep brain stimulation of the subthalamic nucleus on freezing of gait in Parkinson's disease: a prospective controlled study. *J. Neurol. Neurosurg. Psychiatry* 85, 871–877. doi: 10.1136/jnnp-2013-306336

Whitmer, D., de Solages, C., Hill, B., Yu, H., Henderson, J. M., and Bronte-Stewart, H. (2012). High frequency deep brain stimulation attenuates subthalamic and cortical rhythms in Parkinson's disease. *Front. Hum. Neurosci.* 6:155. doi: 10.3389/fnhum.2012.00155

Wu, D., Lance, B. J., and Lawhern, V. J. (2017). Guest editorial for the special section on brain computer interface (BCI). *IEEE Trans. Fuzzy Syst.* 25, 1–2. doi: 10.1109/TFUZZ.2017.2652799

Xie, T., Kang, U. J., and Warnke, P. (2012). Effect of stimulation frequency on immediate freezing of gait in newly activated STN DBS in Parkinson's disease. *J. Neurol. Neurosurg. Psychiatry* 83, 1015–1017. doi: 10.1136/jnnp-2011-302091

Zarkogianni, K., Vazeou, A., Mougiakakou, S. G., Prountzou, A., and Nikita, K. S. (2011). An insulin infusion advisory system based on autotuning nonlinear model-predictive control. *IEEE Trans. Biomed. Eng.* 58, 2467–2477. doi: 10.1109/TBME.2011.2157823

Zavitsanou, S., Chakrabarty, A., Dassau, E., and Doyle, F. (2016). Embedded control in wearable medical devices: application to the artificial pancreas. *Processes* 4:35. doi: 10.3390/pr40 40035

Conflict of Interest: The authors declare that the research was conducted in the absence of any commercial or financial relationships that could be construed as a potential conflict of interest.

frontiers in Neuroscience

ORIGINAL RESEARCH
published: 18 June 2020
doi: 10.3389/fnins.2020.00534

Evoking Apparent Moving Sensation in the Hand via Transcutaneous Electrical Nerve Stimulation

Alessia Scarpelli, Andrea Demofonti, Francesca Terracina, Anna Lisa Ciancio and Loredana Zollo*

Research Unit of Advanced Robotics and Human-Centred Technologies, Università Campus Bio-Medico di Roma, Rome, Italy

The restoration of sensory feedback in amputees plays a fundamental role in the prosthesis control and in the communication on the afferent channel between hand and brain. The literature shows that transcutaneous electrical nerve stimulation (TENS) can be a promising non-invasive technique to elicit sensory feedback in amputees, especially in the lower limb through the phenomenon of apparent moving sensation (AMS). It consists of delivering a sensation that moves along a specific part of the body. This study proposes to use TENS to elicit tactile sensations and adopt AMS to reproduce moving sensations on the hand, such as those related to an object moving in the hand or slipping upward or downward. To this purpose, the developed experimental protocol consists of two phases: (i) the mapping of the evoked sensations and (ii) the generation of the AMS. In the latter phase, the pulse amplitude variation (PAV), the pulse width variation (PWV), and the interstimulus delay modulation (ISDM) methods were compared. For the comparative analysis, the Wilcoxon–Mann–Whitney test with Bonferroni correction ($P < 0.016$) was carried out on the success rate and on the ranking of methods expressed by the subjects. Results from the mapping protocol show that the delivered sensations were mostly described by the subjects as almost natural and superficial tingling. Results from the AMS protocol show that, for each movement direction, the success rate of ISDM method is higher than that of PWV and PAV and significantly higher than that of PAV for the ulnar-median direction. It recreates an AMS in the hand that effectively allows discriminating the type of sensation and distinguishing the movement direction. Moreover, ISDM was ranked by the subjects as the favorite method for recreating a well-defined and comfortable moving sensation only in the median-ulnar direction. For the ranking results, there was not a statistically significant difference among the methods. The experiments confirmed the good potential of recreating an AMS in the hand through TENS. This encourages to push forward this study on amputees and integrate it in the closed-loop control of a prosthetic system, in order to enable full control of grasp stability and prevent the objects from slippage.

Keywords: sensory feedback restoration, transcutaneous electrical nerve stimulation, apparent moving sensation, upper limb prostheses, slippage

OPEN ACCESS

Edited by:
Nitish V. Thakor, Johns Hopkins School of Medicine, United States

Reviewed by:
J. Luis Lujan, Mayo Clinic College of Medicine and Science, United States
Connor Glass, Johns Hopkins Medicine, United States

****Correspondence:***
Alessia Scarpelli
a.scarpelli@unicampus.it

Specialty section:
This article was submitted to Neural Technology, a section of the journal Frontiers in Neuroscience

Received: *20 December 2019*
Accepted: *30 April 2020*
Published: *18 June 2020*

Citation:
Scarpelli A, Demofonti A, Terracina F, Ciancio AL and Zollo L (2020) Evoking Apparent Moving Sensation in the Hand via Transcutaneous Electrical Nerve Stimulation. Front. Neurosci. 14:534. doi: 10.3389/fnins.2020.00534

INTRODUCTION

Upper limb loss is a traumatic event for a human being from a functional and social viewpoint (Ciancio et al., 2016; Cordella et al., 2016). Upper limb prostheses want to replace in the amputee the lost functions and contribute to improve people quality of life. Commercially available hand prostheses use, for hand grasping, an open loop control strategy that does not involve the user in the control loop of the device. Despite that current open loop control strategies have shown good results (Cordella et al., 2014), the amputee can only rely on visual feedback, and this increases the cognitive efforts due to the lack of sensory feedback during manipulation tasks.

For that reason, new approaches aim to insert the user in the control loop of robotic system for upper limb rehabilitation and for prosthetic application. These techniques would lead to monitor the user state and accordingly change the robot behavior (Papaleo et al., 2013). Closed-loop devices for prosthetic application overcome open-loop device limitations: they can improve the performance of the tasks, guarantee a better usability, and a higher embodiment (Wright et al., 2016). Current studies aim to restore the bidirectional communication between the nervous system and the user through closed-loop devices, in order to improve the performance of the motor control and include the user in the loop through the restoration of sensory feedback (Antfolk et al., 2013; Ciancio et al., 2016; Cordella et al., 2016; D'Anna et al., 2017).

It has been demonstrated that invasive interfaces with peripheral nervous system (PNS) [which require surgery to be implanted (Navarro et al., 2005)] are an efficient method to restore a bidirectional communication between the user and the prostheses (Antfolk et al., 2013). Although they allow obtaining promising results, such as the selectivity of the elicited sensation, the discrimination of the hand areas, and the possibility to restore an artificial sensation similar to the real one, they present some disadvantages related to invasiveness, such as the surgery, the fibrotic reaction, and the weak long-term stability of the implant feedback (Raspopovic et al., 2014; Tan et al., 2014; Oddo et al., 2016; D'Anna et al., 2019; George et al., 2019; Zollo et al., 2019).

Different types of non-invasive interfaces have been tested in several studies to close the patient in the prosthesis control loop, e.g., vibrotactile (Cipriani et al., 2011), mechanical (Kim and Colgate, 2012), auditory (Gonzalez et al., 2012), or electrical interfaces. However, they have many drawbacks related to a high cognitive burden that also leads to increase in the response time, a low selectivity in the recognition of the elicited sensation, a low discrimination capabilities of hand areas, a very unnatural sensation, and a long phase of training (Kaczmarek et al., 1991; D'Anna et al., 2017).

Evidence suggests that transcutaneous electrical nerve stimulation (TENS) can be a promising technique as non-invasive closed-loop interface (Johnson and Bjordal, 2011; Chai et al., 2015). TENS uses superficial electrodes placed on the skin to electrically stimulating the PNS and evoke tactile sensation (Chai et al., 2015).

The literature shows that TENS can reduce painful conditions (Johnson and Bjordal, 2011), phantom pain, and stump pain caused by amputation (Johnson et al., 2015). It has also been demonstrated that electrocutaneous stimulation of the median and ulnar nerve can enable the closed-loop control of a prosthesis (Antfolk et al., 2013) and deliver touch and pain sensations (Osborn et al., 2018). This method is safe; it has low energy consumption and high response rate compared to other techniques (Antfolk et al., 2013; D'Anna et al., 2017; Osborn et al., 2017; Vargas et al., 2019).

Recently, a novel feedback principle has been introduced, named apparent moving sensation (AMS). It consists of delivering a sensation that moves along a specific part of the body. The AMS exploits a psychological phenomenon called *tactile phi phenomenon*, which describes a phantom sensation between two stimuli that are simultaneously presented in adjacent locations on the human skin (Pfeifer et al., 2010; Lauretti et al., 2017). If the intensities of the two stimuli are the same, the phantom sensation is felt in the midpoint between their locations. On the other hand, if the two stimuli have different intensities, the phantom sensation is felt around the location of the stimulus with the higher intensity. Therefore, properly modulating the two intensities, the sensation can be moved between the two stimuli locations (Lauretti et al., 2017). In the literature, AMS was applied through TENS to lower limb to make amputees realize how the position of the center of pressure (CoP) changes during gait (Rahal et al., 2009; Pfeifer et al., 2010; Seps et al., 2011; Pagel et al., 2016).

This study considers the aforementioned advantages of non-invasive techniques and focuses on the application of TENS to upper limb amputees in order to elicit tactile sensations in the hand. TENS technique enables a closed-loop control of the prosthesis.

In this study, TENS is aimed to elicit tactile sensations in well-defined hand areas and adopt AMS on the hand in order to reproduce moving tactile sensations on different areas of the hand. This strategy can provide the user with force information when grasping objects and also moving sensations (such as slippage) during object manipulation. To this purpose, an experimental validation has been carried out on nine healthy subjects. The experimental protocol consists of two phases: (i) the mapping of the evoked sensations and (ii) the generation of the AMS on the subjects' hands. In the latter phase, the pulse amplitude variation (PAV), the pulse width variation (PWV), and the interstimulus delay modulation (ISDM) have been compared.

The paper is organized as follows. *Materials and Methods* describes the experimental setup, mapping protocol, and AMS strategy. *Results* reports results of the experimental session. Finally, *Discussion* discuss the results and draws the conclusions.

MATERIALS AND METHODS

Experimental Setup

Nine healthy subjects (four males and five females) with a mean age of 25.2 $\pm$ 3.1 years were recruited for the study. All subjects had no known neurological disorders and no previous experiences with TENS. The study was authorized by the Ethic

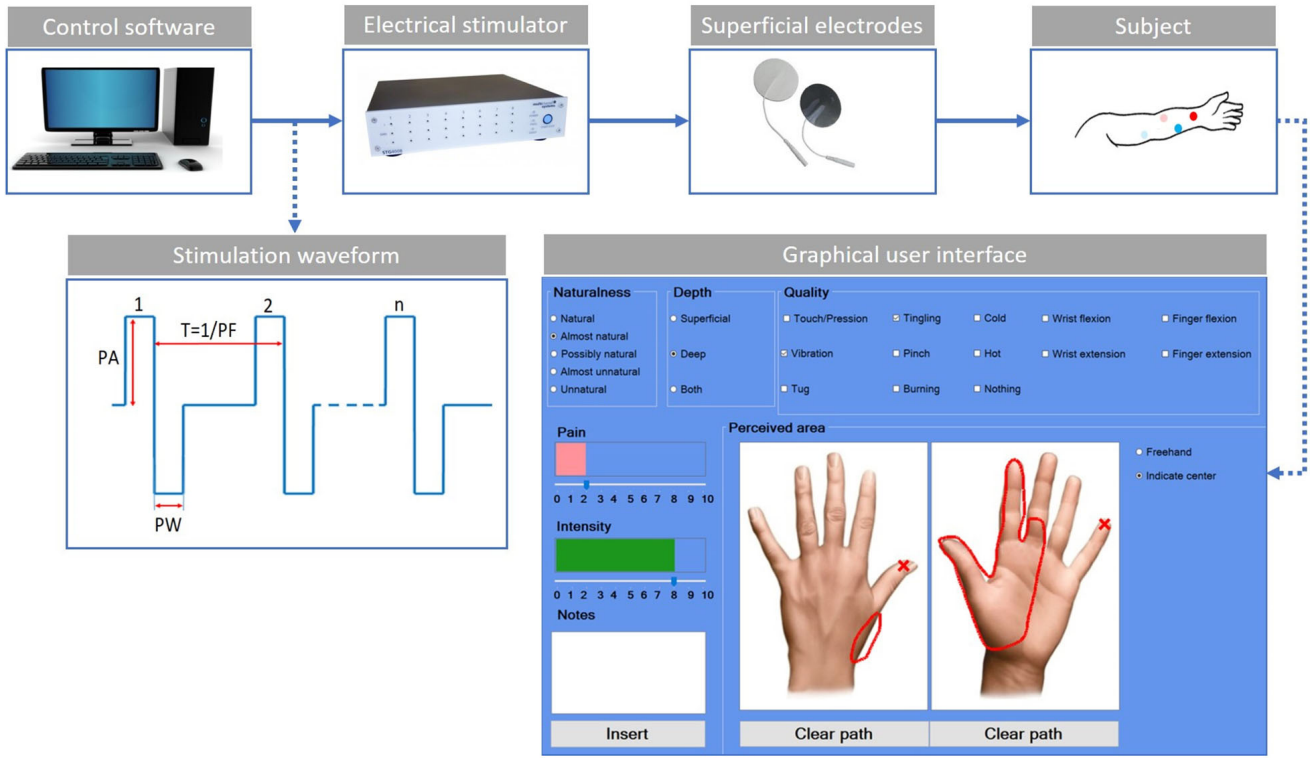

FIGURE 1 | Scheme of the experimental setup. The control software sends the features of the stimulation waveform to the electrical stimulator. The stimulation waveform used in the study is the symmetric biphasic square wave, whose parameters are the pulse amplitude (PA), the pulse width (PW), and the pulse frequency (PF). The current is applied through the use of superficial electrodes to the user's skin. The red dots indicate the electrodes for the median stimulation, while the blue ones are for the ulnar stimulation. The light color is used for the active electrodes and the shaded color for the passive electrodes. The custom-developed graphic user interface is used by the subjects to indicate the main characteristics of the evoked sensations.

Committee of Campus Bio-Medico University of Rome in accordance with the Helsinki Declaration; the main aspects of the study were explained to the subjects, and they signed an informed consent.

The used experimental setup (**Figure 1**) was composed of an electric stimulator, a proprietary control software of the stimulator, four superficial electrodes, and a graphic user interface.

The electrical stimuli were delivered by the multichannel fully programmable stimulator (STG4008, Multichannel System MCS GmbH, Reutlingen, Germany). It has eight independent channels and allows stimulating more than one site simultaneously and independently. The proprietary software (MC_Stimulus II) of the stimulator allows generating arbitrary waveforms for each channel.

The subject sat in a chair in a comfortable position with his/her left arm placed on a table; then, the targeted skin area was cleaned with alcohol. Four commercial autoadhesive, circular, and superficial electrodes (TensCare) with a diameter of 25 mm were applied on the subject's epidermidis and were used to selectively stimulate the subject nerves.

Finally, a custom-developed graphic user interface implemented in C# was used to record the main features of the elicited sensations (**Figure 1**). For each trial, the subject was asked to indicate the naturalness, the depth, the quality of the intensity, and the pain of the sensation. The naturalness of the sensation was assessed using a five-point scale, in which the lowest value means that the subject felt an unnatural sensation and the highest a natural one. Between these two values, other three options have been considered (Flesher et al., 2016; Kim et al., 2018; Petrini et al., 2019; Zollo et al., 2019). Therefore, the naturalness was assessed using the following options: natural, almost natural, possibly natural, almost unnatural, and unnatural. The depth was assessed choosing between superficial, deep, or both. The quality was assessed using the following choices: touch/pression, vibration, tug, tingling, pinch, burning, cold, hot, wrist flexion, wrist extension, finger flexion, finger extension, and nothing. The intensity and/or the pain of the sensation were reported in a scale from 0 to 10. The subject had to indicate the location of the sensation using two pictures representing the dorsal and palmar side of the hand (**Figure 1**).

The symmetric biphasic square wave was found to be the most used since it was shown to be able to elicit a more comfortable sensation among the others (Chai et al., 2015; D'Anna et al., 2017; Li et al., 2018; Shin et al., 2018; Vargas et al., 2019). The stimulation parameters taken into account are shown in **Figure 1**: pulse amplitude (PA), pulse width (PW), and pulse frequency (PF). No interphase delay (ID) has been used.

The experimental setup in **Figure 1** was used both for mapping and AMS protocol.

Mapping of the Elicited Sensations

The mapping protocol (**Figure 2A**) was composed of four phases: the electrodes positioning, the median nerve, the ulnar nerve, and the concurrent stimulation phases. In the concurrent phase, both nerves were stimulated simultaneously. Each stimulation phase included charge modulation and frequency modulation. For each trial, the subject had to report the characteristic of the sensation in the graphic interface shown in **Figure 1**. At the end of each phase, the specific reported characteristics of the evoked sensation were used to set the stimulation parameters for the successive phase.

The first part of the mapping protocol was aimed to identify the optimal position for the two pairs of electrodes. They had to be positioned upon the skin along the superficial path of the median and ulnar nerves in order to stimulate the underlying nerve and elicit a sensation in the areas of hand and fingers innervated by those nerves. The optimal positioning was identified by varying the location of each pair of electrodes. During the three phases of median, ulnar, and both nerves stimulation, the PW and PF parameters were modulated, and the perceived sensations were recorded.

The minimum and maximum values of pulse amplitude of both nerves were defined using the following stimulation parameter: the PW and the PF were fixed, respectively, to 500/600 μs and 500/600 Hz for the median/ulnar nerves, whereas the PA was incremented from 1 mA with a step of 0.1 mA. PA_{min} is the first value of PA at which the subject reported a sensation on the hand; PA_{max} is the value of PA below the motor threshold at which the subject reported a well-defined and conformable sensation. The stimulation duration was settled to 0.5 s.

In the median nerve stimulation phase, during the charge modulation, the PF was fixed at 150 Hz, and the PW was varied in the range of 100–500 μs with a step of 40 μs. At the end of the charge modulation, PW_m and PW_{m0} were selected. PW_m is a value of PW at which the reported sensation intensity was at least 3, and PW_{m0} is the last value of PW at which the reported sensation intensity was 0.

During the frequency modulation, the PW was settled to PW_m, and the PF of the stimulus varied in the range of 50–500 Hz with a step of 50 Hz from 50 to 200 Hz and a step of 100 Hz from 200 to 500 Hz. At the end of the frequency modulation, PF_m and PF_{m0} were selected. PF_m is a value of PF at which the reported sensation intensity is at least 3, and PF_{m0} is the last value of PF at which the reported sensation intensity is 0.

In the ulnar nerve stimulation phase, during the charge modulation, the PF was fixed at 150 Hz, and the PW was varied in the range of 300–600 μs with a step of 40 μs. PW_u and PW_{u0} were selected in the same way as described for the charge modulation of median stimulation phase. During the frequency modulation, the PW was PW_u and the PF of the stimulus varied from 50 to 600 Hz with analogous median nerve stimulation steps. At the end of this section, PF_u and PF_{u0} were selected in the same way as described for the frequency modulation of median nerve stimulation phase.

For the last phase of the mapping protocol, the stimuli parameters should have to be settled for applying the concurrent stimulation. In the charge modulation, the PF was fixed at 150 Hz and the PW varied from PW_{m0} to 500 μs for the median nerve, whereas PW varied from PW_{u0} to 600 μs for the ulnar nerve. At the end of the charge modulation, PW_{mc} and PW_{uc} were selected as the two values of PW for, respectively, the median and ulnar nerve at which the reported sensation intensities are at least 3. In the frequency modulation, the PW were fixed at PW_{mc} and PW_{uc}, respectively, for the median and ulnar stimuli, and PF varied in the frequency ranges of median and ulnar nerves.

For all the three stimulation phases, the maximum pulse amplitude and the stimulus duration (0.5 s) was kept constant during both modulation phases.

A correlation analysis was conducted for the results obtained during the charge and frequency modulation of the mapping protocol. For the charge modulation, the correlation and the linear regression between data of the injected charge to the subjects and the referred intensities reported by the subjects were studied. For the frequency modulation, the correlation and the linear regression between the PF of the stimulus and the referred intensities reported by the subjects were studied.

AMS Strategy

The AMS strategy recreates an apparent movement sensation in the hand of the subject that moves from the fingers innervated by the median nerve to the ones innervated by the ulnar nerve and reverse. AMS is based on the psychological phenomenon called *tactile phi phenomenon*; thus, properly modulating the two stimuli intensities could recreate a slippage sensation. The slippage sensation was delivered by an AMS that flows along the fingers. AMS can be generated by means of three different methods: PAV (Izumi et al., 1988; Rahal et al., 2009), PWV (Pfeifer et al., 2010; Arieta et al., 2011; Seps et al., 2011), and interstimulus delay modulation (ISDM) methods, applied to median, ulnar, and concurrent stimulation phases (**Figure 2B**).

In the median and ulnar stimulation, the type of sensation elicited on the hand of the subjects was investigated for two different time durations (0.5 and 1 s). In the concurrent stimulation phase, a comparison between the PAV and PWV methods in median–ulnar (MU) and ulnar–median (UM) directions in the two different time durations (0.5 and 1 s) was carried out. Moreover, the three methods were further investigated to recreate the AMS on the whole hand, and their effects were compared.

In the PAV method, the pulse amplitude of each subject was modulated in five steps, from PA_{max} to PA_{min}, identified by the subject for each nerve in the mapping protocol. The PW and the PF were kept constant at PW_m/ PW_u for the median/ulnar nerve and at PF_m/PF_u for the median/ulnar nerve.

The PWV method consisted in modulating the pulse width in five steps from PW_m/PW_u to PW_{min} of the median and ulnar nerve. This last value was identified stimulating the subject with PA_{max}, PF_m/PF_u and decreasing PW from PW_m/PW_u with a step of 20 μ s.

The ISDM concerned the modulation of the delay between the two signals sent to the two nerves, keeping constant the PA_{max},

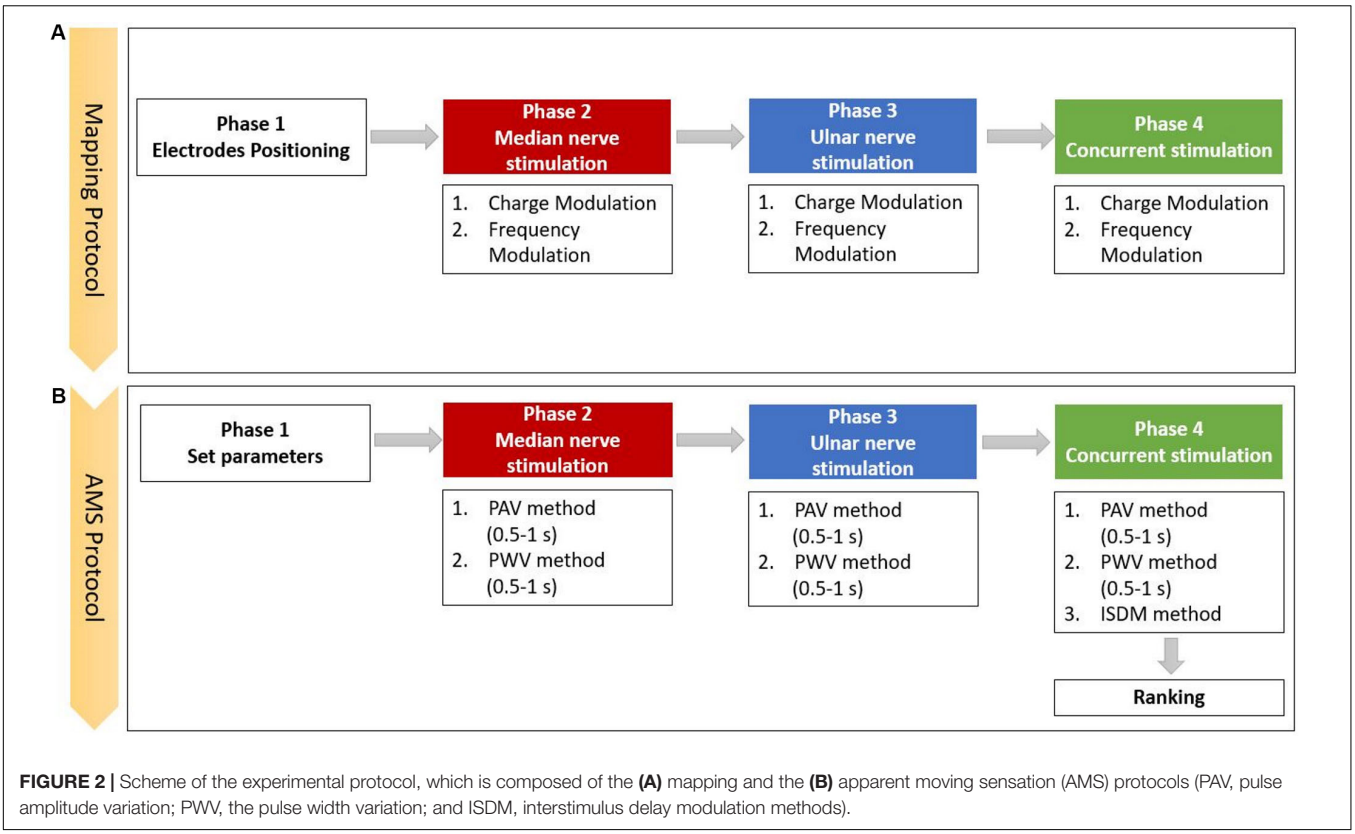

FIGURE 2 | Scheme of the experimental protocol, which is composed of the **(A)** mapping and the **(B)** apparent moving sensation (AMS) protocols (PAV, pulse amplitude variation; PWV, the pulse width variation; and ISDM, interstimulus delay modulation methods).

the PW_m/PW_u, and the PF_m/PF_u. The delay was varied in the range of 0–0.5 s with a step of 0.1 s.

During the concurrent stimulation, in order to generate the AMS from the median region of the hand to the ulnar one with the PAV and PWV methods, a signal with decreasing PA or PW was sent to the median nerve, and one with increasing PA or PW was sent to the ulnar nerve. The signals sent to the nerves were inverted to recreate the AMS in the opposite direction. Applying the ISDM method, the movement of the sensation in the median–ulnar direction was recreated by delaying the ulnar signal; for the opposite direction, the median signal was delayed.

For the single nerve stimulation phases, the subject reported the elicited sensation and indicated the preference between the PAV and PWV methods for each direction.

In the concurrent stimulation, the subject was asked to describe the perceived sensation and indicate the perceived movement direction. A success rate (SR) was introduced in order to evaluate if the subject was able to correctly discriminate the movement direction on the hand. The SR was defined as the number of times the subjects discriminate the movement direction out of the all trials for each movement direction. Moreover, for each trial, the subject was asked to classify the three methods resembling the ranking of preference among them.

Two different statistical significance analyses were conducted: one on the success rate and the other one on the ranking preference of the three methods through the application of the Wilcoxon–Mann–Whitney test with Bonferroni correction (level of significance of $P < 0.016$).

RESULTS

Mapping Protocol

The maximum current amplitude delivered to the participants was specific for each subject; the mean value ± SD among the subjects is 2.9 ± 0.7 mA for the median nerve and 2.6 ± 1.0 mA for the ulnar nerve.

The referred sensations in the hand were indicated by the subjects on a map representing the dorsal and palmar side of the hand on the graphic user interface. The regions indicated by the nine subjects were overlapped in order to obtain a single picture indicating the mean region reported by the subjects for three different level of the stimulus intensity. The elicited regions experienced during the charge and frequency modulation of the median, ulnar, and concurrent stimulations are represented in **Figure 3**. It is worth noticing that, as expected from the literature (D'Anna et al., 2017, 2019; Vargas et al., 2019), the median and the ulnar stimulation elicited, respectively, the regions of the hand innerved by the median and the ulnar nerve, and the concurrent stimulation was able to elicit sensations almost on the whole hand. The areas depicted with a more vivid color indicate the regions reported with a higher number of occurrences than the others.

The extension of the elicited region proportionally increased with the stimulus intensity due to the increase in PW and PF in the charge and frequency modulation. Moreover, the regions reported during the median and ulnar stimulation almost summed up during the concurrent stimulation; these results

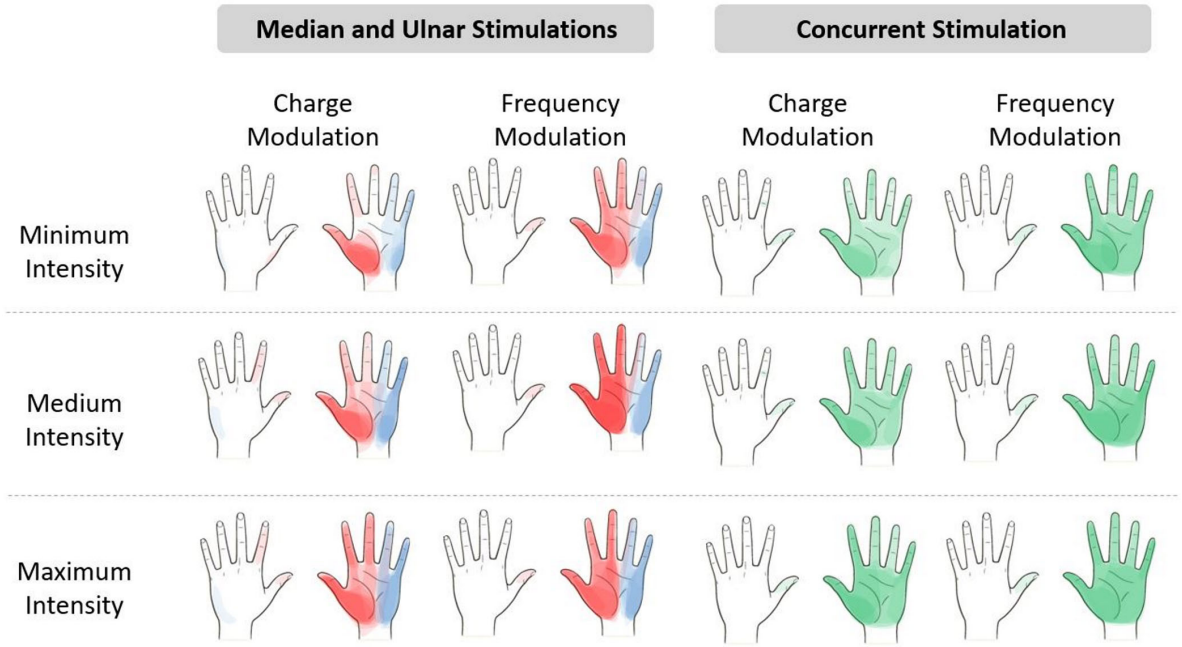

FIGURE 3 | Regions reported by the subjects after the median (red), ulnar (blue), and concurrent (green) stimulations. The regions indicated by the nine subjects have been overlapped in a hand map, which is divided into minimum, medium, and maximum intensity of the electrical stimuli. The areas depicted with a more vivid color indicate the regions with a higher number of occurrences than the others more reported by the subjects. The levels of intensity are the range of values of pulse width (PW) and pulse frequency (PF) provided during the stimuli. Minimum intensity for the median nerve is PW = [220;300] μs and PF = [50;100] Hz and for the ulnar nerve is PW = [380;420] μs and PF = [50;100] Hz. Medium intensity for the median nerve is PW = [340;420] μs and PF = [150;300] Hz and for the ulnar nerve is PW = [460;500] μs and PF = [150;300] Hz. Maximum intensity for the median nerve is PW = [460;500] μs and PF = [400;500] Hz and for the ulnar nerve is PW = [540;580] μs and PF = [400;600] Hz.

confirmed the ones obtained in the literature (D'Anna et al., 2017; Vargas et al., 2019).

Tables 1–**3** show the naturalness, the depth, the pain, and the quality of the sensation of each trial of the mapping protocol for the median, ulnar, and concurrent stimulation for both charge and frequency modulation.

The naturalness of the sensations during the charge modulation of the three stimulation phases was generally perceived natural or almost natural (49% of the trials where the subjects reported a sensation), possibly natural (23%), and almost unnatural and unnatural (28%). During the frequency modulation, the sensations were perceived natural or almost natural for the 46%, possibly natural for the 24%, and almost unnatural and unnatural for the 30%.

Single and concurrent nerve stimulation, during charge and frequency modulation, evoked mostly superficial and painless sensations. However, some subjects reported to feel pain, assigning a value of 1, 2, or 3, especially for the frequency modulation of the ulnar and concurrent stimulations. Nevertheless, only 9% of the total stimulation trials delivered to the subjects produced a pain sensation. In general, the pain was described by the subjects as annoying sensations on the hand or on the forearm.

When the first three stimuli of PW (100, 140, and 180 μs) were applied during the charge modulation of the median nerve, all the subjects reported not to feel any sensations on the hand; the same happened for the first two value of PW (300 and 340 μs) for the ulnar nerve. In **Tables 1**, **2** and for the other results of the paper, these stimuli were not reported from the total amount of charge modulation trials.

During the charge modulation, 21% of the total number of trials of the median stimulation (72) did not elicit any sensation on the subjects, 19% of the total number of trials of the ulnar stimulation (54), and 15% of the total number of trials of the concurrent stimulation (59). In the remaining trials, the subjects reported a sensation of tingling, vibration, and a combination of them (tingling and vibration). These three sensations were prevalent with respect to the others: they were reported with a percentage of 78, 80, and 83%, respectively, for the median, ulnar, and concurrent stimulations.

Moreover, during frequency modulation, 3% of the total number of trials of the median stimulation (63) did not elicit any sensation on the subjects, 4% of the total number of trials of the ulnar stimulation (72), and 2% of the total number of trials of the concurrent stimulation (65). As it can be seen, the number of times when the subjects did not report any sensation during the frequency modulation is less than the charge one. In the remaining trials, the subjects reported a sensation of tingling, vibration, and a combination of them (tingling and vibration). These resulted in the main qualities reported by the subjects with a percentage of 92, 94, and 91%, respectively, for the median, ulnar, and concurrent stimulations.

TABLE 1 | Characteristics of the elicited sensations for the charge modulation and frequency modulation of the median nerve stimulation.

Charge modulation							
Naturalness (57)		**Depth (57)**		**Pain (57)**		**Quality (72)**	
Natural	21	Superficial	42	0 (No pain)	57	Nothing	15
Almost natural	16	Deep	2	1,2,3	0	Tingling	43
Possibly natural	1	Both	13	4,5,6	0	Vibration	7
Almost unnatural	5			7,8,9	0	Tingling and vibration	6
Unnatural	14			10 (Most pain)	0	Others	1
Frequency modulation							
Naturalness (61)		**Depth (61)**		**Pain (61)**		**Quality (63)**	
Natural	12	Superficial	40	0 (No pain)	56	Nothing	2
Almost natural	20	Deep	10	1,2,3	5	Tingling	10
Possibly natural	17	Both	11	4,5,6	0	Vibration	19
Almost unnatural	8			7,8,9	0	Tingling and vibration	29
Unnatural	4			10 (Most pain)	0	Others	3

The total number of trials for the charge modulation (72) and the frequency modulation (63) in naturalness, depth, and pain differ from that of quality because the participant did not always feel a sensation in response to stimulus.

TABLE 2 | Characteristics of the elicited sensations for the charge modulation and frequency modulation of the ulnar nerve stimulation.

Charge modulation							
Naturalness (44)		**Depth (44)**		**Pain (44)**		**Quality (54)**	
Natural	12	Superficial	32	0 (No pain)	38	Nothing	10
Almost natural	8	Deep	11	1,2,3	6	Tingling	27
Possibly natural	8	Both	1	4,5,6	0	Vibration	3
Almost unnatural	4			7,8,9	0	Tingling and vibration	13
Unnatural	12			10 (Most pain)	0	Others	1
Frequency modulation							
Naturalness (69)		**Depth (69)**		**Pain (69)**		**Quality (72)**	
Natural	6	Superficial	48	0 (No pain)	59	Nothing	3
Almost natural	27	Deep	11	1,2,3	10	Tingling	8
Possibly natural	15	Both	10	4,5,6	0	Vibration	23
Almost unnatural	7			7,8,9	0	Tingling and vibration	37
Unnatural	14			10 (Most pain)	0	Others	1

The total numbers of trials for the charge modulation (54) and the frequency modulation (72) in naturalness, depth, and pain differ from that of quality because the participant did not always provide a sensation in response to stimulus.

The relation between the quality of the referred sensation and the injected charge was analyzed. **Figure 4** shows this relation for the median, ulnar, and concurrent stimulations. The thresholds of the qualities of the elicited sensations are shown when the injected charge was modulated. It seems to have a slight increase in the strength of the sensation when there is a higher quantity of charge. The first type of quality perceived by the subjects was the tingling, and it occurred when 2, 2.7, and 4 μC was applied on the skin for the median, ulnar, and concurrent stimulations, respectively.

The correlation between the median value of the injected charge in the subjects was analyzed during the three stimulation and the correspondence referred intensities. They have a moderate correlation for the median nerve ($\rho = 0.5798$, Pearson coefficient) and a weak one for the ulnar nerve ($\rho = 0.3205$, Pearson coefficient) and for the concurrent stimulation ($\rho = 0.3813$, Pearson coefficient). Then, a linear regression was conducted on the three data set in order to determine the coefficients of determination (R^2). In **Figure 5**, the linear regressions are represented: for the median nerve, $R^2 = 0.62$; for the ulnar nerve and for the concurrent stimulation, $R^2 = 0.24$ and $R^2 = 0.34$, respectively.

Moreover, it is relevant that the charge needed to stimulate the ulnar nerve and both nerves simultaneously, with equal reported sensation intensity, was higher with respect to the median nerve (**Figure 5**). The ulnar nerve could be anatomically located more in depth in the segment of the forearm where the superficial electrodes were placed; thus, more charge was needed to obtain the same type and intensity of sensation elicited on the areas innervated by the median nerve. During concurrent stimulation,

TABLE 3 | Characteristics of the elicited sensations for the charge modulation and frequency modulation of the concurrent stimulation.

Charge modulation							
Naturalness (50)		**Depth (50)**		**Pain (50)**		**Quality (59)**	
Natural	11	Superficial	43	0 (No pain)	45	Nothing	9
Almost natural	19	Deep	2	1,2,3	5	Tingling	23
Possibly natural	5	Both	5	4,5,6	0	Vibration	1
Almost unnatural	7			7,8,9	0	Tingling and vibration	25
Unnatural	8			10 (Most pain)	0	Others	1
Frequency modulation							
Naturalness (64)		**Depth (64)**		**Pain (64)**		**Quality (65)**	
Natural	15	Superficial	48	0 (No pain)	56	Nothing	1
Almost natural	9	Deep	8	1,2,3	8	Tingling	3
Possibly natural	15	Both	8	4,5,6	0	Vibration	12
Almost unnatural	13			7,8,9	0	Tingling and vibration	44
Unnatural	12			10 (Most pain)	0	Others	5

The total number of trials for the charge modulation (59) and the frequency modulation (65) in naturalness, depth, and pain differ from that of quality because the participant did not always provide a sensation in response to stimulus.

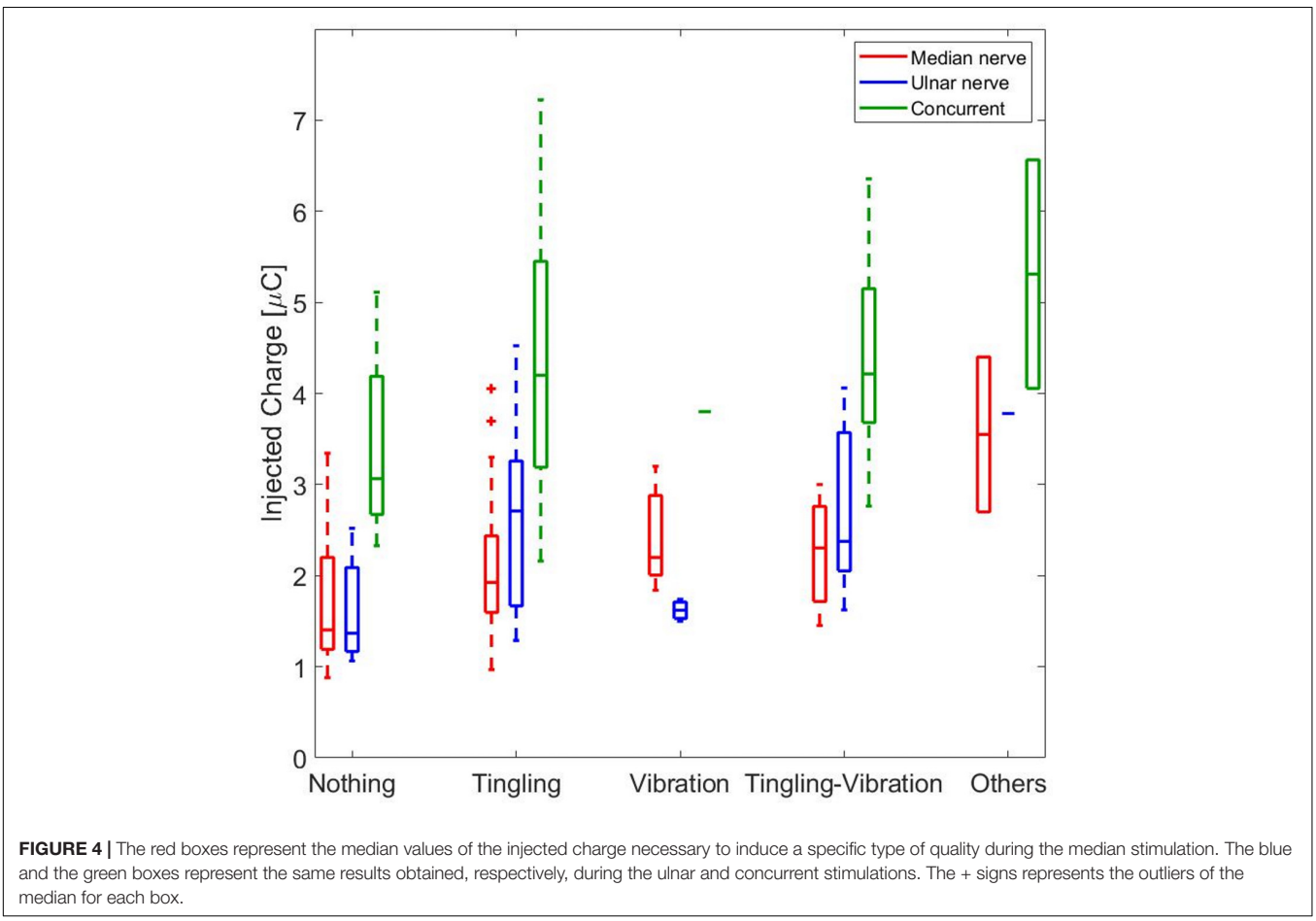

FIGURE 4 | The red boxes represent the median values of the injected charge necessary to induce a specific type of quality during the median stimulation. The blue and the green boxes represent the same results obtained, respectively, during the ulnar and concurrent stimulations. The + signs represents the outliers of the median for each box.

highest values of charge were injected because the sum of the injected charge of the two single nerves was delivered.

For each PF, the median values of the referred intensities reported by the subjects during the frequency modulation were calculated. The correlation between the PF of the stimulus and the referred intensities for the median and the ulnar stimulations was studied. The correlation between PF and referred intensities is moderate for both the median and the ulnar nerve ($\rho = 0.6771$

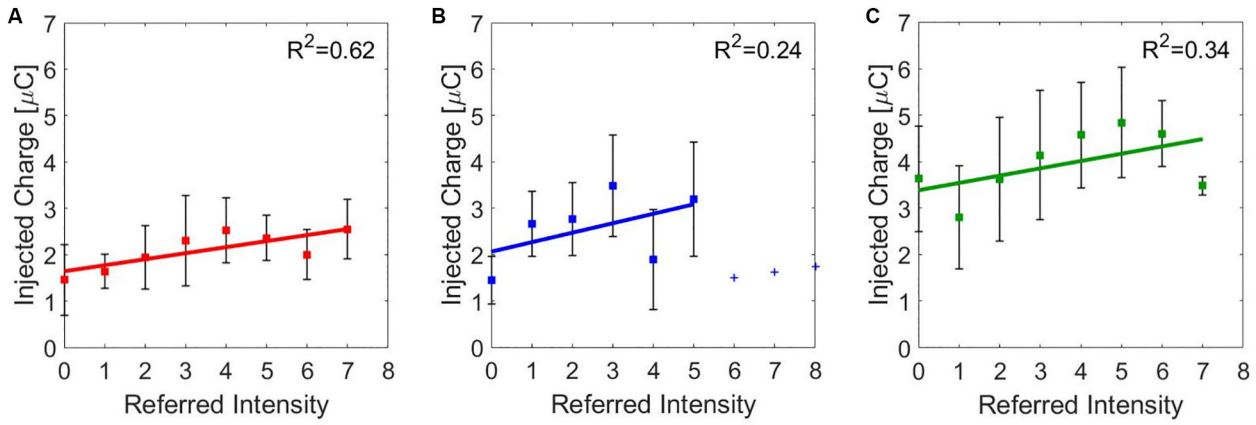

FIGURE 5 | Linear regressions of the median value (±SD, standard deviation) of the injected charge for the referred intensities reported by the subjects during charge modulation of the **(A)** median, **(B)** ulnar, and **(C)** concurrent stimulations. R^2 is the coefficient of determination, which describes the goodness of the linear regression.

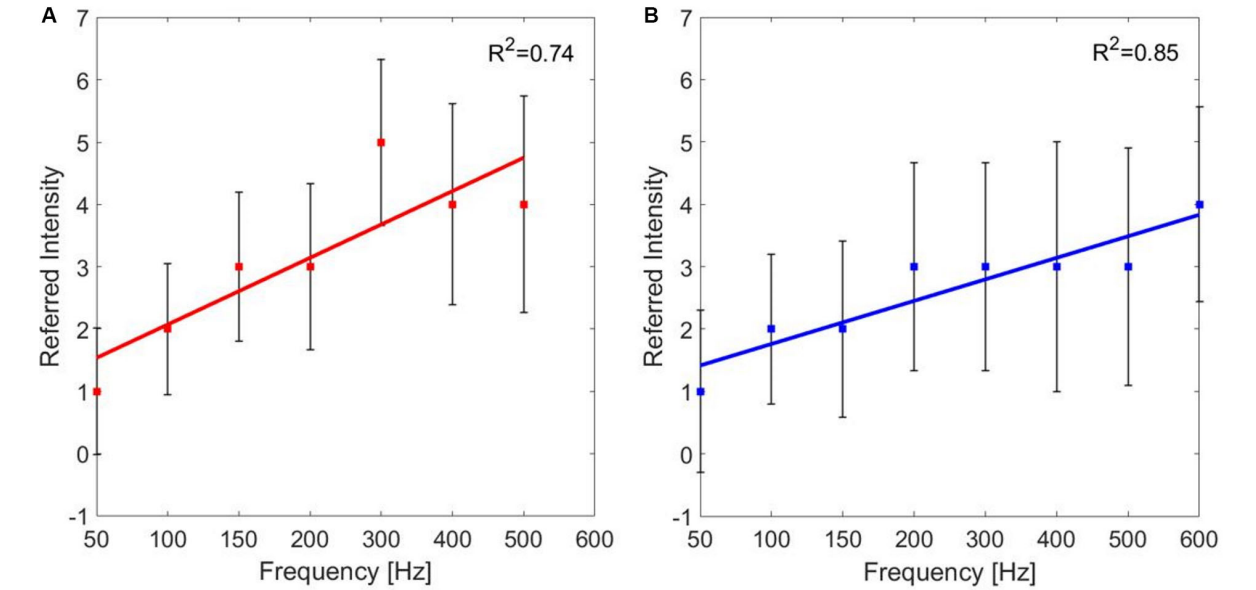

FIGURE 6 | Linear regressions of the median value (±SD, standard deviation) of the referred intensities reported by the subjects for each pulse frequency (PF) of frequency modulation of the **(A)** median and **(B)** ulnar stimulations. R^2 is the coefficient of determination, which describes the goodness of the linear regression.

and $\rho = 0.6015$, Pearson coefficient). Then, the linear regressions of the two data set were studied: for both stimulation phases are $R^2 = 0.74$ and $R^2 = 0.85$, respectively, for the median and ulnar nerve. The median of the referred intensities reported from the nine subjects increases with frequency, as it is shown in **Figure 6**.

AMS Strategy

The aim of the AMS protocol was recreating a sensation of movement in the hand of the subjects. Primarily, the PAV and the PWV were compared during single nerve stimulations. Then, the three methods (i.e., PAV, PWV, and ISDM) were compared during concurrent stimulation.

The single nerve stimulations during the AMS protocol did not revealed any substantial results. The subject perceived a rapid moving sensation starting from the forearm, in correspondence with the electrodes, and reaching the hand and vice versa.

During the concurrent stimulation, the subject had to indicate the perceived direction of the movement elicited during the AMS protocol. **Table 4** reports the SRs obtained during concurrent stimulation of the AMS protocol. The results show that the SR

TABLE 4 | Comparison between success rate (SR) obtained, applying the three methods for each movement directions (MU, median–ulnar; UM, ulnar–median).

	PAV	PWV	ISDM
MU	0.83	0.89	0.98
UM	0.78	0.89	0.98

TABLE 5 | Percentage of preferences expressed by the subjects of the two different time duration of the stimulus (0.5 or 1 s) for each movement directions (MU, median–ulnar; UM, ulnar–median) for the pulse amplitude variation (PAV) and pulse width variation (PWV).

	PAV		PWV			ISDM				
Stimulus Duration (s)	**0.5**	**1**	**0.5**	**1**	**Delays (s)**	**0.1**	**0.2**	**0.3**	**0.4**	**0.5**
MU	67%	33%	44%	56%	MU	11%	33%	33%	11%	11%
UM	33%	67%	22%	78%	UM	11%	22%	22%	33%	11%

For the ISDM, the percentages of preferences expressed by the subjects of delay between the two signals sent to the two nerves (0.1–0.5 s with a step of 0.1 s) are reported for each movement directions.

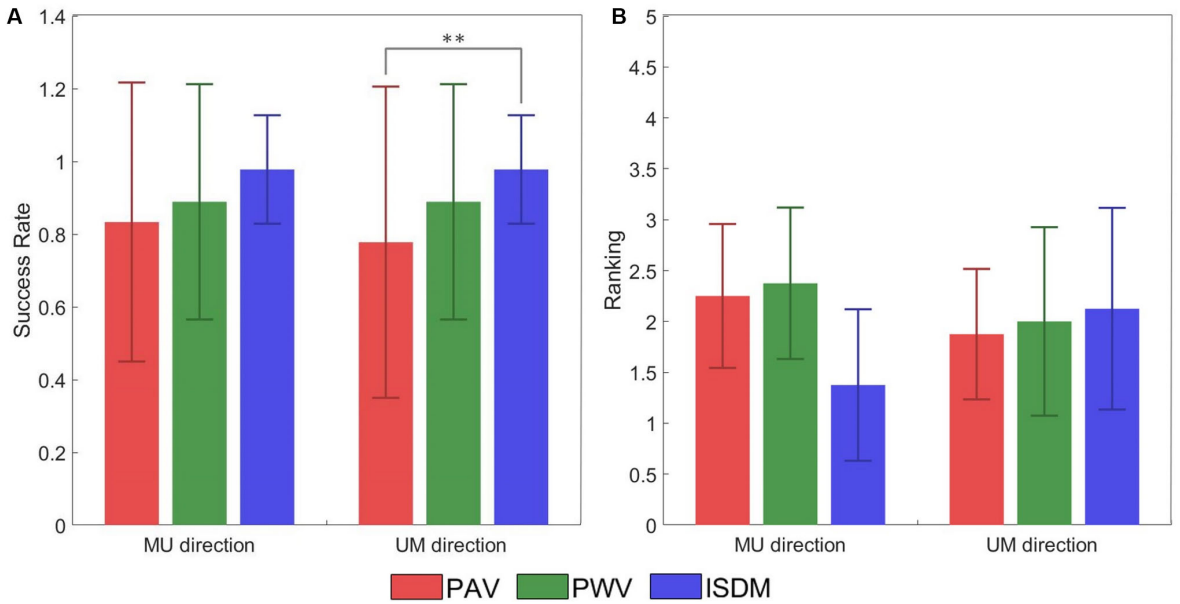

FIGURE 7 | (A) Success rate (±SD, standard deviation) of the discrimination of the movement direction of each subject for each method for both median–ulnar (MU) and ulnar–median (UM) directions. The comparative analysis (Wilcoxon–Mann–Whitney test with Bonferroni correction) reports a statistically significant difference in terms of success rate (SR) between pulse amplitude variation (PAV) and ISDM for the UM direction ($P_{PAV-ISDM}$ = 0.0089). No statistically significant differences were reported for the other comparisons: for the MU direction $P_{PAV-ISDM}$ = 0.0367, $P_{PAV-PWV}$ = 0.6536, and $P_{PWV-ISDM}$ = 0.1432; for the UM direction, $P_{PAV-PWV}$ = 0.3912 and $P_{PWV-ISDM}$ = 0.1432. **(B)** Mean of the ranking position (± SD, standard deviation) for each method for both MU and UM direction. Low mean values indicate that the subjects ranked the method in high positions like 1 or 2. The comparative analysis (Wilcoxon–Mann–Whitney test with Bonferroni correction) reports no statistically significant differences in terms of ranking preference among PAV, PWV, and ISDM: for the MU direction, $P_{PAV-ISDM}$ = 0.0340, $P_{PAV-PWV}$ = 0.8858, and $P_{PWV-ISDM}$ = 0.0297; for the UM direction, $P_{PAV-ISDM}$ = 0.7630, $P_{PAV-PWV}$ = 0.9992, and $P_{PWV-ISDM}$ = 0.9184. Statistically significant differences ($P < 0.0016$) are depicted by asterisks.

of AMS for the median–ulnar direction is 0.83 for PAV method, 0.89 for PWV method, and 0.98 for the ISDM method, whereas, for the ulnar–median direction, the SR is 0.78 for PAV method, 0.89 for PWV method, and 0.98 for the ISDM method (see **Table 4**). This means that, for each movement direction, the SR of ISDM method is higher than that of PAV and PWV for recreating an AMS in the hand that easily allows distinguishing the movement direction. It is a reliable technique also because all the subjects were able to understand the AMS with this method. Subject 9 in fact did not understood the moving sensation with the first two methods.

Table 5 shows the percentage of preferences expressed by the subjects for the two stimulus durations for PAV and PWV and for the delays of the ISDM method.

There was not a clear preference between the two different time durations of the stimuli for the PAV and the PWV, as it is reported in **Table 5**. Among the delays for the median–ulnar direction, the highest percentage of preference was equal for 0.2 and 0.3 s (both 33% of preference); for the ulnar–median direction, the 33% preference was for the 0.4-s delay.

Figure 7A represented the SR of the discrimination of the movement direction of each subject for each method for both MU and UM directions. The statistical analysis (Wilcoxon–Mann–Whitney test with Bonferroni correction) pointed out a significant difference between PAV and ISDM for the UM direction. The *P*-value P_{M1-M2} means the *P*-value of the comparison between two methods, M1 and M2. For the MU direction: $P_{PAV-ISDM}$ = 0.0367, $P_{PAV-PWV}$ = 0.6536, and $P_{PWV-ISDM}$ = 0.1432. For the UM direction: $P_{PAV-ISDM}$ = 0.0089, $P_{PAV-PWV}$ = 0.3912, and $P_{PWV-ISDM}$ = 0.1432.

At the end of the AMS protocol, the three methods were compared, and each subject expressed a preference among them.

Figure 7B reported the ranking position for each method for both MU and UM direction. Low mean values indicate that the subjects ranked the method in high positions like 1 or 2. For the MU direction of movement, seven subjects out of nine reported ISDM as the best method. These results show that ISDM method is indicated by the subjects as the favorite method for recreating a well-defined and conformable AMS for the MU direction. For the UM direction, there was not a clear preference for one of the three methods. The comparative analysis (Wilcoxon–Mann–Whitney test with Bonferroni correction) reported no statistically significant differences in terms of ranking position among PAV, PWV, and ISDM; therefore, there is no significant preference of the three methods. For the MU direction: $P_{PAV-ISDM} = 0.0340$, $P_{PAV-PWV} = 0.8858$, and $P_{PWV-ISDM} = 0.0297$. For the UM direction: $P_{PAV-ISDM} = 0.7630$, $P_{PAV-PWV} = 0.9992$, and $P_{PWV-ISDM} = 0.9184$.

DISCUSSION

This study wanted to investigate the feasibility of using a non-invasive interface based on TENS in a closed-loop device for restoring tactile feedback in terms of forces and slippage. Static tactile sensations and an AMS were recreated in the hand of nine healthy subjects to reproduce sensations occurring during object grasping and manipulation (where the contact between hand and object can be dynamic). An experimental protocol composed of a mapping protocol and AMS protocol was developed.

The mapping protocol allowed characterizing the type of referred sensation in term of naturalness, depth, pain, intensity, and quality. At the end of each trial, for each subject, a hand map was reconstructed where the elicited regions were pointed out. During the charge modulation, the delivered sensations were mostly described by the subjects as an almost natural and superficial tingling. While in the frequency modulation, the sensation was mainly perceived as tingling/vibration. Moreover, the increase in the injected charge intensified the sensation, through the variation of the quality, the referred intensity, and the elicited regions. The correlation analysis for the charge modulation showed that the correlation between the referred intensity and the injected charge is moderate for the median stimulation and weak for the ulnar and concurrent stimulations. For the frequency modulation, the correlation between the PF of the stimulus and the referred intensity is moderate for both nerves.

The obtained results from the mapping protocol matched with the literature background (Chai et al., 2015; Osborn et al., 2017; Shin et al., 2018; Vargas et al., 2019). They strengthened the achievements of TENS studies carried out until now. The data collected from the mapping protocol represent fundamental information for further investigations. In this case, they were used to extend the experimental protocol in order to recreate more complex sensations on the hand, enlarging the literature. In particular, they suggest that there is a common and shared way to characterize sensations, for extrapolating subject-dependent information for specific applications. Further analysis could be the comparison within the subjects among sensation characteristics, such as naturalness or accuracy, or between stimulation methods (charge or frequency modulation) in order to evaluate the ability to perceive different levels of referred intensity and assess the subject acceptance of TENS technique. Moreover, the shifting of the user's tissues in the stump–socket interface from normal movements leads to a variation of the level of impedance. Consequently, this could produce a change in the level of intensity of the referred sensation and/or in the sensation itself. Nevertheless, this would not affect the goodness of TENS since this problem could be overcome by a remodulation of stimulation parameters. In future studies, it will be useful to verify this condition by changing the stimulation parameters in order to compensate the referred sensation perception.

On the other hand, the AMS experimental protocol allowed eliciting an AMS on eight subjects out of nine through three different methods. Only one of the subjects was not able to feel the AMS with the PAV and PWV methods.

In general, the three strategies were able to reach the intended target of discriminating the movement direction: the SR of AMS for the median–ulnar direction is 0.83 for PAV method, 0.89 for PWV method, and 0.98 for the ISDM method, whereas for the ulnar–median direction, the SR is 0.78 for PAV method, 0.89 for PWV method, and 0.98 for the ISDM method (**Table 4**). The comparative analysis (Wilcoxon–Mann–Whitney test with Bonferroni correction) reported a statistically significant difference in terms of SR of movement direction discrimination between PAV and ISDM methods for the UM direction ($P < 0.016$, see **Figure 7A**). The other comparisons did not show significantly differences.

The mean of the ranking position of the three methods for the MU direction is low for the ISDM method, so more subjects indicated it as the favorite method for eliciting a well-defined moving sensation in the hand. The Wilcoxon–Mann–Whitney test with Bonferroni correction did not highlight a statistically significant difference in terms of ranking positions among the three methods (**Figure 7B**).

In this study, AMS protocol permitted to create a moving sensation on the hand of nine healthy subjects in a non-invasive way with the use of TENS. Moreover, TENS guaranteed a somatotopical approach, which recreate a sensation to the corresponding location of missing limb in a physiologically natural way. TENS studies focused on functional tasks in which the objects in contact with the hand is stable. For the first time, it was possible to induce not a static sensation on the hand but a moving one for replicating events that could occur unexpectedly, like slippage. AMS candidates itself as novel tool for feedback restoration during more complex tasks, in which the object is not fixed. Moreover, by this study, high SRs were obtained with healthy subjects, suggesting that it could reasonable to validate this strategy on amputees.

CONCLUSION

The experiments confirmed the good potential of recreating slippage sensations by means of an AMS protocol in the hand via TENS. The AMS protocol is a reliable technique that can

elicit a moving sensation that is easy to distinguish, especially through the application of the ISDM method. It is a promising technique because it could recreate an AMS on the subject fingers that is assimilable to the variation of the contact point of the hand during object manipulation tasks.

In the future, AMS needs to be investigated more in depth in order to elicit a movement sensation passing through the fingers of the hand. In fact, not all the subjects were able to discriminate this type of transition during the AMS; some of them only perceived the sensation moving between the two regions innervated by the median and the ulnar nerves.

After the feasibility study conducted in this paper for recreating AMS by the means of TENS in nine healthy subjects, future improvements will be testing the proposed approach with amputees, whose nerves could have undergone a reorganization into the tissues.

Up to the present, this technique was never studied to recreate a moving sensation in the hand, but it was only examined on lower limb during gait analysis and posture control (Rahal et al., 2009; Pfeifer et al., 2010; Seps et al., 2011; Pagel et al., 2016). Thanks to the promising results, this technique could be integrated in the closed loop of a prosthetic system in order to elicit the moving sensation of an object among the prosthetic fingers, as in the slippage events, and provide the user with information about manipulation forces and slippage event during grasp control.

DATA AVAILABILITY STATEMENT

The datasets generated for this study are available on request to the corresponding author.

ETHICS STATEMENT

The experimental protocol was approved by the local Ethical Committee (Comitato Etico Università Campus Bio-Medico di Roma) and complied with the Declaration of Helsinki. All subjects gave written informed consent in accordance with the Declaration of Helsinki.

AUTHOR CONTRIBUTIONS

AS analyzed the literature, designed the proposed approach, acquired and analyzed the experimental data, and wrote the manuscript. AD analyze the literature, designed the proposed approach, analyze the experimental data, and contributed to wrote the manuscript. FT contributed to analysis of the literature, to design of the proposed approach, and to acquisition of the experimental data. AC contributed to the design of the proposed approach and of the experimental setup, wrote the manuscript, and supervised the study. LZ designed the manuscript and supervised the study. All the authors read and approved the manuscript.

FUNDING

This work was supported partly by Fondazione ANIA with the project "Development of bionic upper limb prosthesis characterized by personalized interfaces and sensorial feedback for amputee patients with macro lesion after car accident" and partly by INAIL prosthetic center with PPR AS 1/3 (CUP: E57B16000160005).

REFERENCES

Antfolk, C., D'alonzo, M., Rosen, B., Lundborg, G., Sebelius, F., and Cipriani, C. (2013). Sensory feedback in upper limb prosthetics. *Expert Rev. Med. Devices* 10, 45–54. doi: 10.1586/erd.12.68

Arieta, A. H., Afthinos, M., and Dermitzakis, K. (2011). Apparent moving sensation recognition in prosthetic applications. *Proc. Comput. Sci.* 7, 133–135.

Chai, G., Sui, X., Li, S., He, L., and Lan, N. (2015). Characterization of evoked tactile sensation in forearm amputees with transcutaneous electrical nerve stimulation. *J. Neural Eng.* 12:066002. doi: 10.1088/1741-2560/12/6/066002

Ciancio, A. L., Cordella, F., Barone, R., Romeo, R. A., Bellingegni, A. D., Sacchetti, R., et al. (2016). Control of prosthetic hands via the peripheral nervous system. *Front. Neurosci.* 10:116. doi: 10.3389/fnins.2016.00116

Cipriani, C., D'Alonzo, M., and Carrozza, M. C. (2011). A miniature vibrotactile sensory substitution device for multifingered hand prosthetics. *IEEE Trans. Biomed. Eng.* 59, 400–408. doi: 10.1109/TBME.2011.2173342

Cordella, F., Ciancio, A. L., Sacchetti, R., Davalli, A., Cutti, A. G., Guglielmelli, E., et al. (2016). Literature review on needs of upper limb prosthesis users. *Front. Neurosci.* 10:209. doi: 10.3389/fnins.2016.00209

Cordella, F., Zollo, L., Salerno, A., Accoto, D., Guglielmelli, E., and Siciliano, B. (2014). Human hand motion analysis and synthesis of optimal power grasps for a robotic hand. *Int. J. Adv. Robot. Syst.* 11:37.

D'Anna, E., Petrini, F. M., Artoni, F., Popovic, I., Simanić, I., Raspopovic, S., et al. (2017). A somatotopic bidirectional hand prosthesis with transcutaneous electrical nerve stimulation based sensory feedback. *Sci. Rep.* 7:10930. doi: 10.1038/s41598-017-11306-w

D'Anna, E., Valle, G., Mazzoni, A., Strauss, I., Iberite, F., Patton, J., et al. (2019). A closed-loop hand prosthesis with simultaneous intraneural tactile and position feedback. *Sci. Robot.* 4:eaau8892.

Flesher, S. N., Collinger, J. L., Foldes, S. T., Weiss, J. M., Downey, J. E., Tyler-Kabara, E. C., et al. (2016). Intracortical microstimulation of human somatosensory cortex. *Sci. Transl. Med.* 8:361ra141.

George, J. A., Kluger, D. T., Davis, T. S., Wendelken, S. M., Okorokova, E. V., He, Q., et al. (2019). Biomimetic sensory feedback through peripheral nerve stimulation improves dexterous use of a bionic hand. *Sci. Robot.* 4:eaax2352.

Gonzalez, J., Soma, H., Sekine, M., and Yu, W. (2012). Psycho-physiological assessment of a prosthetic hand sensory feedback system based on an auditory display: a preliminary study. *J. Neuroeng. Rehabil.* 9:33. doi: 10.1186/1743-0003-9-33

Izumi, T., Hoshimiya, N., Fujii, A., and Handa, Y. (1988). A presentation method of a traveling image for the sensory feedback for control of the paralyzed upper extremity. *Syst. Comput. Jpn.* 19, 87–96.

Johnson, M. I., and Bjordal, J. M. (2011). Transcutaneous electrical nerve stimulation for the management of painful conditions: focus on neuropathic pain. *Expert Rev. Neurotherapeut.* 11, 735–753.

Johnson, M. I., Mulvey, M. R., and Bagnall, A. M. (2015). Transcutaneous electrical nerve stimulation (TEVNS) for phantom pain and stump pain following amputation in adults. *Cochrane Database Syst. Rev.* 5:CD007264.

Kaczmarek, K. A., Webster, J. G., Bach-y-Rita, P., and Tompkins, W. J. (1991). Electrotactile and vibrotactile displays for sensory substitution systems. *IEEE Trans. Biomed. Eng.* 38, 1–16.

Kim, K., and Colgate, J. E. (2012). Haptic feedback enhances grip force control of sEMG-controlled prosthetic hands in targeted reinnervation amputees.

IEEE Trans. Neural Syst. Rehabil. Eng. 20, 798–805. doi: 10.1109/TNSRE.2012.2206080

Kim, L. H., McLeod, R. S., and Kiss, Z. H. (2018). A new psychometric questionnaire for reporting of somatosensory percepts. *J. Neural Eng.* 15:013002. doi: 10.1088/1741-2552/aa966a

Lauretti, C., Pinzari, G., Ciancio, A. L., Davalli, A., Sacchetti, R., Sterzi, S., et al. (2017). "A vibrotactile stimulation system for improving postural control and knee joint proprioception in lower-limb amputees," in *Proceedings of the 2017 26th IEEE International Symposium on Robot and Human Interactive Communication (RO-MAN)*, (Piscataway, NJ: IEEE), 88–93.

Li, M., Zhang, D., Chen, Y., Chai, X., He, L., Chen, Y., et al. (2018). Discrimination and recognition of phantom finger sensation through transcutaneous electrical nerve stimulation. *Front. Neurosci.* 12:283. doi: 10.3389/fnins.2018.00283

Navarro, X., Krueger, T. B., Lago, N., Micera, S., Stieglitz, T., and Dario, P. (2005). A critical review of interfaces with the peripheral nervous system for the control of neuroprostheses and hybrid bionic systems. *J. Peripheral Nervous Syst.* 10, 229–258.

Oddo, C. M., Raspopovic, S., Artoni, F., Mazzoni, A., Spigler, G., Petrini, F., et al. (2016). Intraneural stimulation elicits discrimination of textural features by artificial fingertip in intact and amputee humans. *eLife* 5:e09148. doi: 10.7554/eLife.09148

Osborn, L., Fifer, M., Moran, C., Betthauser, J., Armiger, R., Kaliki, R., et al. (2017). "Targeted transcutaneous electrical nerve stimulation for phantom limb sensory feedback," in *Proceedings of the 2017 IEEE Biomedical Circuits and Systems Conference (BioCAS)*, (Piscataway, NJ: IEEE), 1–4.

Osborn, L. E., Dragomir, A., Betthauser, J. L., Hunt, C. L., Nguyen, H. H., Kaliki, R. R., et al. (2018). Prosthesis with neuromorphic multilayered e-dermis perceives touch and pain. *Science Robot.* 3:eaat3818. doi: 10.1126/scirobotics.aat3818

Pagel, A., Arieta, A. H., Riener, R., and Vallery, H. (2016). Effects of sensory augmentation on postural control and gait symmetry of transfemoral amputees: a case description. *Med. Biol. Eng. Comput.* 54, 1579–1589. doi: 10.1007/s11517-015-1432-2

Papaleo, E., Zollo, L., Spedaliere, L., and Guglielmelli, E. (2013). "Patient-tailored adaptive robotic system for upper-limb rehabilitation," in *Proceedings of the 2013 IEEE International Conference on Robotics and Automation*, (Piscataway, NJ: IEEE), 3860–3865.

Petrini, F. M., Bumbasirevic, M., Valle, G., Ilic, V., Mijović, P., Čvančara, P., et al. (2019). Sensory feedback restoration in leg amputees improves walking speed, metabolic cost and phantom pain. *Nat. Med.* 25, 1356–1363. doi: 10.1038/s41591-019-0567-3

Pfeifer, S., Caldiran, O., Vallery, H., Riener, R., and Arieta, A. H. (2010). "Displaying centre of pressure location by electrotactile stimulation using phantom sensation," in *Proceedings of the 2010 15th Annual Conference of the International Functional Electrical Stimulation Society*, Vienna, 1–3.

Rahal, L., Cha, J., El Saddik, A., Kammerl, J., and Steinbach, E. (2009). "Investigating the influence of temporal intensity changes on apparent movement phenomenon," in *Proceedings of the 2009 IEEE International Conference on Virtual Environments, Human-Computer Interfaces and Measurements Systems*, (Piscataway, NJ: IEEE), 310–313.

Raspopovic, S., Capogrosso, M., Petrini, F. M., Bonizzato, M., Rigosa, J., Di Pino, G., et al. (2014). Restoring natural sensory feedback in real-time bidirectional hand prostheses. *Sci. Transl. Med.* 6:222ra19. doi: 10.1126/scitranslmed.3006820

Seps, M., Dermitzakis, K., and Hernandez-Arieta, A. (2011). "Study on lower back electrotactile stimulation characteristics for prosthetic sensory feedback," in *Proceedings of the 2011 IEEE/RSJ International Conference on Intelligent Robots and Systems*, (Piscataway, NJ: IEEE), 3454–3459.

Shin, H., Watkins, Z., Huang, H. H., Zhu, Y., and Hu, X. (2018). Evoked haptic sensations in the hand via non-invasive proximal nerve stimulation. *J. Neural Eng.* 15:046005. doi: 10.1088/1741-2552/aabd5d

Tan, D. W., Schiefer, M. A., Keith, M. W., Anderson, J. R., Tyler, J., and Tyler, D. J. (2014). A neural interface provides long-term stable natural touch perception. *Sci. Transl. Med.* 6:257ra138. doi: 10.1126/scitranslmed.3008669

Vargas, L., Whitehouse, G., Huang, H., Zhu, Y., and Hu, X. (2019). Evoked haptic sensation in the hand with concurrent non-invasive nerve simulation. *IEEE Trans. Biomed. Eng.* 66, 2761–2767.

Wright, J., Macefield, V. G., van Schaik, A., and Tapson, J. C. (2016). A review of control strategies in closed-loop neuroprosthetic systems. *Front. Neurosci.* 10:312. doi: 10.3389/fnins.2016.00312

Zollo, L., Di Pino, G., Ciancio, A. L., Ranieri, F., Cordella, F., Gentile, C., et al. (2019). Restoring tactile sensations via neural interfaces for real-time force-and-slippage closed-loop control of bionic hands. *Sci. Robot.* 4:eaau9924. doi: 10.1126/scirobotics.aau9924

Conflict of Interest: The authors declare that the research was conducted in the absence of any commercial or financial relationships that could be construed as a potential conflict of interest.

frontiers in Neuroscience

REVIEW
published: 23 June 2020
doi: 10.3389/fnins.2020.00345

A Review of Sensory Feedback in Upper-Limb Prostheses From the Perspective of Human Motor Control

Jonathon W. Sensinger[1]† and Strahinja Dosen[2]*†*

[1] *Institute of Biomedical Engineering, University of New Brunswick, Fredericton, NB, Canada,* [2] *Department of Health Science and Technology, The Faculty of Medicine, Integrative Neuroscience, Aalborg University, Aalborg, Denmark*

This manuscript reviews historical and recent studies that focus on supplementary sensory feedback for use in upper limb prostheses. It shows that the inability of many studies to speak to the issue of meaningful performance improvements in real-life scenarios is caused by the complexity of the interactions of supplementary sensory feedback with other types of feedback along with other portions of the motor control process. To do this, the present manuscript frames the question of supplementary feedback from the perspective of computational motor control, providing a brief review of the main advances in that field over the last 20 years. It then separates the studies on the closed-loop prosthesis control into distinct categories, which are defined by relating the impact of feedback to the relevant components of the motor control framework, and reviews the work that has been done over the last 50+ years in each of those categories. It ends with a discussion of the studies, along with suggestions for experimental construction and connections with other areas of research, such as machine learning.

Keywords: prostheses, sensory feedback, computational motor control, sensory integration, human–machine interfaces

OPEN ACCESS

Edited by:
Max Ortiz-Catalan, Chalmers University of Technology, Sweden

Reviewed by:
Giovanni Di Pino, Campus Bio-Medico University, Italy
Lohitash Karumbaiah, University of Georgia, United States

****Correspondence:***
Jonathon W. Sensinger
j.sensinger@unb.ca
Strahinja Dosen
sdosen@hst.aau.dk

† These authors have contributed equally to this work

Specialty section:
This article was submitted to Neural Technology, a section of the journal Frontiers in Neuroscience

Received: *12 December 2019*
Accepted: *23 March 2020*
Published: *23 June 2020*

Citation:
Sensinger JW and Dosen S (2020) A Review of Sensory Feedback in Upper-Limb Prostheses From the Perspective of Human Motor Control. Front. Neurosci. 14:345. doi: 10.3389/fnins.2020.00345

INTRODUCTION

Anyone who has tried to light a match with cold, numb fingers can appreciate the role that somatosensory feedback plays in accomplishing tasks. And yet although sensory feedback is important, it is only one piece of a complicated story. Cold numb fingers impact both the sensations and the control of finger movements. Small delicate tasks may be influenced by sensory deficits in ways that larger, gross motions would not. And it is possible that one would learn to compensate for numb fingers over time (say after a surgically induced numbing) such that it was only a minor inconvenience, relying on training, experience, and alternative sensory cues (e.g., visual observation). A particularly illustrative example is a well-known deafferented patient Ian Waterman, who was able, after extensive and tedious training, to grasp and manipulate objects despite having completely lost the sense of touch and proprioception (BBC, 1998; Hermsdörfer et al., 2008). Sensory feedback is indeed important, but it is part of a complicated, multifaceted system that makes it difficult to assess the true value and limitations of individual sensory percepts when used to supplement systems with sensory deficits such as prostheses.

Sensory feedback in prostheses is presently a hot topic in research, with the number of studies increasing dramatically over the past few years presenting invasive (Pasluosta et al., 2018) as well as non-invasive solutions (Svensson et al., 2017) (see **Appendix** for chronological list).

In addition, prosthesis companies show an increasing interest in the topic (e.g., https://vincentsystems.de/en/prosthetics/vincent-evolution-2/, http://www.psyonic.co/abilityhand). However, this "boom" is not in any way unique. Something similar happened decades ago, in the 1970's and 1980's. In fact, in 1980 D. Childress wrote a review on sensory feedback in prosthetics from a "historical perspective" (Childress, 1980). The literature from that period is rich, and the manuscripts present methods and prototypes that are in many cases analogous to those that are being developed today. For example, an interested reader can find solutions based on electro (Shannon, 1979; Scott et al., 1980) and vibrotactile stimulation (Shannon, 1976), force applicators (Meek et al., 1989) as well as pressure cuffs (Patterson and Katz, 1992). Yet none of these solutions has been translated into clinical use.

A plausible explanation for this failure to clinically endure could be that the technology of that time was simply not mature enough to be suitable for clinical applications. Since the technology developed immensely in the meantime, one can be far more optimistic that the recent research efforts will indeed lead to a solution that will be accepted and used outside of research labs. However, once the recent literature is carefully examined, the optimism can be tainted by a doubt; the reports in the literature on the benefits of feedback are contradictory. Some studies report that the feedback significantly improves prosthesis performance (Clemente et al., 2016, 2019), whereas the others find no difference in prosthesis performance with and without feedback (Cipriani et al., 2008; Saunders and Vijayakumar, 2011), or report that the feedback is useful in only some subjects and conditions (Chatterjee et al., 2008; Markovic et al., 2018a). And indeed, both authors of the present manuscript experienced the elusiveness of prosthesis feedback when they started working on the topic several years ago. At that time, they designed their first feedback systems (independently from each other) and enthusiastically tested them in amputees, successfully demonstrating that the subjects could accomplish delicate tasks using a sensate prosthesis. However, the excitement was soon replaced by surprise, when the subjects performed the very same tasks equally well without the supplementary feedback.

The thesis of this manuscript is accordingly that the lack of feedback in commercial prostheses is not only due to deficient technology, but also at least in part due to insufficient knowledge and understanding about the fundamental role of feedback in prosthesis control. Our aim here is to shed light on some of these aspects by placing the feedback within the broader framework of human motor control.

This paper attempts to tackle the aspect of sensory feedback in prostheses, which is an integral part of a larger system of prosthetic control. For a holistic overview of prosthesis control in the broader domain, see Sensinger et al. (2019). For an overview focusing explicitly on control and feedback, see Micera et al. (2010).

Several reviews have been published recently on the topic of sensory feedback in prosthetics (Antfolk et al., 2013c; Schofield et al., 2014; Svensson et al., 2017); while they thoroughly describe the technology and methods to elicit tactile sensations, the present manuscript has a different focus. The primary purpose of this paper is to supply a lexicon – and through it a paradigm shift – in how we view the complex phenomenon of closed-loop control of myoelectric prostheses. Our lexicon and paradigm are founded in the language of computational motor control – a field that has proved influential in the broader motor control community to make sense of the way humans move. Therefore, we begin by providing an overview of the main concepts in computational motor control and relate those concepts to the realm of closed-loop prosthesis control. The secondary purpose of this paper is to supply a roadmap that explains how the various aspects work together, and how the literature has landed on the map. To this aim, we provide a comprehensive review of the state-of-the-art and organize the studies using an original categorization that reflects the computational motor control perspective. We then suggest how this roadmap may be used to remember the factors that are important to consider/control/report when experimentally assessing the effectiveness of feedback. Finally, we conclude the paper by discussing psychological factors, emerging and future work as well as connections with other research areas.

MOTOR CONTROL

Motivation

Human movement is coordinated and consistent even within its diversity. These properties have been well known for many years, and are well posed in the pioneering work of Bernstein (Bernstein, 1967). Over the last 70 years scientists and engineers have sought to construct normative laws that describe the "what," "how," and "why" of human movement. These three concepts are formalized in Marr's terminology (Marr, 1982), which divides the three questions into physical, algorithmic, and computational levels. **Table 1** depicts the application of Marr's terminology to the field of closed-loop prosthesis control. Physical and algorithmic levels are dependent on the specific properties of the system – such as the type of prosthetic control, or the fidelity and type of feedback available – whereas the computational level seeks to explain the driving purpose and logic of actions, and thus transcends specific devices. It is accordingly useful to have a clear computational framework when discussing recent advances in specific physical and algorithmic prosthetic solutions, as the computational language can transcend individual technologies. It is the aim of the present manuscript to introduce such a computational framework in the context of closed-loop prosthesis control.

Overview of Computational Motor Control

Human movement is regular – particularly when viewed from an appropriate framework. Through history, paradigm shifts in how we understand human movement have progressed to better explain diverse motor control, while favoring simple, elegant frameworks (Fitts, 1954; Flash and Hogan, 1985; Uno et al., 1989; Harris and Wolpert, 1998; Guiard and Beaudouin-Lafon, 2004; Soukoreff and MacKenzie, 2004). Variability is an inherent aspect of human movement that impacts the types

TABLE 1 | Levels of modeling classification, using levels of Marr, applied to the context of supplementary feedback in upper-limb prostheses.

GRANULARITY				
		CONTROL COMPONENTS	***CONTROL METHODS***	***CONTROL GOALS***
SYSTEM INDEPENDENT	COMPUTATIONAL	Forward model	Sensor fusion	Minimum effort
		Inverse model	Optimal feedback control	Minimum jerk
		Sensor confidence	Prediction of control outcome	Maximum performance
		Cost function	Estimation of current state	Risk avoidance
		Constraints	Intermittent control	
			Heuristics	
		ENCODING	***STIMULATION INTERFACE***	***INTERPRETATION***
SYSTEM DEPENDENT	ALGORITHMIC	Frequency modulation	Squeezing brace	Discrimination
		Amplitude modulation	Surface electrodes	Somatotopy
		Spatial modulation	Linear pusher	Homologous sensation
		Linear mapping	Vibration motors	Natural sensation
		Non-linear mapping	Headphones	Intuitiveness
		Discrete bursts	AR glasses	
		Activation charge rate	Implanted systems	
		FEEDBACK VARIABLES	***STIMULATION METHOD***	***USER IMPACT***
	PHYSICAL	Force	Visual/Sonic	Performance
		Velocity	Force/Torque	Embodiment
		EMG	Squeezing	User experience
		Contact	Stretching	User satisfaction
		Joint position	Electrical pulses	Motivation
		Temperature	Vibrations	Acceptance
		Pain	Hot and cold	
		WHAT	**HOW**	**WHY**
			GENERALITY	

Note that the computational layer, which is the focus of the present manuscript, is not directly dependent on the specifics of a concrete system (layers 1 and 2). Visualization adapted from Schrater et al. (2019).

of stereotypical movements humans make. There is substantial stochastic noise in human movements, as anyone who has tried to learn to throw a ball accurately at a target can appreciate. From the control point of view, the human nervous system is an impressive controller that can cope with the noise and adapt movements in real-time, as well as across trials to achieve the desired goal. Although feedback has long been included as a mechanism within human movement paradigms, it is only within the last 20 years that it has become an intrinsic component in the motor control policy (Todorov and Jordan, 2002), and doing so has yielded substantial insight and generalizability.

A major breakthrough in the field of computational motor control came with the work of Todorov (Todorov and Jordan, 2002; Todorov, 2005) who used the mathematical language of optimal feedback control. Human motor control and sensory feedback both have multiplicative noise, meaning that the variability of the control signal increases relative to the amplitude of the signal (De Luca, 1979; Clancy et al., 2001, 2002; Jones et al., 2002). The nature of variability in control signals affects user behavior (Chhabra and Jacobs, 2006), and is accordingly important to incorporate in any computational model that seeks to explain human behaviors, including those that are relevant for prosthesis use (as explained in later sections). Todorov was able to develop an efficient approach that captured the implications of these noise sources on many types of human behavior in an optimal control context.

Excellent overviews of the approach are provided by Scott (2004); Todorov (2004), Kording (2007), and Shadmehr and Krakauer (2008). In summary, the theory of optimal feedback control states that humans rely on the following components when controlling movements (Todorov, 2004; Shadmehr and Krakauer, 2008):

(1) Costs and rewards: at any time within a motion, there are multiple potential actions. To consider which action to take, we need to know the costs associated with each action, along with the rewarding nature of the sensory states that it may achieve. Given the stochastic nature of control, the costs and rewards are formulated as expectations, rather than as deterministic facts.
(2) Internal models: to map potential actions to the expected states they will produce (and thus the expected rewards they will incur), we need to have learned a mapping between causes (actions) and effects (anticipated state). This mapping is termed an internal model (Kawato, 1999; Cisek, 2009).
(3) Optimal feedback-driven policy: given known costs and known internal models, we need to find the optimal policy that will maximize our reward (or minimize our cost, depending on how the problem is phrased).
(4) State estimation: at every moment in time, we must estimate our state, since combining the estimate of the state with our optimal control policy will yield the control action we should take. Our estimate of state will be

informed by fusing all sensory information that we have, but unfortunately, this sensory information itself has variability, and perhaps more importantly, it also has substantial delays (limiting the gains we could employ in a closed-loop framework). To compensate for this, optimal estimation blends in estimates of our effects, given knowledge of our actions and our internal model.

It seems likely that the same components govern the motor control loop of an upper limb amputee using his/her bionic limb (Johnson et al., 2017a). Therefore, to design and implement an effective closed-loop interface, it is imperative to understand how each of these elements work in an amputee equipped with a prosthesis. However, although these components have been extensively investigated in able-bodied subjects, the literature on how they work in an amputee is nascent. The emerging literature seems to generally confirm what the framework proposes – namely that the computational methods are similar between able-bodied subjects and prosthesis users [e.g., both seem to use Bayesian integration (Risso et al., 2019), internal models (Lum et al., 2014)], but that the parameters (such as control and sensory noise) are different, leading to different internal model uncertainty and ultimately different behaviors and strategies (Johnson et al., 2017a).

Cost Functions

Cost functions define what we care about; the relationship between the quantity of that element and how much we care; and how we prioritize or weight the various things that are important to us. Humans typically care about things such as being accurate or minimizing effort (Todorov and Jordan, 2002; O'Sullivan et al., 2009). Recent work has also suggested that we aim to minimize variability and/or the amount of time a movement takes (Haith et al., 2012). Other studies have proposed we may care about making conservative movements (Nagengast et al., 2010), along with a variety of other costs, but for many upper-limb motions, considering a subset of accuracy, variability, effort, and time describes well human behavior (Shadmehr and Mussa-Ivaldi, 2012). Different relationships (e.g., linear, quadratic, exponential, and hyperbolic) have been used to model how humans penalize costs of increasing magnitudes. Mathematically, cost functions can be formulated as expressions that include these quantities and associated weights, which define the relative importance of those quantities to the human subject. The way that cost functions mathematically describe both the relative importance of small vs. large magnitudes and the relative importance of competing costs enables computational motor control models to evaluate and describe the rationale behind the choices people make when performing a movement.

These choices likely depend on the type of movement being made, as well as the unique preferences of the individual making the movement. Many studies assume quadratic cost functions because they are mathematically tractable and generally describe observed behaviors (Todorov and Jordan, 2002). A few studies have inductively assessed the actual cost functions of humans, and these studies typically find near-quadratic cost functions (Körding and Wolpert, 2004b; Sensinger et al., 2015), with the exception of time, where a hyperbolic cost function seems more representative (Shadmehr and Mussa-Ivaldi, 2012). However, these studies have only been done on a limited number of movements, and none of them have been performed on amputees (although one performed using myoelectric control found similar results, Sensinger et al., 2015). Based on the biological underpinnings of these cost functions (Haith et al., 2012; Shadmehr and Mussa-Ivaldi, 2012), it seems reasonable to assume that the cost functions are similar between able-bodied persons and those using a prosthesis. The weights between competing cost functions, however, are likely to be different across tasks, and may be different between able-bodied persons and those using a prosthesis. No work has yet explored these potential differences, although recent work has suggested flexible control solutions that adjust depending on a particular users preferences (Arunachalam et al., 2019).

Looking specifically at the contribution of supplemental feedback to improve costs, it is clear that the benefits of supplemental feedback depend on the nature and complexity of the task (Markovic et al., 2018a). There are a number of tasks in daily life, many of them included in clinical tests for prosthesis control, that can be accomplished without regulating the grip strength (Schiefer et al., 2016) (e.g., the prosthesis can be closed maximally to grasp a non-breakable object). Obviously, supplying feedback on the grasping force in such tasks is not going to contribute to the performance. Feedback is more likely useful in challenging tasks that require controlled changes of the prosthesis state (Tyler, 2016). It is accordingly useful when considering the role of supplementary feedback to explicitly identify the cost functions relevant for a given task.

Internal Models

Internal models map the relationship between causes and effects, and they may work forward (cause to effect) or inverse (effect to cause) (Kawato, 1999; Cisek, 2009). To determine which action would produce the desired effect, humans use an inverse model. Inverse models are therefore an essential part in feedforward control, which is characteristic of learned (automatic), fast and ballistic movements. Such movements are executed by "releasing" predefined sequences of motor commands (motor programs) that were developed through experience and repeated practice. In contrast, if the aim is to predict the sensory consequence of an action before receiving the delayed sensory reading, you would use a forward internal model – also called an efference copy (Cisek, 2009). Internal models are learned from acquired feedback, but in real-time execution, they do not need feedback and indeed can even be used in place of feedback.

Internal models are important because sensory feedback is delayed. Most sensory feedback work within the realm of prostheses has assumed that supplementary feedback is useful for real-time regulation, but in reality, all sensory feedback – both intrinsic and supplementary, takes time to reach the central nervous system and be processed. This delay is on the order of 50–300 ms, and substantially limits the ability of the central nervous system to respond strongly without losing stability (Whitney, 1977). Studies have shown that for a variety of tasks, humans are able to regulate their motions and forces without any

delay (Flanagan and Wing, 1997). A strong plausible explanation for this result is that they use inverse models to generate motor commands directly from the desired goal (feedforward control) and/or forward internal models to predict the effects of their actions, and then act appropriately (Kawato, 1999; Cisek, 2009). Thus, many attributes that we may assume are provided by feedback are actually subconsciously provided by our internal models.

When the predictions of our internal models are inaccurate, we update them, and there is a vast literature in this area (Shadmehr and Mussa-Ivaldi, 1994; Osu et al., 2003). It is likely that we only update them when we become confident their predictions of our state estimates are wrong (Fishbach et al., 2007). Humans can more quickly adapt their internal models when only parameters must be tuned (e.g., having mastered a badminton racquet, learning to use a tennis racquet) than when the task has different dynamics (e.g., a racquet without a handle) (Braun et al., 2009, 2010). Interestingly, human subjects are capable of updating the internal models of object dynamics after only a few grasping trials (sometimes even one) (Flanagan et al., 2001). When asked to grasp an object of unexpected weight, the subjects produce feedback corrections in load and grasp forces in the very first trial. However, the corrections fade out in later trials with the same object, indicating that the subject recalibrated the anticipatory control. Humans can accordingly update their internal models to improve future control of their motions.

A variety of studies have demonstrated the usefulness of internal models in controlling prostheses. It was shown in Lum et al. (2014) that the subjects properly scaled the grasping forces depending on the object fragility and that this scaling was refined over successive trials (inverse model adaptation). Similarly, as reported in Weeks et al. (2000), the subjects anticipatory increased the force when the weight of the object held by the prosthesis was predictably increased. However, in general, the accuracy of such internal models is poor, and the performance is variable across subjects. This is at least partially related to the uncertainty that characterizes the generation of myoelectric signals, which are imbued with multiplicative signal-dependent noise. For example, when amputees were asked to produce repeatedly the same level of grasping force, they could do that rather consistently if the target level was low but the performance decreased substantially for the high target (Ninu et al., 2014). Strengthening internal models is accordingly a clear way to improve output performance.

The usefulness of internal models vs. feedback depends on the quality and availability of inverse models. If the task is simple and control reliable, supplementary feedback might not be useful since the subjects can control their prosthesis in a purely feedforward fashion. This is nicely demonstrated in Saunders and Vijayakumar (2011), where vibrotactile force feedback did not improve grasping performance with respect to no feedback, even in a condition of full sensory deprivation. Conversely, recent research has used feedback that was specifically designed to exploit and supplement the use of internal models in amputees [see sections "Biofeedback to facilitate forward models (efference copy)" and "Delivering feedback to improve feedforward control (inverse model)"]. There is accordingly a complicated but tractable relationship between feedback and internal models as they affect each other and output performance.

The contribution of feedback is also linked to how much training participants have received. When subjects have not yet received extensive training, feedback is useful – both to develop internal models as well as to execute real-time corrections. Over time, however, as participants develop better internal models, the usefulness of feedback for real-time corrections may fade (Strbac et al., 2017; Markovic et al., 2018a). This is likely because the subjects acquire inverse models and/or learn to perceive and interpret the incidental sources of information. Feedback is not necessarily most beneficial before subjects have received any training, however, as efference copies also enhance the impact of feedback (Cuberovic et al., 2019). Prior to development of these decoding internal models, feedback has been found to be less useful; for example, as demonstrated in Markovic et al. (2018a), the subjects needed some time to learn to control a prosthesis in a delicate task before they were able to exploit the feedback successfully. In summary, the impact of feedback highly depends on how much training a participant has received to develop their inverse and forward internal models.

Optimal Feedback Control Policies

For a given set of costs and a given set of properties, including internal models of system dynamics and estimations of sensory feedback and control stochastic noise sources, an optimal feedback control policy decides on the best course of action for a given state. In contrast to plans that assume a specific sequence of states (fixed trajectory), the policies are general rules that define optimal transitions toward the goal from any state. For example, directions to a destination is an example of a trajectory, whereas traversing the shortest distance using a map is an example of a policy.

Humans use optimal or near-optimal policies across a variety of tasks (Kording, 2007; Liu and Todorov, 2007; Shadmehr and Mussa-Ivaldi, 2012; Acerbi et al., 2014), although it is important to note that for some tasks, their decisions do not seem optimal (Shadmehr and Mussa-Ivaldi, 2012). The challenge of optimal feedback control theories is to explain human abilities to generate these optimal policies in the simplest, most efficient way possible. In a general case, the optimal policies can be derived by applying the framework of optimal control (Todorov, 2006) and dynamic programming (Bertsekas, 2014). For systems with linear dynamics and quadratic costs, this problem substantially reduces to a linear quadratic regulator, and near-optimal solutions can be found using iterative linear quadratic regulators (Li and Todorov, 2007), reinforcement learning (Kositsky and Barto, 2001; Reinkensmeyer et al., 2012), or other strategies (Todorov, 2009). Many of these approaches provide relatively simple explanations, with explanatory value such as being able to describe human movement behavior, uncontrolled manifolds and synergies, or the asymmetrical velocity profiles found in many human movements (Todorov, 2009; Mitrovic et al., 2010; Rigoux and Guigon, 2012; Shadmehr and Mussa-Ivaldi, 2012). Perhaps most importantly for the context of this paper, they provide insight into the contribution of feedback throughout the process. Similar models have only

recently been applied to explain the behavior of a prosthesis user (Johnson et al., 2014, 2017a). However, this research is still in its initial phase and we have yet to develop models that can comprehensively describe the use of a prosthesis in clinically relevant situations.

Optimal feedback control policies help to explain the contribution of supplemental feedback relative to the other properties of the system. The optimal policy of a human controller takes into account the uncertainty of feedforward and feedback pathways. Therefore, the effectiveness of supplementary feedback is also affected by the quality of control. Control quality depends on both the command interface, which determines precision and accuracy in generating command signals, and on the characteristics of a controlled system, which defines the consistency of the system response to those commands. These aspects were investigated in Dosen et al. (2015b) where the subjects used less and more reliable interface (myoelectric versus joystick) to control a system with less and more consistent response (real versus simulated prosthesis), while the grasping force feedback was provided visually (computer screen). The results indeed showed that the properties of the system and control interface affected the quality of developed internal models and closed-loop control of prosthesis grasping force.

State Estimation

Sensory information comes from various sources (exteroception, interoception and proprioception) that are characterized by varying level of stochastic noise along with temporal delays. The brain must integrate this information into a composite estimate of our state that also includes knowledge regarding the expected state (internal model estimate).

Optimal estimation incorporates two sources of information by using a weighted average, where the weight assigned to each estimate is a function of its confidence (Ernst and Banks, 2002; Körding and Wolpert, 2004a). For Gaussian distributions, this process is known as Bayesian inference, and humans have been shown across a number of studies to use something similar (see Ernst and Banks, 2002 for seminal work; Kording, 2007 for review). The resulting composite estimate has its own estimate of confidence and may be used to fuse even more sources of information. Therefore, a multitude of sensors may be incorporated into a single estimate of state. A direct consequence of the sensor fusion is that if one signal has substantially more noise than another, incorporating it adds relatively little value, but does not make the net variability worse. This observation is particularly relevant point for supplementary feedback since it is integrated with intrinsic sources, some of which can provide feedback information with high-fidelity (e.g., vision to assess prosthesis motion).

This same concept of data fusion may be applied to the states that are estimated based on internal models. In this case, the final estimate is obtained as a weighted combination of a state estimated from the measurements (sensor data) and that determined by the model. The weighting is known as the Kalman gain, and the process is known as the Kalman filtering. Humans' state estimation has been well described by Kalman filters (Kording, 2007) and its non-linear extensions (i.e., extended and unscented Kalman filter, particle swarm filter) (Wan and Van Der Merwe, 2001).

The process of state estimation is key to understanding when supplementary sensory feedback in prostheses has worked, and more often, why it has failed. Human subjects can exploit various sources of information to improve motor performance. When somatosensory feedback is missing, as in a deafferented person, the motor control will rely on alternative incidental sensing modalities, such as vision, audition, and vibration (Hermsdörfer et al., 2008). It has been reported a long time ago that amputees can exploit incidental feedback produced by their device (Mann and Reimers, 1970; Prior et al., 1976). In a recent study (Schweisfurth et al., 2019b), it has been shown that visual and auditory cues can be used to estimate prosthesis closing velocity with good precision. Another recent study (Markovic et al., 2018b) demonstrated the ability of subjects to scale prosthesis grasping forces across six different levels from minimum to maximum force by relying only on incidental sources of information (namely, muscle proprioception, vision, and audition). Therefore, contrary to popular thinking, prosthesis control is actually closed-loop even when no explicit somatosensory feedback is transmitted to the prosthesis user.

The contribution of supplementary feedback accordingly depends on its contribution relative to the already-available incidental feedback and the strength of the internal model. As shown in Markovic et al. (2018b), when the supplemental information on the generated force was transmitted through a visual interface after the subjects trained controlling the prosthesis using incidental feedback, the force scaling improved only modestly and mainly at high force levels. It was demonstrated in a recent study (Risso et al., 2019) that an amputee subject with an implanted sensory feedback interface integrated supplementary somatosensory feedback and blurred visual information in a statistically optimal fashion when estimating the size of a hand-held object. If the supplementary feedback is characterized with a higher uncertainty compared to incidental sources, its impact on the control will likely be minimal if any. Therefore, it is critically important that the tactile stimulation profiles used to communicate prosthesis variables through supplementary feedback are easy to discriminate and interpret (Cipriani et al., 2014; Dosen et al., 2017).

Summary and Implications for Supplementary Feedback in Prostheses

In summary, humans make the best use of the actuators and sensors they have, to achieve the best possible reward they may, considering the probabilistic uncertainty in their control and sensory feedback. Given the structure of these noise sources and the complexity of the tasks humans perform, it as a marvel that they achieve optimal or near-optimal solutions. And yet, this observation offers both perspective and hope as it pertains to prostheses. The best thing going for humans is their brain; not their motors or their sensory receptors. Humans will make use of whatever motors or sensory receptors they have available to achieve the best they can, and in light of the sophisticated control policies they can develop, it is no wonder that many attempts

to supplement feedback do not have a significant impact. The brain had already developed an optimal policy that compensated in the control policy for a known deficit in real-time sensory feedback, either through developing internal models, learning to exploit the information from the incidental feedback sources or through navigating control decisions in which sensory feedback was less critical. As we will see below, many studies isolate the role of feedback, but these studies have little explanatory power about the impact of feedback on real-life use of prostheses. In this context, the impact refers not only to the improvement in prosthesis performance (utility), but equally well to enhancing the user experience when interacting with his/her bionic limb by, for example, promoting the feeling of agency and ownership (see section "Psychological aspects").

Whereas we have noted above and will detail below that the majority of supplementary feedback studies in prostheses focus on real-time feedback, the processes described above require learning and adaptation. This learning and adaptation can only happen in the presence of feedback. Thus, it is quite likely that an equally important role for supplementary feedback is to enable better learning of the task, such that it may be used by internal models and motor control policies. Therefore, it is quite likely that efforts to provide such feedback – particularly in areas where it is not redundantly provided by vision, will have substantial impact on the prosthesis performance (e.g., see Dosen et al., 2015a; Shehata et al., 2018a). The use of feedback in this context can be quite different from its application during real time modulation, e.g., the feedback can be an optional feature that can be activated by the subject when they need to learn the system dynamics. For example, the subject can use feedback during initial practice, and then again, when the system changes the properties due to wear and tear. Nevertheless, this application still needs to be implemented thoughtfully since, as it has been already recognized in the field of motor learning, the feedback can be even detrimental for the learning process if not provided properly (Sigrist et al., 2013).

Given that amputees have the same amazing brain to tackle optimal control problems, but also very different sources of control, mechanism dynamics, and sensory feedback, it will be useful to highlight similarities and differences before moving on to focus on the topic of feedback.

Motor control in able-bodied persons typically starts with the visual observation of the target object. Vision is employed to perceive its extrinsic (position and orientation) and intrinsic (size, shape, and material) properties (MacKenzie and Iberall, 2010). These properties are then used to predict the forces that are needed to grasp and lift the object by employing an inverse model to map the desired outcome (lifting an estimated weight) to the motor commands (muscle excitations and forces) required to achieve that goal (Gordon et al., 1991). After contacting the object, the hand produces forces that are normal and tangential to the object surface, known as grasp and load forces, respectively. The grasp forces establish a firm grip to prevent slippage, while the load forces are responsible for lifting. Importantly, both forces increase simultaneously with the rate of change that is proportional to the estimated object weight, thereby indicating anticipatory control (Johansson and Westling, 1988). If the weight is correctly estimated, this leads to a smooth lifting movement while the object is safely held in the hand. If the estimate is wrong, the subjects can use feedback from a dense network of mechanoreceptors as well as other sources (vision, proprioception) to notice the discrepancy and correct the control (Flanagan et al., 2006).

After an amputation, the sound hand is lost and it is replaced by an artificial system such as a myoelectric prosthesis. The biological connection between the neural controller and its end effector is severed, and replaced by a myoelectric interface, with only incidental feedback from the hand to the user. The prosthesis is controlled by generating myoelectric signals, which are characterized with variability that increases with the contraction intensity (Harris and Wolpert, 1998). The signals are processed and mapped into velocity commands that are sent to the prosthesis, and the resulting motion depends on the mechatronic properties of the system (e.g., communication delays and friction). Current myoelectric prostheses are non-backdrivable systems that are still substantially below the dexterity, precision, and accuracy inherent in biological limbs. A prosthetic device supplies intrinsic feedback to the user. The user can see the prosthesis motion, and in addition, he/she receives mechanical (vibration) and/or auditory (motor and motion sound) cues generated by the moving mechanism. Visual feedback, in particular, can provide high-fidelity information regarding a wide range of modalities (e.g., hand position and grasping force).

The control loop for using a prosthetic hand includes all the components that are characteristic for the sensory motor control of a sound hand. **Figure 1** shows how the artificial extremity integrates into the motor control framework of a prosthesis user. The user relies on internal models to generate feedforward commands directly from the task goal (inverse model) as well as to anticipate the system state (forward model) from the generated control signals (reafference) and interoceptive signals (sense of effort). He/she fuses the model-based prediction with the sensory feedback received from the environment to estimate the state of the prosthesis. This estimate is then used to detect deviations from the task goal, and correct the control if required (online controller). However, there are also crucial differences with respect to the control loop of an able-bodied subject. For example, prosthetic hands are non-backdrivable mechanisms with rough modulation of grasping force. Therefore, a nice and coordinated modulation of the load and grasping forces, characteristic to normal grasping, is not possible. In addition, the lack of precise and reliable control and missing somatosensory feedback affect the ability to acquire as well as update the internal models. Nevertheless, this can change with the development of low-impedance end-effectors (Brown et al., 2015), local feedback loops linearizing the prosthesis behavior (Bottomley, 1965), and with the integration of supplementary feedback into prosthetic systems. **Figure 2** highlights the main differences between the components comprising the control loop of an amputee versus an able-bodied subject. Note that the "neural controller" is identical in both cases, emphasizing the assumption that the prosthesis user relies on the same computational mechanisms as an able-bodied subject, but

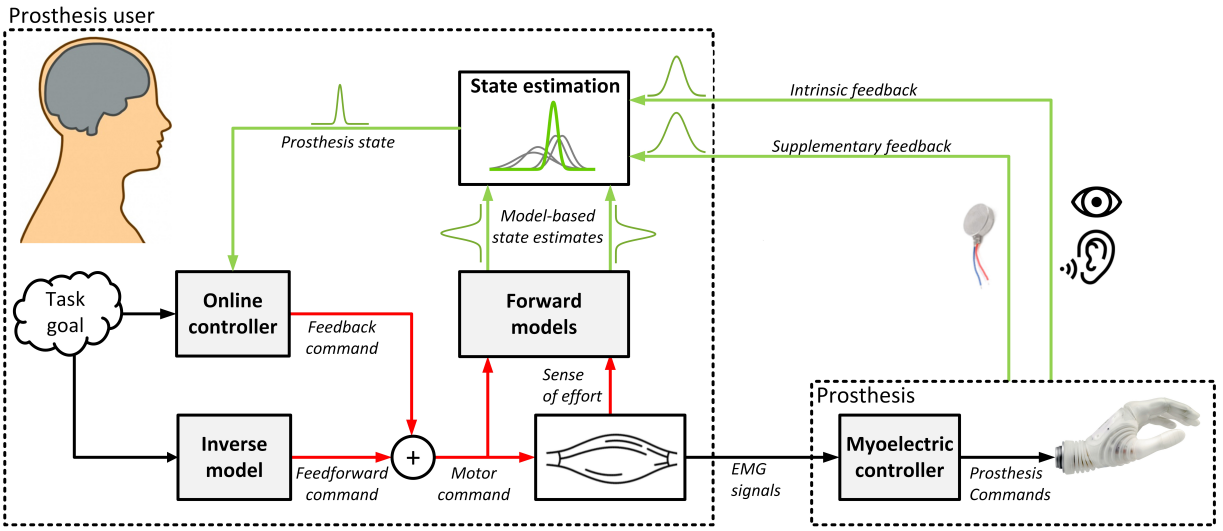

FIGURE 1 | The role of feedback in the larger picture of motor control of a prosthetic arm. The figure illustrates that feedback is only one portion of a broader control paradigm. This should be taken into account when designing methods to provide supplementary feedback. To be successful, the feedback has to make a positive impact within the overall control scheme.

that they must deal with radically different system dynamics and sensory inputs.

THE ROLE OF FEEDBACK FOR PROSTHESIS USERS

The importance of restoring feedback for prosthesis users is not a new idea. As early as 1917, Rosset (1917) (Patent No. DE301108) had patented a mechanism that relayed finger pressure via pneumatic or mechanical means. Describing his motivation, he said "An artificial limb, especially a hand substitute, will always displease the user because of the missing sensation of touch, when grasping objects. Thus the amputee when using the prosthesis, depends entirely on the visual sense . . . It is safe to assume that one of the chief reasons arm amputees prefer to do without an artificial hand is the absence of the tactile sense in the substitute."(Childress, 1980). Work in Italy before 1925 explored similar concepts, mapping finger pressure to thorax skin via pneumatic means (Martin, 1925). Many others followed, including the Vaduz prosthetic hand (Lucaccini et al., 1966) in the 1940's and patents by Goldman (1951) (Patent No. 2567066) and Gonzelman et al. (1953) (Patent No. US2656545 A). Norbert Weiner, a leader in the field of robotics and prostheses in the mid 20th century said "the present artificial limb removes some of the paralyzes caused by amputation but leaves the ataxia. With the use of proper receptors, much of the ataxia should disappear as well, and the patient should be able to learn reflexes." (Childress, 1980). It is clear that engineers have been keen to implement feedback solutions throughout the realm of modern prosthesis design.

For classic reviews of feedback, see Childress (1980); Scott (1990), and Kaczmarek et al. (1991). For recent reviews see Schultz and Kuiken (2011); Antfolk et al. (2013c), Schofield et al. (2014), and Svensson et al. (2017). In these manuscripts, the studies investigating supplementary feedback were organized according to the methods used (e.g., invasiveness, stimulation modality). In the present review, on the contrary, we divide the studies based on how and which components of the motor control framework (**Figure 1**) are impacted by the feedback. Conventional perspectives on feedback in prosthesis control have typically divided feedback into three categories (Childress, 1980). The most popular of these categories—and the focus of this review—is supplementary feedback, i.e., the feedback provided to the user of a prosthesis. Following an extensive review on this topic, the other two categories, which include feedback to change system properties and control-interface feedback, will be briefly summarized (see section "Other applications of feedback").

Supplementary Feedback

The majority of studies have focused on the use of supplementary continuous feedback to improve real-time regulation, as we will see below, but it is important to note that discrete stimulation may also be used, and that the feedback may supply information not only for real-time regulation but also for biofeedback and learning and adaptation. We illustrate these potential impacts of feedback in **Figure 3**, and review the literature within each one in the following subsections.

Continuous Feedback for Real-Time Control

The vast majority of studies have included feedback with a goal of improving real-time closed-loop control (see Antfolk et al., 2013c; Schofield et al., 2014; Svensson et al., 2017 for recent reviews). Childress noted in 1980 that vision was critical as additional source of information (Childress, 1980). Vision supplies information about position and velocity. This information may be used to reliably infer forces – particularly low forces directly after contacting an object (Ninu et al., 2014).

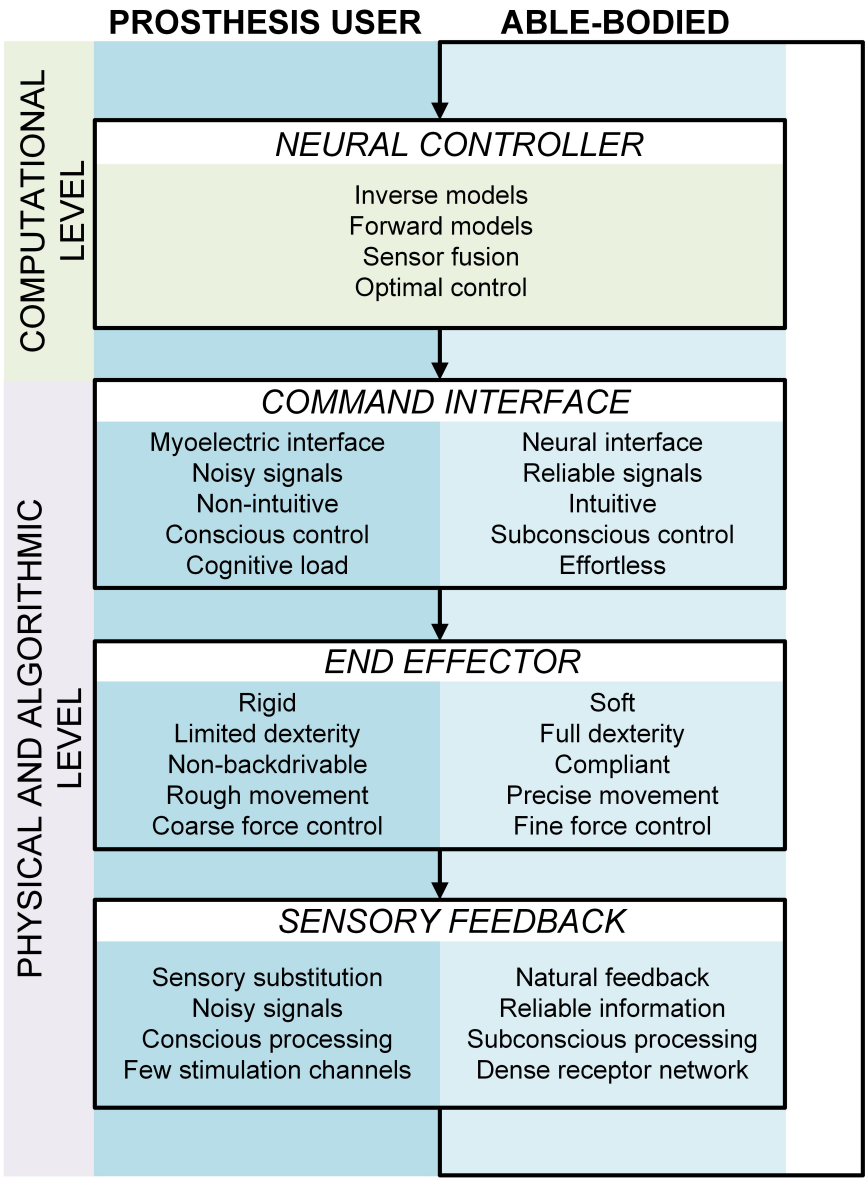

FIGURE 2 | A comparative view of the closed-loop control system in an able-bodied subject (light blue track) versus a prosthesis user (dark blue track). The neural controller (brain) is common to both tracks but the other components (control interface, end effector and sensory feedback) differ fundamentally.

Visual cues from deformable objects and the prosthetic hand also supply a surprising amount of context about grasp force. As a result, it is essential when evaluating the clinical utility of any supplementary feedback source to compare it to a baseline of vision. Yet surprisingly, most studies only evaluate supplementary feedback vs. a baseline that occludes vision. In the absence of vision, somatosensory feedback delivered through different interfaces (e.g., vibro-, electro-, and mechanotactile) was shown to be useful in a variety of tasks, such as, controlling hand aperture (Witteveen et al., 2012), grasping force (Witteveen et al., 2015), joint position (Mann and Reimers, 1970; Erwin and Sup, 2015), object size and stiffness discrimination (D'Anna et al., 2019) etc. Of the many studies exploring real-time feedback (see **Table A1** in the **Appendix**), only a few have shown clinical performance improvements in the presence of vision. Each of these will be reviewed below.

Several studies have shown improvement in a virtual reality environment. Although this is a step in the right direction, virtual environments typically do not have the same richness of visual information (for example, virtual objects are completely non-deformable, unlike the real world, where the cosmesis of the prosthetic hand always deforms). Kim and Colgate (2012) showed that providing grasp force via a manual plunger improved performance of a virtual task, using a patient who had targeted sensory reinnervation – a procedure in which afferent

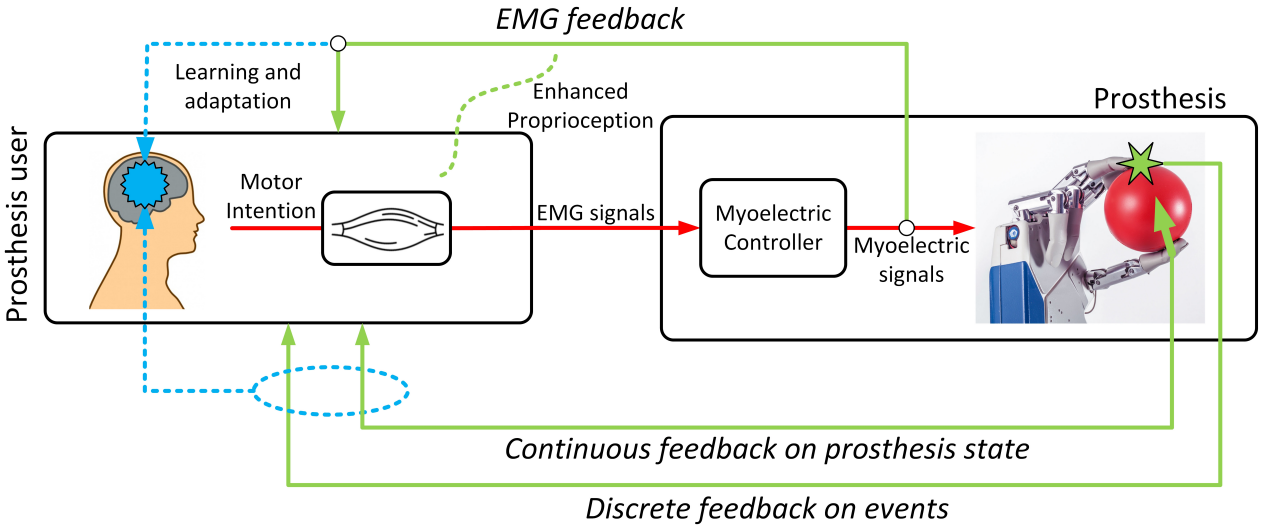

FIGURE 3 | Types of feedback. Feedback is useful for more than real-time continuous regulation. It can supply information about important events (e.g., contact), enhance natural proprioception (sense of effort), and facilitate learning and adaptation through the development of internal models.

fibers that used to go to the hand are rerouted to spare skin (Kuiken et al., 2007a,b; Marasco et al., 2009). Tejeiro et al. (2012) compared mechanical and vibratory feedback of grasp force in a virtual task, and found that both were better than vision alone. Jorgovanovic et al. (2014) used amplitude-modulated electrotactile feedback on grasping force in a virtual prosthesis, and demonstrated that the feedback improved performance while grasping a set of daily life objects of different weights and breaking thresholds. Finally, Dosen et al. (2015a) found that providing visual biofeedback regarding the control signal (processed myoelectric signal) improved control of a virtual hand. In this study, the subjects saw a virtual prosthesis on the computer screen, but they actually controlled a real prosthesis in the background. These studies are each noteworthy in that vision was provided, and yet a convincing improvement was found with supplementary feedback.

There is only one known study in the 20th century that found a clinical improvement using supplementary feedback, namely Meek's 1989 study (Meek et al., 1989), in which grasp force was conveyed via mechanical means. The subjects were more successful in using prosthesis to grasp and manipulate brittle objects without breaking or dropping them when supplementary feedback was provided in presence of vision compared to vision alone. It is likely that with more subjects and proper statistical analysis, Patterson and Katz would have found similar results in their 1992 study (Patterson and Katz, 1992). Zafar and Van Doren (2000) demonstrated a clinical improvement mapping grasping force to surface electrical stimulation in the presence of vision. Although they used video of a sound hand rather than the device itself, the video was of an actual hand deforming an object, and thus supplied realistic visual cues.

Within the last decade, several groups have made impressive progress along both non-invasive and invasive routes. Gonzalez et al. (2012) has shown that providing hand configuration via audio cues improves performance and reduces mental loading (González et al., 2010). Shehata et al. (2018a) has shown that providing pattern recognition error improves the ability to learn internal models and results in an accompanying improvement in performance. Schweisfurth et al. (2016) showed that myoelectric feedback delivered using electrotactile stimulation with mixed frequency and amplitude coding outperformed conventional force feedback during control of grasping with a prosthetic hand. In a recent study, Markovic et al. (2018a) tested multimodal vibrotactile feedback communicating prosthesis state, contact and force in several functional tasks and across multiple sessions, and demonstrated that the benefits of feedback depended on the task and session (training). Marasco et al. (2018) showed that inducing the kinesthetic illusion in TMR amputees improved real-time feedback (as well as other properties, highlighted below). Cipriani's group used discrete-event feedback (expanded below), and found an improvement in performance (Clemente et al., 2016; Aboseria et al., 2018). All these studies share a common theme of tapping into a use for feedback that is not redundant with the role played by vision. More specifically, the feedback in these cases transmits variables that are not assessable through vision (e.g., myoelectric signals, change in active function) and/or variables that are difficult to see clearly (e.g., moment of contact with an object), which according to section "State estimation" is likely to improve the overall quality of state estimation.

Regarding invasive techniques, Tan et al. (2014) produced natural electrical feedback in long-term implanted electrodes that conveyed information of finger forces, and demonstrated improved performance of a cherry-picking task. They used specific stimulation properties to mimic natural sensation (Graczyk et al., 2016), and followed up demonstrating improved performance after at-home use (Graczyk et al., 2018).

Micera's group (Valle et al., 2018a) has recently demonstrated similar success with feedback facilitating a delicate task (e.g., virtual egg test).

Discrete Feedback for Event Confirmation

As early as 1992, Johansen had developed a paradigm in which the primary role of feedback was to confirm the initiation and termination of discrete events (Johansson and Cole, 1992). Cipriani's group pursued this idea, developing actuators embedded in electrodes that were able to supply temporally discrete feedback indicating moment of object contact and release. They showed that humans incorporate this feedback, even in the presence of vision, during a grasp and lift task (Cipriani et al., 2014). More recently they have shown that the discrete feedback improves performance (Clemente et al., 2016) and reduces slips (Aboseria et al., 2018). Discrete feedback was largely off the map of prosthetic feedback until the work of Johansen and Cipriani. It is now commercially available and seems likely to have a positive impact on the field. The feedback on contact was also combined with other continuous and discrete modalities, for example, force and velocity (Ninu et al., 2014) and prosthesis state and force (Markovic et al., 2018a). However, in these studies, the individual effects of these modalities on performance were not investigated. A recent study has explored the interaction between discrete tactile feedback and continuous audio biofeedback focusing on the impact that they have on the formation of internal models (Engels et al., 2019). Contrary to expectations, the results seem to imply that when the two modalities were combined, discrete feedback dominated the continuous information. In several studies, the supplementary feedback was used to communicate the event of object slippage prompting the subject to increase the force and prevent losing the object (Aboseria et al., 2018; Zollo et al., 2019).

Biofeedback to Facilitate Forward Models (Efference Copy)

Dosen et al. (2015a) study provided feedback regarding the myoelectric signal (Dosen et al., 2015a; Schweisfurth et al., 2016). At first glance, this might seem strange, as it is the user who produced the myoelectric signal in the first place, and furthermore, it is a noisy signal. Why not wait until the signal has produced a movement in the prosthesis, and convey seemingly more useful and less noisy information about prosthesis position, velocity, or force? Our review of computational motor control above suggests two key benefits of providing biofeedback, which has long been used for training and therapeutic motives (Ince et al., 1984). First, supplying feedback at an intermediate stage enables the user to develop more precise internal models of the mechanism – models that are based on the output caused by the actual signal, rather than the intended signal (see **Figure 1**). This is a noteworthy enhancement. Second, the process of using the myoelectric signal to generate movement takes time, delaying the feedback. Delayed feedback, as we noted above, reduces stable feedback gains. Thus, by relaying the information sooner and allowing the user to predict (using a forward model, or efference copy), they can compensate initially with higher feedback gains, and then correct any minor discrepancies once the final-state feedback arrives using a lower-gain feedback loop (see **Figure 1**).

Delivering Feedback to Improve Feedforward Control (Inverse Model)

Several groups have recently looked at the role of feedback in enabling the development of better internal models. Gillespie et al. (2010) showed that supplementary feedback improved adaptation rates, and internal model development. Saunders and Vijayakumar (2011) demonstrated the importance of inverse models, particularly when control noise was low. Lum et al. (2014) looked at the internal models developed by body-powered prosthesis users, and Johnson et al. (2014, 2017a) looked at the internal models developed by myoelectric prosthesis users. Ninu et al. (2014) showed how vision could reliably convey force information – presumably through an internal model mapping velocity prior to contact to force after contact. Johnson et al. (2017b) manipulated sensory feedback to show its impact on internal model strength. Marasco et al. (2018) demonstrated improved internal model development when kinesthetic illusion was added to targeted muscle reinnervation (TMR) amputees. Shehata et al. (2018a,b,c) demonstrated that improvements in internal model strength via auditory supplementary feedback resulted in improved efficiency and performance. The ability of feedback to improve internal models is a key area to focus in recent and future work.

To promote the use of feedback for the development of internal models, Dosen et al. (2015b) have introduced the paradigm of routine grasping. In this approach to prosthesis control, the subjects are encouraged to close the prosthesis fast by generating feedforward commands. The feedback is therefore not used for online modulation of force as, for example, during slow and careful closing, but for supplying an end-point feedback on the generated force to help adaptation across trials. They have investigated this paradigm and demonstrated (De Nunzio et al., 2017; Strbac et al., 2017) that feedback is useful initially but that its benefits decrease with training, as the subject becomes better in controlling the prosthesis through developed inverse models.

Psychological Aspects

Several psychological aspects are influenced by feedback. These aspects are important in their own right, but they also indirectly affect performance. For example, agency has been linked to intentional binding – the subjective binding in time of voluntary actions to their sensory consequences (Haggard et al., 2002; Legaspi and Toyoizumi, 2019), suggesting that when a person has agency over their prosthetic limb, movements seems shorter. It is likely that there is a two-way interaction between the computational motor control, as it applies to a user of a prosthetic limb, and the psychological factors, such as agency, ownership and user experience in general (e.g., improved control leads to better embodiment which might further facilitate the control). Because user dissatisfaction with a lack of agency over their movements has been linked to device abandonment (Biddiss and Chau, 2007; Biddiss et al., 2007), some have suggested that improved agency likely leads to better acceptance

of devices (Marasco et al., 2018). These concepts will be briefly reviewed below.

Agency

Agency refers to the feeling of controlling actions that influence events in the outside world (Moore and Fletcher, 2012). Some groups have posited that agency arises from processes involved in motor control (Blakemore et al., 2002; Haggard, 2005), and particularly the forward model aspect of internal models (Blakemore et al., 2000, 2002). Other groups believe that agency is formed when external senses are cued (Wegner, 2002, 2003). Recent research has suggested that both motor control and external cues are integral to establishing a sense of agency (Wegner and Sparrow, 2004; Wegner et al., 2004; Synofzik et al., 2008; Moore et al., 2009). In this context agency fits in well with the concept of computational motor control discussed above (Moore and Fletcher, 2012; Legaspi and Toyoizumi, 2019). Within this framework, sensory feedback is critical to both improving the forward models of motor control, affirming motor control via efference copy, and providing relevant contextual feedback that can help with cueing.

Marasco et al. (2018) recently showed that providing kinesthetic feedback via eliciting kinesthetic illusion in targeted muscle reinnervation subjects established a sense of agency over their prosthetic arms. They hypothesized that kinesthesthetic feedback – the sensation of the limb moving in space – was particularly important in creating a sense of agency. It is hopeful that further research by their group and others will further explore the concept of agency.

Incorporation

Incorporation is the concept that an object, such as a hand or even a tool such as a hammer, has become part of your body schema. It may be assessed using surveys (Marasco et al., 2018), thermal maps (Marasco et al., 2011), or via temporal judgment assessment tests such as the cross-modal congruency effect (Maravita et al., 2003; Holmes et al., 2004; Blustein et al., 2018b). Providing touch feedback via targeted sensory reinnervation has been shown to improve incorporation (Marasco et al., 2011). The other types of supplementary feedback including vibration, mechanical indentation, and electrical stimulation have demonstrated varying degrees of improved incorporation of a prosthetic limb (Blustein et al., 2018b; Graczyk et al., 2018; Valle et al., 2018a; Cuberovic et al., 2019).

It is noteworthy that whereas recent studies have suggested that dynamic feedback, in the form of kinesthesia, is required to obtain agency, event confirmation feedback, in the form of touch, is required to establish incorporation. Although the topics of agency and incorporation are evolving along with their nomenclature, several researchers have suggested that the combination of incorporation and agency results in embodiment (Longo et al., 2008; Marasco et al., 2018), which is accordingly defined as having agency over your body. It therefore appears that to achieve full embodiment, both kinesthetic and tactile forms of feedback are needed, although further research is required to solidify the possibilities.

Phantom Limb Pain

Phantom limb pain is pain perceived as arising from the missing limb due to sources other than stimulation of nociceptive neurons that used to innervate the missing limb (Ortiz-Catalan, 2018). Phantom limb pain can be debilitating and is common after amputation.

It is unclear how phantom limb pain occurs, although there are a number of competing theories including sensory-motor incongruence (similar to motion sickness) (Harris, 1999), cortical reorganization (Flor et al., 1995; Knecht et al., 1998; Lotze et al., 1999, 2001; Grüsser et al., 2001), reduced functional connectivity (Makin et al., 2013), and stochastic entanglement (Ortiz-Catalan, 2018). The latter theory, which is also the most recent one, postulates that stochastic entanglement can occur between networks responsible for sensorimotor processing and paint perception. Many have speculated that phantom limb pain and embodiment are closely connected (Giummarra et al., 2008; Murray, 2008).

Sensory feedback plays a role in all these theories, although not all of them require sensory feedback to alleviate phantom limb pain if motor control is restored.

A number of studies have shown improvements in phantom pain, either through purely therapeutic techniques such as mirror therapy (Chan et al., 2007; Foell et al., 2014) and sensory stimulation/discrimination (Rossini et al., 2010; Horch et al., 2011; Tan et al., 2014), or through actively engaging in the use of the device, as seen through use of myoelectric prostheses (Lotze et al., 1999), targeted muscle reinnervation surgery (Dumanian et al., 2019), or phantom motor execution (Ortiz-Catalan, 2018). Several clinical studies have found that use of devices has reduced phantom limb pain (Lotze et al., 1999; Dumanian et al., 2019), and some laboratory studies have shown reductions in phantom limb pain due to sensory feedback (Rossini et al., 2010; Dietrich et al., 2012, 2018), but no clinical feedback devices are yet available. Based on any of the competing theories, however, it is likely that supplying supplementary sensory feedback would reduce phantom limb pain, and this is a strong area for future research.

Other Applications of Feedback

Although most studies focus on the use of feedback to provide supplemental information to the user, feedback may also be used to change system properties, and as a type of control interface (Childress, 1980). We briefly review these uses below.

Feedback to change system properties refers to the use of feedback as a part of a local loop within the artificial controller. Many designs within this category use feedback to enable shared control [e.g., artificial reflexes (Salisbury and Colman, 1967; Rakic, 1969; Ring and Welbourn, 1969; Kyberd and Chappell, 1994), computer vision based control (Markovic et al., 2014; Marković et al., 2015; Ghazaei et al., 2017)]. Considering the discussion in the section on agency, when these systems work less than perfectly, relinquishment of autonomy to an external agent might cause frustration by users. Other designs modulate system behavior (e.g., decrease control gain after contact detection; Wettels et al., 2009). These designs enable competing costs such as speed and accuracy to be

given prominence during those portions of the task for which they are more likely to be valued, while keeping autonomy with the user. Other designs use feedback to linearize control mechanisms (Bottomley, 1965), which due to static friction, backlash, and resistance from cosmetic gloves are often highly non-linear in prostheses. Although some have commented that this feedback is unnecessary as humans can compensate with visual feedback, the use of feedback to linearize prostheses enables better internal model formation [see Acerbi et al. (2014) for a discussion of difficulties learning more complicated internal models], as well as more reliable control as the local feedback loop can run with less visual delay than the human visual system. Designed properly, these applications of feedback to change system properties can contribute importantly to the closed-loop prosthesis control.

In control-interface feedback, the feedback to the user is inherent in the control process. Driving a powered car is an example of this concept. The control process has been designed in such a way that the user must exert force on the wheel to move it, and if the wheel encounters resistance, this resistance is inherently passed on to the user. Body-powered prostheses provide this form of feedback, as the user can feel the tension in the cable. The Vaduz hand used it as well, routing the force pneumatically (Lucaccini et al., 1966). Simpson termed this concept extended physiological proprioception, and demonstrated its utility across a series of studies in the 1960's and 1970's (Simpson, 1972, 1974; Simpson and Smith, 1977). Others have formally quantified the performance of such systems, which combine both control and sensory aspects (Doubler and Childress, 1984a,b). In non-invasive approaches, the end-effector is actuated by moving a body part (e.g., contralateral shoulder) through the cables attached around the body segment, but there is also an invasive version, where the cable of the end effector is connected to the muscle through a skin tunnel created in a surgical operation [i.e., cineplasty (Gale and Hueston, 1957)]. The last extensive research work in this area was done by Weir (1995), and in recent decades the idea has faltered, and is rarely clinically used outside of body-powered prostheses.

IMPLICATIONS

Guidelines for Experimental Design/Assessment

A variety of experimental approaches have been used to assess supplemental feedback. Importantly, the methods differ substantially with respect to the level of sensory-motor integration that is embodied by the experimental setup (**Figure 4**). This in turn determines which components of the motor control loop will be operative in the task, and this is critical in judging the scope of the study outcomes.

The conventional psychometric assessment, which has been used in a number of studies (Szeto and Saunders, 1982; Kaczmarek et al., 1991), investigates sensory experience. In a typical approach, the subject is passive while stimulation is being delivered and he/she is asked to report on the quality and quantity of elicited sensations. In a more interactive setup, the subject can use a joystick to reproduce the intensity and/or frequency of tactile stimulation (e.g., open-loop electrotactile tracking) (Szeto and Lyman, 1977; Anani and Körner, 1979). This allows testing the quality of perception of versatile and dynamic stimulation profiles, but the sensory-motor loop is essentially open.

In closed-loop tracking, the task for the subject is to control a simulated dynamic system using a command interface (e.g., a joystick or myoelectric control) while the feedback on the state of the system is provided through tactile stimulation (Seeley and Bliss, 1966; Schori, 1970; Schmid and Bekey, 1978; Dosen et al., 2014; Paredes et al., 2015). The aim is to generate the control input so that the system output produces a desired reference trajectory. Most commonly, the tactile feedback transmits the momentary tracking error (i.e., so called compensatory tracking; McRuer and Weir, 1969). Therefore, in this experimental paradigm, the subject not only perceives the tactile feedback but also interprets the information and decides on the control action. Compared to simple psychometric testing, this is closer to controlling a real prosthesis. However, some of the components that exist in the realistic control loop (e.g., incidental feedback) are not available in this paradigm. This method has been used to determine the frequency characteristics of the human controller relying on tactile feedback (Schmid and Bekey, 1978), and the impact of stimulation parameters and precision of feedback information (Schori, 1970; Paredes et al., 2015) on the quality of closed-loop control.

Controlling an actual prosthesis while visually and auditory blinding the subjects is a popular approach that is used in many studies in the literature (Raspopovic et al., 2014; Valle et al., 2018b). In reality, this paradigm is not that different from the aforementioned closed-loop tracking, where an actual prosthesis is used in place of a simulated system. Not surprisingly, such experiments consistently demonstrate that the explicit feedback is beneficial for prosthesis control performance. These studies can be used to demonstrate that a particular feedback interface is effective in transmitting desired information, but they do not tell us much about the expected benefits in the actual clinical applications.

In some studies, the subjects can freely observe the prosthesis motion, but the setup is still not fully realistic. For example, the prosthesis can be placed on the table in front of the subject instead of attaching it to the forearm or residual limb (Ninu et al., 2014; Dosen et al., 2015b). The advantage of this approach is that it is possible to investigate specific aspects of the user-prosthesis interaction, while blocking cofounding factors (e.g., prosthesis weight). Finally, the most realistic setup is when the prosthesis is mounted on the subjects and used to accomplish a functional task (Chatterjee et al., 2008; Brown et al., 2015; Pistohl et al., 2015; Clemente et al., 2016, 2019; Raveh et al., 2017; Markovic et al., 2018a).

The motor control perspective discussed in the present manuscript can be used to propose a set of guidelines for designing and conducting experiments evaluating closed-loop prosthesis control. The underlying principle is that the feedback needs to be approached holistically as a component inseparably connected to the other parts of the motor control loop (**Figure 1**).

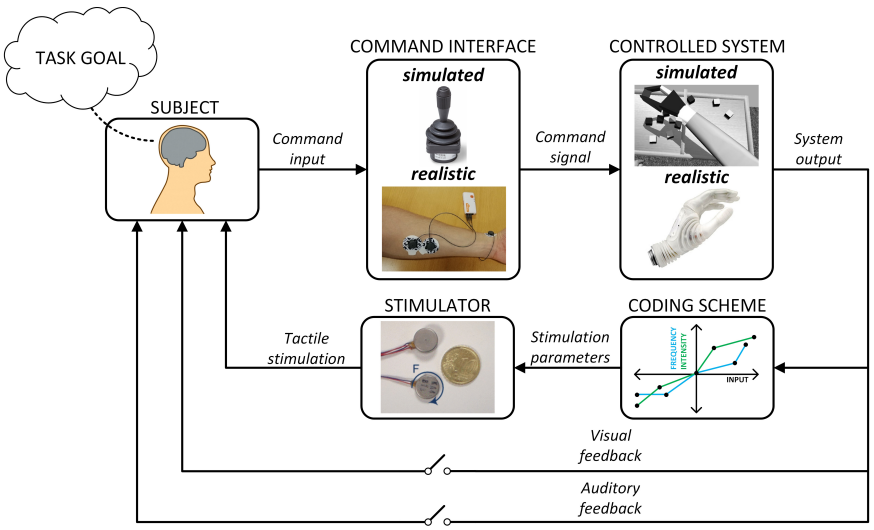

FIGURE 4 | Closed-loop control with supplementary feedback. The interplay between intrinsic feedback sources such as vision and audition with supplementary feedback (including the stimulator and coding scheme) depends on the fidelity of the command interface and the controlled system. These factors can be investigated experimentally by combining virtual and realistic command interfaces and systems, different feedback methods and coding schemes, and allowing or blocking the sources of incidental feedback (e.g., blinded subjects).

Therefore, when designing experiments, it is useful to consider, describe and/or address not only the feedback interface but the other segments of the framework as well. This leads us to the following set of recommendations:

- The operation of a prosthesis control interface needs to be clearly explained, so that the level of variability in the generation of control signals can be estimated (or even better, explicitly reported). This variability relates to signal fluctuations around a desired level as well as to the consistency with which different signal levels can be produced across trials.
- The stimulation method and information-coding scheme translating prosthesis variables into stimulation parameters need to be clearly specified and/or psychometrically tested in order to be able to estimate the uncertainty with which the subject can perceive and interpret the feedback. As discussed in section "State estimation," humans consider both control and sensory noise when developing optimal policies and that is why it is important to describe the characteristics of both noise sources.
- It is important to know the level of experience of a subject participating in the experiment. The experience determines the existence and quality of internal models, and thereby the weight that the subject would place on the feedback versus feedforward approach to control.
- It is relevant to test the proposed closed-loop control interface in subjects with different experience (naïve versus experienced users of myoelectric prostheses) as well as across multiple sessions. The latter is important for assessing the impact of learning and adaptation, and the effect that feedback might have on the development of internal models.
- For studies aiming to demonstrate clinical impact, the performance of developed closed-loop control should be assessed without blocking incidental sources of feedback (e.g., vision and audition) to allow for sensory integration, which will anyway take place during actual clinical use.
- The intended role and application of proposed feedback needs to be clearly stated. For example, is the intention to use the feedback for online modulation or to provide an end-point feedback to facilitate adaptation across trials? Is the feedback aimed at assisting forward and/or inverse model development?

The proposed points are "ideal" requirements and we are fully aware of the challenges that the researchers in this field are facing (e.g., difficulties in recruiting amputee subjects). Therefore, it is clear that it would be very difficult (probably unfeasible) to address all the points within a single study. The aforementioned guidelines should be understood as a list of factors that can be considered and/or discussed to make the study as complete as possible.

Discussion

In this section, we emphasize certain strategic areas that need to be further investigated in order to design effective interfaces for supplementary feedback in prosthetics. These areas arise directly from the framework that is proposed and discussed in the present manuscript.

Our framework advocates that the challenge of effective closed-loop prosthesis control should be approached from the perspective of human motor control. Therefore, we should first develop a better understanding of how different components (internal models) and motor control processes (estimation, optimal policy) operate in an amputee subject. To this

aim, we need theoretical and experimental tools to model, predict and assess those components and processes during myoelectric control and prosthesis operation. We have recently developed methods along this line to measure the strength of internal models in this context (Johnson et al., 2017a; Blustein et al., 2018a; Marasco et al., 2018). In addition, as indicated in sections "Biofeedback to facilitate forward models (efference copy)" and "Delivering feedback to improve feedforward control (inverse model)," some studies have already explicitly addressed the interaction between supplementary feedback and internal models. These tests provided important insights about the interplay between feedforward and feedback mechanisms during prosthesis control as well as some practical guidelines for designing more effective feedback interfaces. The main hypothesis stemming directly from the motor control framework is that to be effective, the feedback needs to be designed so that it makes an impact after it has been integrated with the other components of the motor control loop. Still, almost nothing is known about the cost functions that govern prosthesis control or the optimal policies that amputees use to accomplish different daily life tasks. Shedding light on these components is an imperative to achieve full understanding of optimal control as it applies to prosthetics. This will pave the way for the development of an effective feedback interface, which can make an impact in a daily life of an amputee.

The assessment of feedback is another important topic to be further developed. Presently, it is very difficult to compare the results across different studies since they use substantially different experimental tasks and outcome measures. Most of the clinical tests that are normally used to evaluate prosthesis operation were not really designed to assess the use of closed-loop control. For example, box and blocks, SHAP and clothespin tests can all be accomplished by exerting maximum grasping force, and the grasp economy (e.g., penalizing excessive forces) is not included in the assessment. Therefore, researchers are forced to come up with their own tasks, which leads to a variety of tests. Even in the context of delicate grasping, the selected tasks can be very different, from virtual eggs (Clemente et al., 2016) and sensorized blocks (Meek et al., 1989; Cipriani et al., 2014), which simulate sensitive and brittle objects, to cherry picking (Tyler, 2016) and cup stacking tasks (Markovic et al., 2018a; Clemente et al., 2019) that employ compliant objects. Nevertheless, some of the tests already begin to be applied across research groups (e.g., virtual egg and cup stacking). A promising initiative to develop a standardized battery of tests has been undertaken by the group around HAPTIX project. Importantly, the proposed tests span different scenarios, including an application of Fitts channel capacity to implicit grasp force (Thumser et al., 2018; George et al., 2019), performing functional tasks (e.g., object foraging; Beckler et al., 2019), assessing prosthesis incorporation (Blustein et al., 2018b), and fusing together compensatory motions with eye tracking metrics (Lavoie et al., 2018). A particularly relevant step is the assessment of the prosthesis use longitudinally, across multiple sessions and ideally, in a home environment. And indeed, a recent study has demonstrated that prosthesis performance as well as user experience change dynamically with long-term use (Schofield et al., 2020).

The many methods that are available to provide feedback differ also in the amount of information that they transmit to the subject. Most studies deliver feedback in the form of a continuous tactile signal (e.g., transmitting force through amplitude or frequency of vibrations). Nevertheless, it has been recently proposed to use a low-bandwidth discrete feedback communicating only contact events (Clemente et al., 2016). On the other side, some researchers tested approaches that increase the communication bandwidth, e.g., through the use of visual interfaces [e.g., augmented reality glasses (Clemente et al., 2017; Markovic et al., 2017)] or acoustic signals (Gonzalez et al., 2012; Shehata et al., 2018b). This can be also done through the tactile sense by employing electrodes that integrate a matrix of stimulating pads (Štrbac et al., 2016). Such interfaces can deliver dynamic stimulation patterns that are modulated in location and time and that can communicate multiple feedback variables simultaneously. In addition, matrix electrodes can be used to generate spatially distributed tactile sensations that mimic natural feedback provided by biological hands (e.g., a pressure distribution when grasping an object) (Franceschi et al., 2017; Seminara et al., 2019), especially if coupled with the recent technologies for advanced sensing (e.g., artificial skins; Kim et al., 2014). This research is still in an early stage and it is yet to be investigated what impact such feedback can have on the prosthesis performance and sense of embodiment.

Although outside the scope of this review, the topic of supplementary feedback, particularly seen through the lens of motor control, has important ramifications for our understanding of co-adaptation (e.g., Hahne et al., 2017) and abstract decoding (e.g., Dyson et al., 2018) within the realm of pattern recognition and machine learning. Recent work in this area has benefited from insight within the realm of motor control to provide improved performance (e.g., Ison et al., 2016). As we have argued throughout, the role of feedback is inherently intertwined with that of control and the user (see **Figure 1**). A specific approach to control can directly affect the intrinsic feedback cues that the user can rely upon when estimating the state. For example, in a conventional proportional controller, the user can estimate the prosthesis grasping force using natural muscle proprioception (sense of contraction) (Markovic et al., 2018b), which is not possible when employing a gated-ramp controller (Humbert et al., 2002; Saunders and Vijayakumar, 2011), where the user can instead rely on the time elapsed from the moment of contact. A better appreciation for these interactions will lead to better feedback, better control, and ultimately, better performance and user satisfaction.

CONCLUSION

In summary, supplementary feedback has been investigated for use in prostheses for more than 50 years, but has typically

failed to make a clinical impact due to the availability of incidental feedback, the choice of feedback provided, and the inherent noise in many of the sensory feedback information sources. Recent studies have finally started to make a surge in the amount of impactful work in this area. All these works have been designed so that the supplementary feedback makes an impact after integration with the other components of the motor control loop. Many of them have either targeted lower levels of uncertainty (often through invasive techniques), transmitted information that is not already available through the incidental feedback (e.g., myoelectric control signal) or have looked to the role of feedback in providing information outside the realm of real-time control, given that feedback can be an effective instrument for learning and adaptation. As the field continues to advance it is important that we communicate clearly on how each of our studies addresses the various facets of the complicated process (addressed in the guidelines section), and consider the impact of our focused work within the broader process of motor control. Furthermore, this perspective teaches us that feedback and control are essentially inseparable, and therefore, developing prostheses that allow more reliable and sensitive force and position control is an important push towards an effective closed-loop system.

AUTHOR CONTRIBUTIONS

Both authors listed have made a substantial, direct and intellectual contribution to the work, and approved it for publication.

FUNDING

The present work has been supported by the project ROBIN (8022-00243A) funded by the Independent Research Fund Denmark.

ACKNOWLEDGMENTS

We would like to thank reviewers for their thoughtful contributions. In addition, we would like to thank many of our colleagues, who provided feedback as well, including Dan Blustein and Anjana Garathri Arunachalam. The prosthetic hands in **Figures 3, 4** are developed by Prensilia s.r.l. and Otto Bock, respectively. The eye, ear, and muscle icons in **Figures 1**, **3**, were made by Freepik from www.flaticon.com and the picture of a virtual prosthesis in **Figure 4**, has been taken from Lambrecht et al. (2011).

REFERENCES

Aboseria, M., Clemente, F., Engels, L. F., and Cipriani, C. (2018). Discrete vibrotactile feedback prevents object slippage in hand Prostheses more intuitively than other modalities. *IEEE Trans. Neural. Syst. Rehabil. Eng.* 26, 1577–1584. doi: 10.1109/TNSRE.2018.2851617

Acerbi, L., Vijayakumar, S., and Wolpert, D. M. (2014). On the origins of suboptimality in human probabilistic inference. *PLoS Compu. Biol.* 10:e1003661. doi: 10.1371/journal.pcbi.1003661

Anani, A. B., and Körner, L. M. (1979). Afferent electrical nerve stimulation: human tracking performance relevant to prosthesis sensory feedback. *Med. Biol. Eng. Comput.* 17, 425–434. doi: 10.1007/BF02447053

Antfolk, C., Björkman, A., Frank, S., Sebelius, F., Lundborg, G., and Rosen, B. (2012). Sensory feedback from a prosthetic hand based on air- mediated pressure from the hand to the forearm skin. *J. Rehabil. Med.* 44, 702–707. doi: 10.2340/16501977-1001

Antfolk, C., Cipriani, C., Carrozza, M. C., Björkman, A., Lundborg, G., and Rosén, B. (2013a). Transfer of tactile input from an artificial hand to the forearm: experiments in amputees and able- bodied volunteers. *Disabil. Rehabil.* 8, 249–254. doi: 10.3109/17483107.2012.713435

Antfolk, C., D'Alonzo, M., Controzzi, M., Lundborg, G., Rosen, B., Sebelius, F., et al. (2013b). Artificial redirection of sensation from prosthetic fingers to the phantom hand map on transradial amputees: vibrotactile versus mechanotactile sensory feedback. *IEEE Trans. Neural. Syst. Rehabil. Eng.* 21, 112–120. doi: 10.1109/TNSRE.2012.2217989

Antfolk, C., D'Alonzo, M., Rosén, B., Lundborg, G., Sebelius, F., and Cipriani, C. (2013c). Sensory feedback in upper limb prosthetics. *Expert Rev. Med. Devices* 10, 45–54. doi: 10.1586/erd.12.68

Arunachalam, A. G., Englehart, K. B., and Sensinger, J. W. (2019). "Optimized control mapping through user-tuned cost of effort, time, and reliability," in *IEEE International Conference on Rehabilitation Robotics, 2019-June*, Piscataway, NJ: IEEE.

Battaglia, E., Clark, J., Bianchi, M., Catalano, M., Bicchi, A., and O'Malley, M. K. (2019). "Skin stretch haptic feedback to convey closure information in anthropomorphic, under-actuated upper limb soft Prostheses," in *IEEE Transactions on Haptics*, Piscataway, NJ: IEEE

BBC (1998). *The Man Who Lost His Body*. London: BBC.

Beckler, D. T., Thumser, Z. C., Schofield, J. S., and Marasco, P. D. (2019). Using sensory discrimination in a foraging-style task to evaluate human upper-limb sensorimotor performance. *Scie. Rep.* 9:5806. doi: 10.1038/s41598-019-42086-0

Beeker, T., During, J., and de Hertog, A. (1967). Artificial touch in a hand prosthesis. *Med. Biol. Eng.* 5, 47–49. doi: 10.1007/bf02478841

Bernstein, N. (1967). *The Co-ordination and Regulation of Movements*. New York, NY: Pergamon Press.

Bertsekas, D. P. (2014). *Dynamic Programming and Optimal Control*, 4th Edn. Belmont: Athena Scientific.

Biddiss, E., Beaton, D., and Chau, T. (2007). Consumer design priorities for upper limb prosthetics. *Disabil. Rehabil.*2, 346–357. doi: 10.1080/17483100701714733

Biddiss, E. A., and Chau, T. (2007). Upper-limb prosthetics: critical factors in device abandonment. *Am. J. Phys. Med. Rehabil.* 86, 977–987. doi: 10.1097/PHM.0b013e3181587f6c

Blakemore, S., Wolpert, D., and Frith, C. (2002). Abnormalities in the awareness of action. *Trends Cogn. Sci.* 6, 237–242. doi: 10.1016/s1364-6613(02)01907-1

Blakemore, S. J., Wolpert, D., and Frith, C. (2000). Why can't you tickle yourself? *Neuro Rep.* 11, R11–R16.

Blustein, D., Shehata, A., Englehart, K., and Sensinger, J. (2018a). Conventional analysis of trial-by-trial adaptation is biased: empirical and theoretical support using a Bayesian estimator. *PloS Comput. Biol.* 14:e1006501. doi: 10.1371/journal.pcbi.1006501

Blustein, D., Wilson, A., and Sensinger, J. (2018b). Assessing the quality of supplementary sensory feedback using the crossmodal congruency task. *Sci. Rep.* 8, 6203. doi: 10.1038/s41598-018-24560-3

Bottomley, A. (1965). Myoelectric control of powered Prostheses. *J. Bone Joint Surg. Br.* 47, 411–415.

Braun, D. A., Aertsen, A., Wolpert, D. M., and Mehring, C. (2009). Motor task variation induces structural learning. *Curr. Biol.* 19, 352–357. doi: 10.1016/j.cub.2009.01.036

Braun, D. A., Mehring, C., and Wolpert, D. M. (2010). Structure learning in action. *Behav. Brain Res.* 206, 157–165. doi: 10.1016/j.bbr.2009.08.031

Brown, J. D., Paek, A., Syed, M., O'Malley, M. K., Shewokis, P. A., Contreras-Vidal, J. L., et al. (2015). An exploration of grip force regulation with a low-impedance myoelectric prosthesis featuring referred haptic feedback. *J. Neuroeng. Rehabil.* 12:104. doi: 10.1186/s12984-015-0098-1

Chan, B., Witt, R., Charrow, A., Magee, A., Howard, R., Pasquina, P., et al. (2007). Mirror therapy for phantom limb pain. *N. Engl. J. Med.* 357, 2206–2207.

Chatterjee, A., Chaubey, P., Martin, J., and Thakor, N. (2008). Testing a prosthetic haptic feedback simulator with an interactive force matching task. *J. Prosthetics Orthotics* 20, 27–34. doi: 10.1097/01.JPO.0000311041.61628.be

Chhabra, M., and Jacobs, R. A. (2006). Near-optimal human adaptive control across different noise environments. *J. Neurosci.* 26, 10883–10887. doi: 10.1523/JNEUROSCI.2238-06.2006

Childress, D. S. (1980). Closed-loop control in prosthetic systems - historical perspective. *Ann. Biomed. Eng.* 8, 293–303. doi: 10.1007/BF02363433

Cipriani, C., Segil, J. L., Clemente, F., Richard, R. F., and Edin, B. (2014). Humans can integrate feedback of discrete events in their sensorimotor control of a robotic hand. *Exp. Brain Res.* 232, 3421–3429. doi: 10.1007/s00221-014-4024-8

Cipriani, C., Zaccone, F., Micera, S., and Carrozza, M. C. (2008). On the shared control of an EMG-controlled prosthetic hand: analysis of user-prosthesis interaction. *IEEE Trans. Rob.* 24, 170–184. doi: 10.1109/TRO.2007.910708

Cisek, P. (2009). "Internal Models," in *Encyclopedia of Neuroscience*, ed. L. R. Squire (Amsterdam: Elsevier).

Clancy, E. A., Bouchard, S., and Rancourt, D. (2001). Estimation and application of EMG amplitude during dynamic contractions. *IEEE Eng. Med. Biol. Mag.* 20, 47–54. doi: 10.1109/51.982275

Clancy, E. A., Morin, E. L., and Merletti, R. (2002). Sampling, noise-reduction and amplitude estimation issues in surface electromyography. *J. Electromyogr. Kinesiol.* 12, 1–16. doi: 10.1016/s1050-6411(01)00033-5

Clemente, F., D'Alonzo, M., Controzzi, M., Edin, B. B., and Cipriani, C. (2016). Non-invasive, temporally discrete feedback of object contact and release improves grasp control of closed-loop myoelectric transradial Prostheses. *IEEE Trans. Neural. Syst. Rehabil. Eng.* 24, 1314–1322. doi: 10.1109/TNSRE.2015.2500586

Clemente, F., Dosen, S., Lonini, L., Markovic, M., Farina, D., and Cipriani, C. (2017). Humans can integrate augmented reality feedback in their sensorimotor control of a robotic hand. *IEEE Trans. Hum. Mach. Syst.* 47, 583–589. doi: 10.1109/THMS.2016.2611998

Clemente, F., Valle, G., Controzzi, M., Strauss, I., Iberite, F., Stieglitz, T., et al. (2019). Intraneural sensory feedback restores grip force control and motor coordination while using a prosthetic hand. *J. Neural Eng.* 16:026034. doi: 10.1088/1741-2552/ab059b

Clippinger, F. W., Avery, R., and Titus, B. R. (1975). A sensory feedback system for an upper-limb amputation prosthesis. *Bull. Prosthetics Res.* 22, 247–258.

Cuberovic, I., Gill, A., Resnik, L. J., Tyler, D. J., and Graczyk, E. L. (2019). Learning of artificial sensation through long-term home use of a sensory-enabled prosthesis. *Front. Neurosci.* 13:853. doi: 10.3389/fnins.2019.00853

D'Anna, E., Valle, G., Mazzoni, A., Strauss, I., Iberite, F., and Patton, J. (2019). A closed-loop hand prosthesis with simultaneous intraneural tactile and position feedback. *Sci. Robo.* 4:eaau8892. doi: 10.1101/262741

De Luca, C. J. (1979). Physiology and mathematics of myoelectric signals. *IEEE Trans. Bio Med. Eng.* 26, 313–325. doi: 10.1109/tbme.1979.326534

De Nunzio, A. M., Dosen, S., Lemling, S., Markovic, M., Schweisfurth, M. A., Ge, N., et al. (2017). Tactile feedback is an effective instrument for the training of grasping with a prosthesis at low- and medium-force levels. *Exp. Brain Res.* 235, 2547–2559. doi: 10.1007/s00221-017-4991-7

Dhillon, G. S., and Horch, K. W. (2005). Direct neural sensory feedback and control of a prosthetic arm. *IEEE Trans. Neural. Syst. Rehabil. Eng.* 13, 468–472. doi: 10.1109/TNSRE.2005.856072

Dietrich, C., Nehrdich, S., Seifert, S., Blume, K. R., Miltner, W. H. R., Hofmann, G. O., et al. (2018). Leg prosthesis with somatosensory feedback reduces phantom limb pain and increases functionality. *Front. Neurol.* 9:270. doi: 10.3389/fneur.2018.00270

Dietrich, C., Walter-Walsh, K., Preissler, S., Hofmann, G. O., Witte, O. W., Miltner, W. H. R., et al. (2012). Sensory feedback prosthesis reduces phantom limb pain: proof of a principle. *Neurosci. Lett.* 507, 97–100. doi: 10.1016/j.neulet.2011.10.068

Dosen, S., Markovic, M., Somer, K., Graimann, B., and Farina, D. (2015a). EMG Biofeedback for online predictive control of grasping force in a myoelectric prosthesis. *J. Neuro Eng. Rehabil.* 12:55. doi: 10.1186/s12984-015-0047-z

Dosen, S., Markovic, M., Wille, N., Henkel, M., Koppe, M., Ninu, A., et al. (2015b). Building an internal model of a myoelectric prosthesis via closed-loop control for consistent and routine grasping. *Exp. Brain Res.* 233, 1855–1865. doi: 10.1007/s00221-015-4257-1

Dosen, S., Markovic, M., Strbac, M., Belic, M., Kojic, V., Bijelic, G., et al. (2017). Multichannel electrotactile feedback with spatial and mixed coding for closed-loop control of grasping force in hand Prostheses. *IEEE Trans. Neural. Syst. Rehabil. Eng.* 25, 183–195. doi: 10.1109/TNSRE.2016.2550864

Dosen, S., Schaeffer, M.-C., and Farina, D. (2014). Time-division multiplexing for myoelectric closed-loop control using electrotactile feedback. *J. Neuroeng. Rehabil.* 11:138. doi: 10.1186/1743-0003-11-138

Doubler, J. A., and Childress, D. S. (1984a). An analysis of extended physiological proprioception as a prosthesis-control technique. *J. Rehabil. Restorat. Devices* 21, 5–18.

Doubler, J. A., and Childress, D. S. (1984b). Design and evaluation of a prosthesis control system based on the concept of extended physiological proprioception. *J. Rehabil. Restorat. Devices* 21, 19–31.

Dumanian, G. A., Potter, B. K., Mioton, L. M., Ko, J. H., Cheesborough, J. E., Souza, J. M., et al. (2019). targeted muscle reinnervation treats neuroma and phantom pain in major limb amputees. *Ann. Surg.* 270, 238–246. doi: 10.1097/sla.0000000000003088

Dyson, M., Barnes, J., and Nazarpour, K. (2018). Myoelectric control with abstract decoders. *J. Neural Eng.* 15:056003. doi: 10.1088/1741-2552/aacbfe

Engels, L. F., Shehata, A. W., Scheme, E. J., Sensinger, J. W., and Cipriani, C. (2019). When less is more – discrete tactile feedback dominates continuous audio biofeedback in the integrated percept while controlling a myoelectric prosthetic hand. *Front. Neurosci.* 13:578. doi: 10.3389/fnins.2019.00578

Ernst, M. O., and Banks, M. (2002). Humans integrate visual and haptic information in a statistically optimal fashion. *Nature* 415:433.

Erwin, A., and Sup, F. C. (2015). A haptic feedback scheme to accurately position a virtual wrist prosthesis using a three-node tactor array. *PLoS One* 10:e0134095. doi: 10.1371/journal.pone.0134095

Fishbach, A., Roy, S. A., Bastianen, C., Miller, L. E., and Houk, J. C. (2007). Deciding when and how to correct a movement: discrete submovements as a decision making process. *Exp. Brain Res.* 177, 45–63. doi: 10.1007/s00221-006-0652-y

Fitts, P. M. (1954). The information capacity of the human motor system in controlling the amplitude of movement. *J. Exp. Psychol.* 47, 381–391. doi: 10.1037/h0055392

Flanagan, J. R., Bowman, M. C., and Johansson, R. S. (2006). Control strategies in object manipulation tasks. *Curr. Opin. Neurobiol.* 16, 650–659. doi: 10.1016/j.conb.2006.10.005

Flanagan, J. R., King, S., Wolpert, D. M., and Johansson, R. S. (2001). Sensorimotor prediction and memory in object manipulation. *Cana. J. Exp. Psychol. Rev. Can. Psychol. Exp.* 55, 87–95. doi: 10.1037/h0087355

Flanagan, J. R., and Wing, A. M. (1997). The role of internal models in motion planning and control: evidence from grip force adjustments during movements of hand-held loads. *J. Neurosci.* 17, 1519–1528. doi: 10.1523/jneurosci.17-04-01519.1997

Flash, T., and Hogan, N. J. (1985). The coordination of arm movements: an experimentally confirmed mathematical model. *J. Neurosci.* 5, 1688–1703. doi: 10.1523/jneurosci.05-07-01688.1985

Flor, H., Elbert, T., Knecht, S., Wienbruch, C., Pantev, C., Birbaumers, N., et al. (1995). Phantom-limb pain as a perceptual correlate of cortical reorganization following arm amputation. *Nature* 375, 482–484. doi: 10.1038/375482a0

Foell, J., Bekrater-Bodmann, R., Diers, M., and Flor, H. (2014). Mirror therapy for phantom limb pain: brain changes and the role of body representation. *Eur. J. Pain* 18, 729–739. doi: 10.1002/j.1532-2149.2013.00433.x

Franceschi, M., Seminara, L., Dosen, S., Strbac, M., Valle, M., and Farina, D. (2017). A system for electrotactile feedback using electronic skin and flexible matrix electrodes: experimental evaluation. *IEEE Trans. Haptics* 10, 162–172. doi: 10.1109/TOH.2016.2618377

Gale, A. F., and Hueston, J. T. (1957). Muscle training for biceps cineplasty. *Austr. J. Physiother.* 3, 148–151. doi: 10.1016/S0004-9514(14)60934-X

George, J. A., Kluger, D. T., Davis, T. S., Wendelken, S. M., Okorokova, E. V., He, Q., et al. (2019). Biomimetic sensory feedback through peripheral nerve

stimulation improves dexterous use of a bionic hand. *Sci. Rob.* 4:eaax2352. doi: 10.1126/scirobotics.aax2352

Ghazaei, G., Alameer, A., Degenaar, P., Morgan, G., and Nazarpour, K. (2017). Deep learning-based artificial vision for grasp classification in myoelectric hands. *J. Neural Eng.* 14:036025. doi: 10.1088/1741-2552/aa6802

Gillespie, R. B., Contreras-Vidal, J. L., Shewokis, P. A., O'Malley, M. K., Brown, J. D., and Davis, A. (2010). "Toward improved sensorimotor integration and learning using upper-limb prosthetic devices," in *2010 Annual International Conference of the IEEE Engineering in Medicine and Biology Society*. Piscataway, NJ: IEEE, 5077–5080.

Giummarra, M. J., Gibson, S. J., Georgiou-Karistianis, N., and Bradshaw, J. L. (2008). Mechanisms underlying embodiment, disembodiment and loss of embodiment. *Neurosci. Biobehav. Rev.* 32, 143–160. doi: 10.1016/j.neubiorev.2007.07.001

Goldman, I. (1951). *Robot Controlled Limb*. U.S. Patent 2,567,066.

Gonzalez, J., Soma, H., Sekine, M., and Yu, W. (2012). Psycho-physiological assessment of a prosthetic hand sensory feedback system based on an auditory display: a preliminary study. *J. Neuro Eng. Rehabil.* 9, 1–14. doi: 10.1186/1743-0003-9-33

González, J., Yu, W., and Hernandez Arieta, A. (2010). Multichannel audio biofeedback for dynamical coupling between prosthetic hands and their users. *Ind. Rob.*37, 148–156. doi: 10.1108/01439911011018920

Gonzelman, J., Ellis, H., and Clayton, O. (1953). *Prosthetic Device Sensory Attachment*. U.S. Patent No. 2656545.

Gordon, A. M., Forssberg, H., Johansson, R. S., and Westling, G. (1991). Visual size cues in the programming of manipulative forces during precision grip. *Exp. Brain Res.* 83, 477–482. doi: 10.1007/BF00229824

Graczyk, E. L., Resnik, L., Schiefer, M. A., Schmitt, M. S., and Tyler, D. J. (2018). Home use of a neural-connected sensory prosthesis provides the functional and psychosocial experience of having a hand again. *Sci. Rep.* 8, 1–17. doi: 10.1038/s41598-018-26952-x

Graczyk, E. L., Schiefer, M. A., Saal, H. P., Delhaye, B. P., Bensmaia, S. J., and Tyler, D. J. (2016). The neural basis of perceived intensity in natural and artificial touch. *Sci. Trans. Med.* 8, 1–11. doi: 10.1126/scitranslmed.aaf5187

Grüsser, S. M., Winter, C., Muhlnickel, W., Denke, C., Karl, A., and Flor, H. (2001). The relationship of perceptual phenomena and cortical reorganization in upper extremity amputees. *Neuroscience* 102, 263–272. doi: 10.1016/s0306-4522(00)00491-7

Guiard, Y., and Beaudouin-Lafon, M. (2004). Fitts' law 50 years later: applications and contributions from human–computer interaction. *Int. J. Hum. Comput. Stud.* 61, 747–750. doi: 10.1016/j.ijhcs.2004.09.003

Haggard, P. (2005). Conscious intention and motor cognition. *Trends Cogn. Sci.* 9, 290–295. doi: 10.1016/j.tics.2005.04.012

Haggard, P., Clark, S., and Kalogeras, J. (2002). Voluntary action and conscious awarenes. *Nat. Neurosci.* 5, 382–385. doi: 10.1038/nn827

Hahne, J. M., Markovic, M., and Farina, D. (2017). User adaptation in myoelectric man-machine interfaces. *Sci. Rep.* 7, 1–10. doi: 10.1038/s41598-017-04255-x

Haith, A. M., Reppert, T. R., and Shadmehr, R. (2012). Evidence for hyperbolic temporal discounting of reward in control of movements. *J. Neurosci.* 32, 11727–11736. doi: 10.1523/JNEUROSCI.0424-12.2012

Harris, A. J. (1999). Cortical origin of pathological pain. *Lancet* 354, 1464–1466. doi: 10.1016/S0140-6736(99)05003-5

Harris, C. M., and Wolpert, D. M. (1998). Signal-dependent noise determines motor planning. *Nature* 394, 780–784. doi: 10.1038/29528

Hermsdörfer, J., Elias, Z., Cole, J. D., Quaney, B. M., and Nowak, D. A. (2008). Preserved and impaired aspects of feed-forward grip force control after chronic somatosensory deafferentation. *Neurorehabil. Neural Repair.* 22, 374–384. doi: 10.1177/1545968307311103

Holmes, N. P., Calvert, G. A., and Spence, C. (2004). Extending or projecting peripersonal space with tools? Multisensory interactions highlight only the distal and proximal ends of tools. *Neurosci. Lett.* 372, 62–67. doi: 10.1016/j.neulet.2004.09.024

Horch, K., Meek, S., Taylor, T. G., and Hutchinson, D. T. (2011). Object discrimination with an artificial hand using electrical stimulation of peripheral tactile and proprioceptive pathways with intrafascicular electrodes. *IEEE Trans. Neural. Syst. Rehabil. Eng.* 19, 483–489. doi: 10.1109/TNSRE.2011.2162635

Humbert, S. D., Snyder, S. A., and Grill, W. M. (2002). Evaluation of command algorithms for control of upper-extremity neural Prostheses. *IEEE Trans. Neural. Syst. Rehabil. Eng.* 10, 94–101. doi: 10.1109/TNSRE.2002.1031977

Ince, L. P., Leon, M. S., and Christidis, D. (1984). Experimental foundations of EMG biofeedback with the upper extremity: a review of the literature. *Biofeedback Self Regul.* 9, 371–383. doi: 10.1007/bf00998980

Ison, M., Vujaklija, I., Whitsell, B., Farina, D., and Artemiadis, P. (2016). High-density electromyography and motor skill learning for robust long-term control of a 7-DoF robot arm. *IEEE Trans. Neural. Syst. Rehabil. Eng.* 24, 424–433. doi: 10.1109/TNSRE.2015.2417775

Johansson, R. S., and Cole, K. J. (1992). Sensory-motor coordination during grasping and manipulative actions. *Curr. Opin. Neurobiol.* 2, 815–823. doi: 10.1016/0959-4388(92)90139-c

Johansson, R. S., and Westling, G. (1988). Coordinated isometric muscle commands adequately and erroneously programmed for the weight during lifting task with precision grip. *Exp. Brain Res.* 71, 59–57. doi: 10.1007/BF00247522

Johnson, R. E., Kording, K. P., Hargrove, L. J., and Sensinger, J. W. (2014). Does EMG control lead to distinct motor adaptation? *Front. Neurosci.* 8:302. doi: 10.3389/fnins.2014.00302

Johnson, R. E., Kording, K. P., Hargrove, L. J., and Sensinger, J. W. (2017a). Adaptation to random and systematic errors: comparison of amputee and non-amputee control interfaces with varying levels of process noise. *PLoS One* 12:e0170473. doi: 10.1371/journal.pone.0170473

Johnson, R. E., Kording, K. P., Hargrove, L. J., and Sensinger, J. W. (2017b). EMG versus torque control of human-machine systems: equalizing control signal variability does not equalize error or uncertainty. *IEEE Trans. Neural. Syst. Rehabil. Eng.* 25, 660–667. doi: 10.1109/TNSRE.2016.2598095

Jones, K. E., Hamilton, A. F., and Wolpert, D. M. (2002). Sources of signal-dependent noise during isometric force production. *J. Neurophysiol.* 88, 1533–1544. doi: 10.1152/jn.00985.2001

Jorgovanovic, N., Dosen, S., Djozic, D. J., Krajoski, G., and Farina, D. (2014). Virtual grasping: closed-loop force control using electrotactile feedback. *Comput. Math. Methods Med.* 2014:120357. doi: 10.1155/2014/120357

Kaczmarek, K. A., Webster, J. G., Bach-y-rita, P., and Tompkins, W. J. (1991). Electrotactile and vibrotactile displays for sensory substition systems. *IEEE Trans. Biomed. Eng.* 38, 1–16. doi: 10.1109/10.68204

Kato, I., Yamakawa, S., Ichikawa, K., and Sano, M. (1979). "Multifunctional myoelectric hand prosthesis with pressure sensory feedback system: Waseda hand," in *Advances in External Control of Human Extremities ETAN*, Dubrovnik, 155–170.

Kawamura, Z., and Sueda, O. (1969). "Sensory feedback device for the artificial arm," in *4th Pan Pacific Rehabilitation Conference*, Osaka.

Kawato, M. (1999). Internal models for motor control and trajectory planning. *Curr. Opin. Neurobiol.* 9, 718–727. doi: 10.1016/S0959-4388(99)00028-8

Kim, J., Lee, M., Shim, H. J., Ghaffari, R., Cho, H. R., Son, D., et al. (2014). Stretchable silicon nanoribbon electronics for skin prosthesis. *Nat, Commun.* 5:5747. doi: 10.1038/ncomms6747

Kim, K., and Colgate, J. E. (2012). Haptic feedback enhances grip force control of sEMG-controlled prosthetic hands in targeted reinnervation amputees. *IEEE Trans. Neural. Syst. Rehabil. Eng.* 20, 798–805. doi: 10.1109/TNSRE.2012.2206080

Knecht, S., Henningsen, H., Hohling, C., Elbert, T., Flor, H., Pantev, C., et al. (1998). Plasticity of plasticity? Changes in the pattern of perceptual correlates of reorganization after amputation\rPhantom-limb pain as a perceptual correlate of cortical reorganization following arm amputation. *Brain* 121(Pt 4), 717–724. doi: 10.1093/brain/121.4.717

Kording, K. (2007). Decision theory: what "should" the nervous system do? *Science* 318, 606–610. doi: 10.1126/science.1142998

Körding, K. P., and Wolpert, D. M. (2004a). Bayesian integration in sensorimotor learning. *Nature* 427, 244–247. doi: 10.1038/nature02169

Körding, K. P., and Wolpert, D. M. (2004b). The loss function of sensorimotor learning. *Proc. Natl. Acad. Sci. U.S.A.* 101, 9839–9842. doi: 10.1073/pnas.0308394101

Kositsky, M., and Barto, A. G. (2001). The emergence of multiple movement units in the presence of noise and feedback delay. *Adv. Neural Inform. Process. Syst.* 44-46, 889–895. doi: 10.1016/s0925-2312(02)00488-5

Kuiken, T. A., Marasco, P. D., Lock, B. A., Harden, R. N., and Dewald, J. P. A. (2007a). Redirection of cutaneous sensation from the hand to the chest skin of human amputees with targeted reinnervation. *Proc. Natl. Acad. Sci. U.S.A.* 104, 20061–20066. doi: 10.1073/pnas.0706525104

Kuiken, T. A., Miller, L. A., Lipschutz, R. D., Lock, B. A., Stubblefield, K., Marasco, P. D., et al. (2007b). Targeted reinnervation for enhanced prosthetic arm function in a woman with a proximal amputation: a case study. *Lancet* 369, 371–380. doi: 10.1016/S0140-6736(07)60193-7

Kyberd, P. J., and Chappell, P. H. (1994). The Southampton hand - an intelligent myoelectric prosthesis. *J. Rehabil. Res. Dev.* 31, 326–334.

Lambrecht, J. M., Pulliam, C. L., and Kirsch, R. F. (2011). Virtual reality environment for simulating tasks with a myoelectric prosthesis: an assessment and training tool. *J. Prosthet. Orthot.* 23, 89–94. doi: 10.1097/jpo.0b013e318217a30c

Lavoie, E. B., Valevicius, A. M., Boser, Q. A., Kovic, O., Vette, A. H., Pilarski, P. M., et al. (2018). Using synchronized eye and motion tracking to determine high-precision eye-movement patterns during objectinteraction tasks. *J. Vis.* 18, 1–20. doi: 10.1167/18.6.18

Legaspi, R., and Toyoizumi, T. (2019). A bayesian psychophysics model of sense of agency. *Nat. Commun.* 10, 1–11. doi: 10.1038/s41467-019-12170-0

Li, W., and Todorov, E. (2007). Iterative linearization methods for approximately optimal control and estimation of non-linear stochastic system. *Int. J. Control* 80, 1439–1453. doi: 10.1080/00207170701364913

Liu, D., and Todorov, E. (2007). Evidence for the flexible sensorimotor strategies predicted by optimal feedback control. *J. Neurosci.* 27, 9354–9368. doi: 10.1523/JNEUROSCI.1110-06.2007

Longo, M. R., Schüür, F., Kammers, M. P. M., Tsakiris, M., and Haggard, P. (2008). What is embodiment? A psychometric approach. *Cognition* 107, 978–998. doi: 10.1016/j.cognition.2007.12.004

Lotze, M., Flor, H., Grodd, W., Larbig, W., and Birbaumer, N. (2001). Phantom movements and pain. An fMRI study in upper limb amputees. *Brain A J. Neurol.* 124(Pt 11), 2268–2277. doi: 10.1093/brain/124.11.2268

Lotze, M., Grodd, W., Birbaumer, N., Erb, M., Huse, E., and Flor, H. (1999). Does use of a myoelectric prosthesis prevent cortical reorganization and phantom limb pain? *Nat. Neurosci.* 2, 501–502. doi: 10.1038/9145

Lucaccini, L., Kaiser, P., and Lyman, J. (1966). The French electric hand: some observations and conclusions. *Bull. Prosthetics Res.* 30–51.

Lum, P. S., Black, I., Holley, R. J., Barth, J., and Dromerick, A. W. (2014). Internal models of upper limb prosthesis users when grasping and lifting a fragile object with their prosthetic limb. *Exp. Brain Res.* 232, 3785–3795. doi: 10.1007/s00221-014-4071-1

Lundborg, G., Rosén, B., Lindström, K., and Lindberg, S. (1998). Artificial sensibility based on the use of piezoresistive sensors. Preliminary observations. *J. Hand Surg.* 23, 620–626. doi: 10.1016/s0266-7681(98)80016-8

MacKenzie, C., and Iberall, T. (2010). *The Grasping Hand*. Amsterdam: Elsevier.

Makin, T. R., Scholz, J., Filippini, N., Henderson Slater, D., Tracey, I., and Johansen-Berg, H. (2013). Phantom pain is associated with preserved structure and function in the former hand area. *Nat. Commun.* 4, 1570–1578. doi: 10.1038/ncomms2571

Mann, R., and Reimers, S. (1970). Kinesthetic sensing for the EMG controlled Boston arm. *IEEE Trans. Man Mach. Syst.* 11, 110–115. doi: 10.1109/tmms.1970.299971

Marasco, P. D., Hebert, J. S., Sensinger, J. W., Shell, C. E., Schofield, J. S., and Orzell, B. M. (2018). Illusory movement perception improves motor control for prosthetic hands. *Sci. Trans. Med.* 10, 1–13. doi: 10.1126/scitranslmed.aao6990

Marasco, P. D., Kim, K., Colgate, J. E., Peshkin, M. A., and Kuiken, T. A. (2011). Robotic touch shifts perception of embodiment to a prosthesis in targeted reinnervation amputees. *Brain* 134(Pt 3), 747–758. doi: 10.1093/Brain/Awq361

Marasco, P. D., Schultz, A. E., and Kuiken, T. A. (2009). Sensory capacity of reinnervated skin after redirection of amputated upper limb nerves to the chest. *Brain* 132(Pt 6), 1441–1448. doi: 10.1093/brain/awp082

Maravita, A., Spence, C., and Driver, J. (2003). Multisensory integration and the body schema: close to hand and within reach. *Curr. Biol.* 13, R531–R539. doi: 10.1016/S0960-9822(03)00449-4

Markovic, M., Dosen, S., Cipriani, C., Popovic, D., and Farina, D. (2014). Stereovision and augmented reality for closed-loop control of grasping in hand Prostheses. *J. Neural Eng.* 11:046001. doi: 10.1088/1741-2560/11/4/046001

Marković, M., Dosen, S., Popović, D. B., Graimann, B., and Farina, D. (2015). Computer vision and sensor fusion for semi-autonomous control of a multi degree-of-freedom prosthesis. *J. Neural Eng.* 12:066022. doi: 10.1088/1741-2560/12/6/066022

Markovic, M., Karnal, H., Graimann, B., Farina, D., and Dosen, S. (2017). GLIMPSE: google Glass interface for sensory feedback in myoelectric hand Prostheses. *J. Neural Eng.* 14:036007. doi: 10.1088/1741-2552/aa620a

Markovic, M., Schweisfurth, M. A., Engels, L. F., Bentz, T., Wüstefeld, D., Farina, D., et al. (2018a). The clinical relevance of advanced artificial feedback in the control of a multi-functional myoelectric prosthesis. *J. Neuroeng. Rehabil.* 15:28. doi: 10.1186/s12984-018-0371-1

Markovic, M., Schweisfurth, M. A., Engels, L. F., Farina, D., and Dosen, S. (2018b). Myocontrol is closed-loop control: incidental feedback is sufficient for scaling the prosthesis force in routine grasping. *J. Neuro Eng. Rehabil.* 15:81. doi: 10.1186/s12984-018-0422-7

Marr, D. (1982). *A Computational Investigation into the Human Representation and Processing of Visual Information*. New York, NY: Henry Holt and Co.

Martin, F. (1925). *Artificial Limbs*. Geneva: International Labour Office, Studies and Reports, Series No. 5.

McRuer, D., and Weir, D. (1969). Theory of manual vehicular control. *IEEE Trans. Man Mach. Syst.* 10, 257–291. doi: 10.1109/TMMS.1969.299930

Meek, S. G., Jacobsen, S. C., and Goulding, P. (1989). Extended physiologic taction: design and evaluation of a proportional force feedback system. *J. Rehabil. Res. Dev.* 26, 53–62.

Micera, S., Carpaneto, J., and Raspopovic, S. (2010). Control of hand Prostheses using peripheral information. *IEEE Rev. Biomed. Eng.* 3, 48–68. doi: 10.1109/rbme.2010.2085429

Mitrovic, D., Klanke, S., Osu, R., Kawato, M., and Vijayakumar, S. (2010). A computational model of limb impedance control based on principles of internal model uncertainty. *PLoS One* 5:e13601. doi: 10.1371/journal.pone.0013601

Moore, J., Wegner, D., and Haggard, P. (2009). Modulating the sense of agency with external cues. *Conscious Cogn.* 18, 1056–1064. doi: 10.1016/j.concog.2009.05.004

Moore, J. W., and Fletcher, P. C. (2012). Sense of agency in health and disease: a review of cue integration approaches. *Conscious Cogn.* 21, 59–68. doi: 10.1016/j.concog.2011.08.010

Murray, C. D. (2008). "Embodiment and Prosthetics," in *Psychoprosthetics: State of the Knowledge*, eds P. Gallagher, D. M. Desmond, and M. MacLachlan (Berlin: Springer).

Nagengast, A. J., Braun, D. A., and Wolpert, D. M. (2010). Risk-sensitive optimal feedback control accounts for sensorimotor behavior under uncertainty. *PLoS Comput. Biol.* 6:e1000857. doi: 10.1371/journal.pcbi.1000857

Ninu, A., Dosen, S., Muceli, S., Rattay, F., Dietl, H., and Farina, D. (2014). Closed-loop control of grasping with a myoelectric hand prosthesis: which are the relevant feedback variables for force control? *IEEE Trans. Neural Syst. Rehabil. Eng.* 22, 1041–1052. doi: 10.1109/TNSRE.2014.2318431

Ortiz-Catalan, M. (2018). The stochastic entanglement and phantom motor execution hypotheses: a theoretical framework for the origin and treatment of Phantom limb pain. *Front. Neurol.* 9:748. doi: 10.3389/fneur.2018.00748

Ortiz-Catalan, M., Håkansson, B., and Brånemark, R. (2014). An osseointegrated human-machine gateway for long-term sensory feedback and motor control of artificial limbs. *Sci. Trans. Med.* 6:257re6. doi: 10.1126/scitranslmed.3008933

Osborn, L. E., Dragomir, A., Betthauser, J. L., Hunt, C. L., Nguyen, H. H., Kaliki, R. R., et al. (2018). Prosthesis with neuromorphic multilayered e-dermis perceives touch and pain. *Sci. Rob.* 3:eaat3818. doi: 10.1126/scirobotics.aat3818

Osu, R., Burdet, E., Franklin, D. W., Milner, T. E., and Kawato, M. (2003). Different mechanisms involved in adaptation to stable and unstable dynamics. *J. Neurophysiol.* 90, 3255–3269. doi: 10.1152/jn.00073.2003

O'Sullivan, I., Burdet, E., and Diedrichsen, J. (2009). Dissociating variability and effort as determinants of coordination. *PLoS Comput. Biol.* 5:e1000345. doi: 10.1371/journal.pcbi.1000345

Panarese, A., Edin, B. B., Vecchi, F., Carrozza, M. C., Johansson, R. S., Member, A., et al. (2009). Humans can integrate force feedback to toes in their sensorimotor control of a robotic hand. *IEEE Trans. Neural. Syst. Rehabil. Eng.* 17, 560–567. doi: 10.1109/TNSRE.2009.2021689

Paredes, L. P., Dosen, S., Rattay, F., Graimann, B., and Farina, D. (2015). The impact of the stimulation frequency on closed-loop control with electrotactile feedback. *J. Neuro Eng. Rehabil.* 12:35. doi: 10.1186/s12984-015-0022-8

Pasluosta, C., Kiele, P., and Stieglitz, T. (2018). Paradigms for restoration of somatosensory feedback via stimulation of the peripheral nervous system. *Clin. Neurophysiol.* 129, 851–862. doi: 10.1016/j.clinph.2017.12.027

Patel, G. K., Dosen, S., Castellini, C., and Farina, D. (2016). Multichannel electrotactile feedback for simultaneous and proportional myoelectric control. *J. Neural Eng.* 13:056015. doi: 10.1088/1741-2560/13/5/056015

Patterson, P. E., and Katz, J. A. (1992). Design and evaluation of a sensory feedback-system that provides grasping pressure in a myoelectric hand. *Bull. Prosthetics Res.* 29, 1–8.

Pena, A. E., Rincon-Gonzalez, L., Abbas, J. J., and Jung, R. (2019). Effects of vibrotactile feedback and grasp interface compliance on perception and control of a sensorized myoelectric hand. *PLoS One* 14:e0210956. doi: 10.1371/journal.pone.0210956

Pistohl, T., Joshi, D., Ganesh, G., Jackson, A., and Nazarpour, K. (2015). Artificial proprioceptive feedback for myoelectric control. *IEEE Trans. Neural. Syst. Rehabil. Eng.* 23, 498–507. doi: 10.1109/TNSRE.2014.2355856

Prior, R., and Lyman, J. (1975). Electrocutaneous feedback for artificial limbs. *Bull. Prosthetics Res.* 10, 3–37.

Prior, R. E., Lyman, J., Case, P. A., and Scott, C. M. (1976). Supplemental sensory feedback for the VA/NU myoelectric hand. Background and preliminary designs. *Bull. Prosthetics Res.* 10–26, 170–191.

Pylatiuk, C., Kargov, A., and Schulz, S. (2006). Design and evaluation of a low-cost force feedback system for myoelectric prosthetic hands. *J. Prosthetics Orthotics* 18, 57–61. doi: 10.1097/00008526-200604000-00007

Rakic, M. (1969). The Belgrade hand prosthesis. *Proc. Inst. Mech. Eng.* 183, 60–67. doi: 10.1243/pime_conf_1968_183_179_02

Raspopovic, S., Capogrosso, M., Petrini, F. M., Bonizzato, M., Rigosa, J., and Micera, S. (2014). Restoring natural sensory feedback in real-time bidirectional hand Prostheses. *Sci. Trans. Med.* 6:222ra19. doi: 10.1126/scitranslmed.3006820

Raveh, E., Friedman, J., and Portnoy, S. (2017). Visuomotor behaviors and performance in a dual-task paradigm with and without vibrotactile feedback when using a myoelectric controlled hand. *Assist. Technol.* 30, 274–280. doi: 10.1080/10400435.2017.1323809

Reinkensmeyer, D. J., Guigon, E., and Maier, M. A. (2012). A computational model of use-dependent motor recovery following a stroke: optimizing corticospinal activations via reinforcement learning can explain residual capacity and other strength recovery dynamics. *Neural Networks* 2, 60–69. doi: 10.1016/j.neunet.2012.02.002

Reswick, J., Mooney, V., Schwartz, A., McNeal, D., Su, N., and Sperry, C. (1975). "Sensory feedback prosthesis using intraneural electrodes," in *Proceedings of the 5th International Symposium on External Control of Human Extremities*, Dubrovnik, 9–24.

Rigoux, L., and Guigon, E. (2012). A model of reward- and effort-based optimal decision making and motor control. *PLoS Comput. Biol.* 8:e1002716. doi: 10.1371/journal.pcbi.1002716

Ring, N., and Welbourn, D. (1969). A self-adaptive gripping device: its design and performance. *Proc. Inst. Mech. Eng.* 183, 45–49. doi: 10.1243/pime_conf_1968_183_176_02

Risso, G., Valle, G., Iberite, F., Strauss, I., Stieglitz, T., Controzzi, M., et al. (2019). Optimal integration of intraneural somatosensory feedback with visual information: a single-case study. *Scie. Rep.* 9:7916. doi: 10.1038/s41598-019-43815-1

Rohland, T. (1975). Sensory feedback for powered limb Prostheses. *Med. Biol. Eng.* 13, 300–301. doi: 10.1007/bf02477743

Rosset, F. (1917). *Patent No. DE301108. Germany*.

Rossini, P. M., Micera, S., Benvenuto, A., Carpaneto, J., Cavallo, G., Citi, L., et al. (2010). Double nerve intraneural interface implant on a human amputee for robotic hand control. *Clin. Neurophysiol.* 121, 777–783. doi: 10.1016/j.clinph.2010.01.001

Salisbury, L., and Colman, A. (1967). A mechanical hand with automatic proportional control of prehension. *Med. Biol. Eng.* 5, 505–511. doi: 10.1007/bf02479145

Saunders, I., and Vijayakumar, S. (2011). The role of feed-forward and feedback processes for closed-loop prosthesis control. *J. Neuroeng. Rehabil.* 8:60. doi: 10.1186/1743-0003-8-60

Schiefer, M., Tan, D., Sidek, S. M., and Tyler, D. J. (2016). Sensory feedback by peripheral nerve stimulation improves task performance in individuals with upper limb loss using a myoelectric prosthesis. *J. Neural Eng.* 13:016001. doi: 10.1088/1741-2560/13/1/016001

Schiefer, M. A., Graczyk, E. L., Sidik, S. M., Tan, D. W., and Tyler, D. J. (2018). Artificial tactile and proprioceptive feedback improves performance and confidence on object identification tasks. *PLoS One* 13:e0207659. doi: 10.1371/journal.pone.0207659

Schmid, H. P., and Bekey, G. A. (1978). Tactile information processing by human operators in control systems. *IEEE Trans. Syst.ManCybern.* 8, 860–866. doi: 10.1109/TSMC.1978.4309886

Schmidl, H. (1973). The INAIL-CECA Prostheses. *Orthotics Prosthetics* 27, 6–12.

Schmidl, H. (1977). The importance of information feedback in Prostheses for the upper limbs. *Prosthetics Orthotics Int.* 1, 21–24. doi: 10.3109/03093647709164601

Schofield, J. S., Evans, K. R., Carey, J. P., and Hebert, J. S. (2014). Applications of sensory feedback in motorized upper extremity prosthesis: a review. *Expert Rev. Med. Devices* 11, 499–511. doi: 10.1586/17434440.2014.929496

Schofield, J. S., Shell, C. E., Beckler, D. T., Thumser, Z. C., and Marasco, P. D. (2020). Long-term home-use of sensory-motor-integrated bidirectional bionic prosthetic arms promotes functional, perceptual, and cognitive changes. *Front. Neurosci.* 14:120. doi: 10.3389/fnins.2020.00120

Schori, T. R. (1970). Tracking performance as a function of precision of electrocutaneous feedback information. *Hum. Fact.*12, 447–452. doi: 10.1177/001872087001200503

Schrater, P., Kording, K. P., and Blohm, G. (2019). "Modeling in neuroscience as a decision process," in *Conference on Cognitive Computational Neuroscience*, San Francisco, CA.

Schultz, A. E., and Kuiken, T. A. (2011). Neural interfaces for control of upper limb Prostheses: the state of the art and future possibilities. *J. Inj. Funct.Rehabil.* 3, 55–67. doi: 10.1016/j.pmrj.2010.06.016

Schultz, A. E., Marasco, P. D., and Kuiken, T. A. (2009). Vibrotactile detection thresholds for chest skin of amputees following targeted reinnervation surgery. *Brain Res.* 1251, 121–129. doi: 10.1016/j.brainres.2008.11.039

Schweisfurth, M. A., Hartmann, C., Schimpf, F., Farina, D., and Dosen, S. (2019a). "The interaction between feedback type and learning in routine grasping with myoelectric Prostheses," in *IEEE Transactions on Haptics*, Piscataway, NJ.

Schweisfurth, M. A., Niethammer, C., Meyer, B., Farina, D., and Dosen, S. (2019b). Psychometric characterization of incidental feedback sources during grasping with a hand prosthesis. *J Neuro Eng. Rehabil.* 16:155.

Schweisfurth, M. A., Markovic, M., Dosen, S., Teich, F., Graimann, B., and Farina, D. (2016). Electrotactile EMG feedback improves the control of prosthesis grasping force. *J. Neural Eng.* 13:056010. doi: 10.1088/1741-2560/13/5/056010

Scott, R. N. (1990). Feedback in myoelectric Prostheses. *Clin. Orthop.* 256, 58–63.

Scott, R. N., Brittain, R. H., Caldwell, R. R., Cameron, A. B., and Dunfield, V. A. (1980). Sensory-feedback system compatible with myoelectric control. *Med. Biol. Eng. Compu.* 18, 65–69. doi: 10.1007/bf02442481

Scott, S. H. (2004). Optimal feedback control and the neural basis of volitional motor control. *Nat. Rev. Neurosci.* 5, 532–546. doi: 10.1038/nrn1427

Seeley, H. F., and Bliss, J. C. (1966). Compensatory tracking with visual and tactile displays. *IEEE Trans. Hum. Fact. Electron.* 7, 84–90. doi: 10.1109/THFE.1966.232328

Seminara, L., Fares, H., Franceschi, M., Valle, M., Strbac, M., Farina, D., et al. (2019). Dual-parameter modulation improves stimulus localization in multichannel electrotactile stimulation. *IEEE Trans. Haptics.* doi: 10.1109/TOH.2019.2950625 [Epub ahead of print].

Sensinger, J. W., Aleman-Zapata, A., and Englehart, K. (2015). Do cost functions for tracking error generalize across tasks with different noise levels? *PloS one* 10:e0136251. doi: 10.1371/journal.pone.0136251

Sensinger, J. W., Schultz, A. E., and Kuiken, T. A. (2009). Examination of force discrimination in human upper limb amputees with reinnervated limb sensation following peripheral nerve transfer. *IEEE Trans. Neural. Syst. Rehabil. Eng.* 17, 438–444. doi: 10.1109/TNSRE.2009.2032640

Sensinger, J. W., Hill, W., and Sybring, M. (2019). "Prostheses-Assistive Technology-Upper," in *Encyclopedia of Biomedical Engineering*, Editor in Chief

R. Narayan, eds M. Wang, C. Laurencin, and X. Yu (Amsterdam: Elsevier), 632–644. doi: 10.1016/b978-0-12-801238-3.99912-4

Shadmehr, R., and Krakauer, J. W. (2008). A computational neuroanatomy for motor control. *Exp. Brain Res.* 185, 359–381. doi: 10.1007/s00221-008-1280-5

Shadmehr, R., and Mussa-Ivaldi, F. A. (1994). Adaptive representation of dynamics during learning of a motor task. *J. Neurosci.* 74, 3208–3224. doi: 10.1523/jneurosci.14-05-03208.1994

Shadmehr, R., and Mussa-Ivaldi, S. (2012). *Biological Learning and Control: How the Brain Builds Representations, Predicts Events, and Makes Decisions*. Cambridge, MA: The MIT Press.

Shannon, G. F. (1976). A comparison of alternative means of providing sensory feedback on upper limb Prostheses. *Med. Biol. Eng. Comput.* 14, 289–294. doi: 10.1007/bf02478123

Shannon, G. F. (1979). A myoelectrically-controlled prosthesis with sensory feedback. *Med. Biol. Eng. Comput.* 17, 73–80. doi: 10.1007/bf02440956

Shehata, A. W., Engels, L. F., Controzzi, M., Cipriani, C., Scheme, E. J., and Sensinger, J. W. (2018a). Improving internal model strength and performance of prosthetic hands using augmented feedback. *J. Neuro Eng. Rehabil.* 15, 1–12. doi: 10.1186/s12984-018-0417-4

Shehata, A. W., Scheme, E. J., and Sensinger, J. W. (2018b). Audible feedback improves internal model strength and performance of myoelectric prosthesis control. *Sci. Rep.* 8, 1–10. doi: 10.1038/s41598-018-26810-w

Shehata, A. W., Scheme, E. J., and Sensinger, J. W. (2018c). Evaluating internal model strength and performance of myoelectric prosthesis control strategies. *IEEE Trans. Neural Syst. Rehabil. Eng.* 26, 1046–1055. doi: 10.1109/TNSRE.2018.2826981

Sigrist, R., Rauter, G., Riener, R., and Wolf, P. (2013). Augmented visual, auditory, haptic, and multimodal feedback in motor learning: a review. *Psychon. Bull. Rev.* 20, 21–53. doi: 10.3758/s13423-012-0333-8

Simpson, D. C. (1972). Externally powered prosthesis for complete arm replacement. *Phys. Med. Biol.* 17, 110.

Simpson, D. C. (1974). "The choice of control system for the multimovement prosthesis: extended physiological proprioception," in *The Control of Upper-Extremity Prostheses and Orthoses*, eds P. Herberts, R. Kadefors, R. Magnusson, and I. Petersen (Springfield, IL: Charles Thomas), 146–150.

Simpson, D. C., and Smith, J. G. (1977). Externally powered controlled complete arm Prosthesis. *J. Med. Eng. Technol.* 1, 275–277. doi: 10.3109/03091907709162194

Soukoreff, R. W., and MacKenzie, I. S. (2004). Towards a standard for pointing device evaluation, perspectives on 27 years of Fitts' law research in HCI. *Int. J. Hum. -Comput. Stud.* 61, 751–789. doi: 10.1016/j.ijhcs.2004.09.001

Stepp, C. E., and Matsuoka, Y. (2010). "Relative to direct haptic feedback, remote vibrotactile feedback improves but slows object manipulation. 2010," in *Annual International Conference of the IEEE Engineering in Medicine and Biology*, Piscataway, NJ: IEEE, 2089–2092.

Stepp, C. E., and Matsuoka, Y. (2012). Vibrotactile sensory substitution for object manipulation: amplitude versus pulse train frequency modulation. *IEEE Trans. Neural Syst. Rehabil. Eng.* 20, 31–37. doi: 10.1109/TNSRE.2011.2170856

Štrbac, M., Belić, M., Isaković, M., Kojić, V., Bijelić, G., Popović, I., et al. (2016). Integrated and flexible multichannel interface for electrotactile stimulation. *J. Neural Eng.* 13:046014. doi: 10.1088/1741-2560/13/4/046014

Strbac, M., Isakovic, M., Belic, M., Popovic, I., Simanic, I., Farina, D., et al. (2017). Short- and long-term learning of feedforward control of a myoelectric prosthesis with sensory feedback by amputees. *IEEE Trans. Neural. Syst. Rehabil. Eng.* 25, 2133–2145. doi: 10.1109/TNSRE.2017.2712287

Svensson, P., Wijk, U., Björkman, A., and Antfolk, C. (2017). A review of invasive and non-invasive sensory feedback in upper limb Prostheses. *Expert Rev Med. Devices* 14, 439–447. doi: 10.1080/17434440.2017.1332989

Synofzik, M., Vosgerau, G., and Newen, A. (2008). Beyond the comparator model: a multifactorial two-step account of agency. *Conscious Cogn.* 17, 219–239. doi: 10.1016/j.concog.2007.03.010

Szeto, A. Y., and Saunders, F. A. (1982). Electrocutaneous stimulation for sensory communication in rehabilitation engineering. *IEEE Trans. Biomed. Eng.* 29, 300–308. doi: 10.1109/tbme.1982.324948

Szeto, A. Y. J., and Lyman, J. (1977). Comparison of codes for sensory feedback using electrocutaneous tracking. *Ann. Biomed. Eng.* 5, 367–383. doi: 10.1007/BF02367316

Tan, D. W., Schiefer, M. A., Keith, M. W., Anderson, J. R., Tyler, J., and Tyler, D. J. (2014). A neural interface provides long-term stable natural touch perception. *Sci. Transl. Med.* 6:257ra138. doi: 10.1126/scitranslmed.3008669

Tan, D. W., Schiefer, M. A., Keith, M. W., Anderson, J. R., Tyler, J., and Tyler, D. J. (2014). A neural interface provides long-term stable natural touch perception. *Sci. Trans. Med.* 6:257ra138. doi: 10.1126/scitranslmed.3008669

Tejeiro, C., Stepp, C. E., Ieee, M., Malhotra, M., Rombokas, E., and Matsuoka, Y. (2012). "Comparison of Remote Pressure and Vibrotactile Feedback for Prosthetic Hand Control," in *2012 4th IEEE RAS & EMBS International Conference on Biomedical Robotics and Biomechatronics (BioRob)*, Piscataway, NJ: IEEE, 521–525.

Thumser, Z. C., Slifkin, A. B., Beckler, D. T., and Marasco, P. D. (2018). Fitts' law in the control of isometric grip force with naturalistic targets. *Front. Psychol.* 9:560. doi: 10.3389/fpsyg.2018.00560

Todorov, E. (2004). Optimality principles in sensorimotor control. *Nat. Neurosci.* 7, 907–915. doi: 10.1038/nn1309

Todorov, E. (2005). Stochastic optimal control and estimation methods adapted to the noise characteristics of the sensorimotor system. *Neural Comput.* 17, 1084–1108. doi: 10.1162/0899766053491887

Todorov, E. (2006). Optimal control theory. *Environ. Plan. Gov. Policy* 4, 1–28. doi: 10.1068/c040121

Todorov, E. (2009). Efficient computation of optimal actions. *Proc. Natl. Acad. Sci. U.S.A.* 106, 11478–11483. doi: 10.1073/pnas.0710743106

Todorov, E., and Jordan, M. I. (2002). Optimal feedback control as a theory of motor coordination. *Nat. Neurosci.* 5, 1226–1235. doi: 10.1038/nn963

Tupper, C. N. (1989). Improved prosthesis control. 39–40.

Tyler, D. J. (2016). Restoring the human touch: prosthetics imbued with haptics give their wearers fine motor control and a sense of connection. *IEEE Spectrum* 53, 28–33. doi: 10.1109/MSPEC.2016.7459116

Uno, Y., Kawato, M., and Suzuki, R. (1989). Formation and control of optimal trajectory in human multijoint arm movement: minimum torque-change model. *Biol. Cybern.* 61, 89–101.

Valle, G., Petrini, F. M., Strauss, I., Iberite, F., D'Anna, E., Granata, G., et al. (2018b). Comparison of linear frequency and amplitude modulation for intraneural sensory feedback in bidirectional hand Prostheses. *Sci. Rep.* 8:16666. doi: 10.1038/s41598-018-34910-w

Valle, G., Mazzoni, A., Iberite, F., D'Anna, E., Strauss, I., Granata, G., et al. (2018a). Biomimetic intraneural sensory feedback enhances sensation naturalness, tactile sensitivity, and manual dexterity in a bidirectional prosthesis. *Neuron* 100, 37.e7–45.e7. doi: 10.1016/j.neuron.2018.08.033

Wan, E. A., and Van Der Merwe, R. (2001). *The Unscented Kalman Filter. Kalman Filtering and Neural Networks*. Hoboken, NJ: John Wiley & Sons, 62.

Wang, G., Zhang, X., Zhang, J., and Gruver, W. A. (1995). "Gripping force sensory feedback for a myoelectrically controlled forearm prosthesis," in *IEEE International Conference on Intelligent Systems for the 21st Century*, Vol. 1 (Vancouver, BC), 501–504.

Weeks, D. L., Wallace, S. A., and Noteboom, J. T. (2000). Precision-grip force changes in the anatomical and prosthetic limb during predictable load increases. *Exp. Brain Res.* 132, 404–410. doi: 10.1007/s002210000337

Wegner, D. (2002). *The Illusion of Conscious Will*. Cambridge, MA: MIT Press.

Wegner, D. (2003). The mind's best trick: how we experience conscious will. *Trends Cogn. Sci.* 7, 65–69. doi: 10.1016/s1364-6613(03)00002-0

Wegner, D., and Sparrow, B. (2004). *Authorship Processing. In The new Cognitive Neurosciences*. Cambridge, MA: MIT Press.

Wegner, D., Sparrow, B., and Winerman, L. (2004). Vicarious agency: experiencing control over the movements of others. *J. Pers. Soc. Psychol.* 86, 838–848. doi: 10.1037/0022-3514.86.6.838

Weir, R. F. (1995). *Direct Muscle Attachment as a Control Input for a Position Servo Prosthesis Controller*. Evanston: Northwestern University.

Weir, R. F., Heckathorne, C. W., and Childress, D. S. (2001). Cineplasty as a control input for externally powered prosthetic components. *J. Rehabil. Res. Dev.* 38, 357–463.

Wettels, N., Parnandi, A. R., Loeb, G. E., and Sukhatme, G. S. (2009). Grip control using biomimetic tactile sensing systems. *IEEE/ASME Trans. Mech.* 14, 718–723. doi: 10.1109/TMECH.2009.2032686

Wheeler, J., Bark, K., Savall, J., and Cutkosky, M. (2010). Investigation of rotational skin stretch for proprioceptive feedback with application to myoelectric

systems. *IEEE Trans. Neural. Syst. Rehabil. Eng.* 18, 58–66. doi: 10.1109/Tnsre.2009.2039602

Whitney, D. E. (1977). Force feedback control of manipulator fine motions. *J. Dyn. Syst. Measu. Control* 99, 91–97. doi: 10.1115/1.3427095

Witteveen, H. J., Rietman, H. S., and Veltink, P. H. (2015). Vibrotactile grasping force and hand aperture feedback for myoelectric forearm prosthesis users. *Prosthetics Orthotics Int.* 39, 204–212. doi: 10.1177/0309364614522260

Witteveen, H. J. B., Droog, E. A., Rietman, J. S., and Veltink, P. H. (2012). Vibro- and electrotactile user feedback on hand opening for myoelectric forearm Prostheses. *IEEE Trans. Biomedi. Eng.* 59, 2219–2226. doi: 10.1109/TBME.2012.2200678

Zafar, M., and Van Doren, C. L. (2000). Effectiveness of supplemental grasp-force feedback in the presence of vision. *Med. Biol. Eng. Comput.* 38, 267–274. doi: 10.1007/BF02347046

Zollo, L., Pino, G., Di, Ciancio, A. L., Ranieri, F., Cordella, F., et al. (2019). Restoring tactile sensations via neural interfaces for real-time force-and-slippage closed-loop control of bionic hands. *Sci. Rob.* 4, 1–12. doi: 10.1126/scirobotics.aau9924

Conflict of Interest: The authors declare that the research was conducted in the absence of any commercial or financial relationships that could be construed as a potential conflict of interest.

APPENDIX – LIST OF SUPPLEMENTARY FEEDBACK STUDIES IN PROSTHESIS CONTROL

TABLE A1 | Supplementary sensory feedback in prostheses.

				Quantitative improvement in performance (vision and feedback) compared with vision alone?		
Input	**Output**	**Experimental group**	**Stimulation position**	**Virtual environment**	**Real life**	**References**
Contact pressure	E	TR	RL			Beeker et al., 1967
Grasp force	V	TR	RL			Kawamura and Sueda, 1969
Joint position	V	TH	RL			Mann and Reimers, 1970
Grasp force	N	TR and TH	Median n.			Clippinger et al., 1975
Grasp force	E	TH	RL			Prior and Lyman, 1975
Grasp force, position	N	TR	Radial and Ulnar nerve			Reswick et al., 1975
Grasp force	E	TR	RL			Rohland, 1975
Position, Grasp force	V,E	N.A.	N.A.			Shannon, 1976
Grasp force, position	E	TR	RL			Schmidl, 1973, 1977
Grasp force	E	N.A.	N.A.			Shannon, 1979
Grasp force	E	TR	RL			Kato et al., 1979
Grasp force	E	TR	RL			Scott et al., 1980
Grasp force	D	AB	Forearm		Yes	Meek et al., 1989
Position	E	AB	Array of electrodes in belt			Tupper, 1989
Grasp force	V,D	AB	Upper arm		Yes, but not significant	Patterson and Katz, 1992
Grasp force	E	AB				Wang et al., 1995
Grasp force	E	Nerve injury patients and amputees	Upper arm			Lundborg et al., 1998
Grasp force	E	AB	Neck		Yes	Zafar and Van Doren, 2000
Grasp force, finger position	EPP	Amputees with cineplasty	RL			Weir et al., 2001
Position	N	TR	Median nerve			Dhillon and Horch, 2005
Grasp force	V	TR	RL			Pylatiuk et al., 2006
Touch	D	TSR	Reinnervated area			Kuiken et al., 2007a
Touch	D	TSR	Reinnervated area			Kuiken et al., 2007b
Grasp force	V	AB	Upper arm			Chatterjee et al., 2008
Grasp force	V	AB	Upper arm			Cipriani et al., 2008a
Grasp force	D	AB	Toes			Panarese et al., 2009
Grasp force	D	TSR	Reinnervated area			Sensinger et al., 2009
Vibration	V	TSR	Reinnervated area			Schultz et al., 2009
Orientation, discrimination	D	TSR	Reinnervated area			Marasco et al., 2009
Position	Auditory	AB	Auditory			González et al., 2010
Gripping force	Haptic stylus	AB	Fingers			Stepp and Matsuoka, 2010
Position	Skin stretch	AB	Upper arm			Wheeler et al., 2010
Position and force	N	TR	Ulnar and median n.			Horch et al., 2011
Grasp force	V	AB	Forearm – array			Saunders and Vijayakumar, 2011
Touch	D	TSR	RL			Marasco et al., 2011
Passive hand touch	D	TR	RL			Antfolk et al., 2012
Hand configuration	Auditory	AB	Auditory		Yes	Gonzalez et al., 2012
Grasp force	D	TSR	Reinnervated area	Yes		Kim and Colgate, 2012
Grasp force	V	AB	Upper arm			Stepp and Matsuoka, 2012
Grasp force	V,D	AB	Index finger	Yes		Tejeiro et al., 2012
Pressure	V,D	TR	RL			Antfolk et al., 2013b

(Continued)

TABLE A1 | Continued

Input	Output	Experimental group	Stimulation position	Quantitative improvement in performance (vision and feedback) compared with vision alone?		References
				Virtual environment	Real life	
Passive hand touch	V,D	TR	RL			Antfolk et al., 2013a
Contact	V	AB	Fingers			Cipriani et al., 2014
Grasp force, velocity	V,D	AB	Forearm			Ninu et al., 2014
Grasp type, aperture size	Augm. reality	AB	Visual			Markovic et al., 2014
Grasping force	E	AB	Forearm	Yes		Jorgovanovic et al., 2014
N.A.	N	TH	Ulnar nerve			Ortiz-Catalan et al., 2014
Grasping force	N	TR	Median, Radial, Ulnar nerves		Yes	Tan et al., 2014
Grasping force	V, joint torque	AB, TR	Forearm			Brown et al., 2015
EMG amplitude	Visual	AB, TR	Visual	Yes		Dosen et al., 2015a
Grasping force	Visual	AB	Visual			Dosen et al., 2015b
Grasp force, position	N	TR	Median, Radial, Ulnar nerves			Schiefer et al., 2016
Contact	V	TR	RL		Yes	Clemente et al., 2016
EMG amplitude	E	AB, TR	Forearm			Schweisfurth et al., 2016
Finger positions	E	AB	Forearm			Patel et al., 2016
Grasp force	V	TR	RL		Yes	Strbac et al., 2017
Grasp force	E	AB	Forearm			Dosen et al., 2017
Grip force, hand aperture	Augm. reality	AB	Visual			Clemente et al., 2017
EMG amplitude, hand aperture, force and contact	Augm. reality, sound	AB	Visual, Audio		Yes	Markovic et al., 2017
Grasp force	V	AB	Forearm			De Nunzio et al., 2017
Grasp force, position	N	TR	Median, Radial, Ulnar nerves			Schiefer et al., 2018
Grasp force, position	N	TR	Median, Radial, Ulnar nerves		Yes	Graczyk et al., 2018
Position	Kinesthetic illusion	TMR	RL		Yes	Marasco et al., 2018
Contact	V	AB	Forearm			Raveh et al., 2017
Pattern rec class velocity	Auditory	AB	Audio		Yes	Shehata et al., 2018a
Contact	V,D	AB	Forearm		Yes	Aboseria et al., 2018
Grasping force	Visual	AB	Visual			Markovic et al., 2018b
Grasping force, state change and contact	V	TR	RL		Yes	Markovic et al., 2018a
Touch, pain	E	TR	RL			Osborn et al., 2018
Grasp force	N	TR	Median, Ulnar		Yes	Valle et al., 2018a
Contact, Grasp force, position	N	TR	Median, Ulnar			George et al., 2019
Grasp force, position	N	TR	Median, Ulnar			Zollo et al., 2019
Grasp force	V, visual	AB	Forearm			Schweisfurth et al., 2019a
Grasp force	E	TR	Ulnar nerve		Yes	Clemente et al., 2019
Grasp force, hand aperture	V	AB	Forearm			Pena et al., 2019
Grasp force, hand aperture	E	TR	Ulnar and median nerves			D'Anna et al., 2019
Hand aperture	Skin stretch	AB, TR	Upper arm			Battaglia et al., 2019
Grasping force	D	TMR	RL			Schofield et al., 2020

E, electrical surface stimulation; EPP, extended physiological proprioception (combination of sensory feedback and control); N, nerve stimulation; D, direct pressure; V, vibration; AB, able-bodied; TR, transradial amputation; TH, transhumeral amputation; TMR, targeted muscle reinnervation; TSR, targeted sensory reinnervation; RL, residual limb.

frontiers in Neuroscience

ORIGINAL RESEARCH
published: 21 August 2020
doi: 10.3389/fnins.2020.00882

Effects of Gamification in BCI Functional Rehabilitation

Martí de Castro-Cros[1], Marc Sebastian-Romagosa[2], Javier Rodríguez-Serrano[2], Eloy Opisso[3], Manel Ochoa[3], Rupert Ortner[2], Christoph Guger[2,4,5] and Dani Tost[1,6,7]*

[1] Universitat Politecnica de Catalunya, Barcelona, Spain, [2] g.tec medical engineering Spain S.L., Barcelona, Spain, [3] Guttmann Institute, Badalona, Spain, [4] g.tec medical engineering GmbH, Schiedlberg, Austria, [5] Guger Technologies (Austria), Graz, Austria, [6] Research Center in Biomedical Engineering (CREB), Barcelona, Spain, [7] Sant Joan de Déu Research Institute, Esplugues de Llobregat, Spain

Objective: To evaluate whether introducing gamification in BCI rehabilitation of the upper limbs of post-stroke patients has a positive impact on their experience without altering their efficacy in creating motor mental images (MI).

Design: A game was designed purposely adapted to the pace and goals of an established BCI-rehabilitation protocol. Rehabilitation was based on a double feedback: functional electrostimulation and animation of a virtual avatar of the patient's limbs. The game introduced a narrative on top of this visual feedback with an external goal to achieve (protecting bits of cheese from a rat character). A pilot study was performed with 10 patients and a control group of six volunteers. Two rehabilitation sessions were done, each made up of one stage of calibration and two training stages, some stages with the game and others without. The accuracy of the classification computed was taken as a measure to compare the efficacy of MI. Users' opinions were gathered through a questionnaire. *No potentially identifiable human images or data are presented in this study.*

Results: The gamified rehabilitation presented in the pilot study does not impact on the efficacy of MI, but it improves users experience making it more fun.

Conclusion: These preliminary results are encouraging to continue investigating how game narratives can be introduced in BCI rehabilitation to make it more gratifying and engaging.

Keywords: brain computer interface, gamification, stroke, rehabilitation, functional rehabilitation, serious game

OPEN ACCESS

Edited by:
Nicolas Garcia-Aracil, Miguel Hernández University of Elche, Spain

Reviewed by:
Xiaoli Li, Beijing Normal University, China
Juan Antonio Barios Heredero, University of Castilla La Mancha, Spain

****Correspondence:***
Martí de Castro-Cros
marti.de.castro@upc.edu

Specialty section:
This article was submitted to Neural Technology, a section of the journal Frontiers in Neuroscience

Received: *13 February 2020*
Accepted: *28 July 2020*
Published: *21 August 2020*

Citation:
de Castro-Cros M, Sebastian-Romagosa M, Rodríguez-Serrano J, Opisso E, Ochoa M, Ortner R, Guger C and Tost D (2020) Effects of Gamification in BCI Functional Rehabilitation. Front. Neurosci. 14:882. doi: 10.3389/fnins.2020.00882

INTRODUCTION

Stroke is a leading cause of severe physical disability. According to the World Health Organization, 15 million people suffer from stroke worldwide each year, five million of them die, and five million are permanently disabled (Donkor, 2018). Impairments in the upper limbs affect 60% of stroke survivors. Rehabilitation of these patients is key to improve patients' capabilities of realizing daily life activities and, consequently, to improve their independence and quality of life (Pindus et al., 2018). Various technologies have been used to support upper limb rehabilitation including assistive robotic systems, camera tracking and motion sensors. Among them, the Mental Imagery Brain Computer Interface (MI-BCI) has emerged as a cost-effective, non-invasive rehabilitation technology, specially indicated for patients with a low range of motor motion, having fatigue, or pain (van Dokkum et al., 2015; Remsik et al., 2016; Cervera et al., 2018).

The strategy of MI-BCI rehabilitation is to exploit the capability of users to create a mental image of a movement. BCI systems use ElectroEncephaloGraphy (EEG) placing electrodes over the patients' head to capture functional cortical activation changes while patients are trying to create a mental image of a functional motor movement. The EEG signal exhibit event-related synchronization and desynchronization of neural rhythms that can be correlated with the laterality of the mental image (McFarland et al., 2000; Neuper et al., 2006). Thus, machine learning algorithms can be trained to determine in real time if the mental image is correct (Chavarriaga et al., 2017).

Feedback is an essential feature of EEG-BCI rehabilitation. EEG-BCI signal analysis can be used to trigger functional electrostimulation (FES) (Quandt and Hummel, 2014) and to control robotic ortheses in order to assist the realization of motor activity (Ang et al., 2015). In this way, the disrupted sensorimotor loop is closed. It has been proven that this loop closure is a key factor to induce neural plasticity changes, therefore to improve functional behavior. Visual feedback is necessary to learn how to create mental images. In addition, during the routine use of BCI, it provides users with self-awareness and assessment of how they are performing. The suitability of different forms of feedback has been discussed (Lotte et al., 2013; Jeunet et al., 2016). On one hand, symbolic widgets such as progress bars and arrows are simple and fast to implement, but they have been found to be difficult to understand and may even distract users (Kosmyna and Lécuyer, 2017; Škola et al., 2019). On the other hand, embodied avatar representations of the patient's limb promote Action Observation mechanisms and activate the Mirror Neuron Network (MNN) inducing thus cortical plasticity (Pichiorri et al., 2015; Zhang et al., 2018). Moreover, the sense of embodiment that a realistic avatar provides impacts positively on BCI control (Petit et al., 2015; Alimardani et al., 2016).

BCI sessions are based on repetition of exercises, they are cognitively demanding and can lead to a reduced patient engagement in rehabilitation. Gamification is defined as the introduction of game-design elements and principles such as narratives, scores and awards in non-game contexts to increase a person satisfaction and interest in performing activities by bringing intrinsically motivational playful experiences (Richter et al., 2015). Gamification has become a popular research topic with applications in a variety of domains from corporate business transformation to education and health (Zichermann and Linder, 2013). However, some studies in domains such as education, have shown that it is not always effective. Moreover, it can even yield to a reduction of the efficacy of the activity it aims at making more motivating (Hamari et al., 2014). The effects of gamification are greatly dependent on the context and on the users. In particular, rewards, badges and leaderboards should be used with precaution as they may backfire (Hanus and Fox, 2015).

Gamification has been largely used in conventional upper-arm rehabilitation in order to alleviate the repetitiveness of sessions, increase motivation, and engagement (Burke et al., 2009; Bermúdez-Badia et al., 2016). Commercial computer games have been adapted and new games have been designed on purpose to enhance the rehabilitation experience (Bermúdez-Badia and Cameirão, 2012). These games use the movement of the patients as the input system of the game. The movement is measured through various tracking systems (Llorens et al., 2015), and it substitutes conventional devices such as mouse and joysticks.

The introduction of gamification in BCI rehabilitation is quite challenging because using brain signals as the only user input reduces the scope of possible game narratives. Moreover, in order to keep the benefits of embodiment (Borrego et al., 2019), games should somewhat integrate the patient's upper limb avatar. This is why existing studies typically involve driving or navigation tasks: for instance, destroying asteroids using left/right hand (Vourvopoulos et al., 2016) or rowing boats while trying to collect flags (Vourvopoulos et al., 2019). Existing gamified BCI solutions have been basically tested with volunteer participants that have not been affected by a stroke, thus there is a lack of data on actual patients. Little is known about the impact of introducing external stimuli such as game elements aside from the avatar's limb on the efficacy of the training activity.

In this paper, we present a preliminary experimental study on gamified BCI post-stroke functional rehabilitation of the upper limbs. The goal of the study is to analyze how gamification impacts on the efficacy of the treatment and on patients' experience.

MATERIALS AND METHODS

Setup

The BCI system used on this study is recoveriX® (g.tec medical engineering GmbH, Austria). The system analyzes the EEG brain signals and provides multimodal feedback through a virtual reality avatar of the upper limbs and a FES proprioceptive feedback stimulation (Irimia et al., 2016, 2017; Cho et al., 2016). The EEG caps were equipped with 16 active electrodes (g.LADYbird or g.Scarabeo, g.tec medical engineering GmbH) located according to international 10/10 system (extended 10/20 system): FC5, FC1, FCz, FC2, FC6, C5 C3, C1, Cz, C2, C4, C6, Cp5, Cp1, Cp2, Cp6. A reference electrode was placed on the right earlobe and a ground electrode at position of Fpz.

Game Design

The game was developed on top of this system with two main requirements. First, it could not alter the pace of the rehabilitation. Second, in order to avoid altering the sense of identification of the user with the virtual forehand, the game could not modify the gesture of the avatar. With these limitations, the narrative was restricted to a game in which the unique action of the avatar was raising and lowering the wrist. Moreover, to make the virtual situation as similar as possible to the real one, we avoided driving-like actions that imply a virtual navigation of the avatar. We also wanted to have feedback of the current exercise and of the total training stage so far. Hence, the goal of the game is to compete with a mouse in order to preserve food. **Figure 1** shows the "standard" avatar and the new game appearance. At the beginning of the session 80 pieces of cheese (one for each exercise) are set between the two virtual arms. At each exercise, a mouse appears from the right or left corner of the room (the side of the wrist that must move) and stands

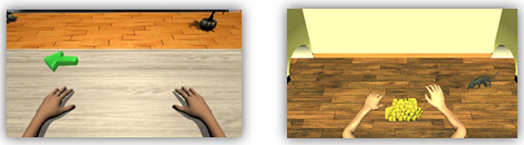

FIGURE 1 | Standard avatar and new game appearance. In the left side, is the avatar used in recoveriX system, the green arrow indicates in which hand the movement should be performed. In the right side is the new animated game, both arms are in the same position than the standard avatar. In front of the virtual subject there are 80 pieces of cheese that the user should try to keep. The rat indicates which hand should move.

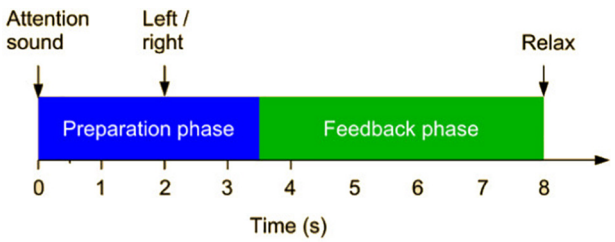

FIGURE 2 | RecoveriX trial description.

nearby the pile of cheese pieces during the cue sub-stage. In the feedback sub-stage, the game receives a cue of Boolean events that indicate if the mental image is being correct or not. The avatar's hand moves accordingly, and the FES is activated. When a cue is incorrect, both the visual feedback and the electrical stimulation are disabled. In the relax sub-stage, if five consecutive events are considered correct, when the virtual arm lowers, the mouse runs away empty-handed. Otherwise, it takes a piece of cheese. The size of the pile is thus an indicator of the overall progress of the training stage. In addition, a scoring panel was added to reinforce the awareness of the user. This panel could be deactivated, shown intermittently or constantly displayed. The game was implemented with Unity and connected to the recoveriX® replacing the non-gamified version. It is available upon request by mail to the corresponding author.

Participants

Ten stroke patients with hemiparesis in the upper limb and six healthy subjects were recruited for this study. The stroke subjects were patients from Institut Guttmann. All participants were volunteers. The inclusion criteria for stroke patients were: (i) residual hemiparesis, (ii) the stroke occurred at least 4 days before the first assessment, (iii) functional restriction in the upper extremities. Additionally, for all participants, the following criteria were applied: (iv) to be able to understand written and spoken instructions, (v) stable neurological status, (vi) willing to participate in the study and to understand and sign the informed consent, (vii) to be able to attend meetings. Ethics approval was obtained from the Ethic committee of Institut Guttmann, Barcelona, Spain. Finally, all participants were informed about the goals of the project, and they provided their written informed consent before participating in the study.

Experimental Design

All participants took part in the same procedure: control users in the research lab and patients in the rehabilitation institution. They performed two training sessions separated in time by a minimum of 1 day and a maximum of 2 weeks. Each session was composed of three runs or stages: Calibration (C-S1, C-S2), Training 1 (T1-S1, T1-S2), and Training 2 (T2-S1 and T2-S2). Each run was composed of 80 trials (80 movements) and lasted 12 min. There was a resting time of about 5 min between stages.

Figure 2 describes the timing of each trial. Each movement started with a cue, and 2 s later the system presented an arrow pointing to the movement direction. The participant was instructed to start the MI just after the cue for the next 6 s. During this period the user had to imagine the wrist dorsiflexion, and the feedback devices were activated. After the feedback period the system provided a sound to mark the end of the exercise and gave 2 s of rest before the next trial.

Motor Imagery Accuracy Calculation

The EEG data was bandpass filtered (0.5–30 Hz) to increase the signal to noise ratio (SNR) and to remove unnecessary components. We also applied a 50 Hz notch filter to reduce line noise. We then created 8 s epochs of EEG data for every trial and divided them into two classes: left and right.

Each epoch was bandpass filtered (8–30 Hz) and an artifact rejection was applied (the same as in the lateralization coefficient). Using the current frames, a CSP filter was created. Next, it was used to get 4 spatially filtered channels from the 16 EEG channels. For every frame we defined 14 timepoints, separated 0.5 s one from each other, from 1.5 to 8 s of the frames. For each timepoint we calculated a set of 4 features.

For each timepoint, we calculated the variance of each spatially filtered signal using a window of 1.5 s. The resulting four features for each timepoint were normalized, and we then derived their logarithmic values. Using all the features from all the timepoints and the entire frame collection, we calculated a linear discriminant analysis (LDA) classifier.

Using the CSP filter and the LDA classifier, the classifier accuracy is assessed with a 10-fold cross validation process. During this process, a classifier is created for every fold using 90% of the frames (training set). The classifier is then assessed with the other frames (testing set). This is done 10 times, and ultimately yields a mean accuracy for each class (left and right hand) and every timepoint. Finally, for each class, the MI accuracy is calculated as the maximum (Max. Accuracy) or as the mean (Mean Accuracy), among all timepoints. The LDA classifier was not modified from the original version (Irimia et al., 2016) to support the gamification pilot. Its code is not publicly available.

The calibration run is used to train the LDA classifier, thus, during this run the online feedback provided to users is always positive. After the calibration run, all participants were moved to the "Training" mode, where the feedback is triggered by the MI in real time. During Training 1 feedback is based on the classifier

built after Calibration, and during Training 2 it is based on an enhanced version of the classifier using data from the previous two stages. Each session started from scratch; thus Session 2 did not use the classifier of Session 1.

During the two sessions subjects sat at a table with the computer screen in front. They wore headphones to listen to the instructions and sounds.

In the first session, calibration (C-S1) and Training 1 (T1-S1) were without the game, only with the regular avatar, while Training 2 (T2-S1) used the game without any feedback of time and scoring *(no feedback)*. In the second session, all stages used the game: C-S2 (*no feedback),* T1-S2 showing score and time every ten exercises *(intermittent feedback)* and T2-S2 showing time and score constantly *(constant feedback)*.

The feedback received by the users is shown in **Figure 1**. As mentioned, there are two kinds of feedback: time and score. The time is shown through a cheese-shape clock while the score is shown literally differentiating the user score, under the name of Jasper, and the rat score.

Assessment Test

For this study two variables were analyzed: BCI performance and users' experience. BCI performance was studied using the MI accuracy of each run computed as exposed above. Users' experience was assessed using a questionnaire.

Questionnaire

The opinions of users about the game were gathered through a customized version of the System Usability Scale (SUS) composed by 8-items to be answered in a Likaert scale of 1–5, being 1 the worst case and 5 the best (see **Table 1**).

In addition, all participants were asked about how often they played videogames in a 5-values scale (never, sometimes, often, usually, always), and if they had previous experience with BCI technology. The answers and all collected data are available at the git repository: https://github.com/nosepas1/BCI_gamification_data.

Statistical Analysis

The software used for the statistical analysis was MATLAB R2017a and a python script using scipy stats, numpy and pandas. The first step of the statistical analysis is the comparison of the baselines of each group of participants; age, gender, and precision. First, the Shapiro-Wilk Test (SWT) test was performed to analyze the normality of the variables. For the comparison between groups ("Healthy" and "Stroke"), *t*-test for independent samples (in case of assumption of normality) and Mann–Whitney *U* test (in case of non-normality) were used.

For the analysis of the impact of the serious game combined with BCI on the user's concentration, since no independence could be assumed, the MI accuracies of every subject in all games mode were compared. The selected test for the analysis was "repeated measures ANOVA" (Girden, 1992; Norman and Streiner, 2008; Singh et al., 2013; Verma, 2015), which allows the results' comparison of the same group of participants at different time points. For that, two assumptions are needed: normality distribution (Shapiro-Wilk test > 0.05) and assumption of sphericity (Mauchly's sphericity test > 0.05).

Finally, a quantitative analysis of the answers in the questionnaire of each participant was carried out.

RESULTS

Participants Baseline

Six healthy subjects and ten stroke patients were enrolled in the study, seven of them were females and nine males. The average age of the healthy group was 35.3 years old (SD = 16.0), with the maximum and minimum age in this group was 58 and 23 years old, respectively. The mean age of the stroke group was 55.8 years old and the maximum and minimum age was 79 and 26 years old. In the Stroke group, four patients had been affected on their right side, and 6 on their left side. The mean time since stroke was 33 months (SD = 22.8), seven in subacute phase, Three in chronic phase, and 0 in acute phase. Neither patients nor control users had previous experience in BCIs, except two patients that had used the recoveriX® system years ago. Control users had neither previous known neurological disorder, nor previous experience in BCIs.

The accuracy obtained after the first training run in the first session (T1-S1) is taken as a baseline reference for each subject. As mentioned above, in run T1-S1, participants used the standard visual feedback with a personalized classifier generated in the calibration run of Session 1(T1-C1). Thus, the accuracy obtained in T2-S1, T1-S2, and T2-S2 is compared with that of T1-S1. The equality of the baselines cannot be assumed, because there is a statistical difference in the age between groups. The age variable of the healthy group is not normally distributed (SWT: $P = 0.022$) and Mann-Whitney U test shows a significant difference between both age groups, $P = 0.031$. In order to see how much the age differences can influence the BCI performance, the correlation between the age and the maximum classification accuracy (maximum accuracy of the second run in the first session T1-S2) has been studied. The age variable with all participants and MI accuracy data follow a normal distribution (SWT age, $P = 0.075$, SWT accuracy, $P = 0.096$). The Pearson correlation test shows that there is no significant correlation between age and accuracy (rho = −0.195, $P = 0.505$). Thus, the comparison of the MI accuracy between groups is allowed. However, because of the small size of sample no general conclusion can be extracted about the relationship age and accuracy.

The comparison of the accuracy obtained in the first training run T1-S1 (after system calibration), shows that there is no statistical difference in the BCI performance between healthy and stroke group using unpaired t-test, t-value = $|1.475|$ and $P = 0.166$ (SWT > 0.05).

Impact of the Game in the BCI Performance

In order to detect differences in the accuracy using different visual feedback modalities, the MI accuracy of each run has been analyzed using repeated measures ANOVA. All the datasets can be considered normally distributed. Shapiro-Wilk test did

TABLE 1 | Users' experience questionnaire.

#	Question	Score
Q1	Evaluate the level of fun in the game.	[1] no fun; [2] little fun; [3] indifferent; [4] fun; [5] very fun
Q2	Evaluates the visual aspect of the game.	[1] very bad; [2] bad; [3] indifferent; [4] good; [5] very good
Q3	Evaluate the easeiness of use of the game.	[1] very hard; [2] hard; [3] normal; [4] easy; [5] very easy
Q4	Evaluate the clarity of rules of the game.	[1] very confusing; [2] confusing; [3] indifferent; [4] clear; [5] very clear
Q5	With regard to the narrative plot (the fight against the mouse to protect the cheese), you thought so.	[1] very inadequate; [2] inadequate; [3] indifferent; [4] adequate; [5] very adequate
Q6	With regard to the level of concentration required to perform the exercise, in your opinion, adding the game to the rehabilitation session has contributed to:	[1] has distracted me a lot; [2] has distracted me; [3] has not influenced me; [4] has helped me to concentrate; [5] has helped me to concentrate a lot
Q7	With regard to possible boredom while exercising, in your opinion, adding the game to the rehabilitation session has contributed to:	[1] It's increased a lot more boredom; [2] It's bored me more; [3] It has not influenced me; [4] It alleviated boredom more; [5] It alleviated boredom a lot more
Q8	In general, the idea of introducing a game (not necessarily this one) into rehabilitation therapy, seems:	[1] very bad; [2] bad; [3] indifferent; [4] good; [5] very good

not show significant results at alpha level. Mauchly's Test of Sphericity indicated that the assumption of sphericity has not been violated, $\chi 2(2) = 9.595$, $P = 0.088$.

Table 2 shows the results of the accuracy comparison using repeated measures ANOVA. The multiple comparison did not show statistical differences in the accuracy based on the gamification with different visual feedback modalities (see **Figure 3** and **Table 3**). The same comparison has been done using only the data from the healthy or stroke group, and no significant differences have been detected.

While no significant differences are shown in several ANOVA tests, from inspection of **Figure 3**, a trend toward an improvement of mean accuracy along the sessions seems plausible. However, no conclusive results can be drawn because of the small number of subjects.

Users' Satisfaction With the Serious Game

The users' satisfaction was assessed after the last session using a questionnaire with eight questions rated from 1 to 5. For the quantification of the results the average of the individual score and the average of each question in the questionnaire has been computed.

Table 4 shows the results in the questionnaire based on groups and gaming experience. The first column shows the group name, the second column the group size, the third column is the averaged total questionnaire score based on the average score in each question, and the next eight columns show the average result for each group of each question. **Figure 4** shows the questionnaire results of each group.

All participants gave high scores in all questions: users' satisfaction is 4.20 points (SD = 0.45) up to five, the stroke group gave higher score in the questionnaire with 4.23 points (SD = 0.35), whereas the healthy group was 4.15 points (SD = 0.63). In general, the best aspect of the game is the clarity of the rules (Q4). The healthy group also highlighted the easiness of use (Q3). The worst aspect is the fun level of the game (Q1). In the informal debriefing after the sessions, users declared being pleased with the game, but suggested some enhancements such as introducing variations in the animation of the rat, which is always the same, and adding new auditory stimuli. The attention and somnolence in stroke patients are always a problem, which is not always discussed and should be considered in the design of experiments. In this case, patients agreed that the activity had the proper duration to avoid these problems. Stress was not quantitatively measured. However, in the debriefing session, patients did not mention any change in the level of fatigue and stress using the gamified version of training.

Finally, no significant correlation was found between the questionnaire score and accuracy.

DISCUSSION

The objective of this experiment was to explore how the proposed serious game can affect users' concentration and performance of a BCI system for stroke functional rehabilitation.

Although the Healthy and Stroke groups presented significant differences in age, this unevenness does not seem to harm the analysis, because there is no lineal correlation between age and accuracy (Pearson's test; rho = −0.195, P = 0.505). However, the number of subjects is too small to generalize this conclusion. In future experiments, with more subjects, ages will be stratified. Furthermore, there was no differences in the MI accuracy between the Healthy group and the Stroke group (t-test, t-value = |1.475| and $P = 0.166$).

The BCI performance has been studied through a multiple comparison analysis using the MI accuracy calculated after each run using different avatar versions. The comparison using repeated measures ANOVA test, showed no significant results, in the mean accuracy as well as in the maximum accuracy (**Tables 2**, **3** and **Figure 3**). The results of this first analysis demonstrate that there is no negative effect in the BCI performance when it is combined with a new gamified avatar. However, as shown in **Figure 3A**, the point cloud of T1-S2 and T2-S2 are slightly higher than T1-S1 (MI accuracy baseline measure). This difference is more evident in the mean accuracy plot (**Figure 3C**). The most probable explanation for that is that the pop-up scoring window can encourage the user to be more focused in the MI task.

TABLE 2 | Multiple comparison of MI accuracy using repeated measures ANOVA.

	SumSq	*df*	MeanSq	*F*	*p*-Value	*p*-ValueGG	*p*-ValueHF	*p*-ValueLB
Maximum accuracy								
Intercept	72.272	2	36.136	1.4213	0.265	0.266	0.266	0.261
run2_ses1	49.236	2	24.618	0.96826	0.397	0.374	0.382	0.348
Error	508.50	20	25.425					
Mean accuracy								
Intercept	72.508	2	36.254	1.3514	0.284	0.280	0.281	0.275
run2_ses1	48.422	2	24.211	0.90249	0.423	0.385	0.392	0.367
Error	482.88	18	26.827					

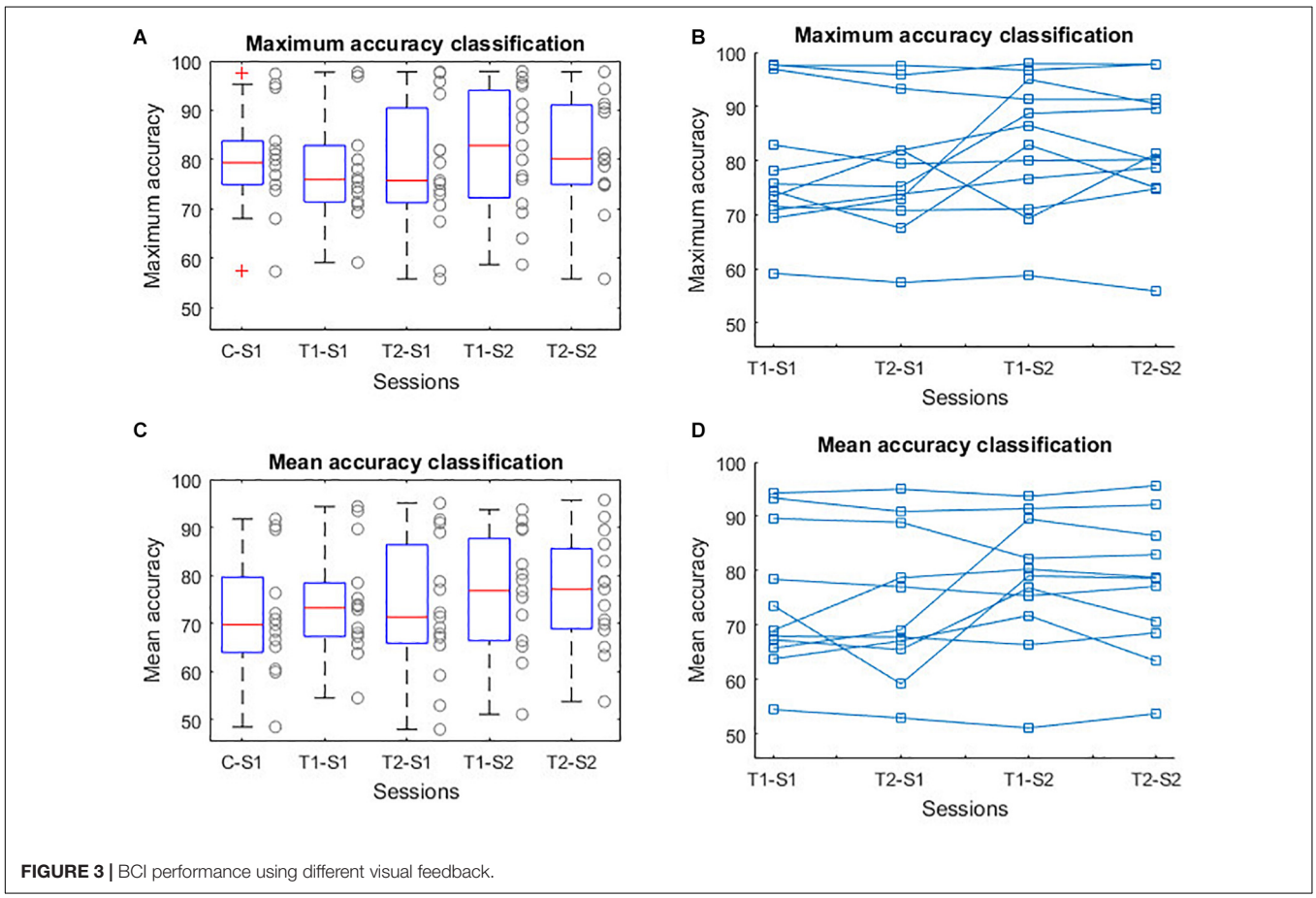

FIGURE 3 | BCI performance using different visual feedback.

TABLE 3 | Summary of MI accuracy of each group.

	C-S1	T1_S1	T2_S1	T1_S2	T2_S2
Maximum accuracy					
All (mean)	80.09 (10.76)	78.86 (11.47)	78.49 (13.32)	82.03 (12.48)	82.08 (11.61)
Healthy (mean)	84.78 (12.9)	85.70 (14.25)	83.68 (16.9)	86.42 (15.39)	88.42 (11.41)
Stroke (mean)	78.21 (9.91)	76.12 (9.65)	75.02 (9.9)	79.11 (10.02)	77.86 (10.22)
Mean accuracy					
All (mean)	71.53 (12.82)	74.29 (11.47)	73.07 (14.15)	76.09 (12.33)	76.45 (11.63)
Healthy (mean)	80.40 (17.77)	81.86 (14.26)	77.84 (18.17)	81.93 (14.37)	83.77 (11.83)
Stroke (mean)	68.87 (10.71)	71.27 (9.31)	69.88 (10.75)	72.20 (9.73)	71.57 (9.07)

TABLE 4 | Summary of questionnaire results based on group and gaming experience.

	n	Mean (*SD*)	P1	P2	P3	P4	P5	P6	P7	P8
All	**16**	**4.20 (0.45)**	**3,31**	**3,75**	**4,44**	**4,69**	**4,38**	**4,25**	**4,25**	**4,50**
Healthy	**6**	**4.15 (0.68)**	**2,83**	**3,83**	**4,83**	**4,83**	**4,33**	**3,83**	**4,00**	**4,67**
Often	3	4.54 (0.56)	3,33	4,33	5,00	5,00	4,67	4,33	4,67	5,00
Sometimes	2	3.81 (0.80)	2,50	3,50	4,50	4,50	4,50	3,50	3,00	4,50
Never	1	3.63 (1.06)	2,00	3,00	5,00	5,00	3,00	3,00	4,00	4,00
Stroke	**10**	**4.23 (0.37)**	**3,60**	**3,70**	**4,20**	**4,60**	**4,40**	**4,50**	**4,40**	**4,40**
Often	1	3.75 (1.04)	3,00	2,00	4,00	4,00	3,00	5,00	4,00	5,00
Sometimes	3	4.13 (0.56)	3,00	3,67	4,00	4,33	4,67	4,67	4,33	4,33
Almost never	1	3.13 (0.83)	3,00	2,00	2,00	4,00	4,00	3,00	4,00	3,00
Never	5	4.6 (0.24)	4,20	4,40	4,80	5,00	4,60	4,60	4,60	4,60

The bold values differentiate between the two groups of users that participate in the experiment. People that have suffer the stroke and healthy people.

The results obtained from the questionnaire show a high satisfaction level from the users (see **Figure 4**). In one hand, the easiness of use and the clarity of the rules are the features best scored by both groups. It is important to point out that previous experience on gaming is not related with better user experience or a better BCI performance. All users also reported that this new avatar helped them to improve their concentration (Q6) and reduce their boredom (Q7). This is consistent with the results obtained in **Figure 3C**. On the other hand, all participants gave the lowest score to the entertainment level (Q1) and visual attractiveness (Q2). As observed in previous experiments (Lledó et al., 2016), visual attractiveness is a desired objective but sometimes patients prefer simpler versions of a task. Future versions of the game could provide different versions of the game appearance. The difficult part is to improve the entertainment level of the game without increasing the cognitive task and, consequently, decreasing the BCI performance. Hence, other narrative threads could be tested and stratified into levels to assess how a story impacts on users' performance and motivation. Moreover, the game difficulty level could be adapted to the user's performance: the better the results, the higher the correct response threshold.

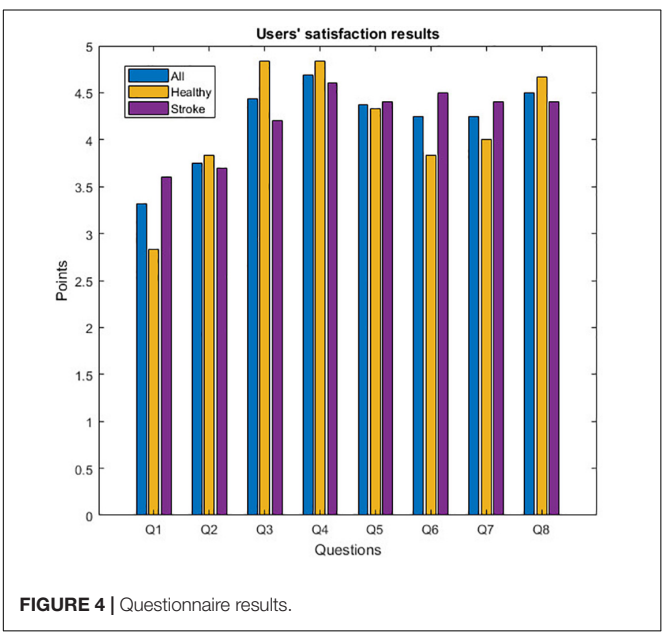

FIGURE 4 | Questionnaire results.

The main limitation of the study is small number of subjects and the age difference between groups. In addition, more sessions are needed to evaluate if the results observed in this pilot study are generalizable. Furthermore, new variables can be considered such us stress and fatigue, frequent in this type of rehabilitation. Finally, some emotional variables can be included to compare with the user performance.

Nevertheless, the idea of introducing games combined with BCI therapy seems to be an promising step to take to improve user experience, increase adherence to treatment and improve the functional outcome of patients.

CONCLUSION

A game-based rehabilitation instrument has been developed as an improvement of the existing recoveriX system for post-stroke upper limb rehabilitation. A pilot study has been carried out to test the impact of the game in the rehabilitation process. Sixteen subjects were recruited (6 healthy and 10 stroke patients) to perform 2 sessions of BCI therapy using different visual feedback modalities. The first run (80 trials) of each session was used to calibrate the system creating a personal LDA classifier. In the second run of the first session (T1-S1) all participants performed 80 trials using the "standard" VR avatar. In the third run of the first session (T2-S1) the participants used a new animated version based on the standard avatar. In the second run of the second session (T2-S2) users trained with the new avatar combined with a pop-up window that was appearing for a short period every 10 min showing the score. In the third run of the second session (T2-S2) the appearance was like the T2-S2, but the score window was appearing all the time. The objective of these last two runs was to add more cognitive responses to improve the concentration without harming the MI accuracy.

The results show there is no significant difference in the MI accuracy baseline between the healthy group and the stroke group. Moreover, there were no significant differences either between training with or without game. Results also show that there are no significant differences in the accuracies using the different forms of scoring feedback. Thus, the added stimuli of

scoring and time does not affect performance. Concerning users' opinions, they were all positive about the game level of entertainment, clarity of rules, narrative and visual attractiveness. Participants declared not having been affected by the game to create a mental image but having felt less bored. Finally, there was a consensus about the interest of gamifying stroke rehabilitation sessions. The main limitation of this study is the small size of the sample and small number of rehabilitation sessions. However, the results are encouraging to continue investigating how to bring gamification elements to post-stroke rehabilitation.

DATA AVAILABILITY STATEMENT

The datasets generated for this study are available on request to the corresponding author.

ETHICS STATEMENT

The studies involving human participants were reviewed and approved by the Institut Guttmann ethics committee. The patients/participants provided their written informed consent to participate in this study. Written, informed consent was obtained from the individuals for the publication of any potentially identifiable images or data included in this article.

AUTHOR CONTRIBUTIONS

MC-C contributed to the implementation and execution of the methodology and writing the manuscript. MS-R collaborated in the design of the experiment, the analysis of the results, and writing the manuscript. JR-S participated in the design of the experiment and in the set up of the brain computer interface, and the integration of the game. EO and MO collaborated in the organization of the pilot study with patients. EO reviewed the manuscript. RO and CG contributed to the design of the BCI technology. DT supervised the research and contributed to the design of the game, the analysis of the results, and writing the manuscript. All authors contributed to the article and approved the submitted version.

SUPPLEMENTARY MATERIAL

The Supplementary Material for this article can be found online at: https://www.frontiersin.org/articles/10.3389/fnins.2020.00882/full#supplementary-material

REFERENCES

Alimardani, M., Nishio, S., and Ishiguro, H. (2016). The importance of visual feedback design in BCIs; from embodiment to motor imagery learning. *PLoS One* 11:e0161945. doi: 10.1371/journal.pone.0161945

Ang, K. K., Chua, K. S. G., Phua, K. S., Wang, C., Chin, Z. Y., Kuah, C. W. K., et al. (2015). A Randomized controlled trial of EEG-based motor imagery brain-computer interface robotic rehabilitation for stroke. *Clin. EEG Neurosci.* 46, 310–320. doi: 10.1177/1550059414522229

Bermúdez-Badia, S., and Cameirão, M. S. (2012). The neurorehabilitation training toolkit (NTT): a novel worldwide accessible motor training approach for at-home rehabilitation after stroke. *Stroke Res. Treat.* 2012:802157.

Bermúdez-Badia, S., Fluet, G. G., Llorens, R., and Deutsch, J. E. (2016). "Virtual reality for sensorimotor rehabilitation post stroke: design principles and evidence," in *Neurorehabilitation Technology*, eds D. Reinkensmeyer, and V. Dietz, (Cham: Springer), 573–603. doi: 10.1007/978-3-319-28603-7_28

Borrego, A., Latorre, J., Alcañiz, M., and Llorens, R. (2019). Embodiment and presence in virtual reality after stroke. a comparative study with healthy subjects. *Front. Neurol.* 10:1061. doi: 10.3389/fneur.2019.01061

Burke, J. W., McNeill, M. D. J., Charles, D. K., Morrow, P. J., Crosbie, J. H., and McDonough, S. M. (2009). Optimising engagement for stroke rehabilitation using serious games. *Vis. Comput.* 25:1085. doi: 10.1007/s00371-009-0387-4

Cervera, M. A., Soekadar, S. R., Ushiba, J., Millán, J. D. R., Liu, M., Birbaumer, N., et al. (2018). Brain-computer interfaces for post-stroke motor rehabilitation: a meta-analysis. *Ann. Clin. Transl. Neurol.* 5, 651–663. doi: 10.1002/acn3.544

Chavarriaga, R., Fried-Oken, M., Kleih, S., Lotte, F., and Scherer, R. (2017). Heading for new shores! Overcoming pitfalls in BCI design. *Brain Comput. Interfaces* 4, 60–73. doi: 10.1080/2326263x.2016.1263916

Cho, W., Sabathiel, N., Ortner, R., Lechner, A., Irimia, D. C., Allison, B. Z., et al. (2016). Paired Associative stimulation using brain-computer interfaces for stroke rehabilitation: a pilot study. *Eur. J. Transl. Myol.* 26:6132.

Donkor, E. S. (2018). Stroke in the 21st century: a snapshot of the burden, epidemiology, and quality of life. *Stroke Res. Treat.* 2018:3238165.

Girden, E. R. (1992). *ANOVA: Repeated Measures*, 1st Edn. Thousand Oaks, CA: SAGE Publications, Inc.

Hamari, J., Koivisto, J., and Sarsa, H. (2014). "Does gamification work? - A literature review of empirical studies on gamification," in *Proceedings of the 2014 47th Hawaii International Conference on System Sciences*, (Piscataway, NJ: IEEE), 3025–3034.

Hanus, M. D., and Fox, J. (2015). Assessing the effects of gamification in the classroom: a longitudinal study on intrinsic motivation, social comparison, satisfaction, effort, and academic performance. *Comput. Educ.* 80, 152–161. doi: 10.1016/j.compedu.2014.08.019

Irimia, D., Sabathiel, N., Ortner, R., Poboroniuc, M., Coon, W., Allison, B. Z., et al. (2016). "recoveriX: a new BCI-based technology for persons with stroke," in *Proceedings of the 2016 38th Annual International Conference of the IEEE Engineering in Medicine and Biology Society (EMBC)*, (Piscataway, NJ: IEEE), 1504–1507.

Irimia, D. C., Cho, W., Ortner, R., Allison, B. Z., Ignat, B. E., Edlinger, G., et al. (2017). Brain-computer interfaces with multi-sensory feedback for stroke rehabilitation: a case study. *Artif. Organs* 41, E178–E184.

Jeunet, C., Jahanpour, E., and Lotte, F. (2016). Why standard brain-computer interface (BCI) training protocols should be changed: an experimental study. *J. Neural Eng.* 13:036024. doi: 10.1088/1741-2560/13/3/036024

Kosmyna, N., and Lécuyer, A. (2017). Designing guiding systems for brain-computer interfaces. *Front. Hum. Neurosci.* 11:396. doi: 10.3389/fnhum.2017.00396

Lledó, L. D., Díez, J. A., Bertomeu-Motos, A., Ezquerro, S., Badesa, F. J., Sabater-Navarro, J. M., et al. (2016). A comparative analysis of 2D and 3D tasks for virtual reality therapies based on robotic-assisted neurorehabilitation for post-stroke patients. *Front. Aging Neurosci.* 8:205. doi: 10.3389/fnagi.2016.00205

Llorens, R., Noé, E., Naranjo, V., Borrego, A., Latorre, J., and Alcañiz, M. (2015). Tracking systems for virtual rehabilitation: objective performance vs. subjective experience. a practical scenario. *Sensors* 15, 6586–6606. doi: 10.3390/s150306586

Lotte, F., Larrue, F., and Mühl, C. (2013). Flaws in current human training protocols for spontaneous brain-computer interfaces: lessons learned from instructional design. *Front. Hum. Neurosci.* 7:568. doi: 10.3389/fnhum.2013.00568

McFarland, D. J., Miner, L. A., Vaughan, T. M., and Wolpaw, J. R. (2000). Mu and beta rhythm topographies during motor imagery and actual movements. *Brain Topogr.* 12, 177–118.

Neuper, C., Müller-Putz, G. R., Scherer, R., and Pfurtscheller, G. (2006). Chapter 25 Motor imagery and EEG-based control of spelling devices and neuroprostheses. *Prog. Brain Res.* 159, 393–409. doi: 10.1016/s0079-6123(06)59025-9

Norman, G., and Streiner, D. (2008). *Biostatistics: The Bare Essentials*, 3rd Edn. Toronto: McGraw-Hill Education, 200.

Petit, D., Gergondet, P., Cherubini, A., and Kheddar, A. (2015). "An integrated framework for humanoid embodiment with a BCI," in *Proceedings of the 2015 IEEE International Conference on Robotics and Automation (ICRA)*, (Piscataway, NJ: IEEE), 2882–2887.

Pichiorri, F., Morone, G., Petti, M., Toppi, J., Pisotta, I., Molinari, M., et al. (2015). Brain-computer interface boosts motor imagery practice during stroke recovery. *Ann. Neurol.* 77, 851–865. doi: 10.1002/ana.24390

Pindus, D. M., Mullis, R., Lim, L., Wellwood, I., Rundell, A. V., Aziz, N. A. A., et al. (2018). Stroke survivors' and informal caregivers' experiences of primary care and community healthcare services – A systematic review and meta-ethnography. *PLoS One* 13:e0192533. doi: 10.1371/journal.pone.0192533

Quandt, F., and Hummel, F. C. (2014). The influence of functional electrical stimulation on hand motor recovery in stroke patients: a review. *Exp. Transl. Stroke Med.* 6:9.

Remsik, A., Young, B., Vermilyea, R., Kiekoefer, L., Abrams, J., Evander-Elmore, S., et al. (2016). A review of the progression and future implications of brain-computer interface therapies for restoration of distal upper extremity motor function after stroke. *Expert Rev Med Devices* 13, 445–454. doi: 10.1080/17434440.2016.1174572

Richter, G., Raban, D. R., and Rafaeli, S. (2015). "Studying gamification: the effect of rewards and incentives on motivation," in *Gamification in Education and Business*, eds T. Reiners, and L. C. Wood, (Cham: Springer), 21–46. doi: 10.1007/978-3-319-10208-5_2

Singh, V., Rana, R. K., and Singhal, R. (2013). Analysis of repeated measurement data in the clinical trials. *J. Ayurveda Integr. Med.* 4:77. doi: 10.4103/0975-9476.113872

Škola, F., Tinková, S., and Liarokapis, F. (2019). Progressive training for motor imagery brain-computer interfaces using gamification and virtual reality embodiment. *Front. Hum. Neurosci.* 13:329. doi: 10.3389/fnhum.2019.00329

van Dokkum, L. E. H., Ward, T., and Laffont, I. (2015). Brain computer interfaces for neurorehabilitation-its current status as a rehabilitation strategy post-stroke. *Ann. Phys. Rehabil. Med.* 58, 3–8. doi: 10.1016/j.rehab.2014.09.016

Verma, J. (2015). *Repeated Measures Design for Empirical Researchers*, 1st Edn. India: Wiley, 288.

Vourvopoulos, A., Ferreira, A., and Badia, S. B. I. (2016). "NeuRow: an immersive VR environment for motor-imagery training with the use of Brain-Computer Interfaces and vibrotactile feedback," in *Proceedings of the International Conference on Physiological Computing Systems*, Vol. 2, (Portugal: SCITEPRESS), 43–53.

Vourvopoulos, A., Pardo, O. M., Lefebvre, S., Neureither, M., Saldana, D., Jahng, E., et al. (2019). Effects of a brain-computer interface with virtual reality (VR) neurofeedback: a pilot study in chronic stroke patients. *Front. Hum. Neurosci.* 13:210. doi: 10.3389/fnhum.2019.00210

Zhang, J. J. Q., Fong, K. N. K., Welage, N., and Liu, K. P. Y. (2018). The activation of the mirror neuron system during action observation and action execution with mirror visual feedback in stroke: a systematic review. *Neural Plast.* 2018:2321045.

Zichermann, G., and Linder, J. (2013). *The Gamification Revolution*, 1st Edn. New York, Ny: McGraw Hill Professional.

Conflict of Interest: MC-C, MS-R, JR-S, and RO were employed by the company g.tec medical engineering Spain S.L. CG is CEO of the company g.tec medical engineering Spain S.L. and g.tec medical engineering GmbH.

The remaining authors declare that the research was conducted in the absence of any commercial or financial relationships that could be construed as a potential conflict of interest.

Advantages of publishing in Frontiers

OPEN ACCESS
Articles are free to read for greatest visibility and readership

FAST PUBLICATION
Around 90 days from submission to decision

HIGH QUALITY PEER-REVIEW
Rigorous, collaborative, and constructive peer-review

TRANSPARENT PEER-REVIEW
Editors and reviewers acknowledged by name on published articles

Frontiers
Avenue du Tribunal-Fédéral 34
1005 Lausanne | Switzerland

Visit us: www.frontiersin.org
Contact us: frontiersin.org/about/contact

REPRODUCIBILITY OF RESEARCH
Support open data and methods to enhance research reproducibility

DIGITAL PUBLISHING
Articles designed for optimal readership across devices

FOLLOW US
@frontiersin

IMPACT METRICS
Advanced article metrics track visibility across digital media

EXTENSIVE PROMOTION
Marketing and promotion of impactful research

LOOP RESEARCH NETWORK
Our network increases your article's readership